Phaeophyceae

General characteristics

- ca 265 genera, 1500 - 2000 species
- multicellular thallus, attached to the surface
- marine, only 3-5 species in freshwater habitats
- rocky coastline – litoral, sublitoral (min. 0,6% of residual light – up to depth of 260 m, but most species are not shade-loving organisms)
- high primary production, DMS production
- economically and culturally important – aquacultures, seaweed art

Cell structure

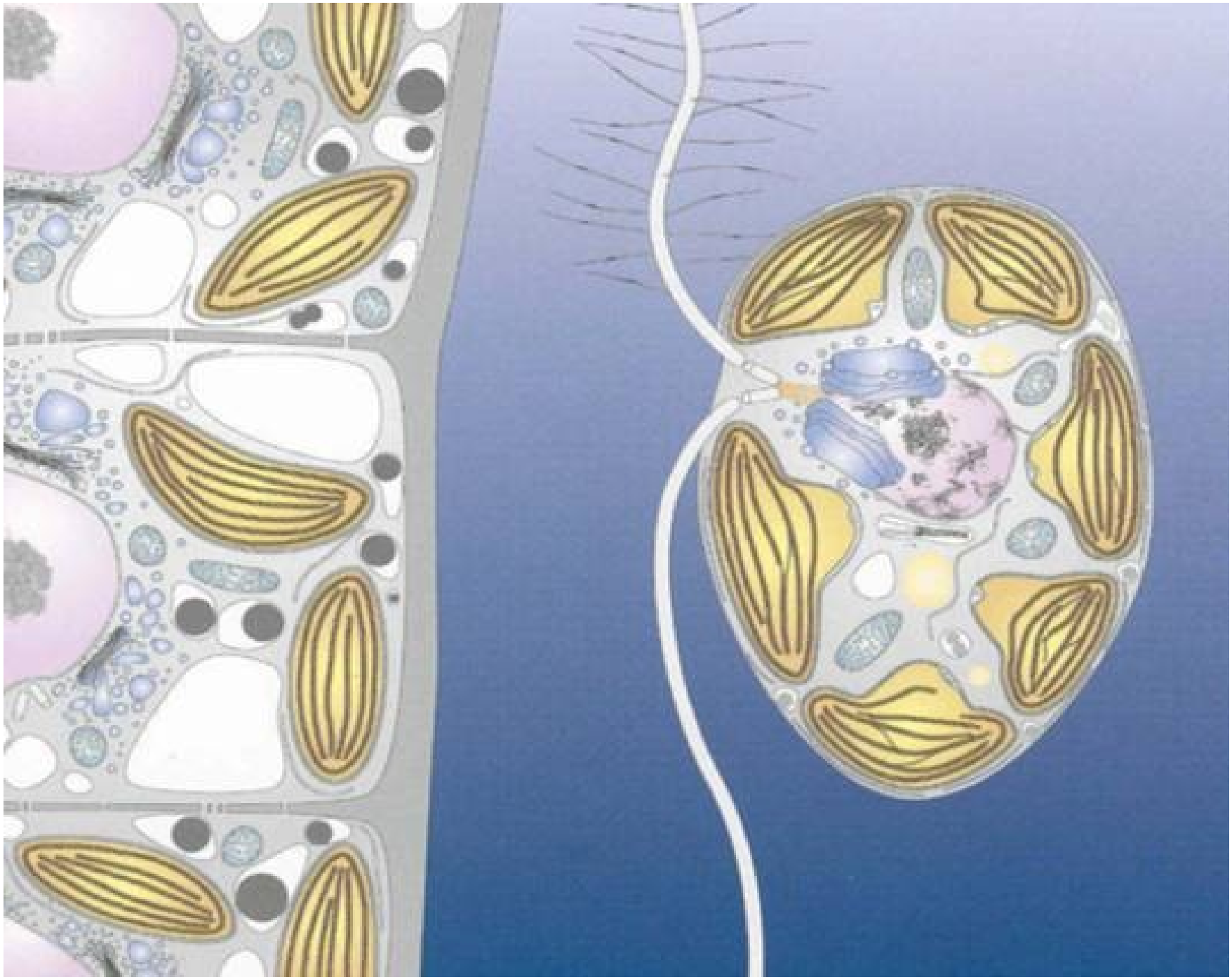

Plastids

- chl a, c_1 , c_2, β-carotene, fukoxanthin (like in Chrysophyceae) Bacillariophyceae) , violaxanthin, dinoxanthin, diadinoxanthin
- discoid plastids, 1 or more pyrenoids
- heterokont structure

Plastids

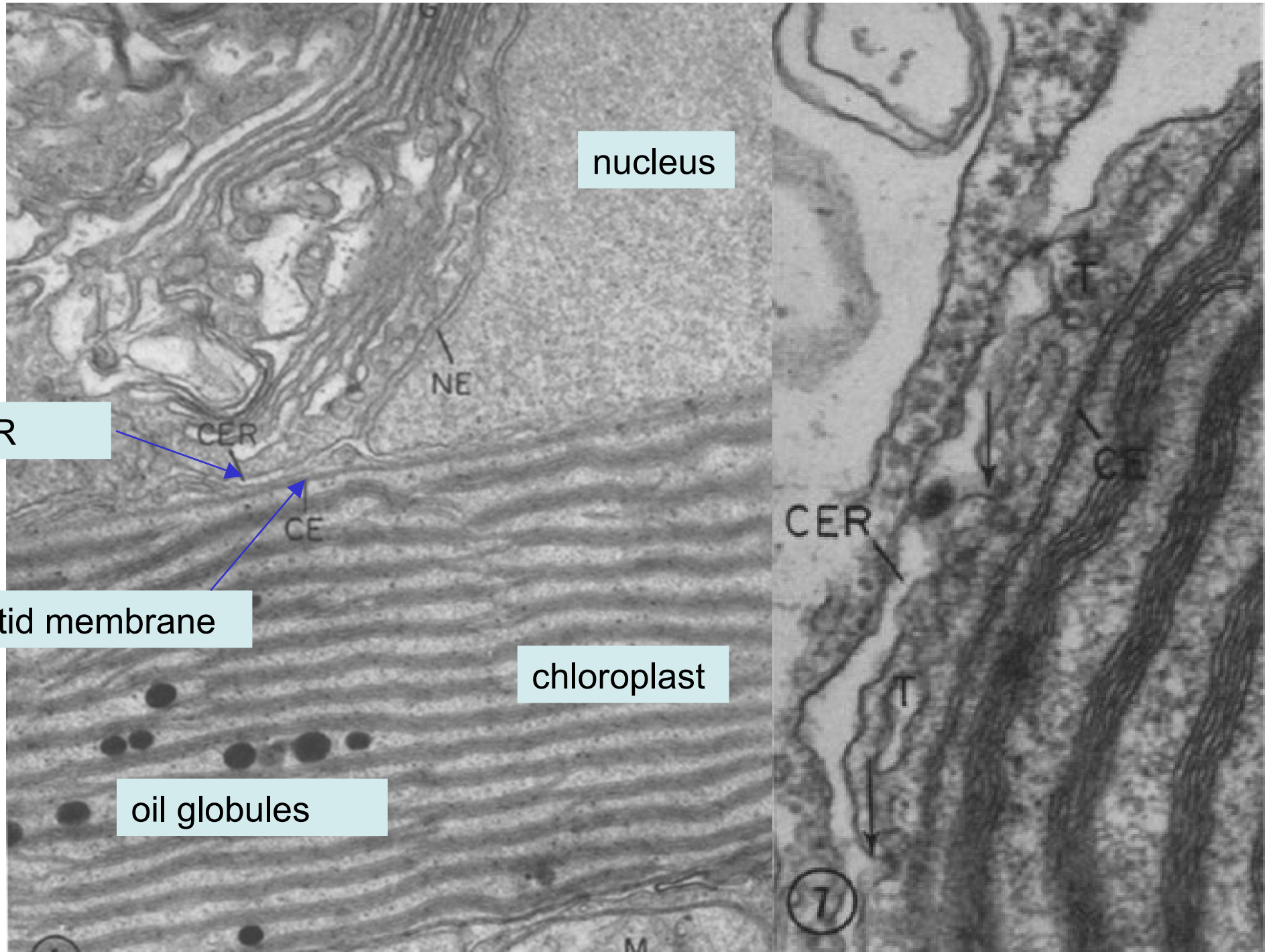
nucleus
NE
chloroplast ER
CER
CE
2layered plastid membrane
chloroplast
oil globules
T
CE
CER
T
7

Pyrenoid

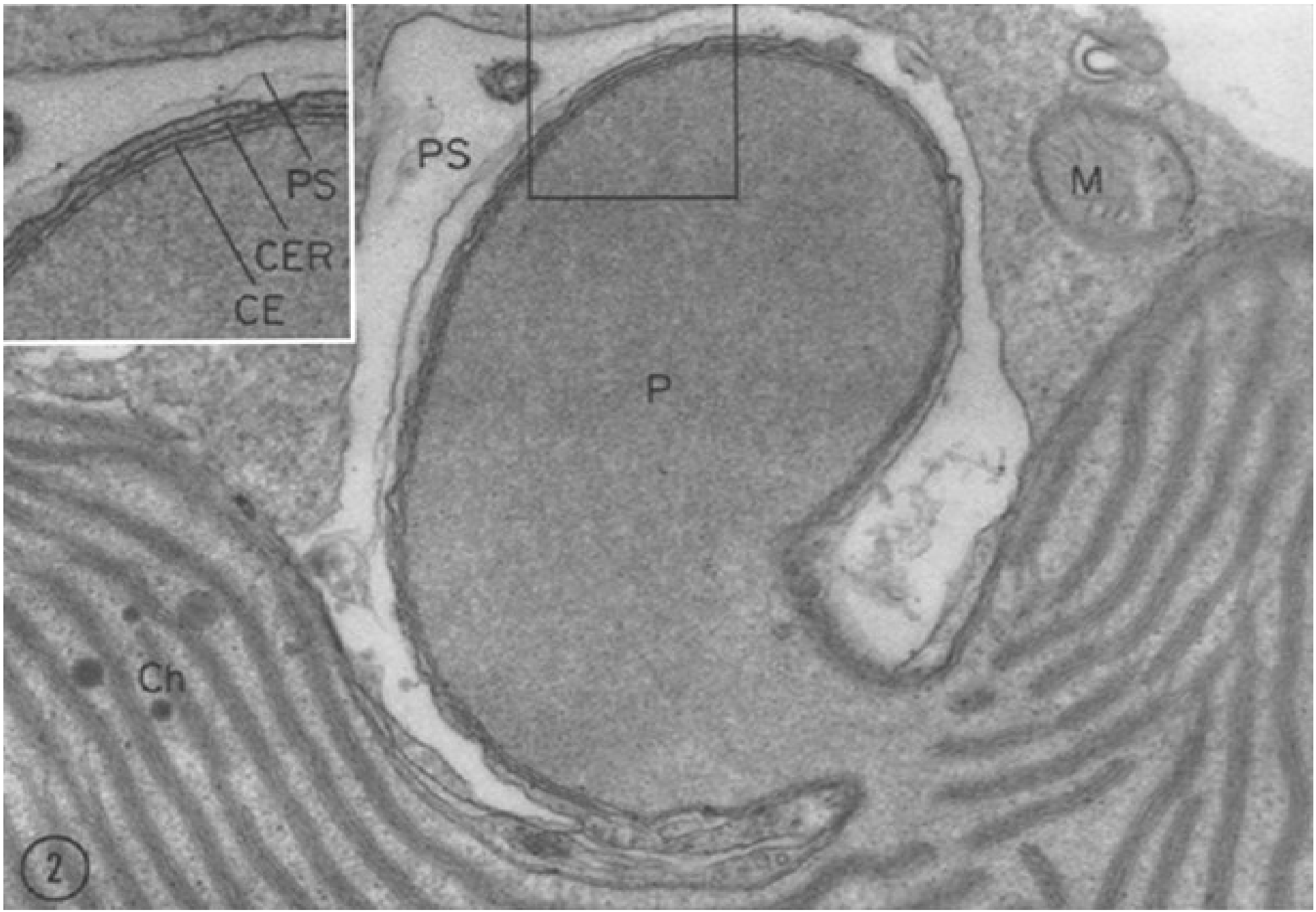

Metabolism products

- storage products (chrysolaminaran, manitol)
- florotanins – stored in physodes, when oxidized, they case brown colour of water
- iodine (0,03 – 0,3% of weight)
- organobromids – destruction of ozone layer

- dimethylsulphopropionate – osmotic regulation

  production of DMS (in parallel to haptophytes)

Cell wall composition

- alginates – salts of Alginic acid (gelatinous)
  - Na-alginates – soluble
  - Ca-alginates – insoluble
- cell wall structure
  - fibrilar component – cellulose, Ca-alginates
  - amorphous component – soluble Na-alginates
- fucoidane – mucilage surrounding cell wall
  - against desiccation
  - environment for gamete fusion

Zoids

features similar to other heterokont groups

features typical for brown algae

heterokont flagella, mastigonemata

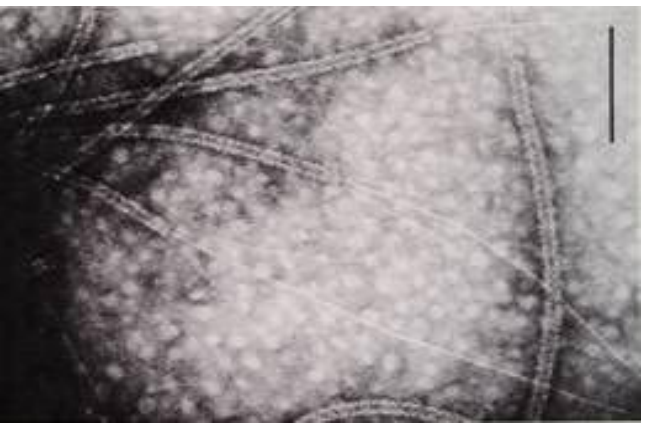

photoreceptor

periplastidial reticulum

four membranes, girdle lamella

lateral flagella insertion

flagella terminated by acronemates

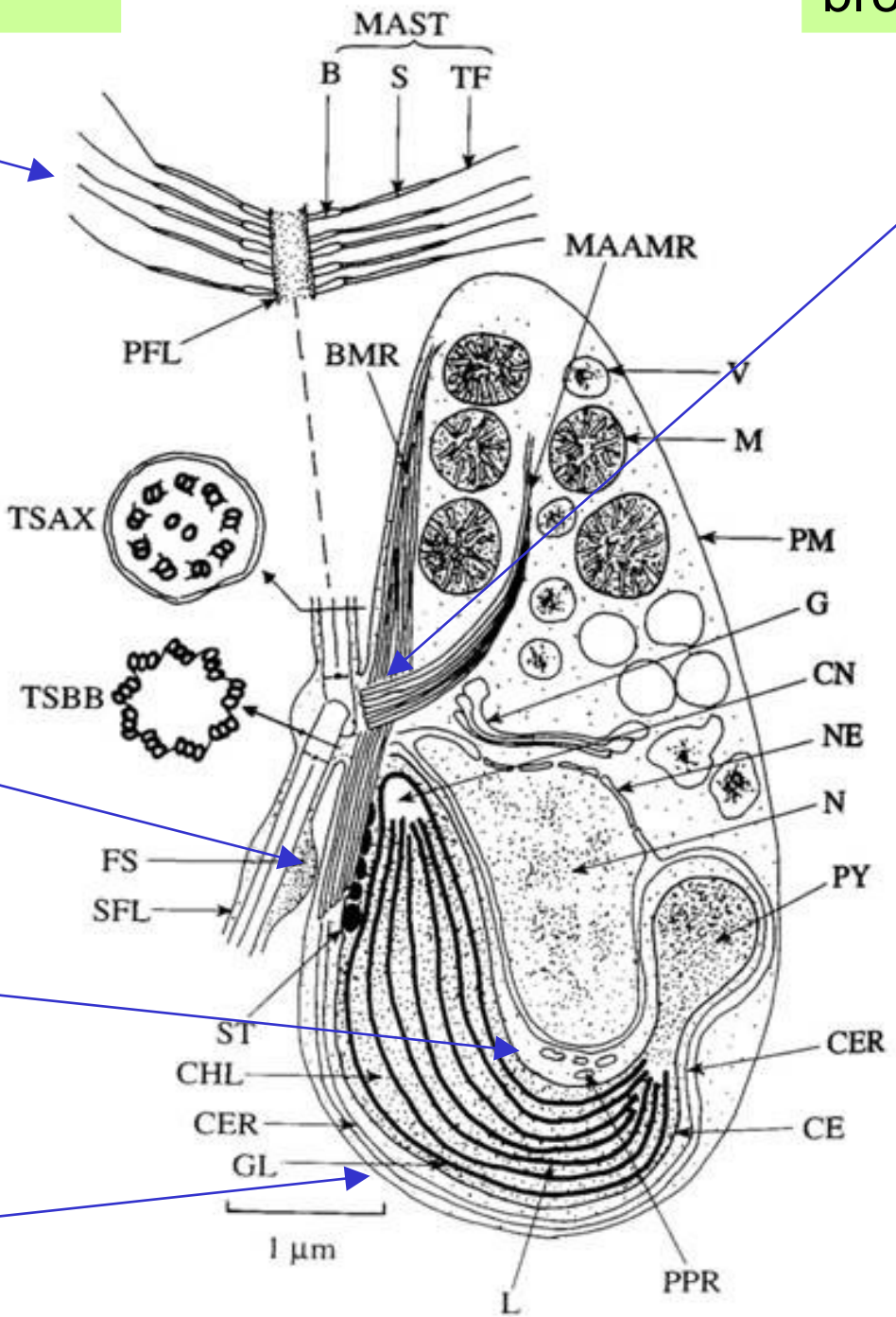

Zoids

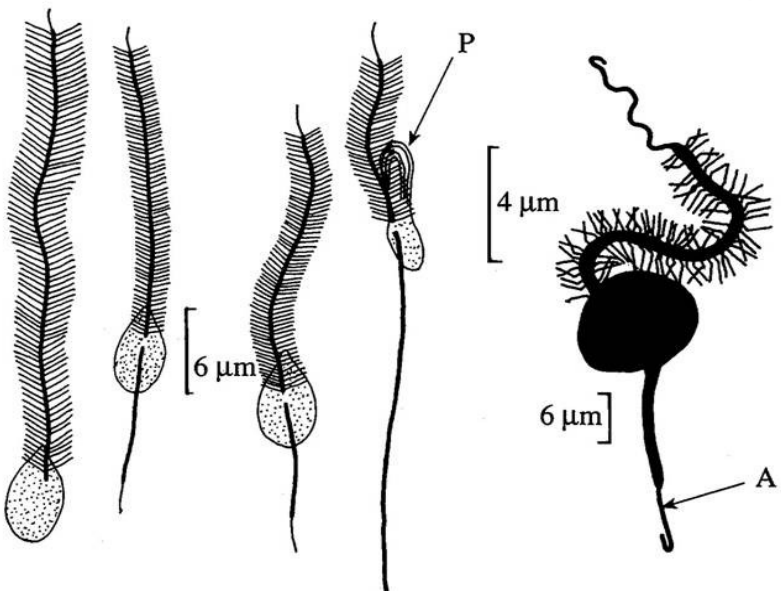

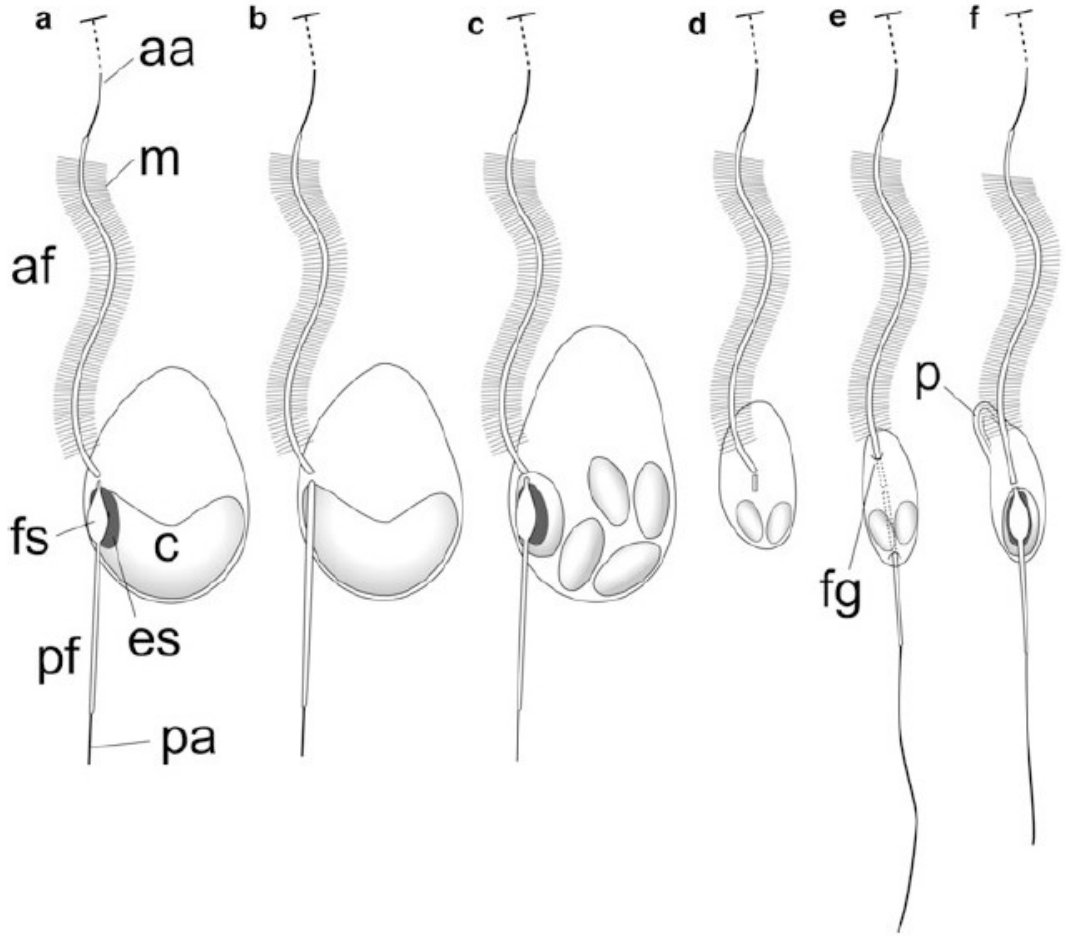

Fig. 7 Schematic representation of brown algal flagellated cells. (**a**) Typical (perhaps plesiomorphic) type with long anterior flagellum (*af*) and short posterior flagellum (*pf*). Chloroplast (*c*) has eyespot (*es*) spatially associated with flagellar swelling (*fs*) on the basal part of the posterior flagellum. Anterior flagellum has long acronema (*aa*), which is easily detached by fixation. Posterior flagellum has relatively short, but more persistent acronema (*pa*). (**b**) Laminarialean type without eyespot and flagellar swelling and lacking phototaxis. (**c**) Female anisogamous gamete with multiple chloroplasts. (**d**) Dictyotalean sperm with remnant posterior flagellum and reduced chloroplast. (**e**) Laminarialean sperm with long posterior flagellum, reduced chloroplasts, and deep flagellar gullet (*fg*). (**f**) Fucalean sperm with proboscis (anterior protuberance) and eyespot

Kawai & Henry, 2017, Phaeophyta in Handbook of Protists

Sexual reproduction

- diplohaplontic cell cycle, isomorphic and heteromorphic
- plurilocular zoidangia

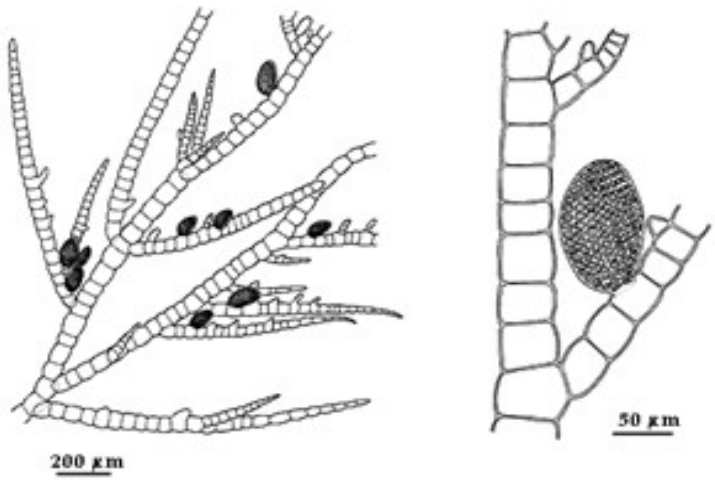

- unilocular zoidangia

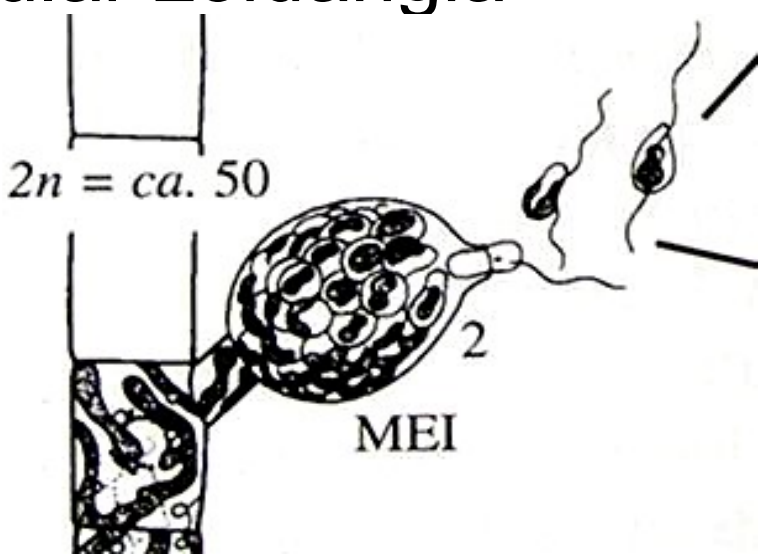

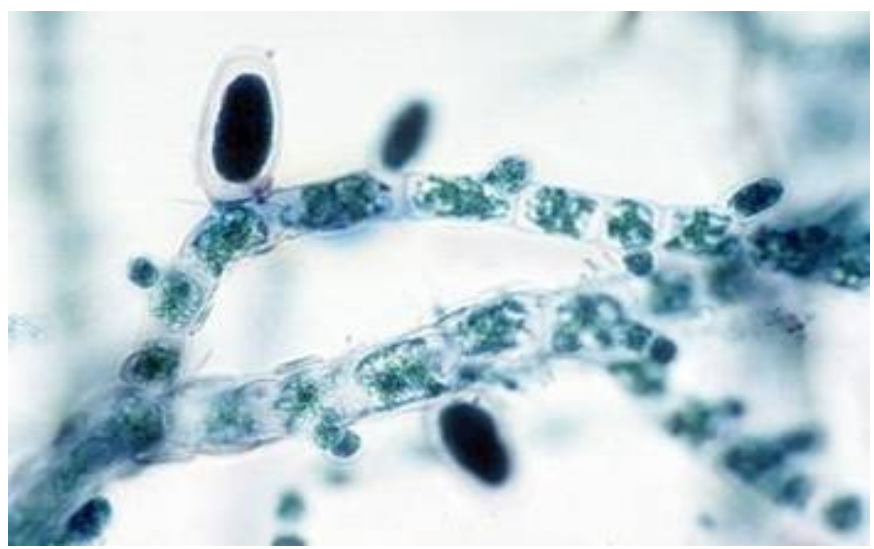

unilocular sporangia (unangia)

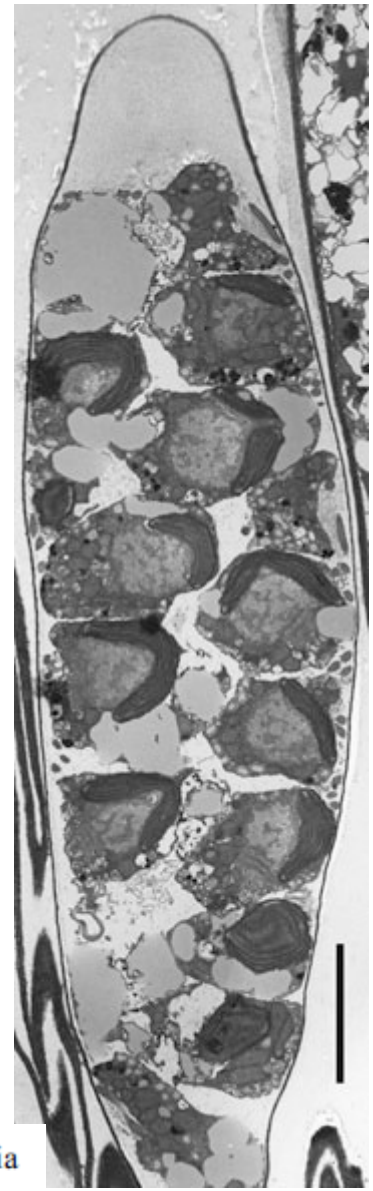

Fig. 4 Unilocular sporangia of *Saccharina japonica* in longitudinal section (TEM micrograph courtesy of Taizo Motomura). Scale bar, 5 µm

plurilocular sporangia (plurangia)

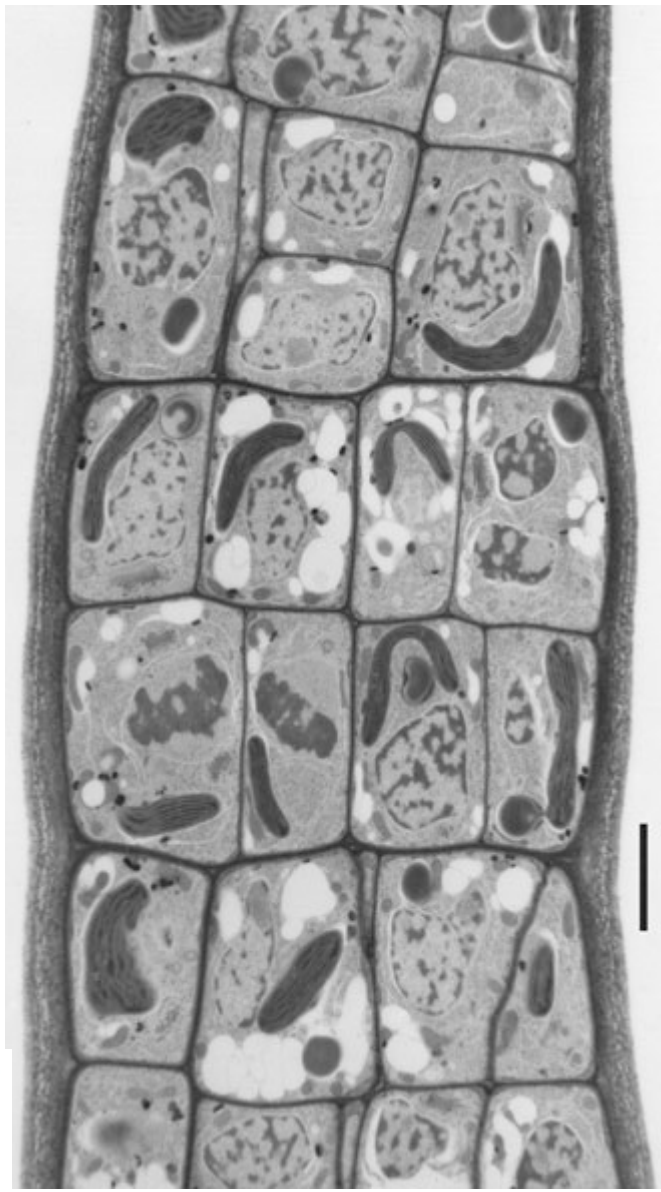

Fig. 5 Immature plurilocular sporangia of *Ectocarpus* sp. Freeze substitution (TEM micrograph courtesy of Taizo Motomora). Scale bar, 2 µm

Kawai & Henry, 2017, Phaeophyta in Handbook of Protists

Thallus structure

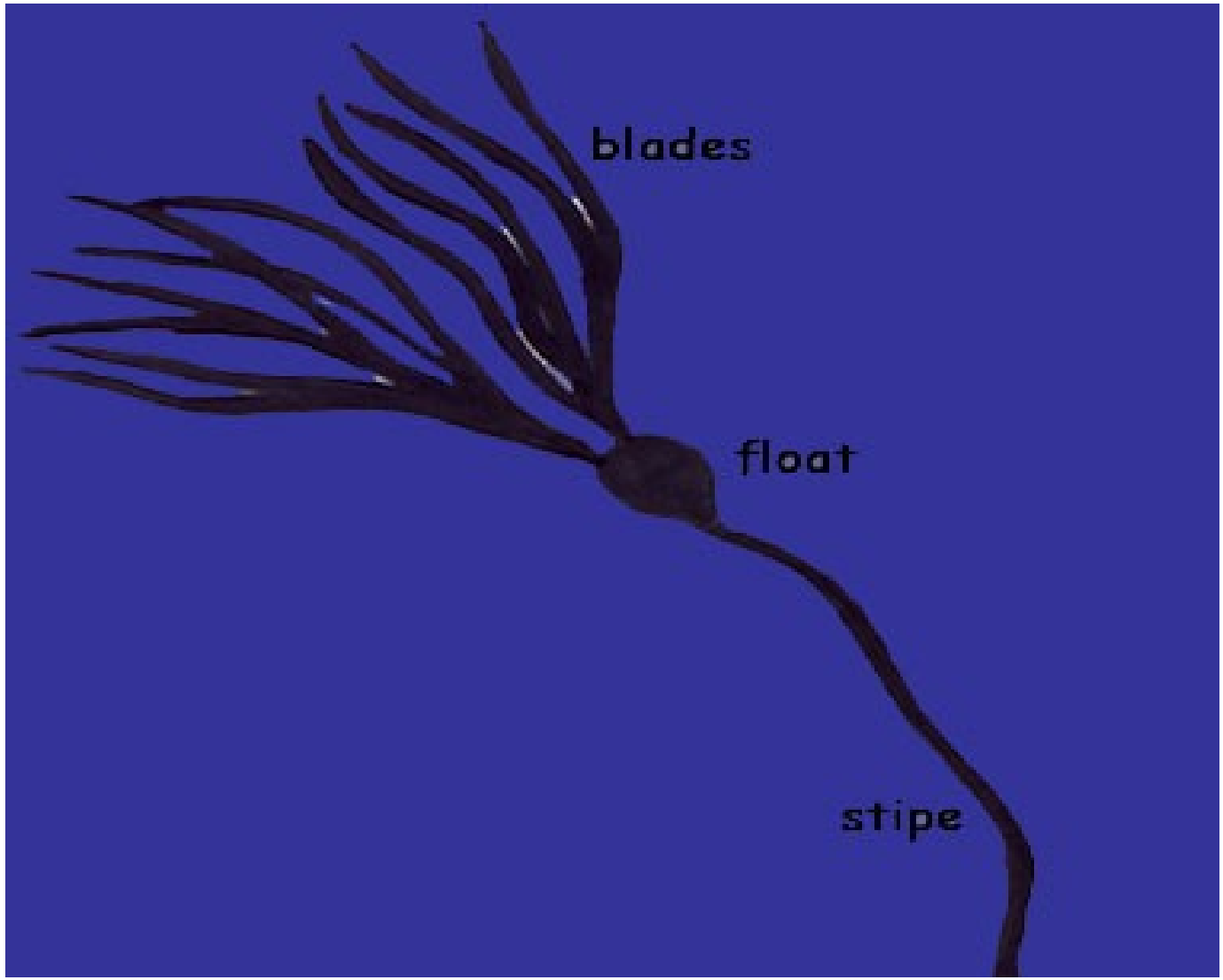

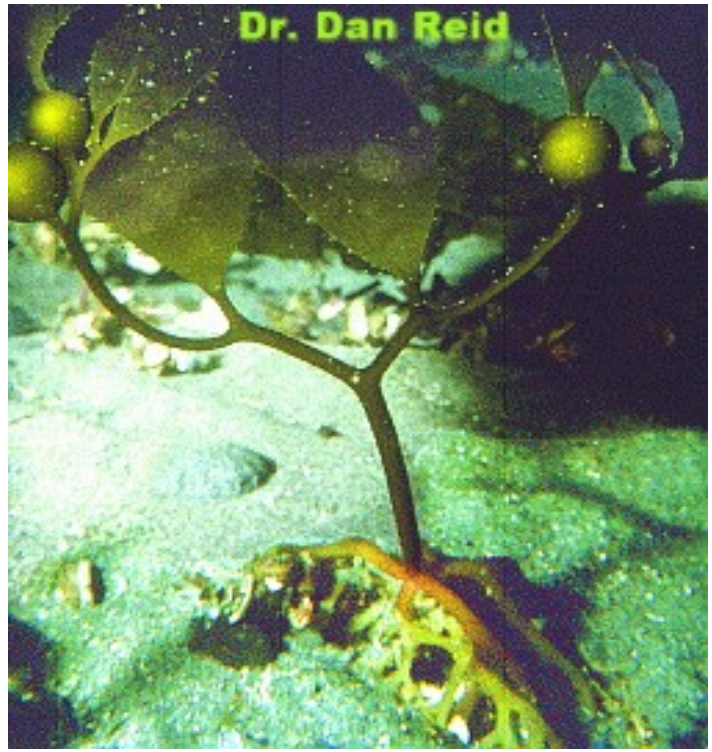

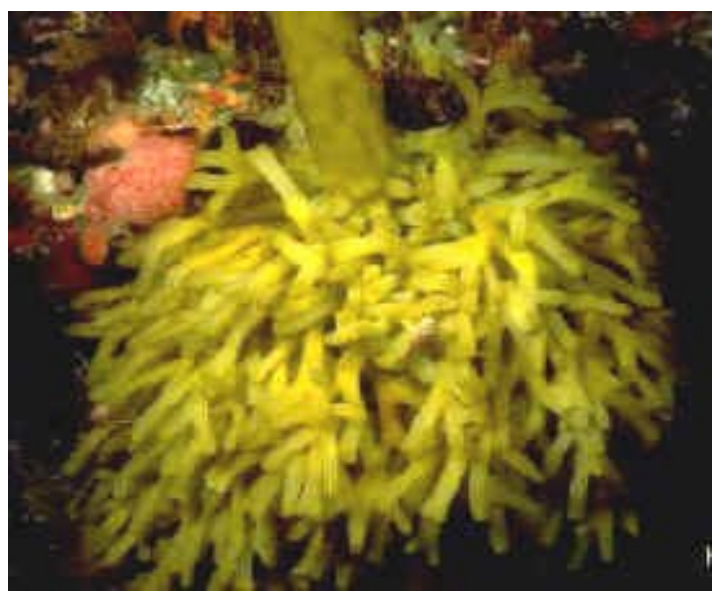

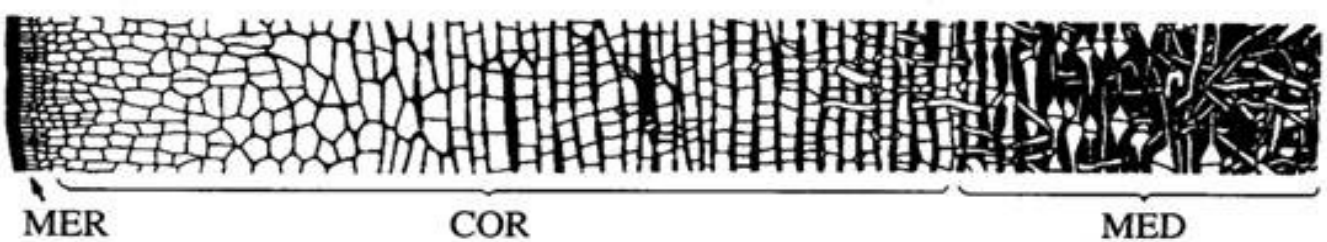

Thallus structure

filament developmental patterns

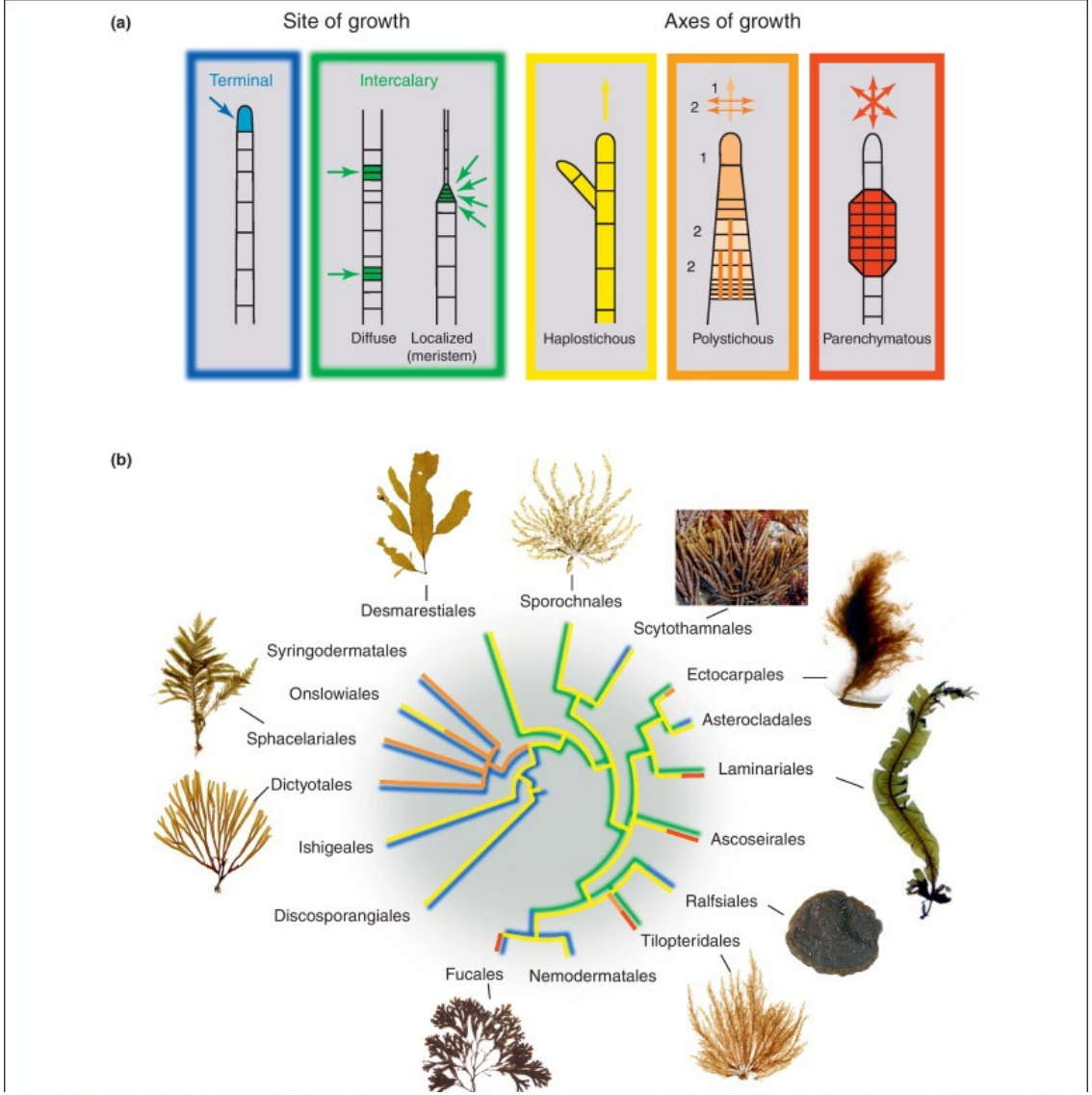

Figure 3. Main developmental patterns observed in brown algae. **(a)** Primary growth. Localization and axes of cell division that are observed in brown algal development. Cell division occurs either in a terminal–apical position (blue), or in an intercalary position (green: either diffuse growth or localized growth: e.g. trichothallic growth). Cell division axes are either unidirectional (haplostichous, uni- or multi-axial: yellow), or multidirectional. In the latter, division occurs either in two steps (polystichous: orange; with or without secondary thickening of the axes in the Sphacelariales, the auxocaulus and leptocaulus construction modes, respectively, as defined by [104]) or simultaneously along different axes (parenchymatous: red). **(b)** Distribution of cell division patterns on the phylogenetic tree of brown algae. The cell division patterns (localization and axes) for each brown algal order are indicated by the color and style (defined or blurred) of the branches of the circular tree, in agreement with those indicated in (a). The haplostichous growth pattern is the most widely distributed. Note that Desmarestiales and Sporochnales develop haplostichous structures (uniaxial in Desmarestiales and multi-axial in Sporochnales), which generate pseudo-parenchymes. Structures produced by a two-step cell division process (polystichous construction) with a terminal growth arose only once and are synapomorphic for the orders Syringodermatales, Sphacelariales, Dictyotales and Onslowiales (SSDO). However, polystichous construction analogous to that in the SSDO group also appeared in Tilopteridales (Tilopteridaceae, Cutleriaceae) and in numerous Ectocarpales, but as a result of intercalary growth rather than of terminal growth, such as that seen in the SSDO group. Parenchymatous growth appeared several times, and shows convergence in the most diverged brown algae (Fucales, Laminariales, Phyllariaceae in Tilopteridales and Ascoseirales) [1]. Interestingly, some distant orders comprise macroalgae with similar morphologies (e.g. *Himantothallus* in the Desmarestiales and the kelps in Laminariales) [105] and, conversely, some closely related orders show different morphologies, as illustrated by the 'crusts' morphology observed in Nemodermatales (not shown), which are a sister order to Fucales, as well as in Petrodermataceae, which are a sister family to Ishigeaceae (Ishigeales) and Lithodermataceae within Sphacelariales. Photographs are displayed for brown algal orders containing at least three genera: Dictyotales, *Dictyota linearis;* Sphacelariales, *Halopteris filicina*; Desmarestiales, *Desmarestia dresnayi*; Sporochnales, *Sporochnus pedunculatus;* Scytothamnales, *Splachnidium rugosum*; Ectocarpales, *Ectocarpus fasciculatus*; Laminariales, *Alaria esculenta*; Ralfsiales, *Ralfsia verrucosa*; Tilopteridales, *Tilopteris mertensii*; Fucales, *Fucus vesiculosus*. Image reproduced, with permission, from AlgaeBase (M.D. Guiry; *Splachnidium rugosum*).

Charrier et al., 2012, Trends Pl. Sci

Systematics and diversity

- class **Phaeophyceae**, syn. Fucophyceae
- traditionally - ca 14 orders (van den Hoek 1995)

Phylogeny

- traditional concepts of phylogeny and taxonomy:

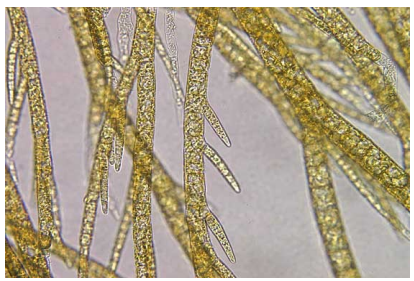

Ectocarpales G,S,[iso]

Sphacelariales G,S,iso

Dictyotales G,S,iso

Cutleriales G,S,hetero

Laminariales S,hetero

Fucales S,hetero

Time-calibrated multigenic molecular phylogeny of Phaeophyceae

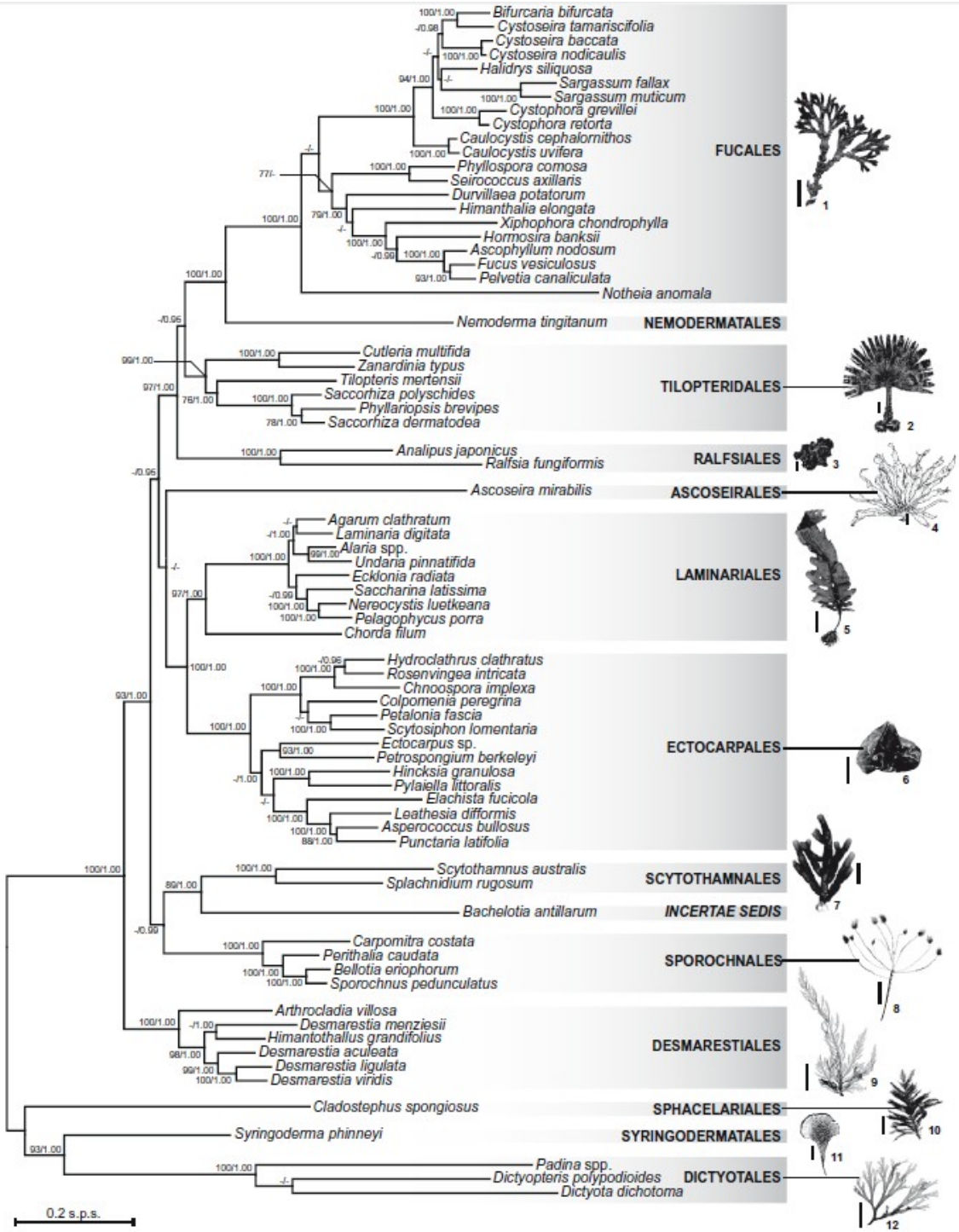

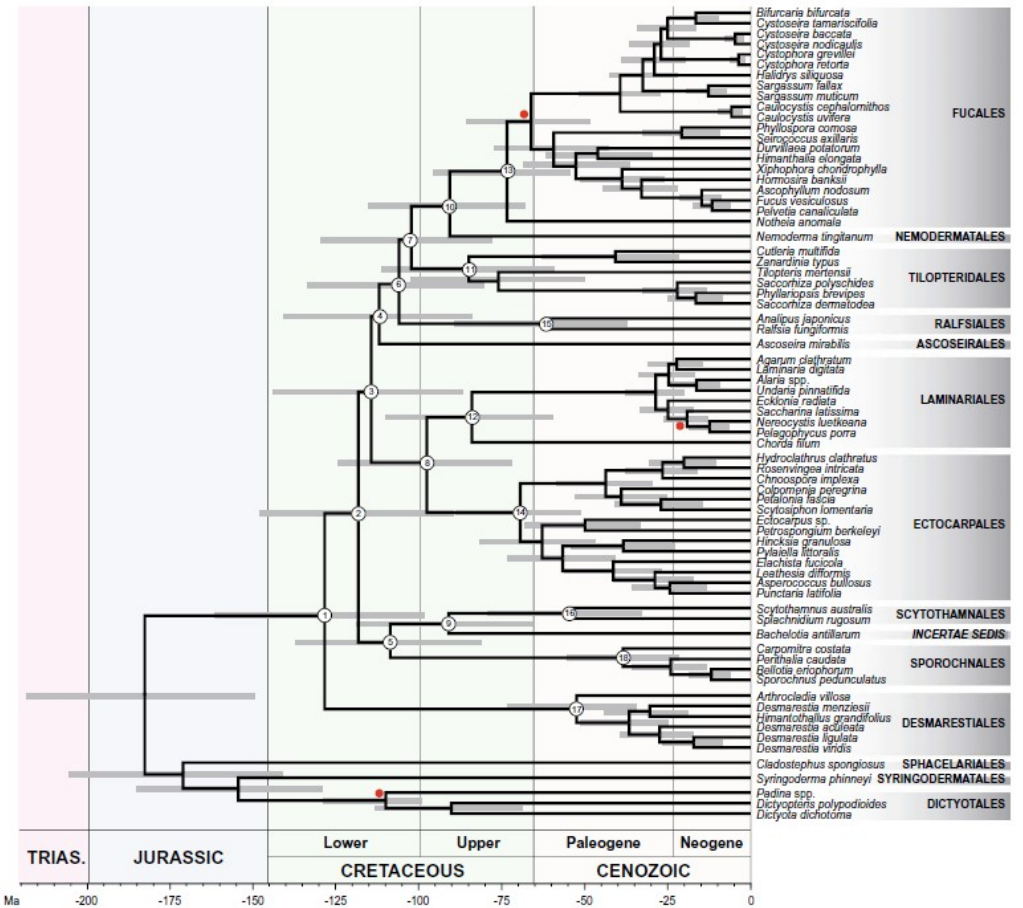

Fig. 2. Chronogram resulting from the Bayesian relaxed molecular clock analysis performed with BEAST (Drummond and Rambaut, 2007). The grey bars display the 95% HPD (highest probability density) interval of node ages. Details for nodes labelled with numbers are provided in Table 3. The red circles mark the three nodes that were time-constrained with fossils as described in text: the Sargassaceae and the (*Nereocystis–Pelagophycus*) lineage were constrained under a uniform prior with 13 Ma as lower boundary for their respective stem nodes, and the Dictyotales were constrained under a uniform prior with 13 Ma as lower boundary for their crown node. (For interpretation of the references to color in this figure legend, the reader is referred to the web version of this article.)

Silberfeld et al., 2010, Mol Phyl Evol 56: 659-674.

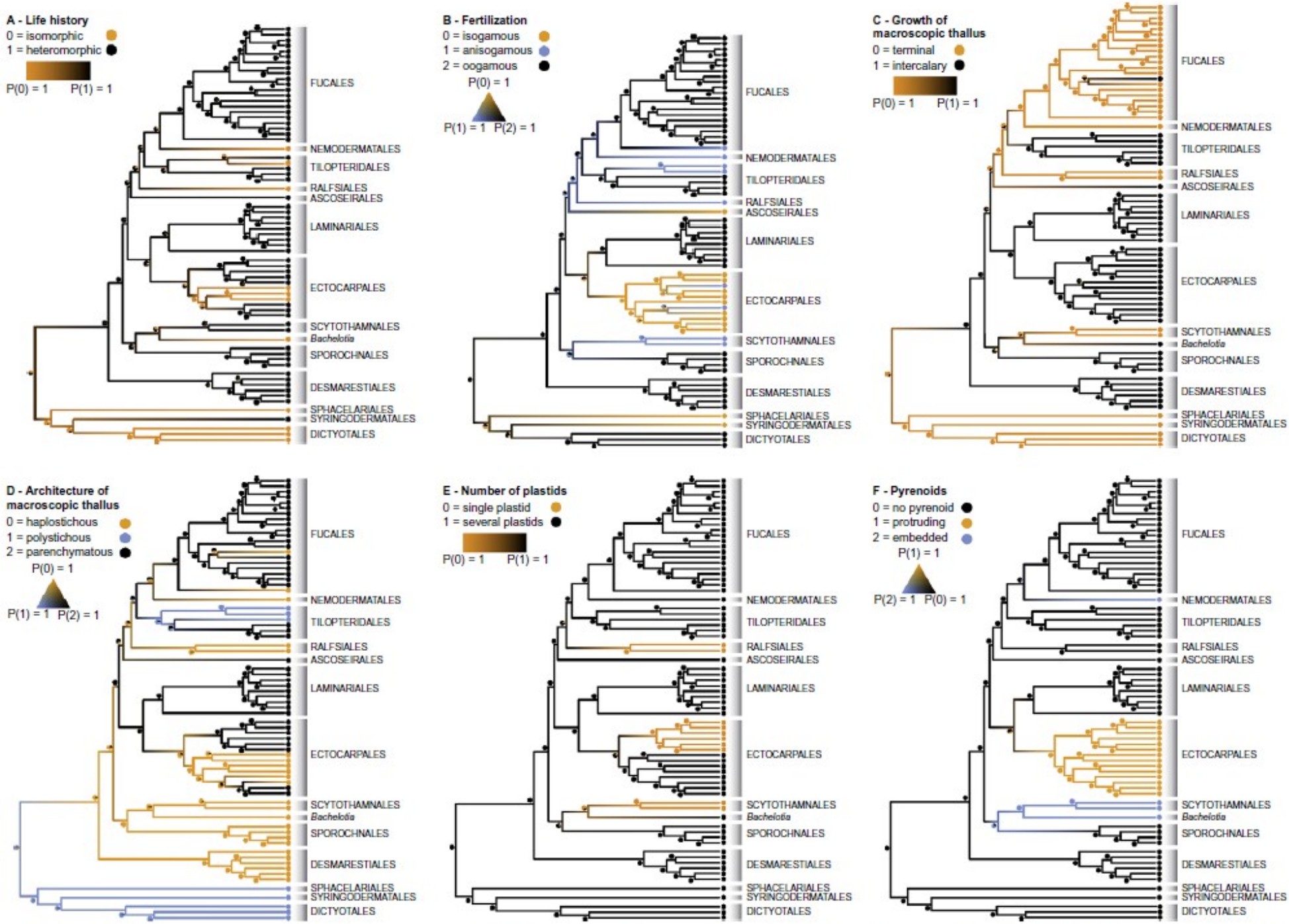

Fig. 4. Results of the ML-based ancestral character state estimation for six non-molecular characters on the chronogram topology of the Fig. 2. The six characters, traditionally considered as the most relevant in the field of brown algal systematics, are: A, type of life history; B, type of fertilization; C, growth of macroscopic thallus; D, architecture of macroscopic thallus; E, number of plastids; F, occurrence and structure of pyrenoid. The ML procedure provides a probabilistic assessment of the ancestral states; these probabilities are reflected in branch colors and pie diagrams at nodes. Each character state has been assigned a color and intermediate colors indicate uncertainty about the character state. For details, see the color caption associated with each tree.

Silberfeld et al., 2010, Mol Phyl Evol 56: 659-674.

DISCOSPORANGIOPHYCIDAE
Discosporangiales

ISHIGEOPHYCIDAE
Ishigeales

DICTYOTOPHYCIDAE
Dictyotales *
Onslowiales
Sphacelariales *
Syringodermatales

FUCOPHYCIDAE
Ascoseirales
Asterocladales
Desmarestiales *
Ectocarpales **
Fucales **
Laminariales **
Nemodermatales
Phaeosiphoniellales
Ralfsiales
Scytothamnales
Sporochnales
Tilopteridales *

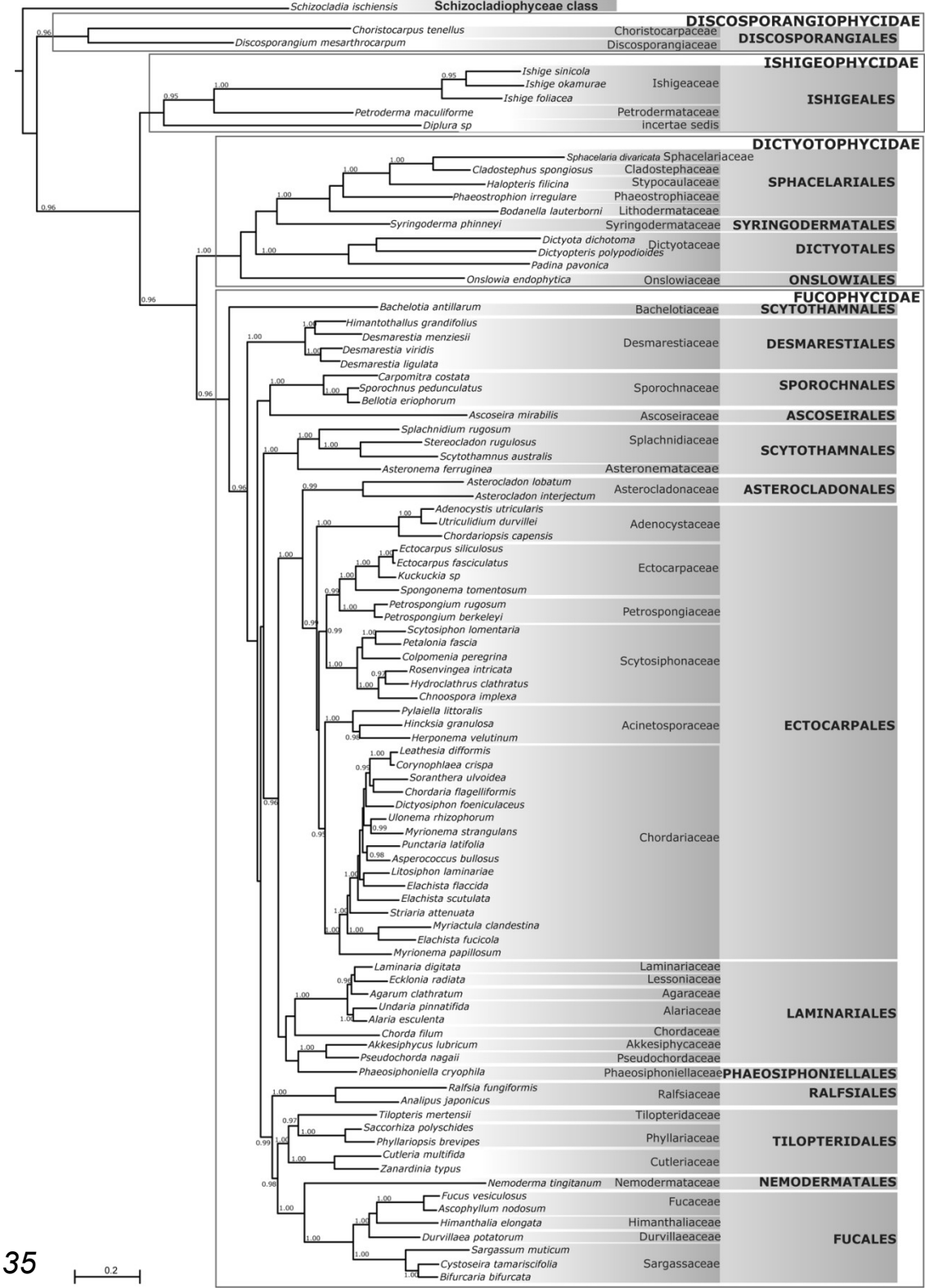

Silberfeld et al., 2014, Crypt. Algol. 35

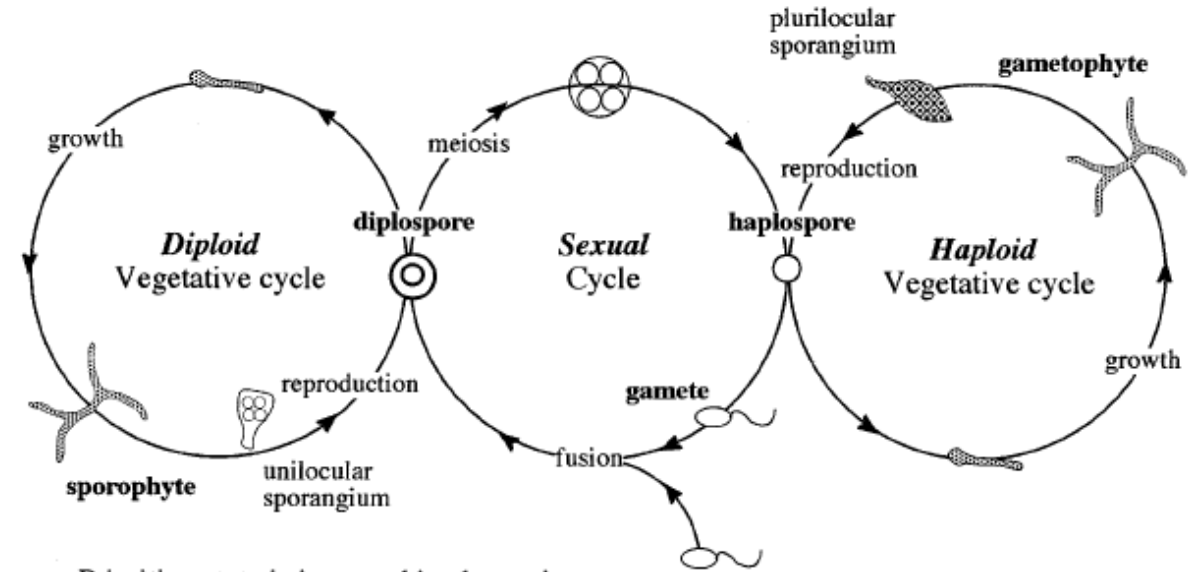

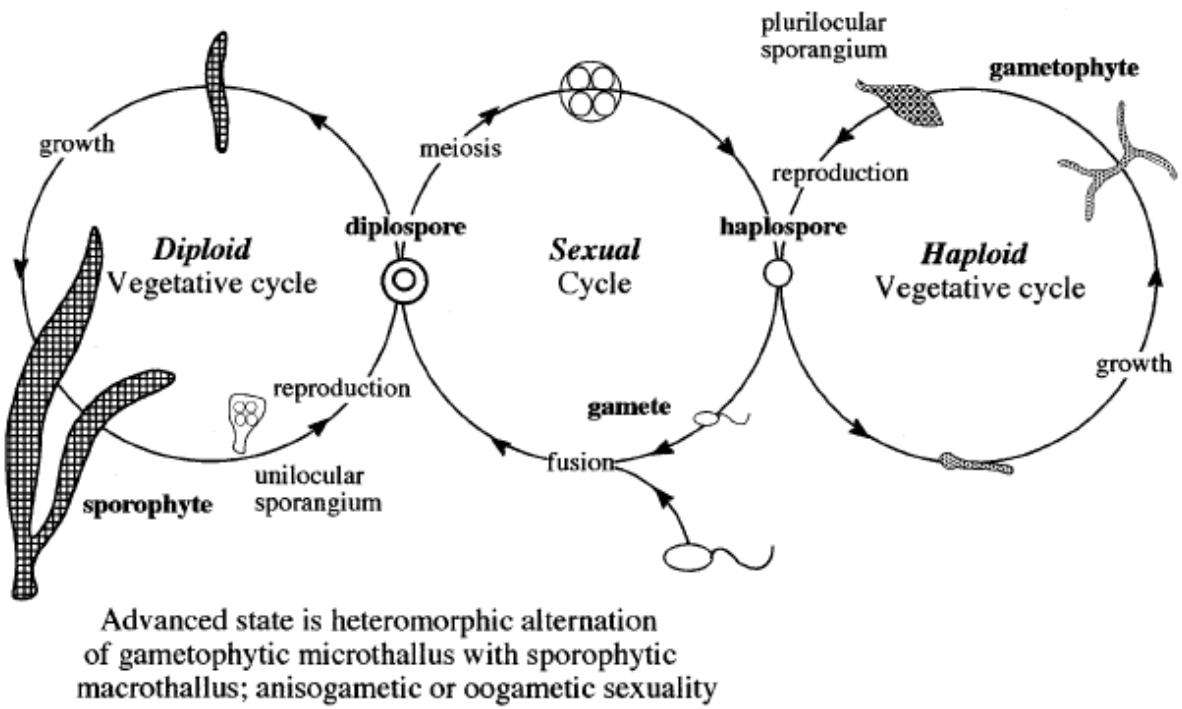

Figure 1. The classical interpretation of the sexual life cycle in Phaeophyta. This way of representing the life cycle, as a series of linked cycles, was introduced by Bell (1994).

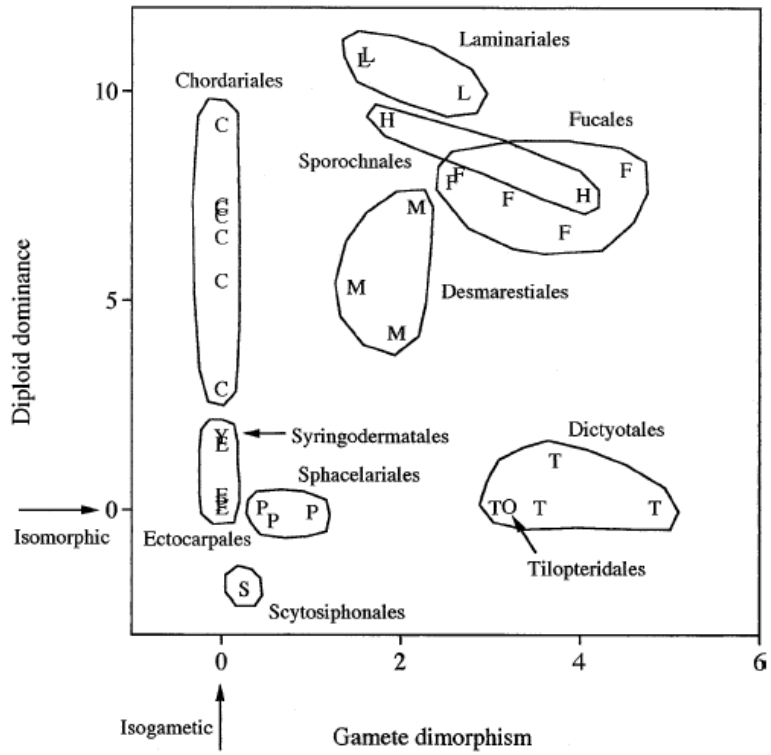

Figure 5. How the balance of haploid and diploid growth varies with the disparity in gamete size. Diploid dominance is expressed as log (diploid size/haploid size), and gamete dimorphism as log (macrogamete size/microgamete size).

the traditional view of the life cycle evolution in Phaeophyceae

Bell, 1997, Biol. J. Linn. Soc. 60

Time calibration of phaeophycean phylogenetic history

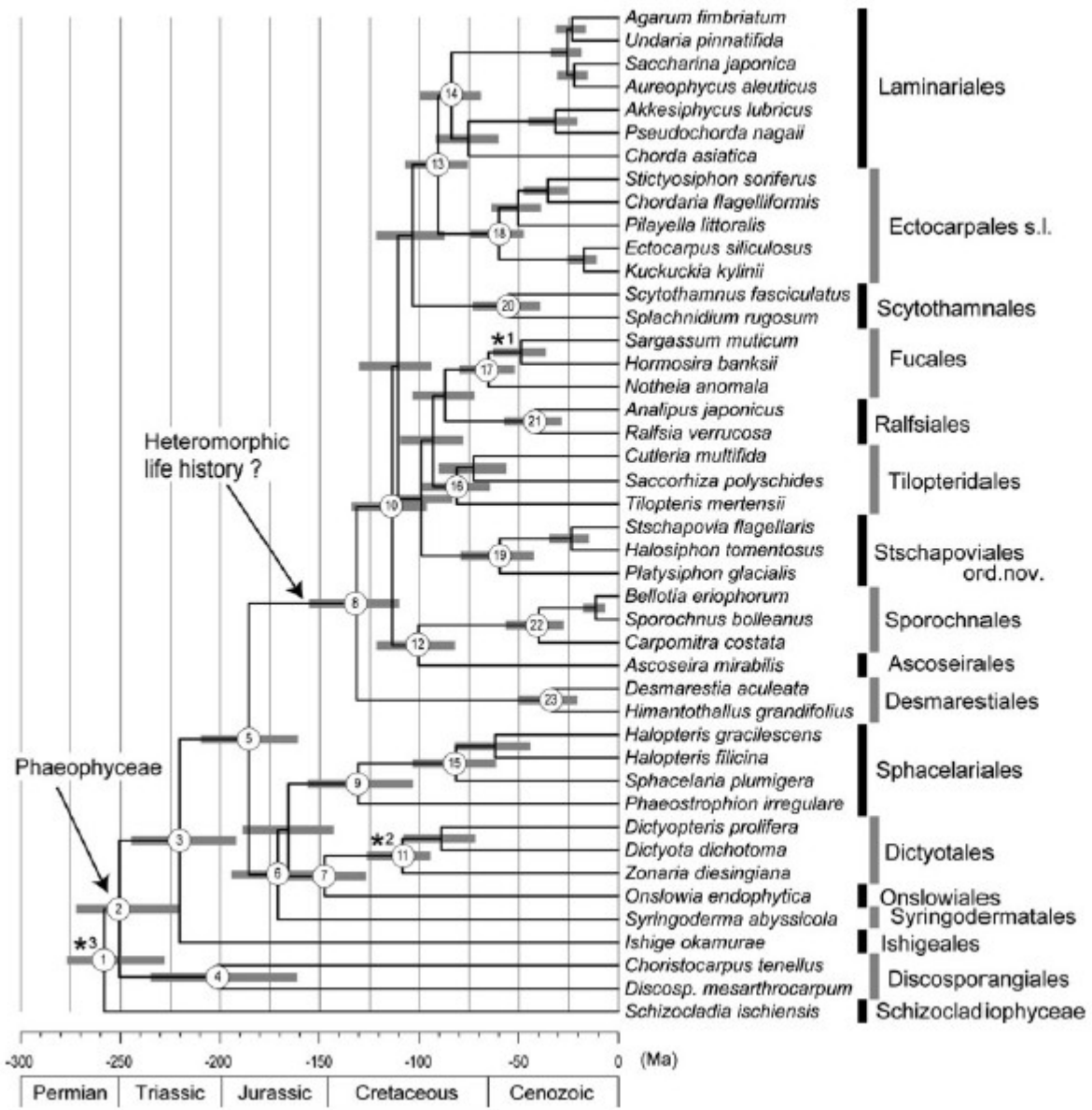

FIG. 3. Time tree derived from relaxed molecular clock method implemented in MCMCTREE in PAML 4.7 (Yang 2007). Horizontal bars indicate 95% credible intervals of divergence time estimates. Asterisks on nodes correspond to calibration points. Asterisks 1 and 2 indicate calibration points with fossils (Parker and Dawson 1965 and Rajanikanth 1989, respectively), and minimum time constraints used for nodes were 13 and 99.6 Ma, respectively. Asterisk 3 shows calibration point based on previous molecular clock study (Brown and Sorhannus 2010), and maximum (267 Ma) and minimum (124 Ma) time constraints used on node. Estimated ages and their 95% credible intervals are listed in Table 2 with node numbers.

[phaeophyceans have very poor fossil record (only from upper Miocene)]

Kawai et al., 2015, J. Phycol.

Discosporangium
(**Discosporangiales**)

- uniserial epiphytic filaments, up to 4 cm
- apical growth (thus, formerly classified in Sphacelariales)
- numerous discoid plastids
- plurilocular zoidangia form single-layered plate of locules

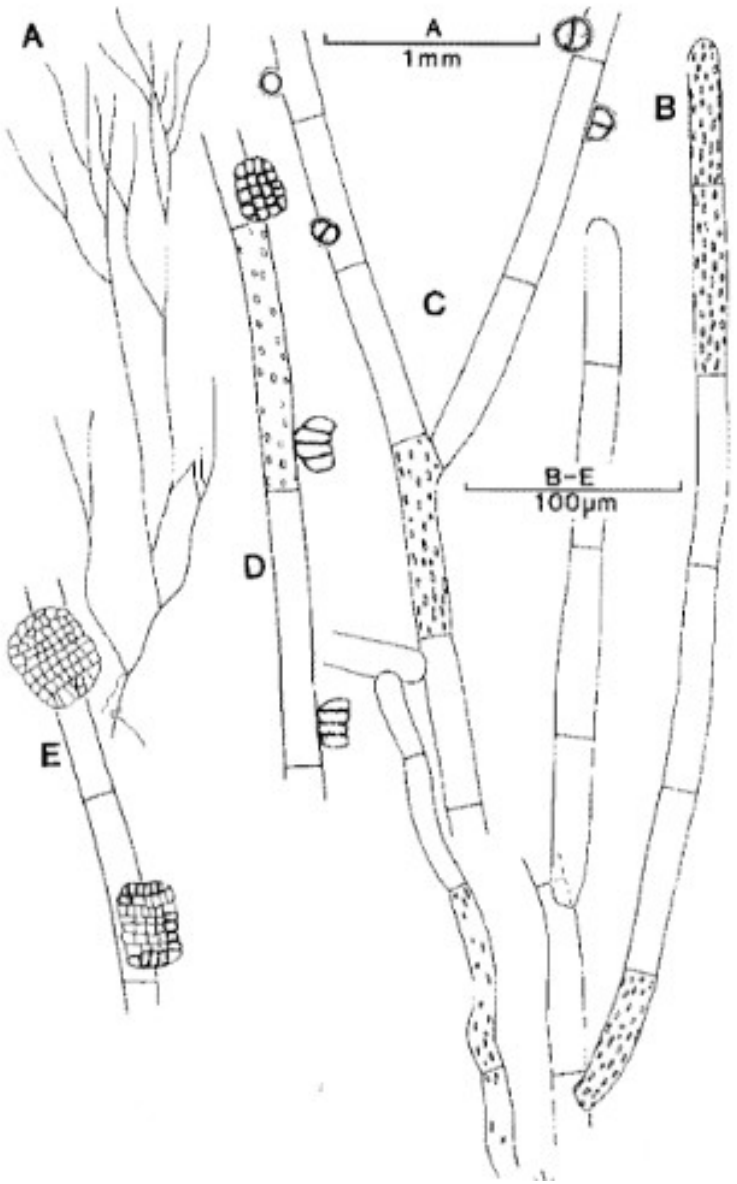

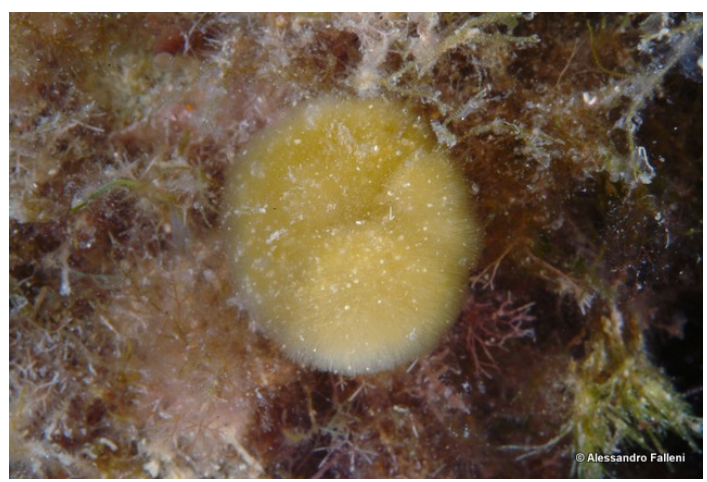

subtropics, tropics (Mediterranean, Australia)

Ishige okamurae

(**Ishigeales**)

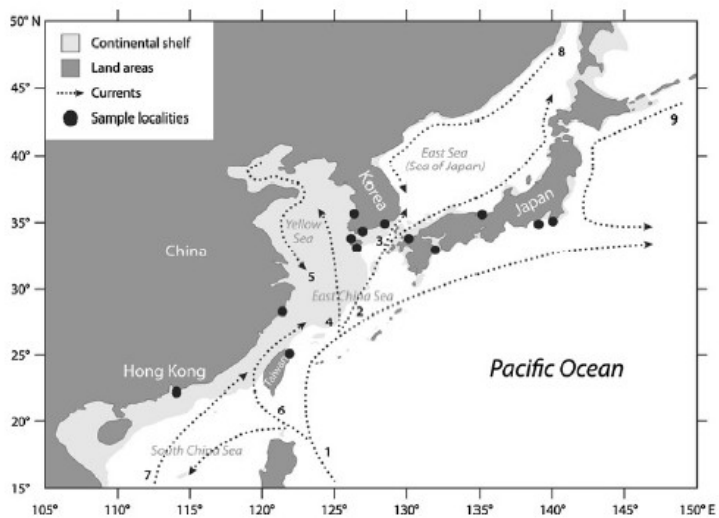

Fig. 1 Map of the study area depicting the sample locations and schematic map of currents (Liu et al. 2007). *Shaded sea* areas are continental shelves that would have been dry during period of low sea level. *1* Kuroshio Current, *2* Tsushima Current, *3* East Korea Warm Current, *4* Yellow Sea Warm Current, *5* China Coastal Current, *6* Taiwan Warm Current, *7* South China Sea Warm Current, *8* Liman Current, *9* Oyashio Current

- irregular dichotomous branching
- thalli up to 20 cm
- unilocular and plurilocular sporangia
- presumably isomorphic life cycle

occurs in temperate and subtropical W Pacific

Lee et al., 2012, Mar. Biol.

Diversity centers of *I. okamurae* in N Taiwan and S Korea (glacial refugia)

Fig. 3 Geographical distribution of *Ishige okamurae* haplotypes. *Shaded areas* in light *gray* color are continental shelves that would have been covered by ice sheet during the Pleistocene glaciation. Letters correspond to the code in Table 1

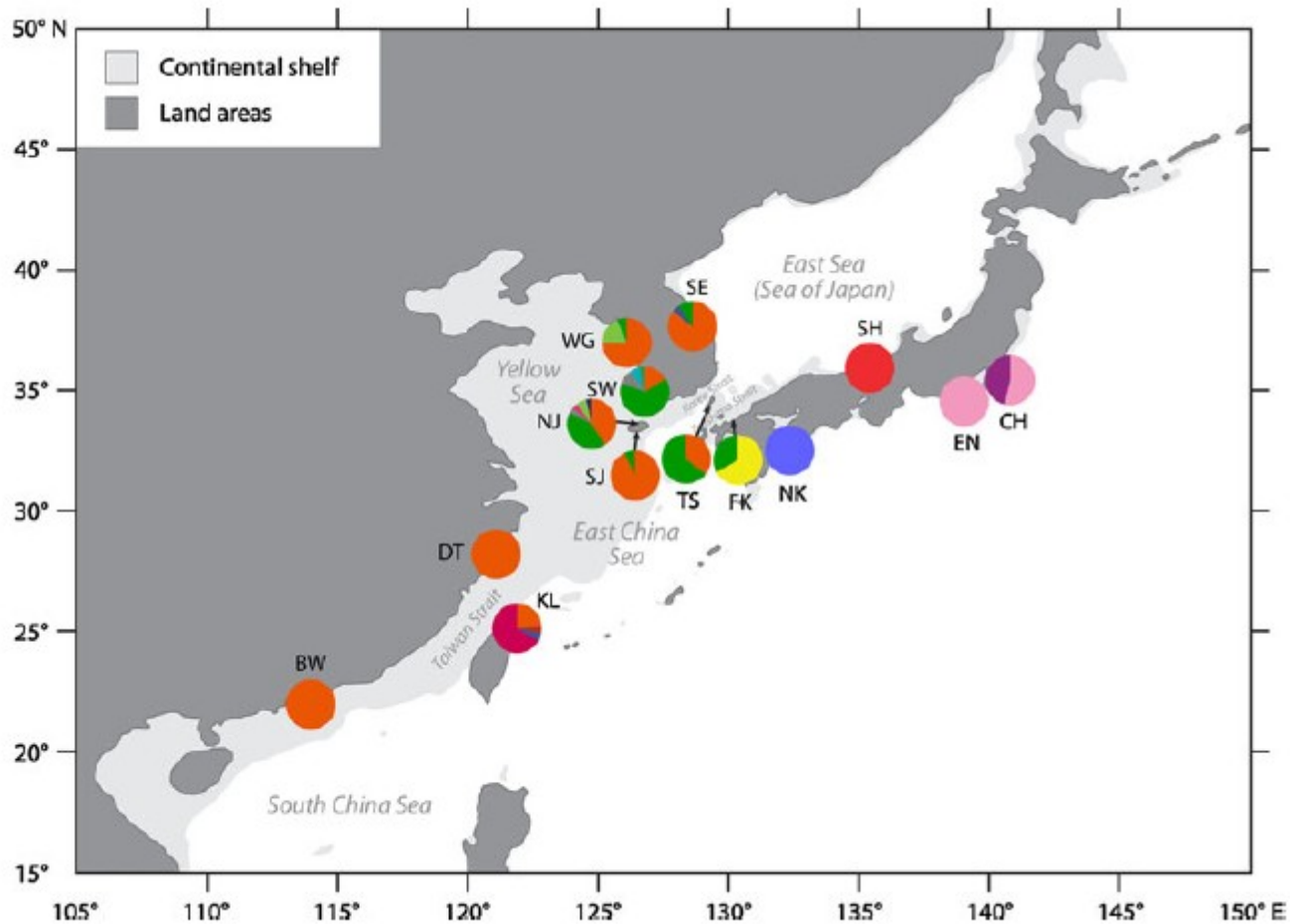

Lee et al., 2012, Mar. Biol.

Petroderma maculiforme (Ishigeales)

- lichen photobiont – *Verrucaria tavaresiae* as a mycobiont

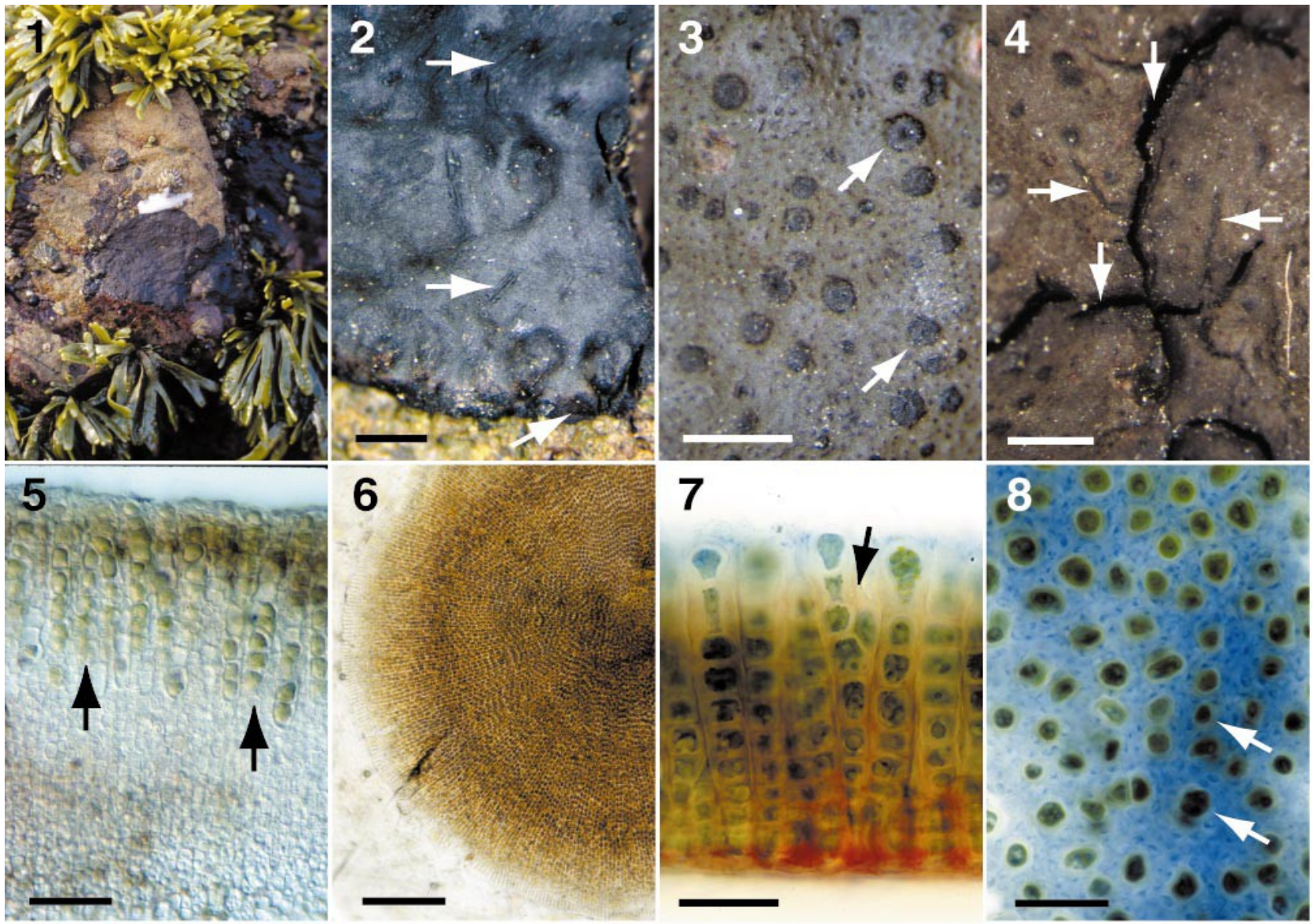

occurs in supralittoral / eulittoral of temperate and boreal seas (incl. European coasts – Baltic, North Sea, Atlantic)
two other species in subtropics/tropics

Dictyotales

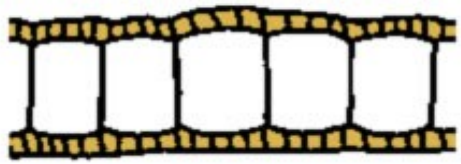

- typically fan-shaped, parenchymatic thallus (2-3 layers of cells)
- diplohaplontic cell cycle, isomorphic, always oogamy

Dictyotales

Dictyota dichotoma

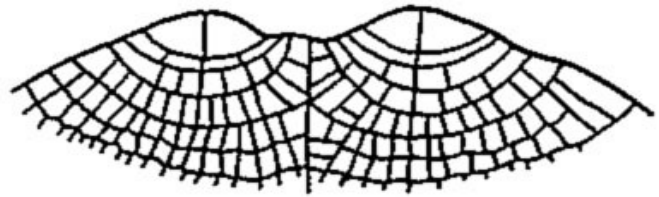

- true dichotomy, growth by division of apical cell
- temperate, cosmopolitan species

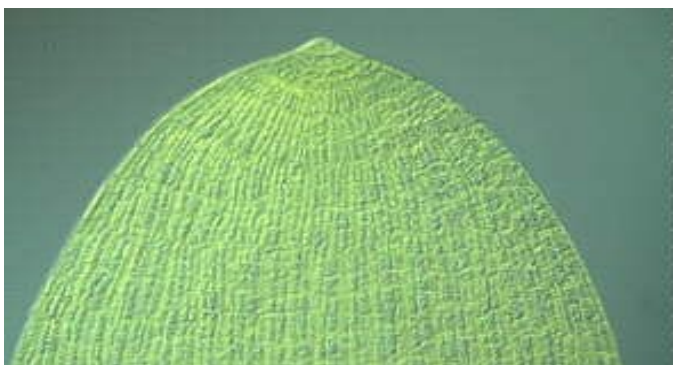

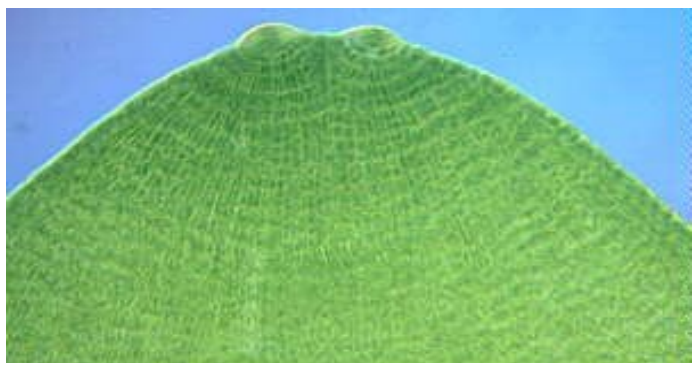

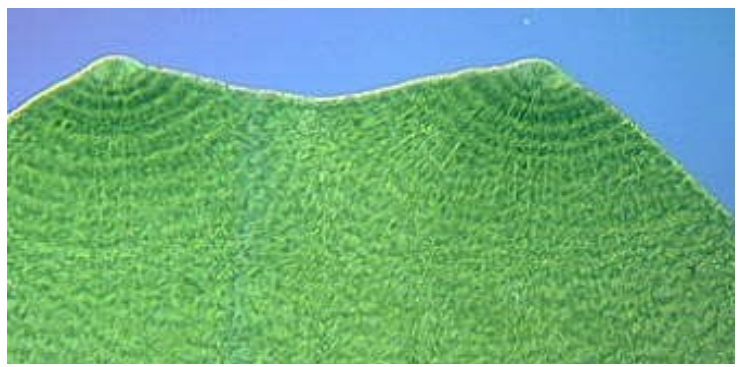

♀ gametophyte

♂ gametophyte

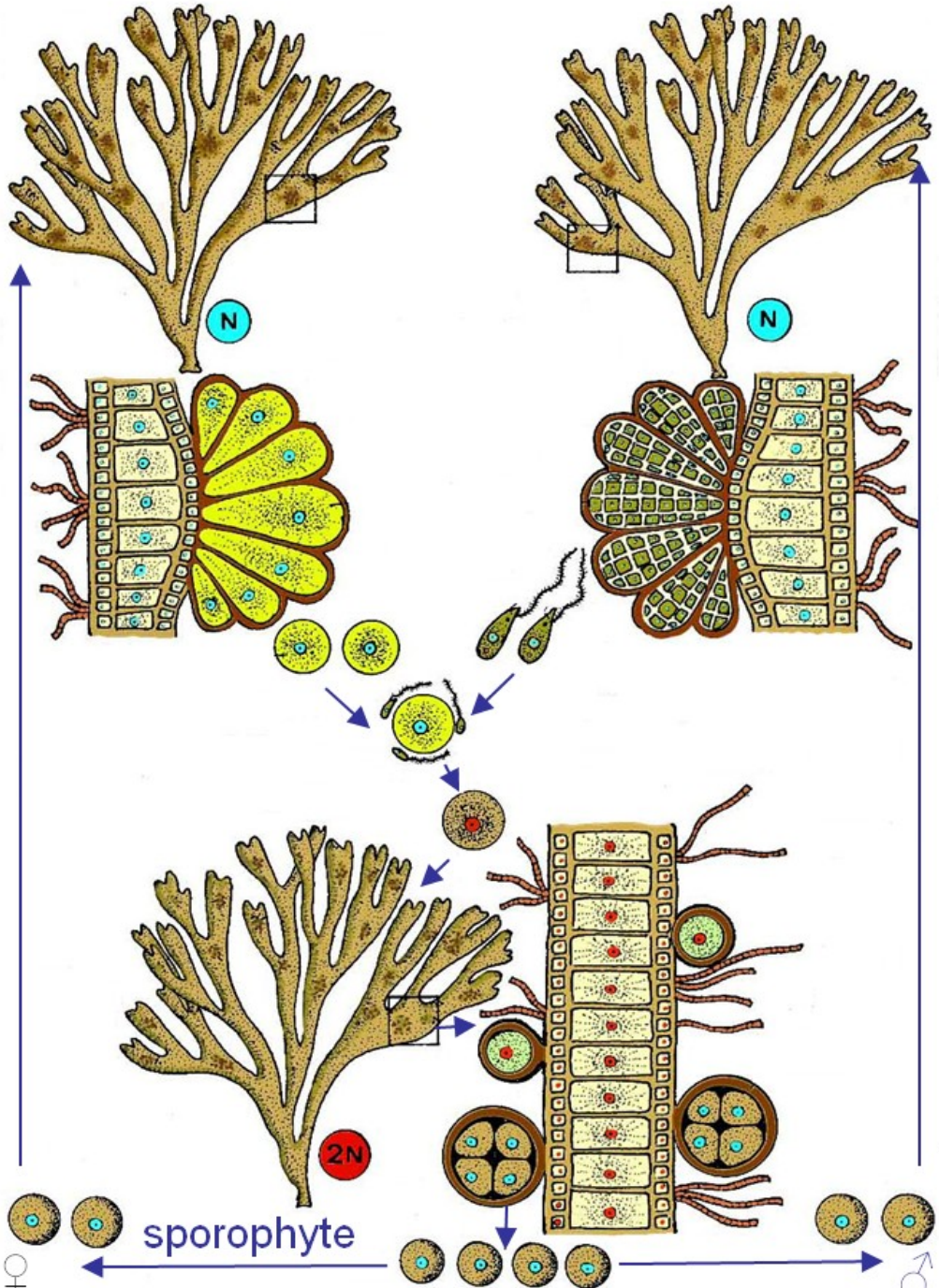

dark brown
sorus – oogonia
(unilocular gametangia)

light brown
sorus – antheridia
(plurilocular gametangia)

unilocular
sporangia

= tetrasporangia

Dictyota

Dictyota bartayresiana

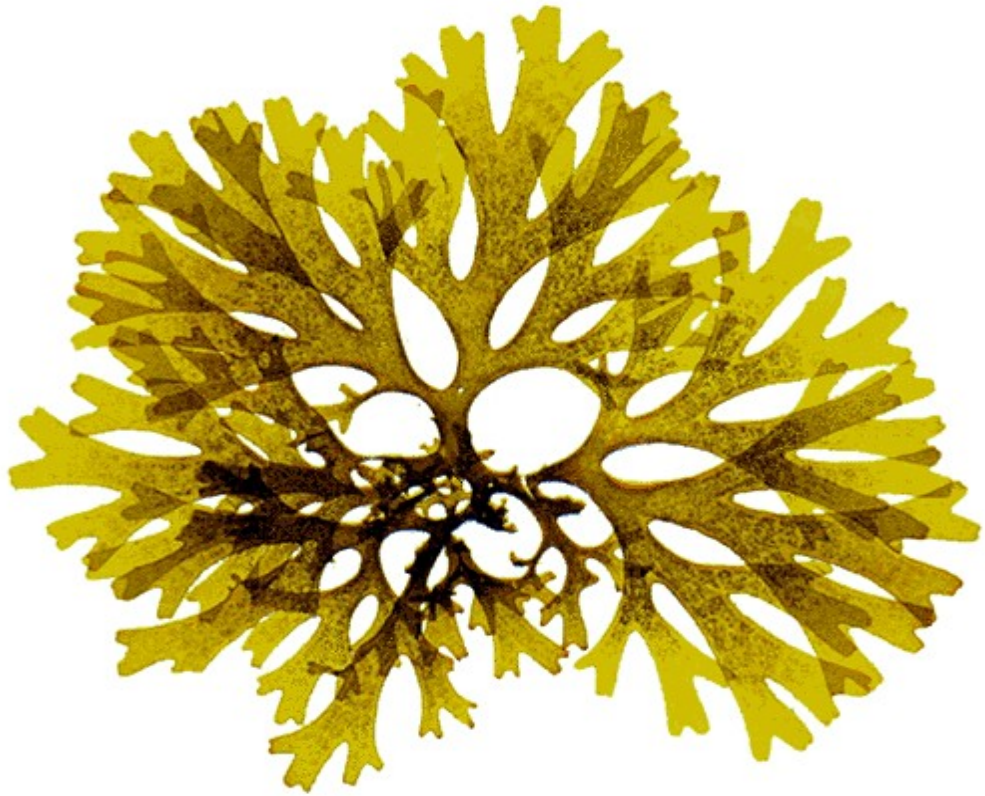

Dictyota dichotoma

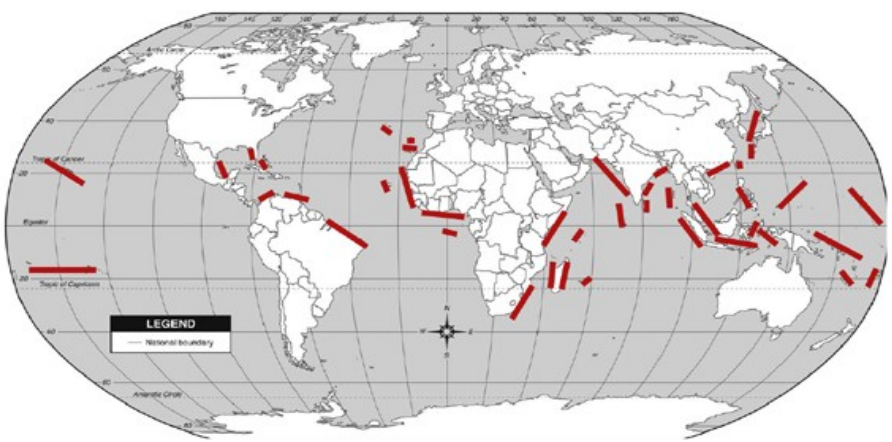

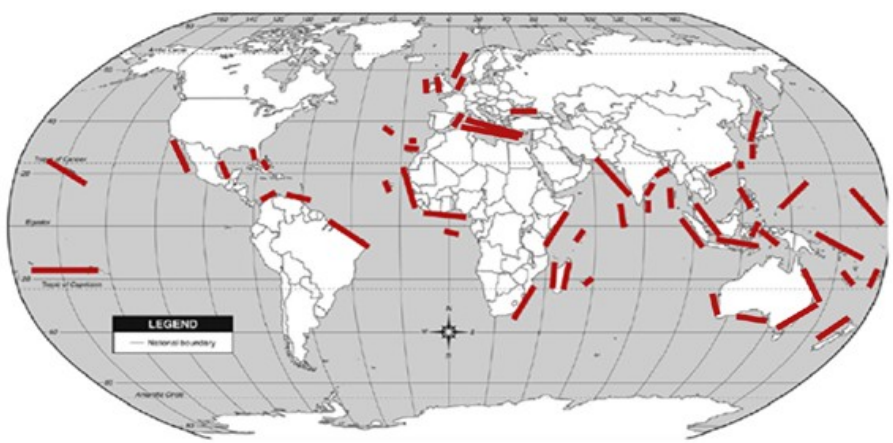

Dictyota

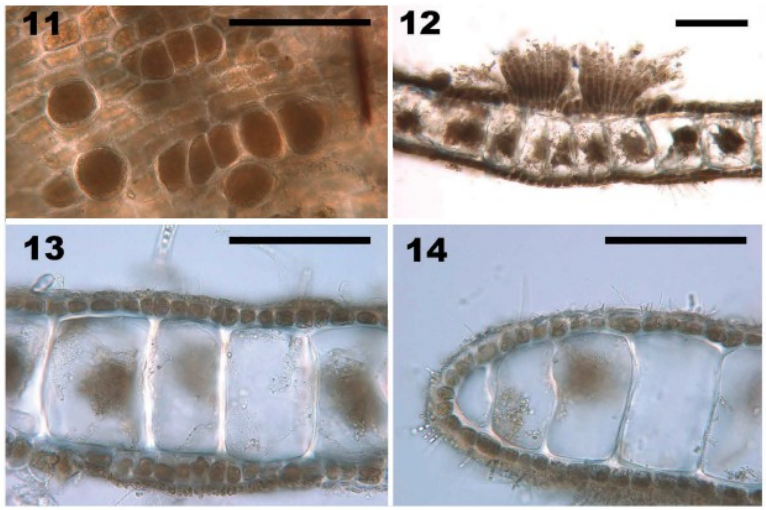

Figs 7–14. Herbarium specimens and micrographs of *Dictyota falklandica sp. nov.*
Fig. 7. Isotype (PC accession no. 0776066). Scale bar = 5 cm.
Fig. 8. Surface view, with walls of larger medullar cells indicated by black lines. Scale bar = 50 µm.
Fig. 9. Holotype specimen (BM accession no. BM013828094). Scale bar = 5 cm.
Fig. 10. Apical region of branching thallus, with actively growing apical cells (asterisks) as well as marginal dormant apical cells (arrowheads). Scale bar = 1 mm.
Fig. 11. Spores on thallus surface in irregular longitudinal groups. Scale bar = 50 µm.
Fig. 12. Cross section of thallus with two hair tufts. Scale bar = 100 µm.
Fig. 13. Cross section of central blade area. Scale bar = 100 µm.
Fig. 14. Cross section of blade margin. Scale bar = 100 µm.

Fig. 5 Fortnightly release periodicity of *Dictyota dichotoma* sporophytes (*grey bars*) using gametophytes as a control (*black bars*) near l'Ancient Fort Croix (Wimereux, France). The histogram shows the percentage of total release of eggs (*black*) and spores (*grey*) for the hatched part of the lunar cycle (*error bars* denote standard errors). Approximate positions of spring and neap tides in Wimereux are marked on the lunar cycle with *arrowheads*. *Black circle* new moon, *half darkened circle* second quarter, *white circle* full moon

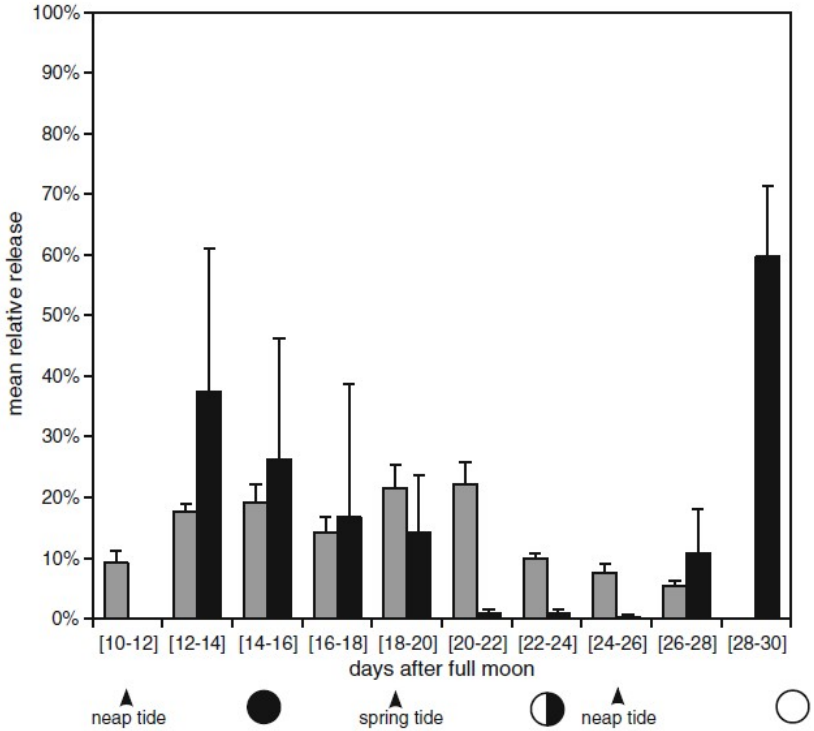

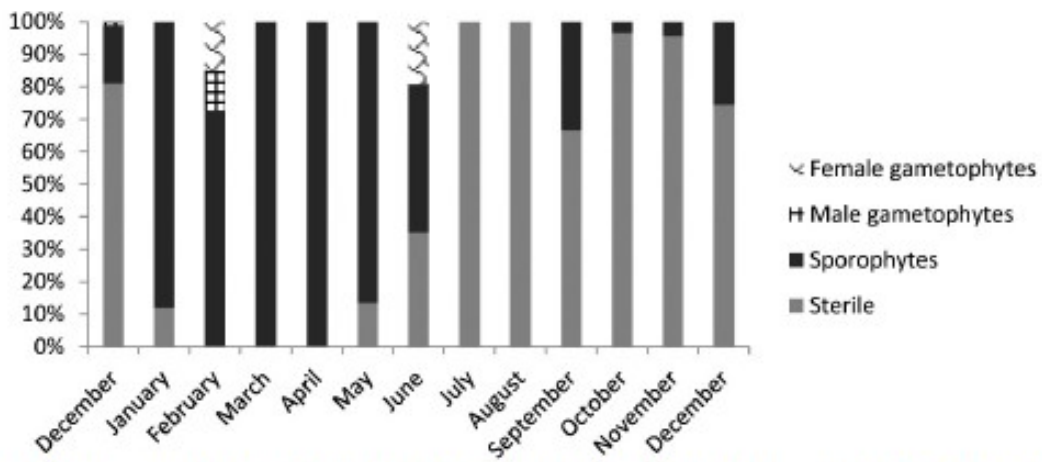

Fig. 4: Percentage of female gametophytes (patron), male gametophytes (squares), sporophytes (black colour) and sterile individuals (grey colour) of *Dictyota cyanoloma* per month.

structure, seasonal cycles, phenology

Bogaert et al., 2016, J. Appl. Phycol. 28
Aragay et al., 2016, Med. Mar. Sci.
Küpper et al., 2019, Phycologia

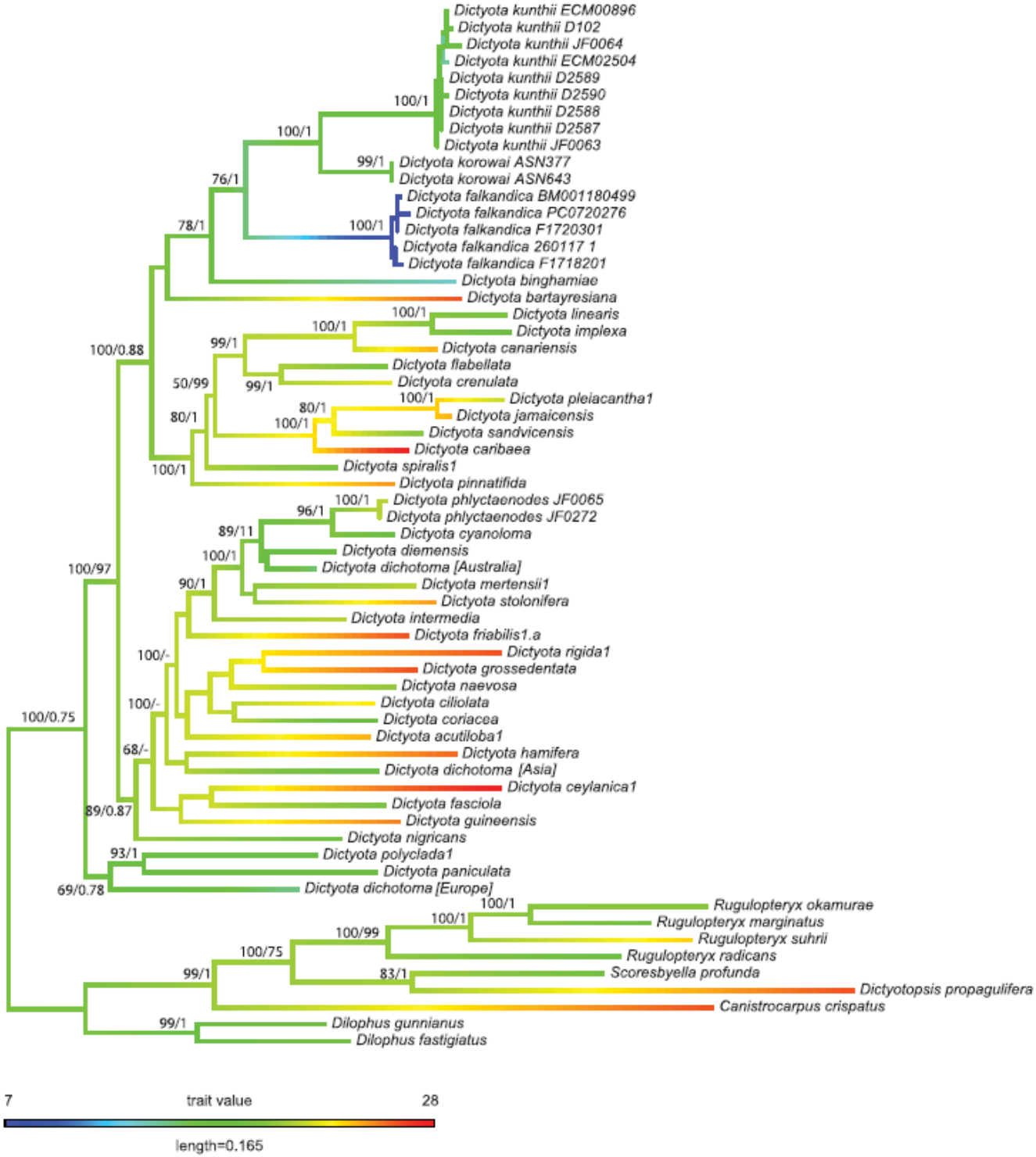

Fig. 6. Maximum-likelihood tree of the concatenated alignment (-Ln = 45270.45) with rapid bootstrap (left) and posterior probabilities (right) values shown on branches. Branch colours are the maximum-likelihood estimates of the ancestral states of mean sea surface temperature.

Küpper et al., 2019, Phycologia

Phylogenetic species structure of *Dictyota* in Europe

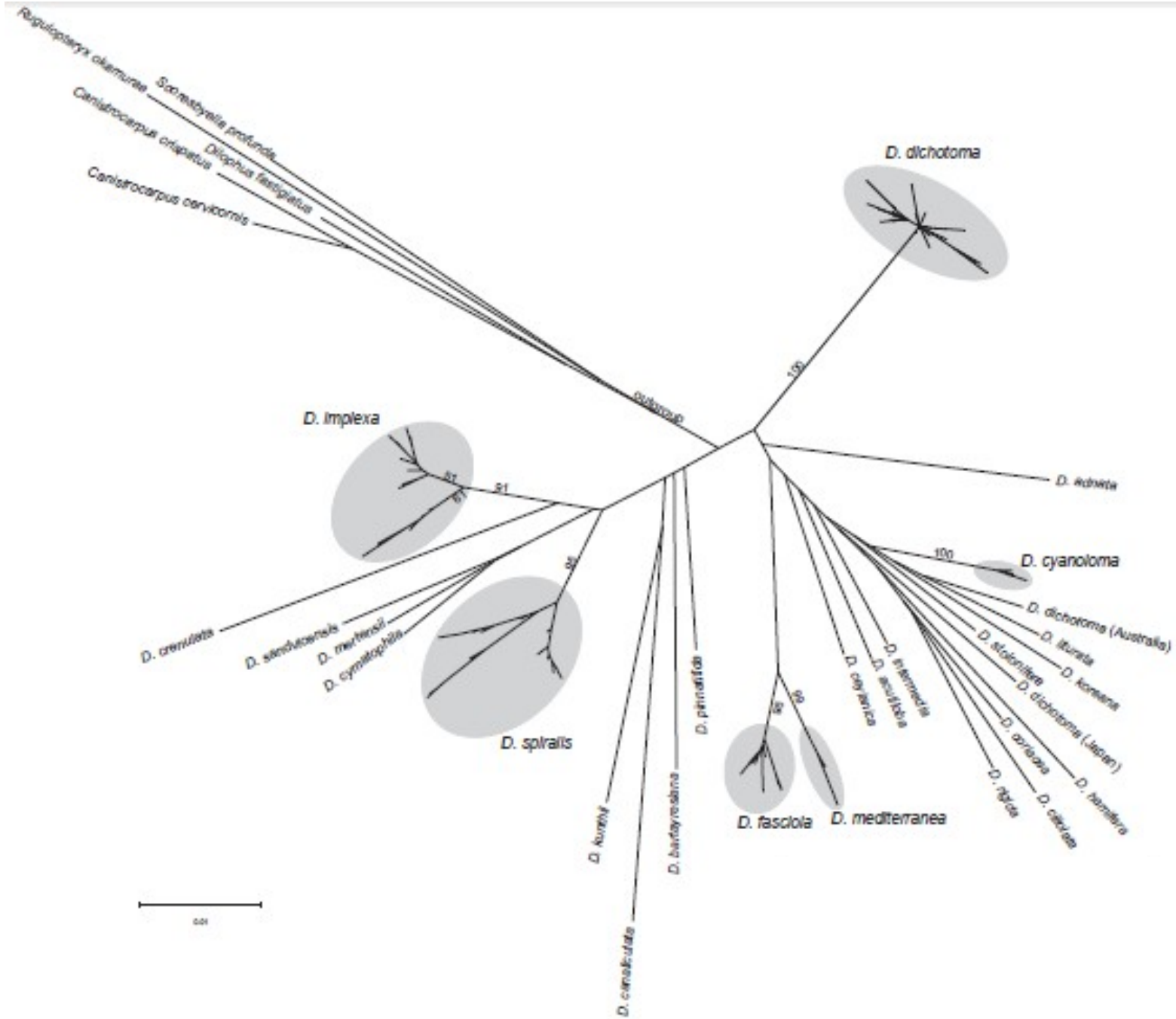

psbA based phylogeny of European species

Tronholm et al., 2010, J Phycol 46: 1301-1321

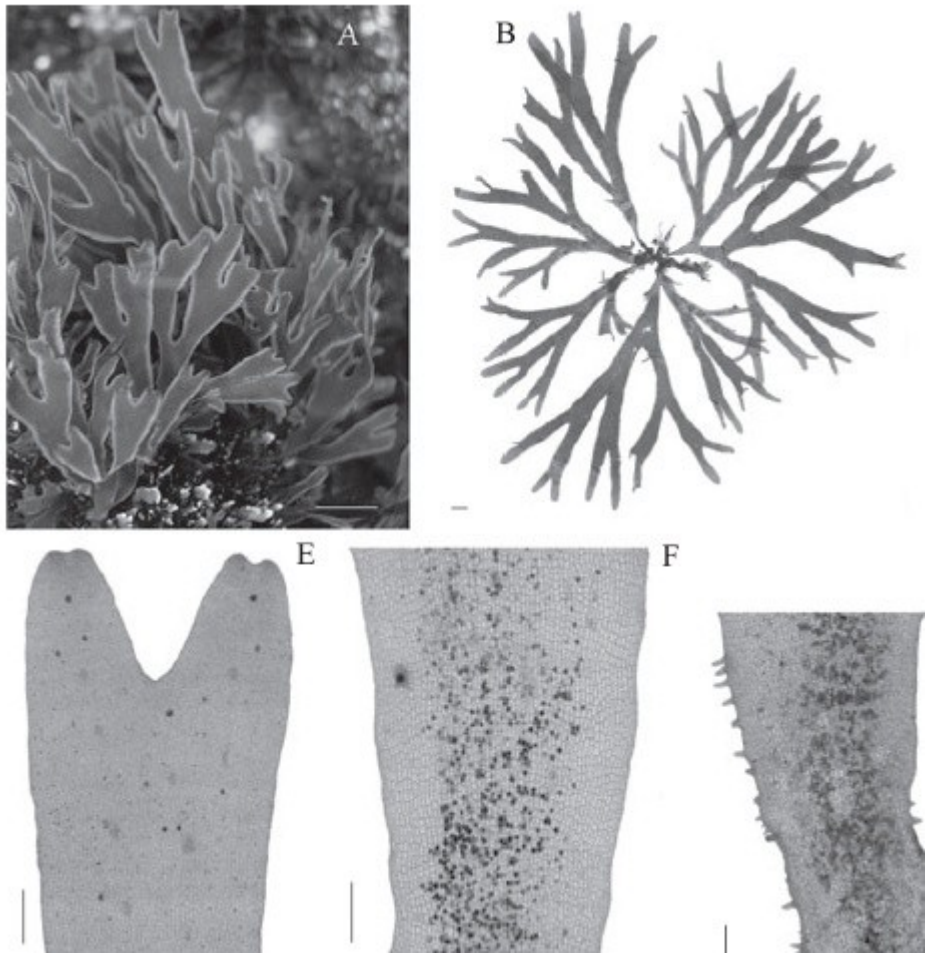

Dictyota cyanoloma

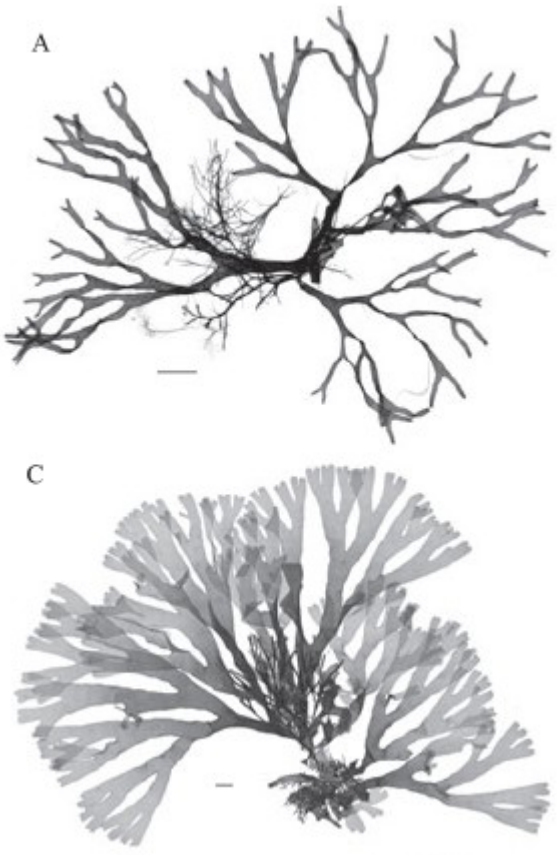

Dictyota dichotoma

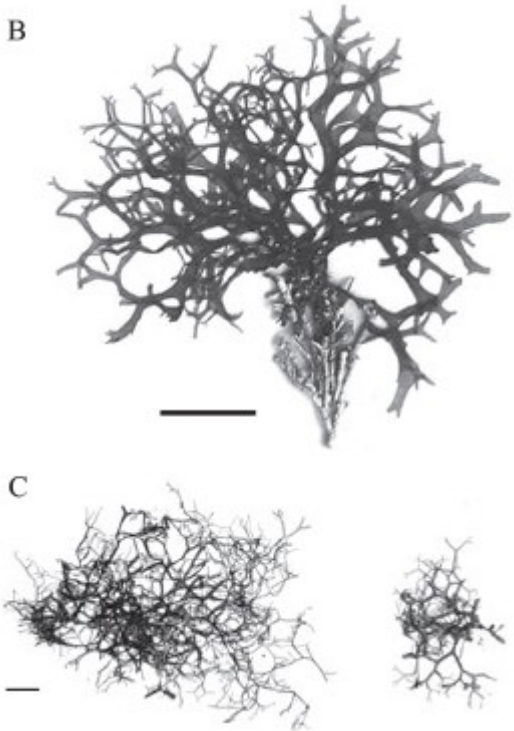

Dictyota implexa

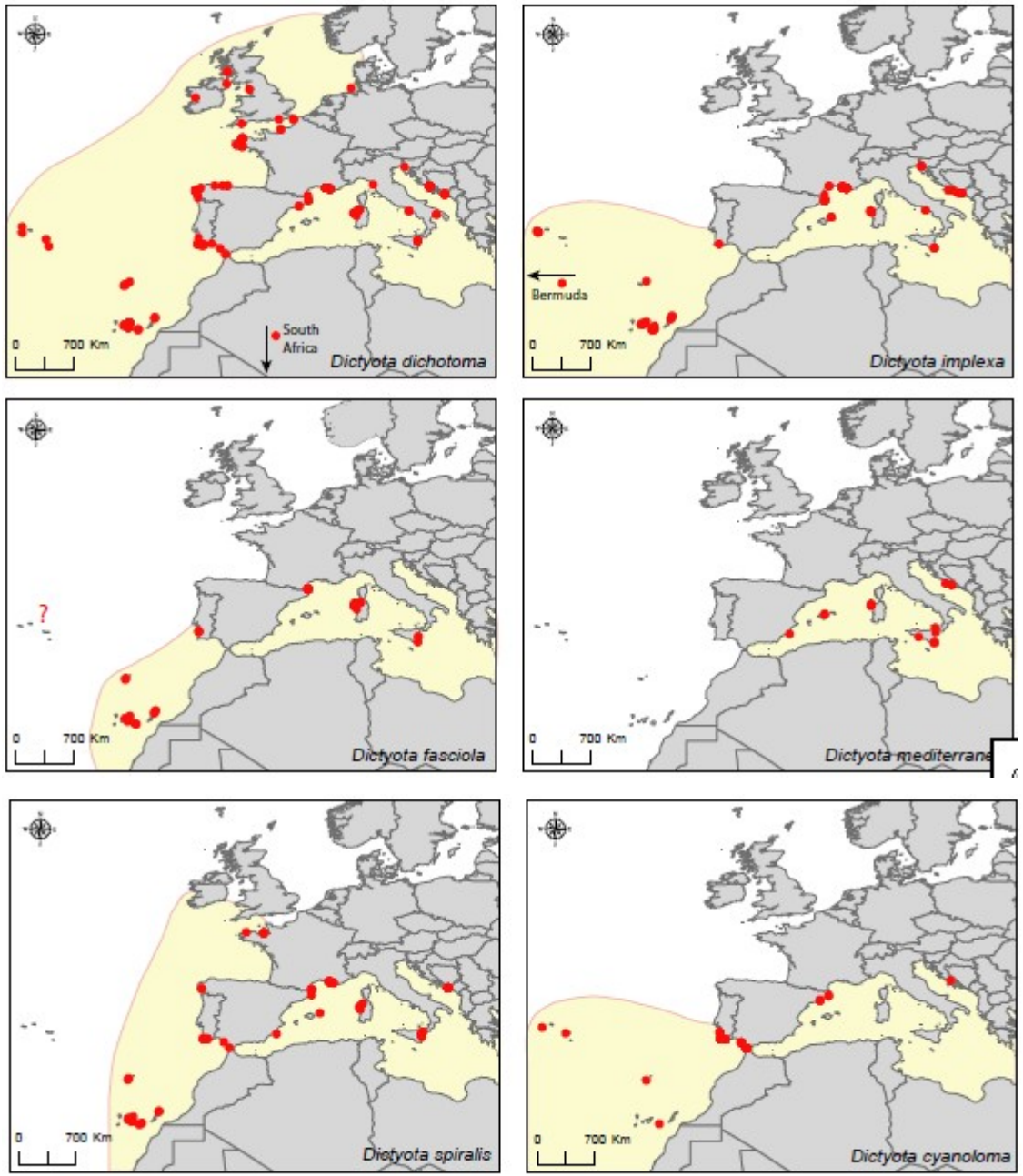

FIG. 2. Distribution maps of European *Dictyota* species. Dots represent DNA-confirmed distribution records; shaded areas indicate the estimated distribution range.

Tronholm et al., 2010, J Phycol 46: 1301-1321

D. cyanoloma
anthropogenically introduced into the Mediterranean

Figs 5 and 6. *Dictyota cyanoloma*. **Fig. 5**. *Dictyota cyanoloma* clearly showing its characteristic blue iridescent margin, photograph taken by Joana Aragay, port of Almeria, 2013. **Fig. 6**. Boat hull fouled by *Dictyota cyanoloma*, photograph taken by Olivier De Clerck at Garachico Bay, Tenerife, 2014.

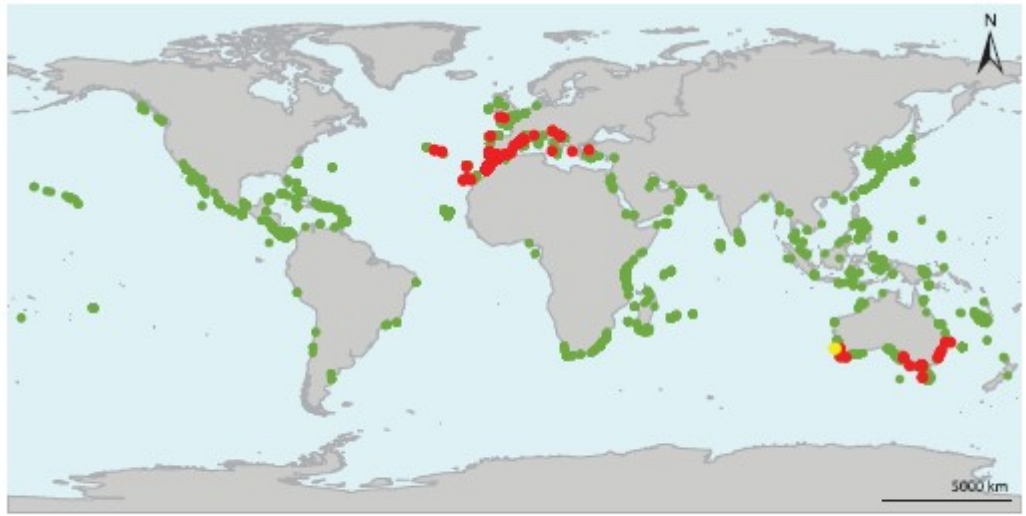

Fig. 2. Distribution map of a global *Dictyota* data set (green) highlighting the occurrences of *D. cyanoloma* (red) and *D.* sp8

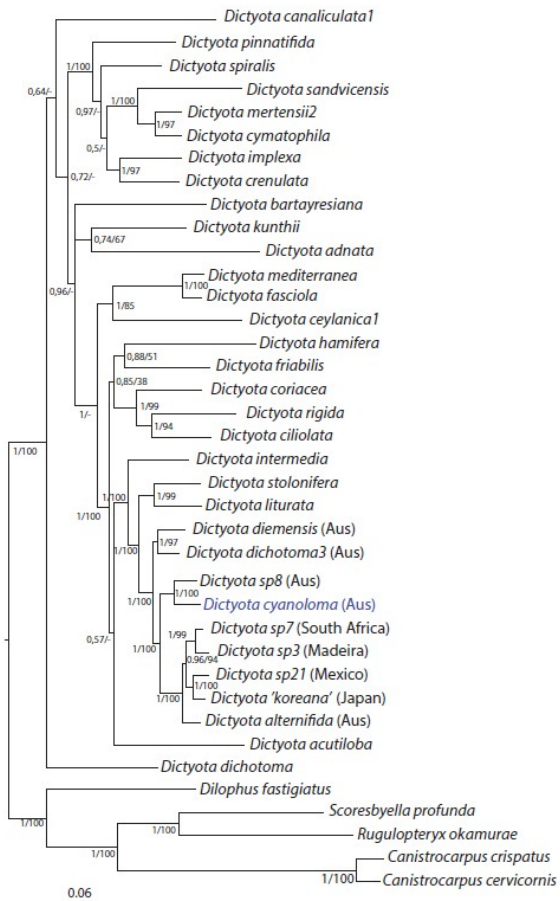

Fig. 1. Phylogenetic tree obtained by ML-inference of a dataset containing six genes (partial LSU rDNA, *rbc*L, *psb*A, *cox*1, *cox*3 and *nad*1). Numbers at the nodes indicate posterior probabilities followed by ML-bootstrap values.

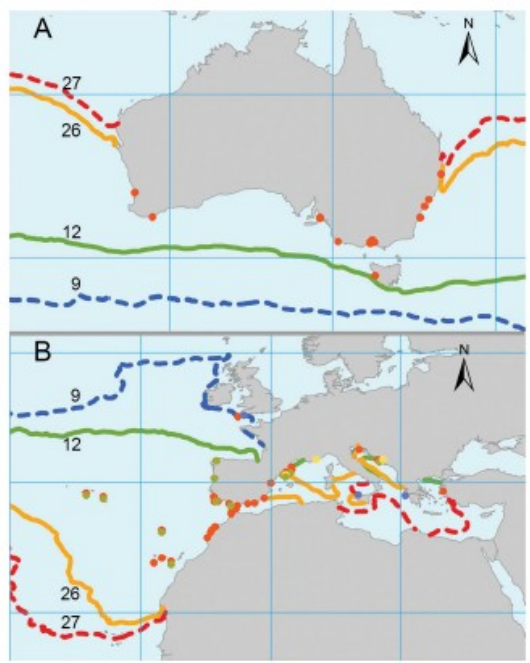

Fig. 3. The sample locations (dots) within the native range (**A**) and the region of introduction (**B**) are reported. The reported isotherms on both maps are the annual mean maximum and minimum sea surface temperatures bordering the distribution range of *Dictyota cyanoloma* within the native region (full lines) contrasted with the annual mean maximum and minimum sea surface temperatures bordering the distribution within the introduced range (dashed lines). A distinction is made between samples from this study (red), earlier published records (green), photographic evidence (blue) and herbarium samples (yellow).

Steen et al., 2017, Eur. J. Phycol.

Dictyopteris

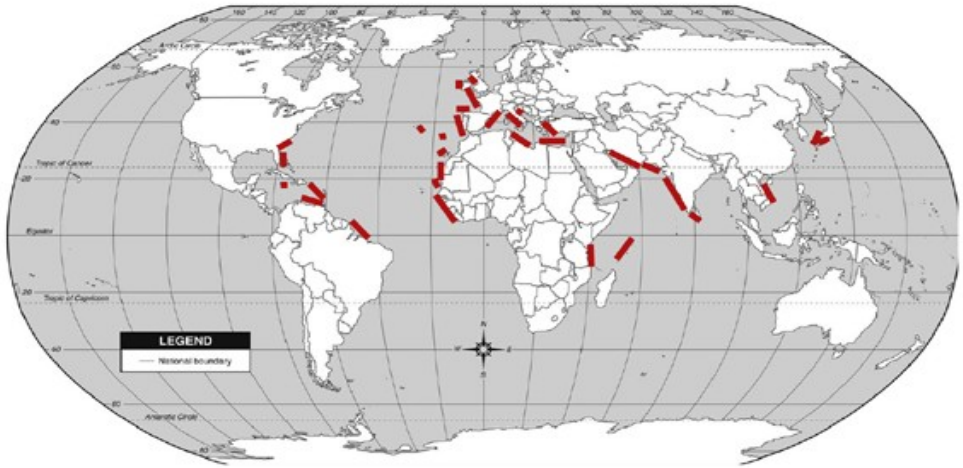

Dictyopteris polypodioides

shade-loving species, mesotrophic, moderately disturbed habitats

Lobophora

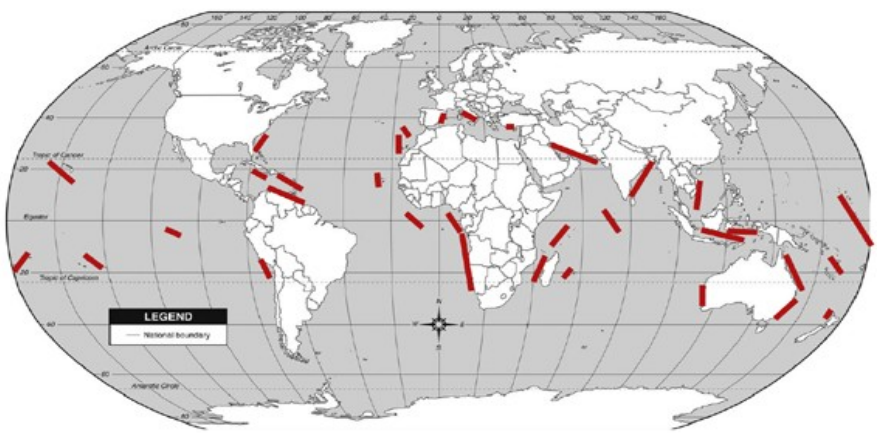

Lobophora variegata

Mediterranean Lobophora – several hemicryptic species (and not L. variegata...)

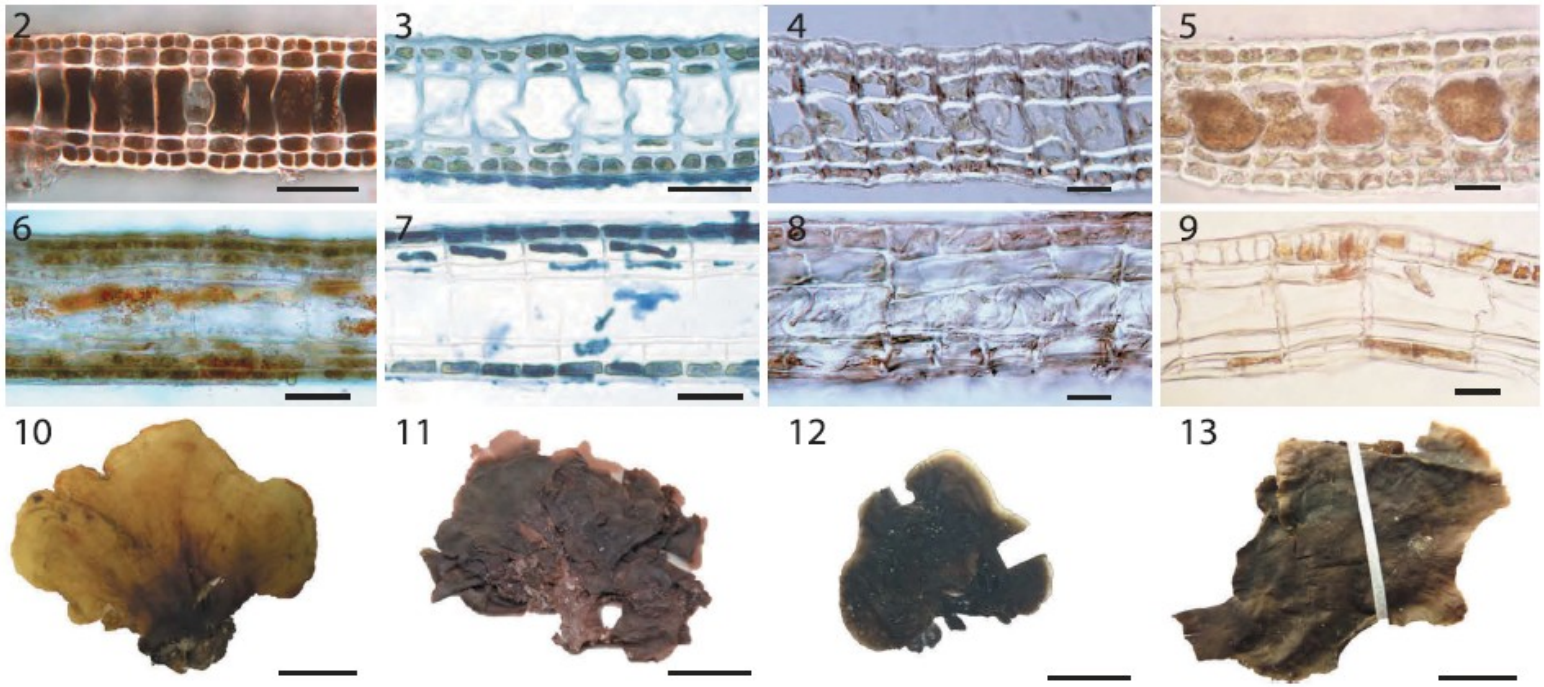

L. schneideri 10-11
L. delicata 12
L. lessepsiana 13

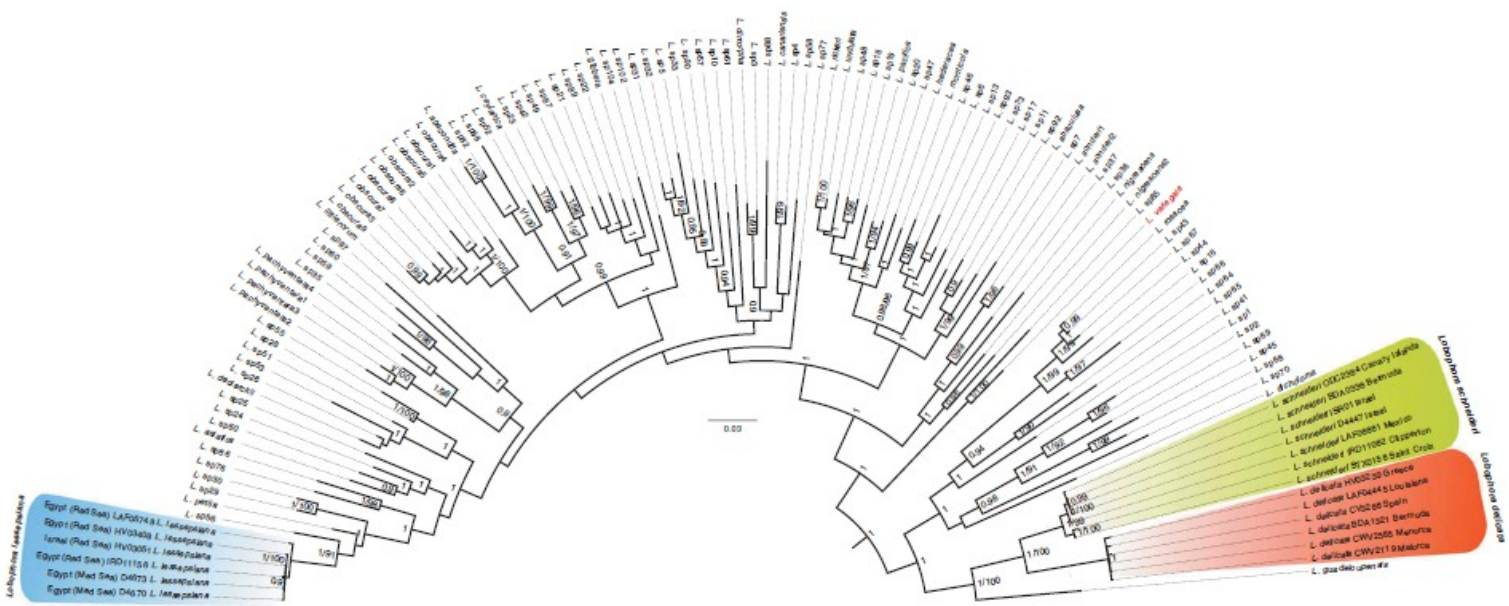

Fig. 1. Bayesian tree of *Lobophora* based on *cox*3. The values shown at each node represent Bayesian posterior probabilities (on the right) and the maximum likelihood bootstrap values (on the left). The asterix indicate *L. variegata*.

Vieira et al., 2019, Phycologia 58

Padina

- fan-shaped, slightly calcified thalli


Palau
Celebes Sea
Malaysia
Indonesia
Makassar
Laut Banda
Papua New Guinea
Timor-Leste
Kupang
Timor Sea
Arafura Sea

Padina – morphology and calcification

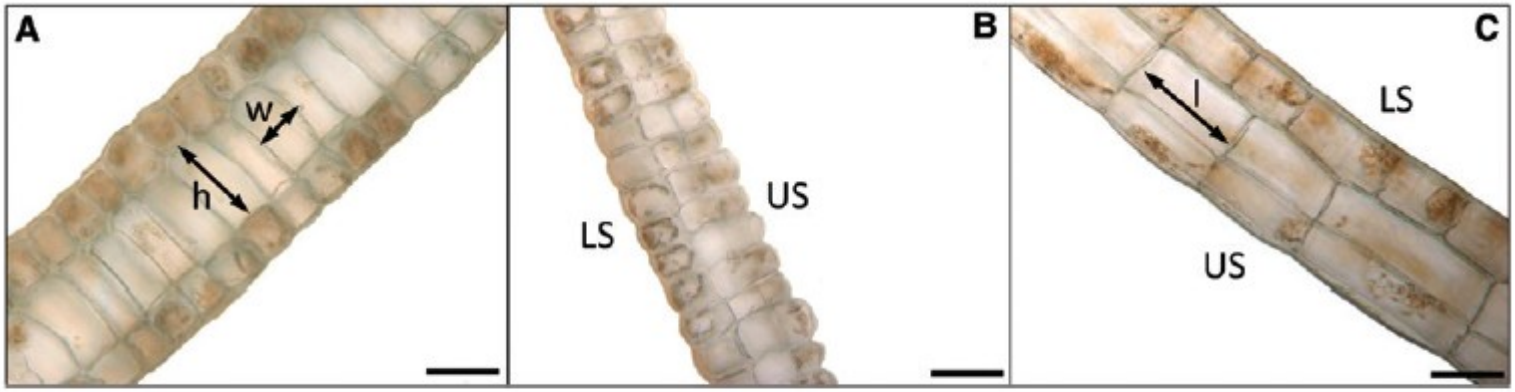

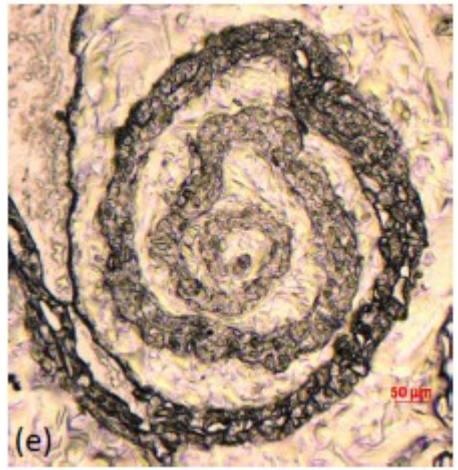

Figure 1: *Padina pavonica* – thin sections of fronds (scale bars: 50 µm) consisting of three cell layers: lower surface (LS), middle, and upper surface (US).
Arrows show the dimensions cell height (h), width (w) and length (l). (A) Transverse section of thallus in spring. Cells of the middle cell layer are visibly larger, containing almost no chloroplasts. LS and US are difficult to distinguish but both show chloroplasts. (B) Transverse section of thallus in autumn. (C) Longitudinal section of thallus in autumn with pigments located in the US cells.

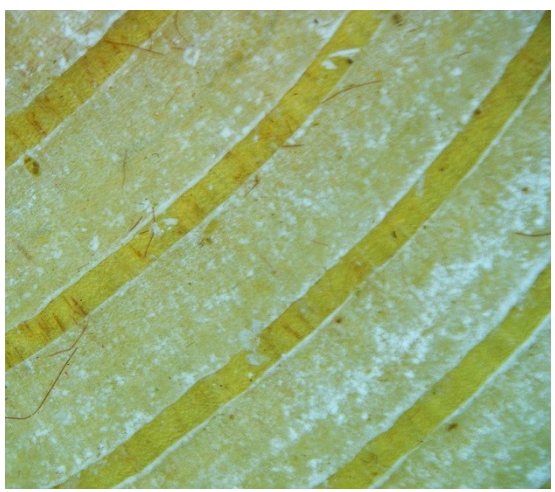

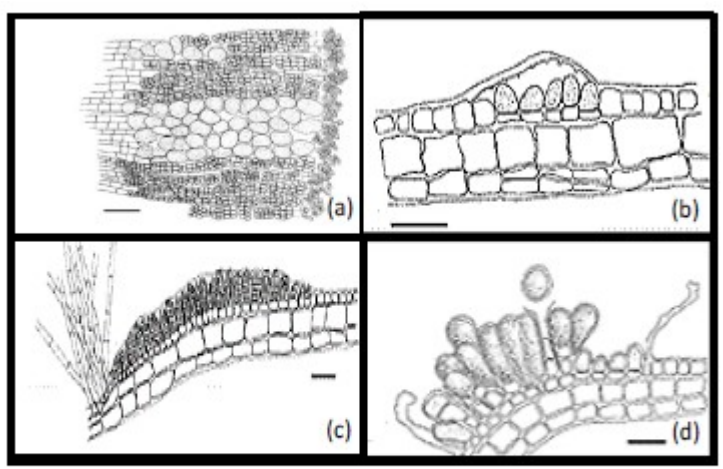

Figure 4. *P. pavonica* reproductive cells. (a) Radial section of monoecious sori; (b) Radial section of the indusium (arrow) over young oogonial sori; (c) Antheridial sori (with basal stalk cells and condensed hair); and (d) The indusium (arrows) torn over mature oogonial sori. Scale bar (a)-(d) 100 µm [27].

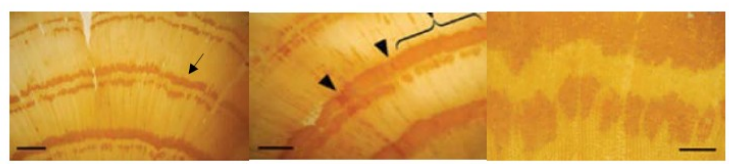

Figure 5. The sorus stripes of *P. pavonica*. (a) Dioecism, female thallus oogonia are arranged as two dark lines (arrow) [27]; (b) Monoecism, Antheridia ({) in between narrow oogonia (arrowheads) [27]. Scale bar (a) and (b), 2 mm; and (c) close-up of the sorus's perpendicular rows. Scale bar 400 µm.

Benita et al., 2018, Am. J. Plant Sci.
Bürger et al., 2017, Bot. Mar.

Global biogeography of Padina

FIG. 1. Species-level diversity and biogeography of *Padina* based on literature reports. (A) Global map with indication of marine realms following Spalding et al. (2007); (B and C) Richness, percentage of endemism (i.e., species only found in a single realm) and species shared across ocean basin, based on the data provided in supplementary Table S1.

A

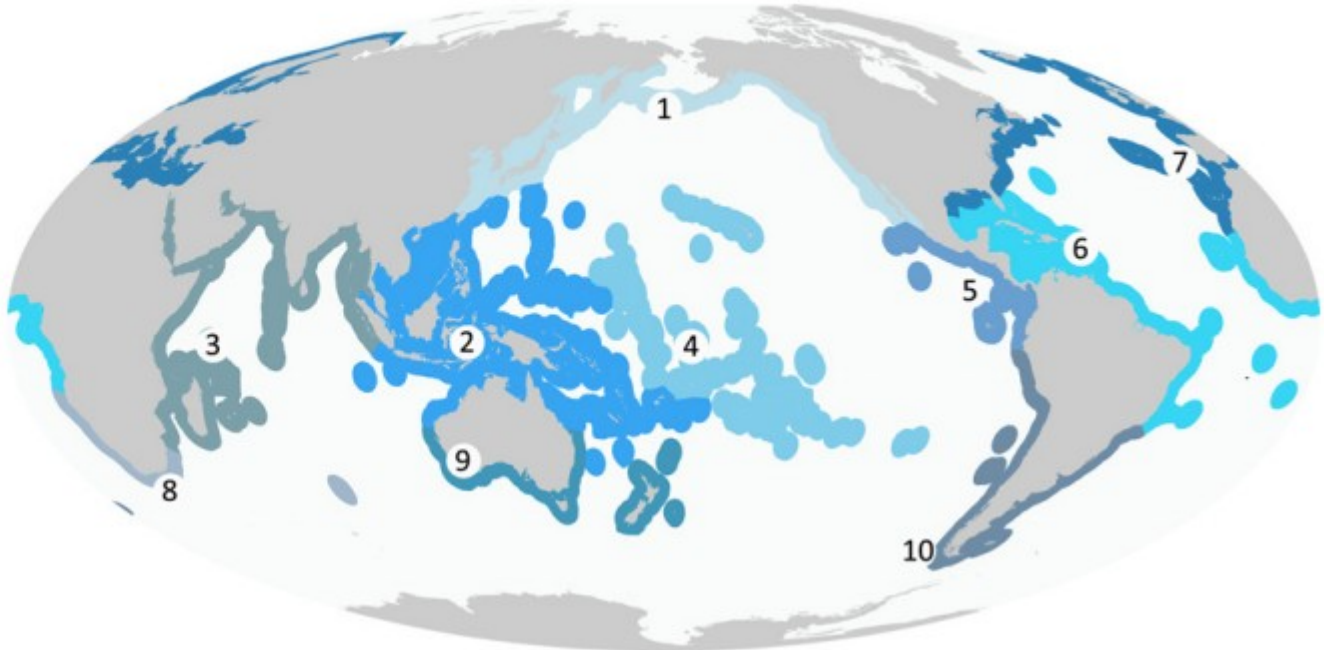

B

Marine Realm	*richness*	*% endemism*	*% > 1 basin*
1. Temperate Northern Pacific	20	40	25
2. Central Indo-Pacific	15	13	47
3. Western Indo-Pacific	13	15	62
4. Eastern Indo-Pacific	10	0	60
5. Tropical Eastern Pacific	4	0	50
6. Tropical Atlantic	14	21	78
7. Temperate N Atlantic	5	0	78
8. Temperate Southern Africa	6	17	83
9. Temperate Australasia	10	20	80
10. Temperate South America	4	50	50

C

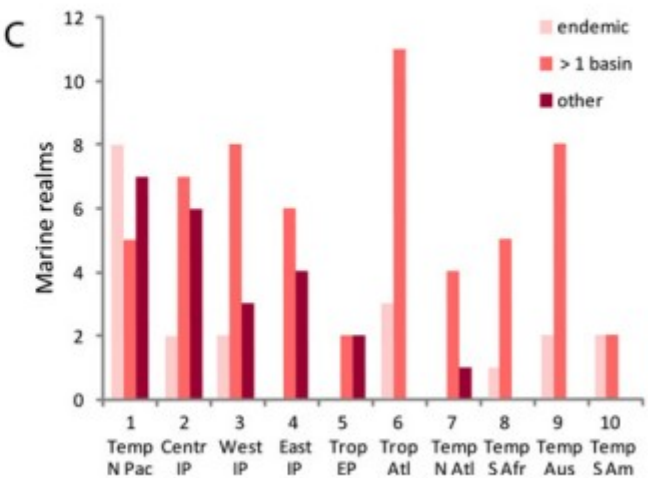

species limited to either Indo-Pacific or Atlantic, usually into a single region of these oceans

Silberfeld et al., 2013, J Phycol 49

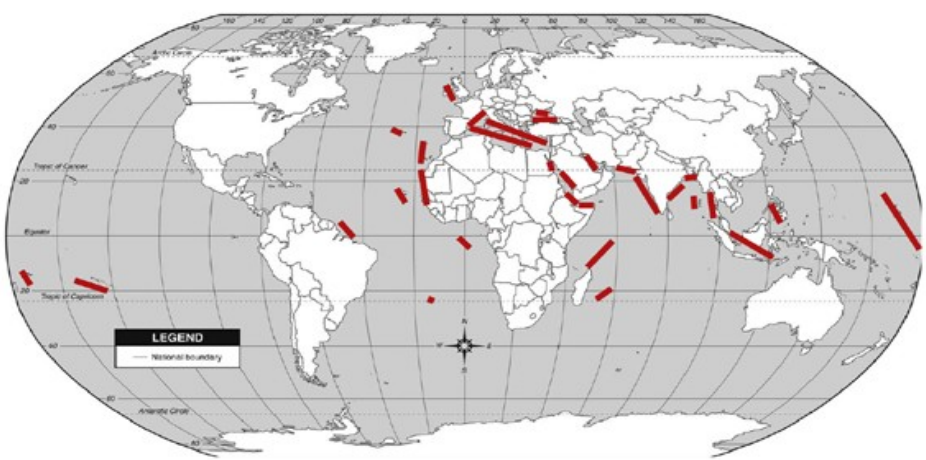

abundant Mediterranean species,
shallow eutrophicated habitats

Padina pavonica

Padina pavonica at the northern-most expanse of the distribution area – S and SW England/Wales

Table 2 Longevity of site record of *Padina pavonica* in southern Britain. For locations of numbered 'sites', see Fig. 1

Site No.	Position	Location	1650–1700	1701–1750	1751–1800	1801–1850	1851–1900	1901–1950	1951–1975	1976–2000	2001–2010	2011	2012	2013	2014
1	51° 56′ 21.47″N; 01° 17′ 52.53″E	Harwich		1730 +											
2	51° 19′ 34.83″N; 01° 24′ 12.21″E	Margate				1806–46+	1868+								
3	51° 24′ 08.91″N; 01° 25′ 42.75″E	Ramsgate													
4	51° 07′ 05.58″N; 01° 18′ 36.53″E	Dover				1846	1868								
5	51° 04′ 59.41″N; 01° 11′ 57.19″E	Folkestone													
6	50° 44′ 50.82″N; 01° 16′ 00.29″E	Eastbourne													
7	50° 45′ 24.07″N; 00° 08′ 37.20″E	Seaford													
8	50° 46′ 51.08″N; 00° 02′ 21.89″E	Newhaven													
9	50° 46′ 43.93″N; 00° 40′ 02.20″W	Bognor Rocks		1750		1831									
10	50° 41′ 22.08″N; 01° 04′ 13.73″W	Bembridge					1860				2009 C	C	C	C	C
11	50° 37′ 04.77″N; 01° 10′ 15.34″W	Shanklin					1872				2009 C	C	C	C	C
12	50° 36′ 54.02″N; 01° 10′ 15.42″W	Luccombe					1860								A
13	50° 35′ 19.04″N; 01° 13′ 23.65″W	Steephill Cove					1883								
14	50° 35′ 08.34″N; 01° 14′ 10.15″W	St Lawrence				1836									
15	50° 39′ 09.19″N; 01° 27′ 53.51″W	Compton Bay						1911			2009 C	R	F	R	R
16	50° 41′ 27.20″N; 01° 32′ 11.72″W	Colwell Bay						1922			2009 C	O	C	C	F
17	50° 38′ 33.74″N; 01° 56′ 35.40″W	Studland					1890								
18	50° 38′ 33.74″N; 01° 56′ 25.87″W	Swanage			1799			1902							
19	50° 35′ 32.52″N; 02° 03′ 52.18″W	Chapmans Pool					1894				2009	C			R
20	50° 36′ 31.36″N; 02° 08′ 06.50″W	Kimmeridge							1965		2009	C	R	C	C
21	50° 37′ 04.94″N; 02° 14′ 47.90″W	Lulworth Cove			1799			1924	1972						
22	50° 38′ 10.55″N; 02° 23′ 27.10″W	Osmington						1921			2009				C
23	50° 36′ 18.70″N; 02° 26′ 53.99″W	Weymouth			1796		1854	1909+	1925+		2010 R	R	R	R	O
24	50° 35′ 51.35″N; 02° 27′ 31.65″W	Portland Harbour				1850			1967		2010 R				A
25	50° 35′ 32.60″N; 02° 29′ 29.32″W	East Fleet								2000					
26	50° 40′ 14.46″N; 02° 56′ 51.79″W	Lyme Regis				1802+					2009 A				A
27	50° 43′ 04.40″N; 03° 15′ 45.23″W	Sidmouth				1828	+				2009				
28	50° 39′ 38.02″N; 03° 16′ 36.42″W	Ladram Bay					1852		+		2009 C			R	O
29	50° 37′ 44.80″N; 03° 19′ 12.54″W	Budleigh Salterton				1810									
30	50° 36′ 35.69″N; 03° 23′ 54.21″W	Exmouth	1680–83			1850	1889+	1902							
31	50° 35′ 34.73″N; 03° 26′ 38.13″W	Dawlish			1799		1876								
32	50° 32′ 21.10″N; 03° 29′ 56.75″W	Teignmouth					1889+								
33	50° 27′ 09.06″N; 03° 32′ 46.06″W	Torbay				1825+	+	1930 +			2009 F				O
34	50° 23′ 44.10″N; 03° 20′ 29.79″W	Brixham							1953		2005				
35	50° 20′ 05.10″N; 04° 07′ 54.37″W	Plymouth					End 19th				2004				
36	51° 12′ 31.67″N; 04° 07′ 03.85″W	Ilfracombe				1837									
37	50° 41′ 32.63″N; 04° 42′ 09.15″W	Boscastle						1906		1993					
38	51° 33′ 41.30″N; 04° 18′ 57.30″W	Worms Head				Early19th									
39	51° 40′ 19.89″N; 04° 42′ 04.66″W	Tenby						1930							
40	51° 42′ 20.24″N; 05° 11′ 13.55″W	Westdale Bay								1997					

Black indicates presence during period shown. Grey indicates periods when *Padina* was not found in searches. Dates are shown to indicate first, last records or single record for the period. Recent records of 'Abundance' (A–R) are as shown in Table 1. Years when anecdotal historical records and accounts indicate *Padina* was 'common' or 'abundant' are shown as '+'

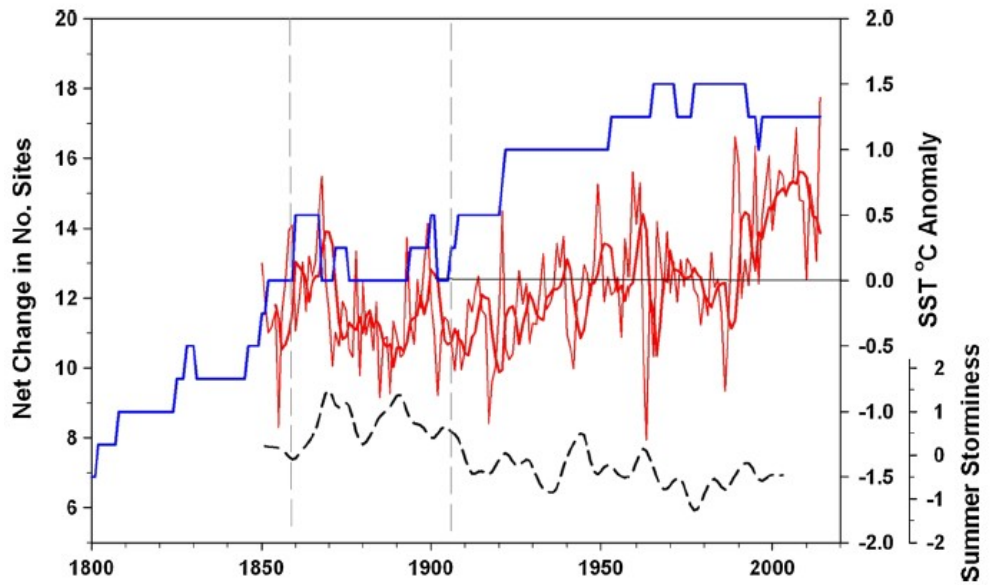

Fig. 4 Net changes in number of sites with *P. pavonica* populations on the south coast of England (cumulative site gains minus cumulative site loss) between 1800 and 2014. Annual SST (and 5-year smoothed mean) anomalies (1960–1991 baseline) from 1850 to 1869 were extracted from the HadSST 3.1.1.0 data (Kennedy et al. 2011a, b) and from 1870 to 2014 extracted from the HadISST1 data set (Rayner et al. 2003). Summer storm index data from Cornes and Jones (2011). *Vertical dashed lines* indicate cooler and stormier period in mid-nineteenth century

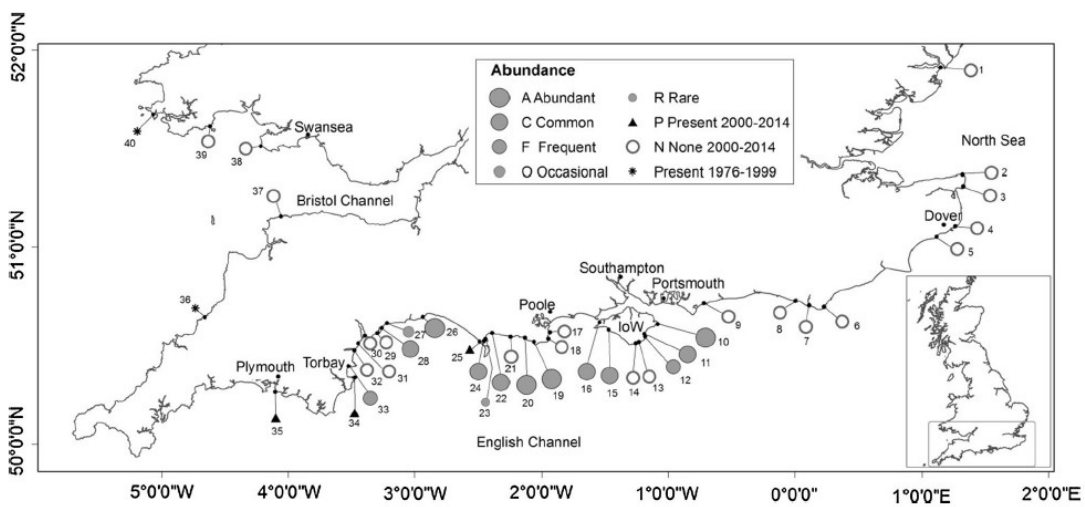

Fig. 1 Distribution and abundance of *Padina pavonica* in southern Britain. *Symbols* show the maximum recorded abundance at each site over the period 2000–2014 and records from other localities subsequent to the previous main survey (Price et al. 1979). To our best knowledge, there have been no records north of this region subsequent to those in Price et al. (1979). The abundance scale and site reference numbers are given in Tables 1 and 2, respectively

Herbert et al., 2016, Mar. Biol. 163

Sphacelariales

- branching multiseriate filaments
- diplohaplontic cell cycle, isomorphic [or slightly heteromorphic?]
- iso-, aniso- and oogamy

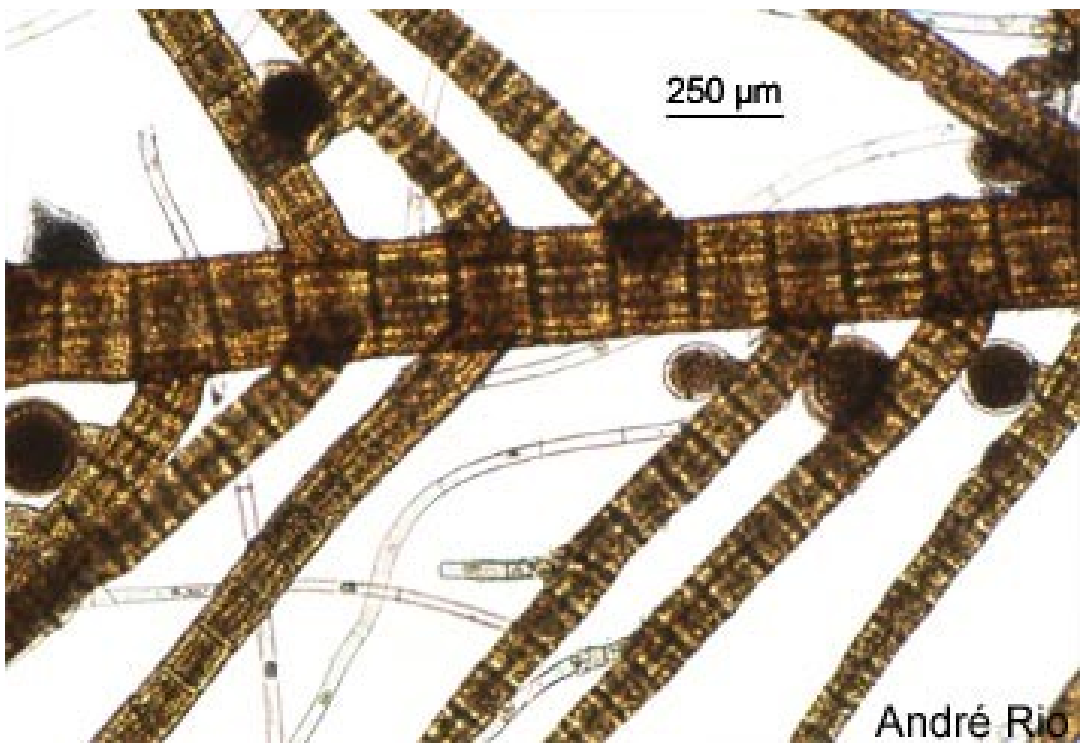

Sphacelariales

Sphacelaria rigidula

- tiny brown tufts
- cosmopolitan, on rocks or epiphytic
- triradiate asexual propagules

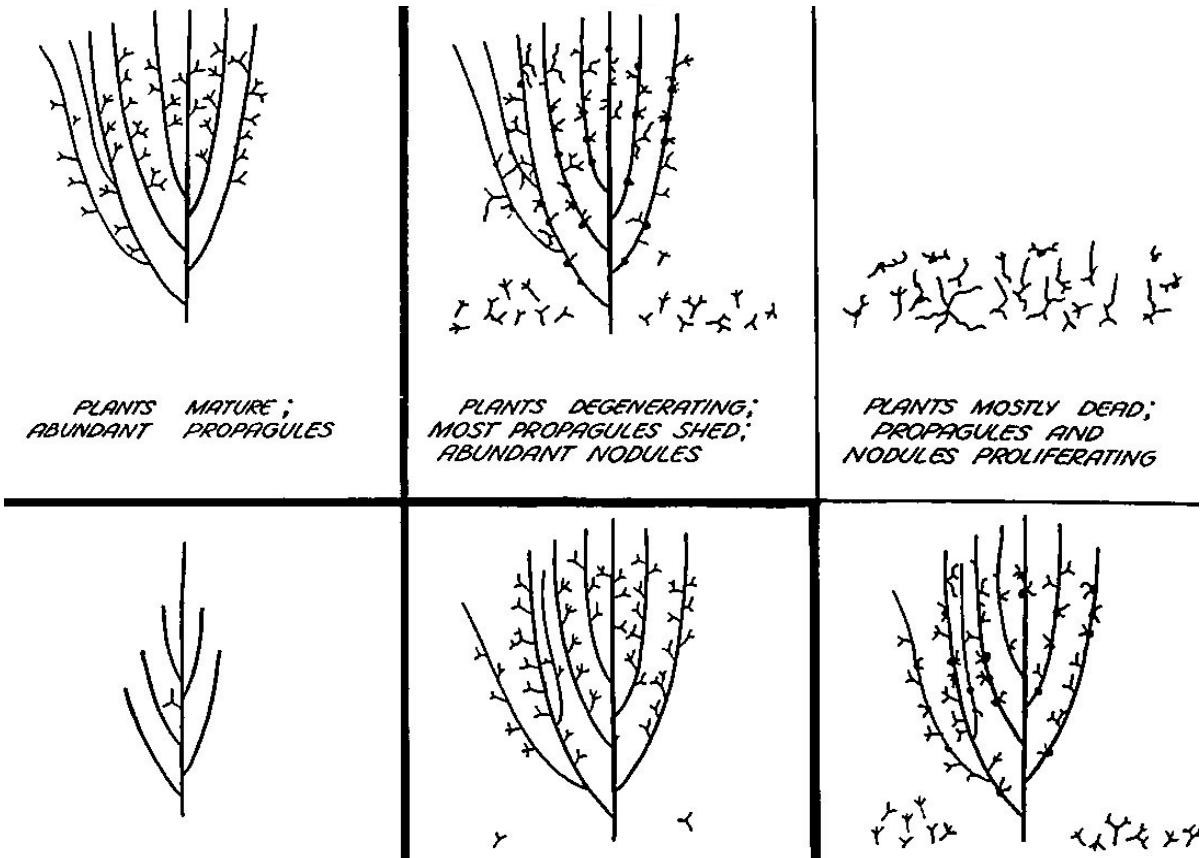

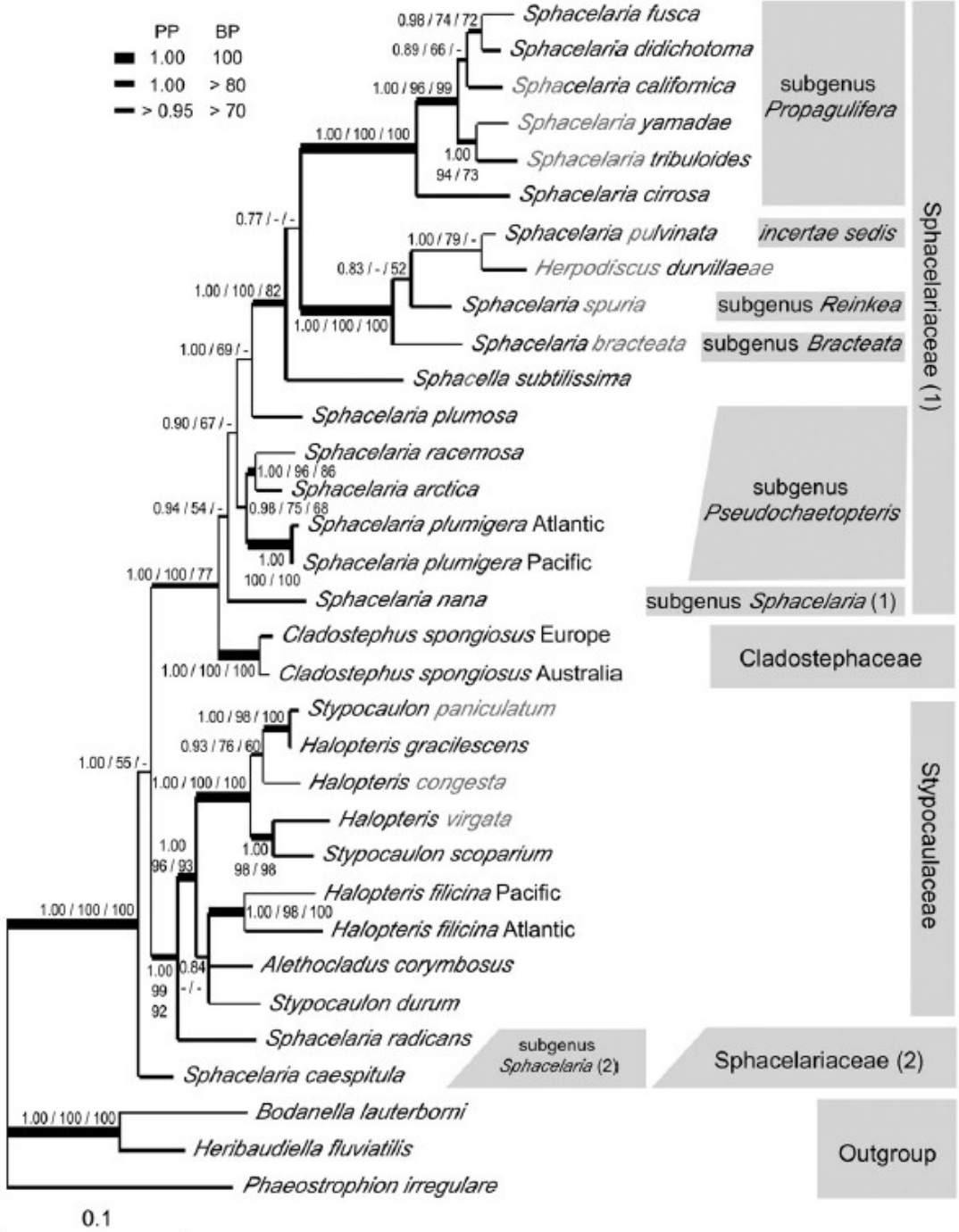

Fig. 2. Bayesian Inference (BI) phylogeny for the Sphacelariales based on a combined analysis of *psb*C and *rbc*L DNA sequence data. Traditional family classification and *Sphacelaria* subgenera are indicated in grey boxes. BI Posterior Probabilities (PP) and Maximum Likelihood (ML) Bootstrap Percentages (BP) and Maximum Parsimony (MP) BP are given near nodes (BI PP/ML BP/MP BP). Dashes (-) indicate percentages <50% (or that the node did not occur in the MP or ML tree). Branch support is also indicated by branch thickness (see inset upper left). In cases where a taxon was

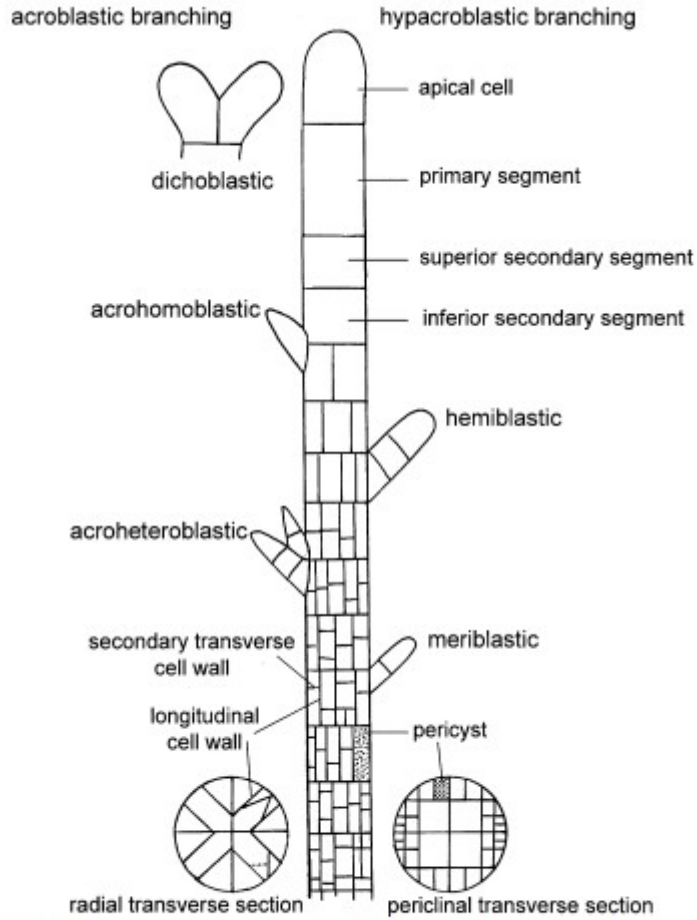

Fig. 1. Diagrammatic representation of anatomical characters used in taxonomic descriptions of the Sphacelariales.

Draisma et al., 2010, Eur. J. Phycol.
Draisma et al., 2002, Eur. J. Phycol.

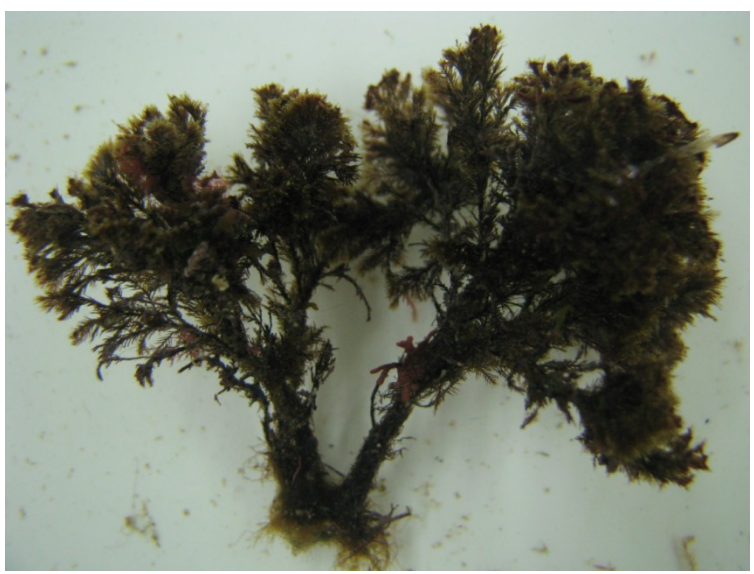

Halopteris filicina
abundant Mediterranean species

Sphacelaria arctica
cold water, slowly growing, deep sea species
Baltic – lower sublittoral

Cladostephus spongiosus
(temperate, cosmopolitan)

Sphacelaria cirrosa

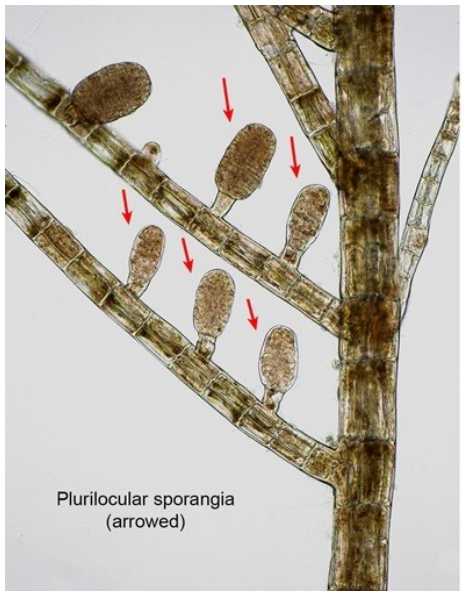

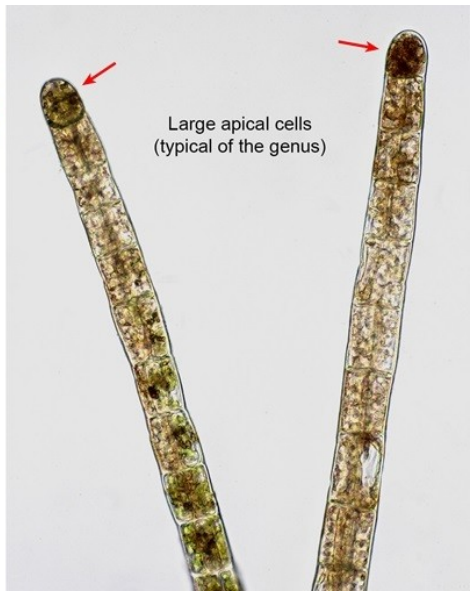

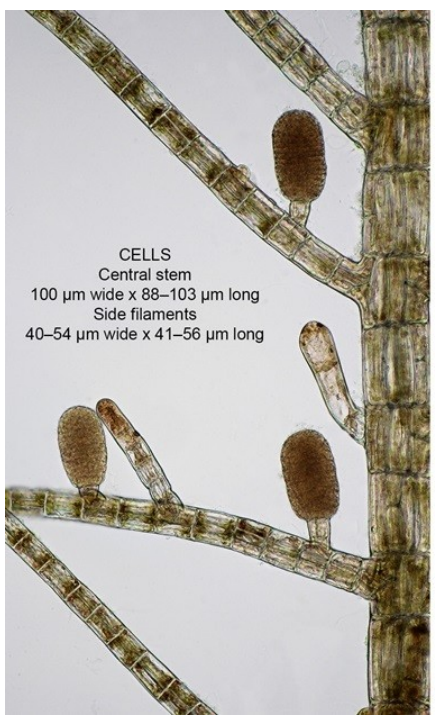

freshwater brown algae

- *Pleurocladia*, *Heribaudiella*, [*Ectocarpus*]

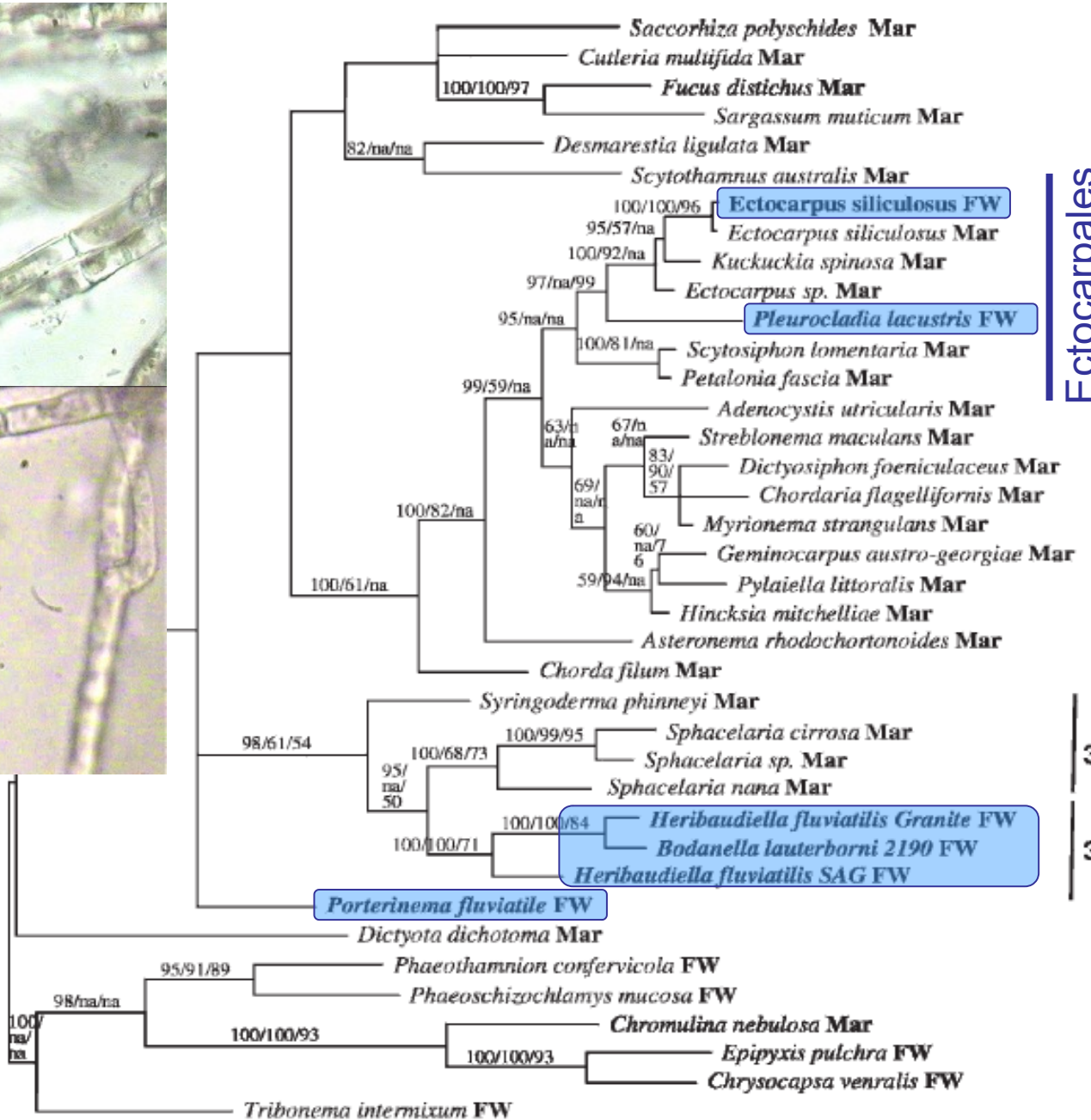

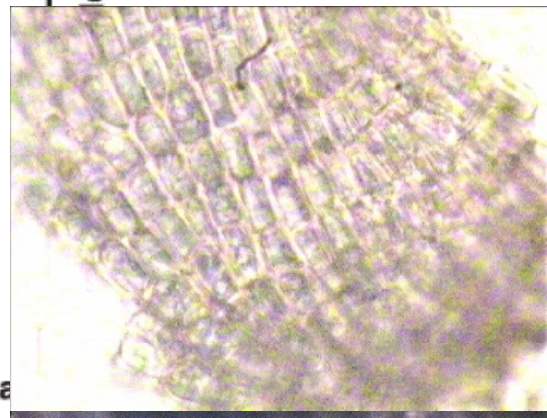

TABLE 1 Species of Brown Algae Reported from Freshwater Environments, with Morphology (UF = Uniseriate Filaments; CR = Crustose, MF = Multiseriate Filaments), Habitats, and Localities

Taxon	*Morphology*	*Habitat*	*Localities*
Ectocarpales			
Bodanella lauterbornii	UF	Lake	North America: unknown Other: Lake Constance,[a] Europe
Ectocarpus siliculosus[b]	UF	Stream, estuary	North America: unknown Other: Hopkins River, Australia
Pleurocladia lacustris	UF	Stream, lake	North America: Green River (UT, CO), Devon Island (NWT) Other: Austria, Germany, Poland, Scandinavia, England
Heribaudiella fluviatilis[c]	CR	Stream, lake	North America: at least 30 sites Other: many locations in Europe, also Japan, China
Porterinema fluviatile	UF	Lake	North America: unknown[d] Other: Germany, Netherlands, United Kingdom
Sphacelariales			
Sphacelaria fluviatilis	MF	Stream, lake	North America: Gull Lake, MI Other: China
S. lacustris	MF	Lake	North America: Lake Michigan Other: unknown

[a] Known locally as Bodensee.
[b] *Ectocarpus confervoides* has been collected from the River Werra, Germany, polluted by potassium mines (Geißler, 1983).
[c] Previously reported as *Lithoderma arvernensis*, *L. fluviatile*, and *L. fontanum*; *L. zonatum* (Jao, 1941) is retained by some authors.
[d] Freshwater and euryhaline (= *Pseudobodanella peterfii*) reported from North America from marine and estuarine sites only.

Wehr, 2002, Brown Algae

Heribaudiella fluviatilis

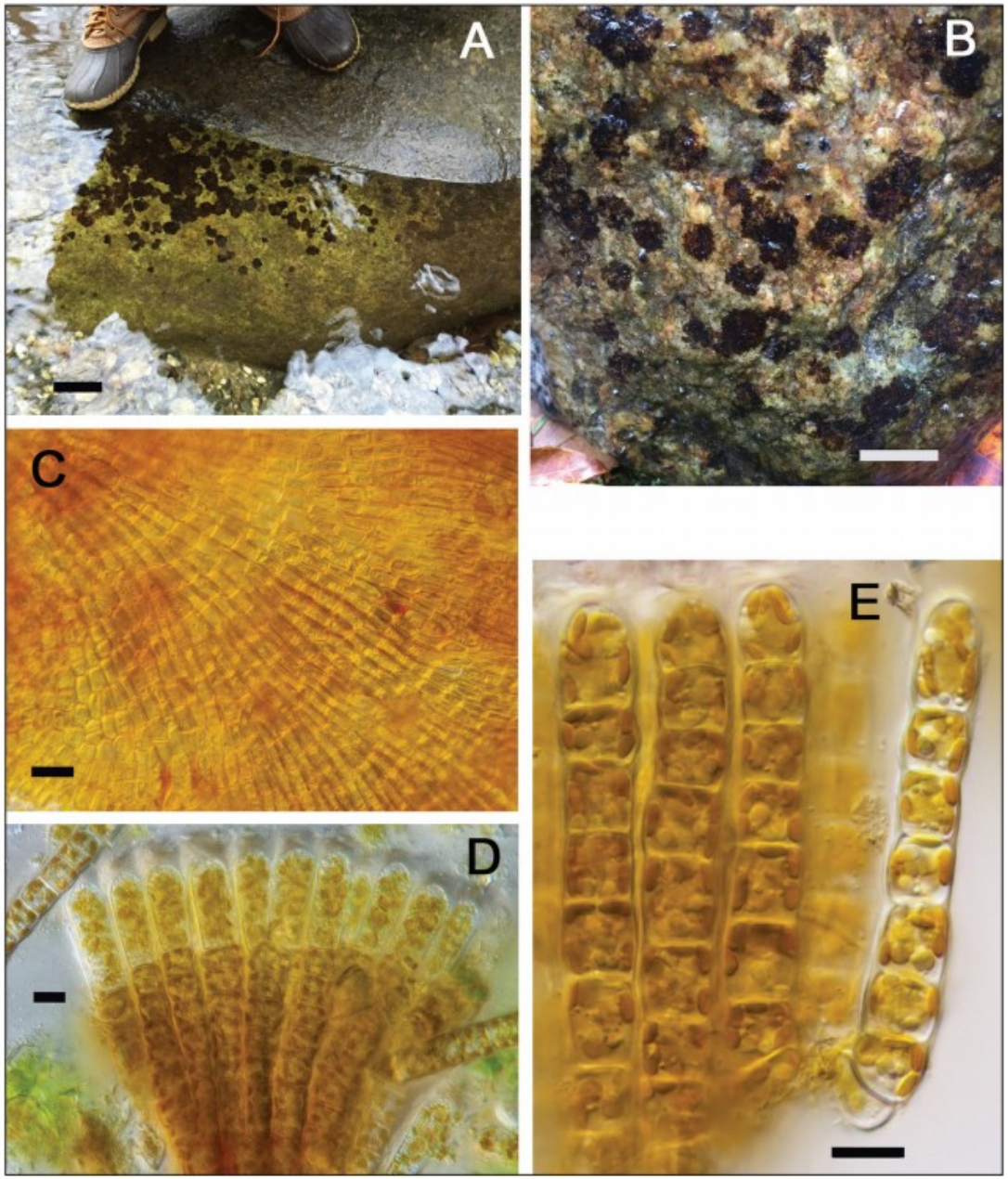

Figure 3. Images of *Heribaudiella fluviatilis* collected from contemporary populations in western Connecticut. (A): Brown macroscopic crusts on a large boulder in Gunn Creek (scale bar = 5 cm); (B): close-up view of crusts on a rock from Macedonia Brook (scale bar = 2 cm); (C): microscopic appearance of prostrate form with densely arranged, dichotomously-branched filaments; (D): series of vertically arranged, tightly packed filaments with terminal unilocular sporangia; (E): details of cells in vertical filaments with multiple

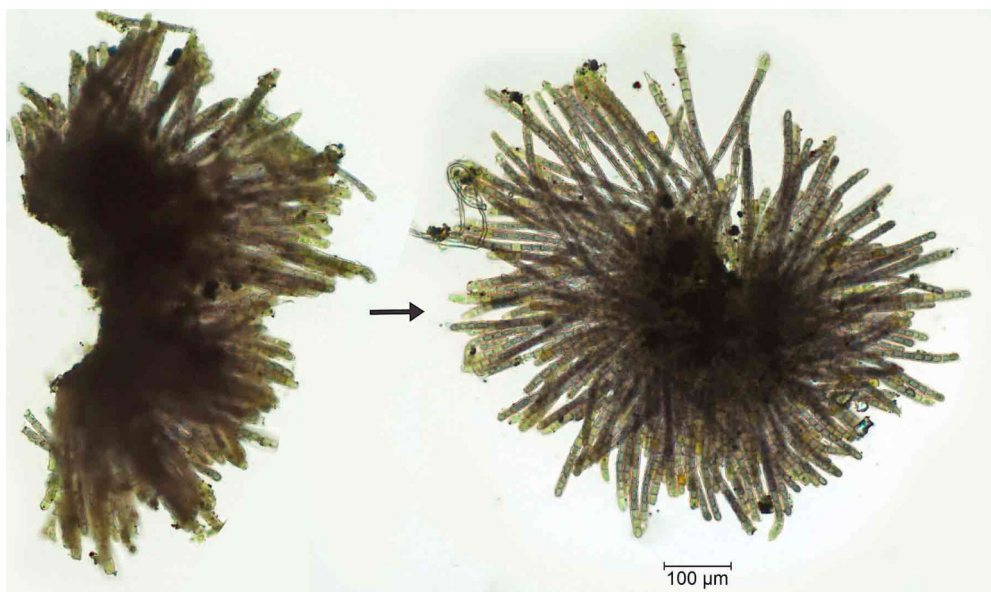

Wehr et al., 2019, NorthE. Nat. 26

Bodanella lauterbornii

only known from deeper sublittoral of Bodensee, Traunsee and two other Austrian Alpine lakes

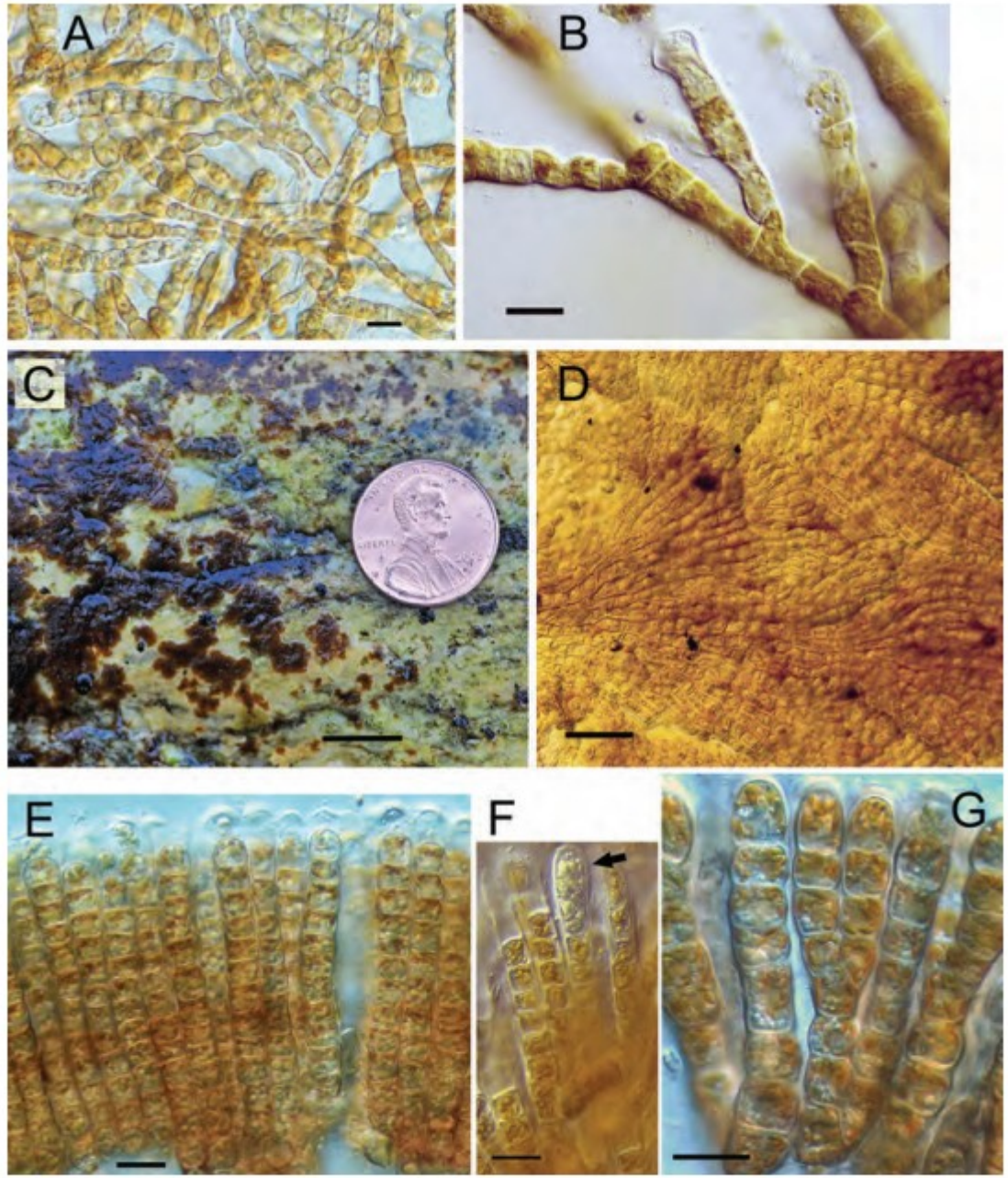

FIGURE 6 Heribaudiales.[3] *Bodanella lauterborni* (A) undulating or wavy filaments with irregular branching, forming mat-like network (in culture); (B) detail of filaments with inflated, quadrate irregularly shaped cells containing multiple disc-like chloroplasts and refractive physodes; terminal cells may be developing unilocular sporangia. *Heribaudiella fluviatilis* (C) forming raised, crusts on rocks colonies; (D) spreading, densely branched prostrate system; (E) vertical series of filaments; (F) terminal unilocular sporangium (arrow); (G) vertical filaments with dichotomous branching and detail of cells showing numerous disc-like chloroplasts and refractive bodies, which may be physodes and/or oil droplets (scale bar for A-B, E-G = 20 µm; C = 1 cm; D = 50 µm). *(Photo (C) by Kam Truhn, with permission).*

Wehr, 2015, Brown Algae, Freshw. Algae N. Am.

Desmarestiales

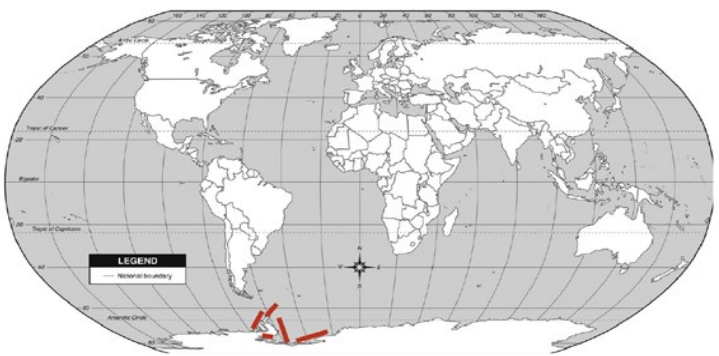

D. anceps

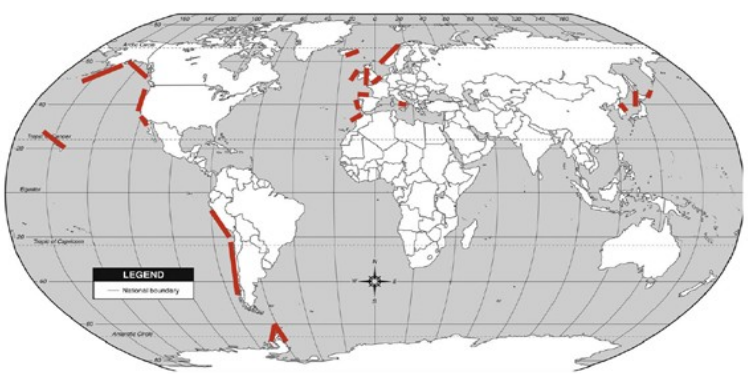

D. ligulata

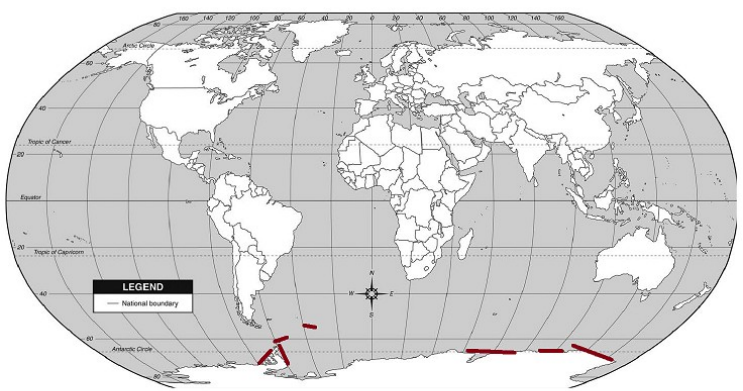

Himantothallus grandifolius

sporophytes - feathery and usually lithophytic thalli
pseudoparenchymatous thallus is derived from apical meristems situated at the base of a hair (trichothallic growth)

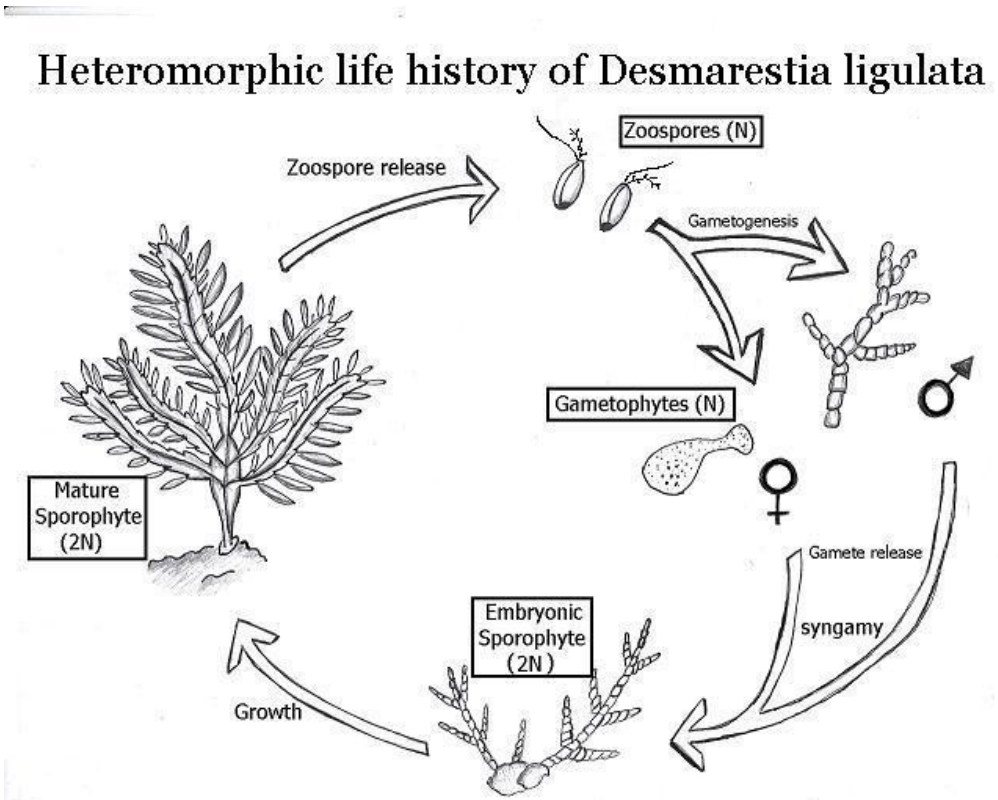

branched or foliose macroscopic thalli in the genus Desmarestia (D. viridis, D. ligulata, etc.) and others contain free sulfuric acid (pH up to 1.0) – in intracellular vacuoles (traditional name: acidweed); apparently this feature has originated only once in the evolution of the group

D. ligulata

D. menziesii

Himantothallus grandifolius

D. viridis

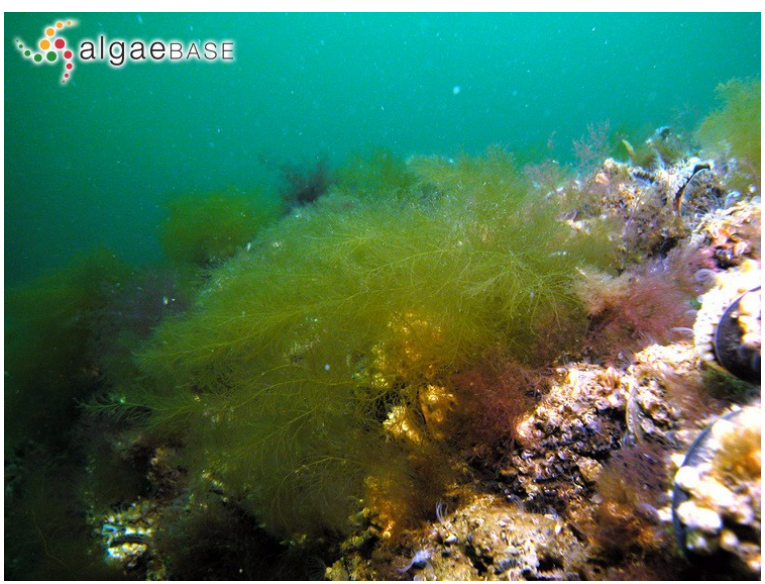

Ralfsiales

crustose thallus (erect, tightly adherent filaments)
unangia and plurangia (these in vertical rows with one or more sterile terminal cells)
often with bright margins
typically in supralittoral, intertidal or upper subtidal

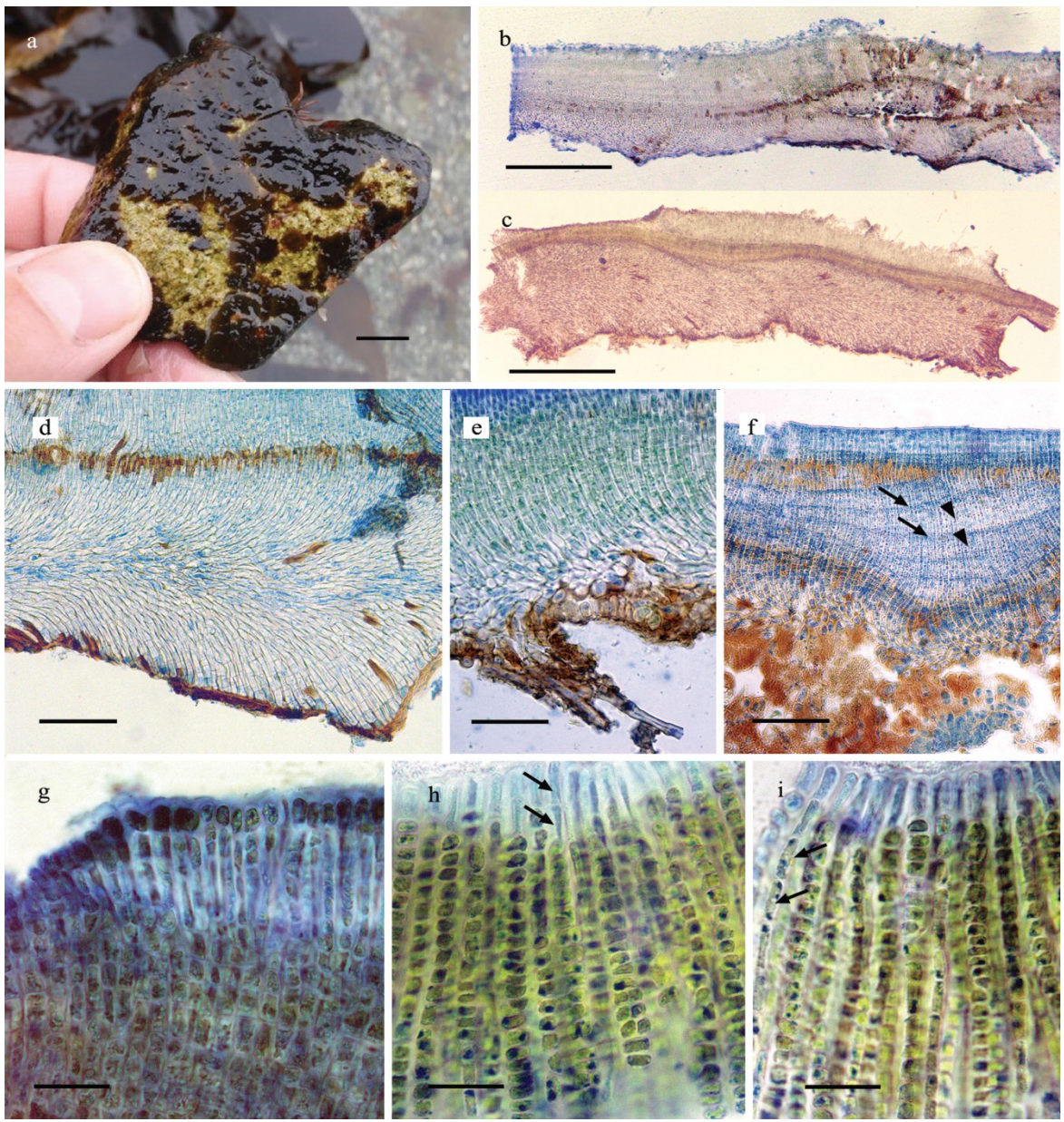

R. verrucosa

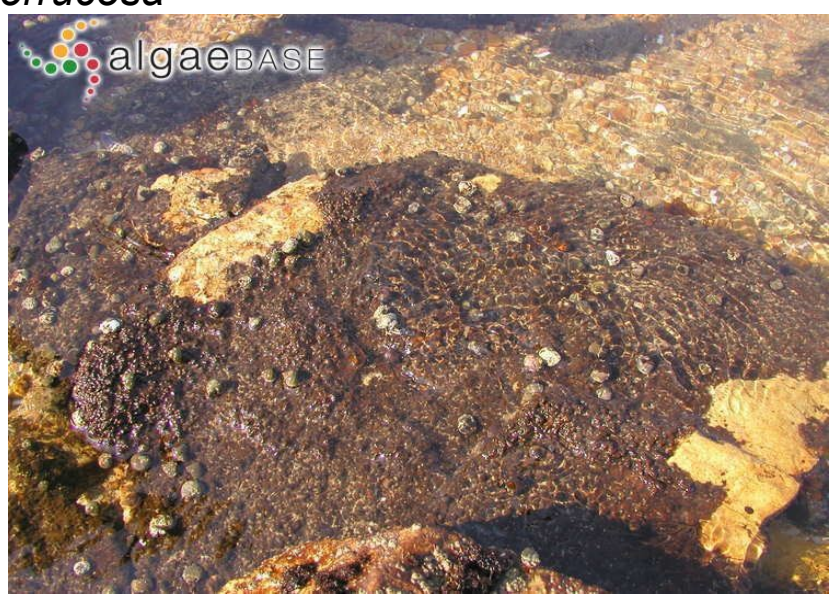

Parente & Saunders, 2019, Botany 97

Fucales

- only macrothallus (S)
- diplont cell cycle, mostly oogamy
- conceptacula – cavities in thallus, containing gametangia

sporophyte (♀)

receptacula

sporophyte (♂)

receptacula

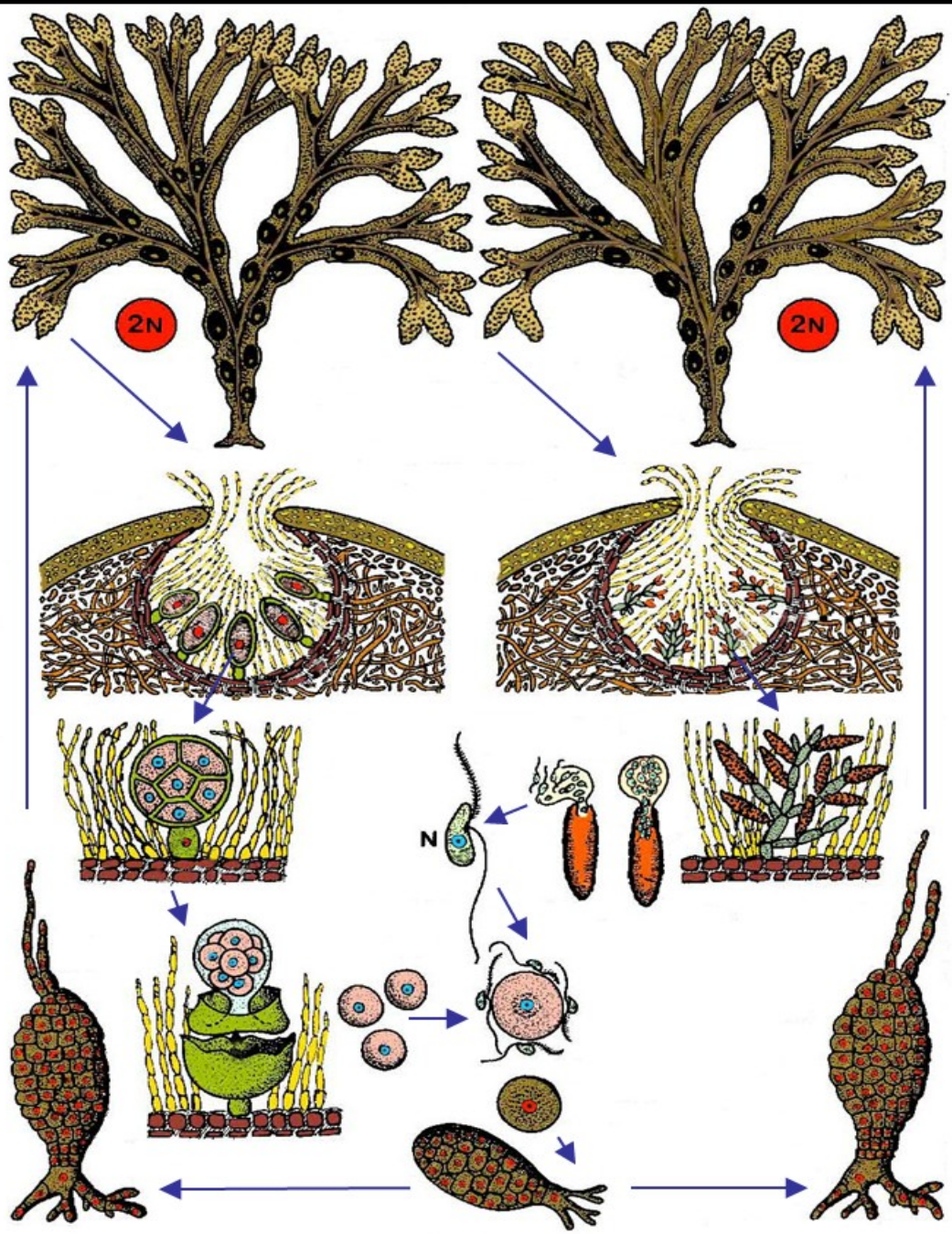

♀ conceptacula

♂ conceptacula

oogonium
(♀ gametophyte)

antheridium
(♂ gametofyt)

→ analogy to flowering plants

Fucales

Fucus – conceptacula

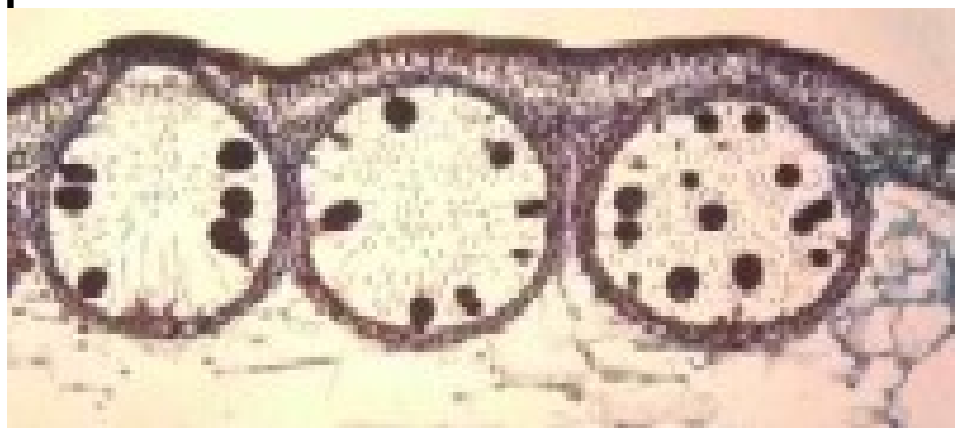

Concepticle

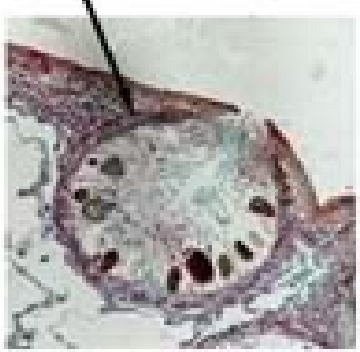

Fucales

systematic overview

[Xiphophoraceae - 1 g, 3 sp, endemic to southern Australia and NZ]

[Bifurcariopsidaceae – 1 g, 1 sp, endemic to Cape region]

Durvillaeaceae - 1 g, 7 sp, cold temperate and subantarctic regions of the southern hemisphere
- Durvillaea

Fucaceae - 5 g, 18 sp
- Silvetia - N Pacific (vyčleněno z Pelvetia v roce 1999)
- Ascophyllum - N Atl, 1 druh
- Pelvetiopsis - NE Pacific (Neiva et al. 2017)
- Pelvetia - N Atl, 1 druh
- Fucus - N Atl

Himanthaliaceae - 1 g, 1-2 sp, N Atl – Eur
- Himanthalia

[Hormosiraceae – 1 g, 2 sp, endemic to southern Australia and NZ]

[Notheiaceae – 1 g, 1 sp (N. anomala), epiphytic in intertidal on Hormosira and Xiphophora; S Australia and NZ]

Sargassaceae - 33 g, 510 sp
- Cystoseira (+ Carpodesmia, Treptacantha)
- Cystophora - Australia, NZ
- Halidrys (H. siliquosa) - N Atl - Eur
- [Myriodesma - Austr, NZ]
- Sargassum
- Turbinaria

[Seirococcaceae - Cystosphaera (end. Ant. Pen.), Marginariella (end. NZ), Phyllospora, Seirococcus (end. S Austr)]

Durvillaea

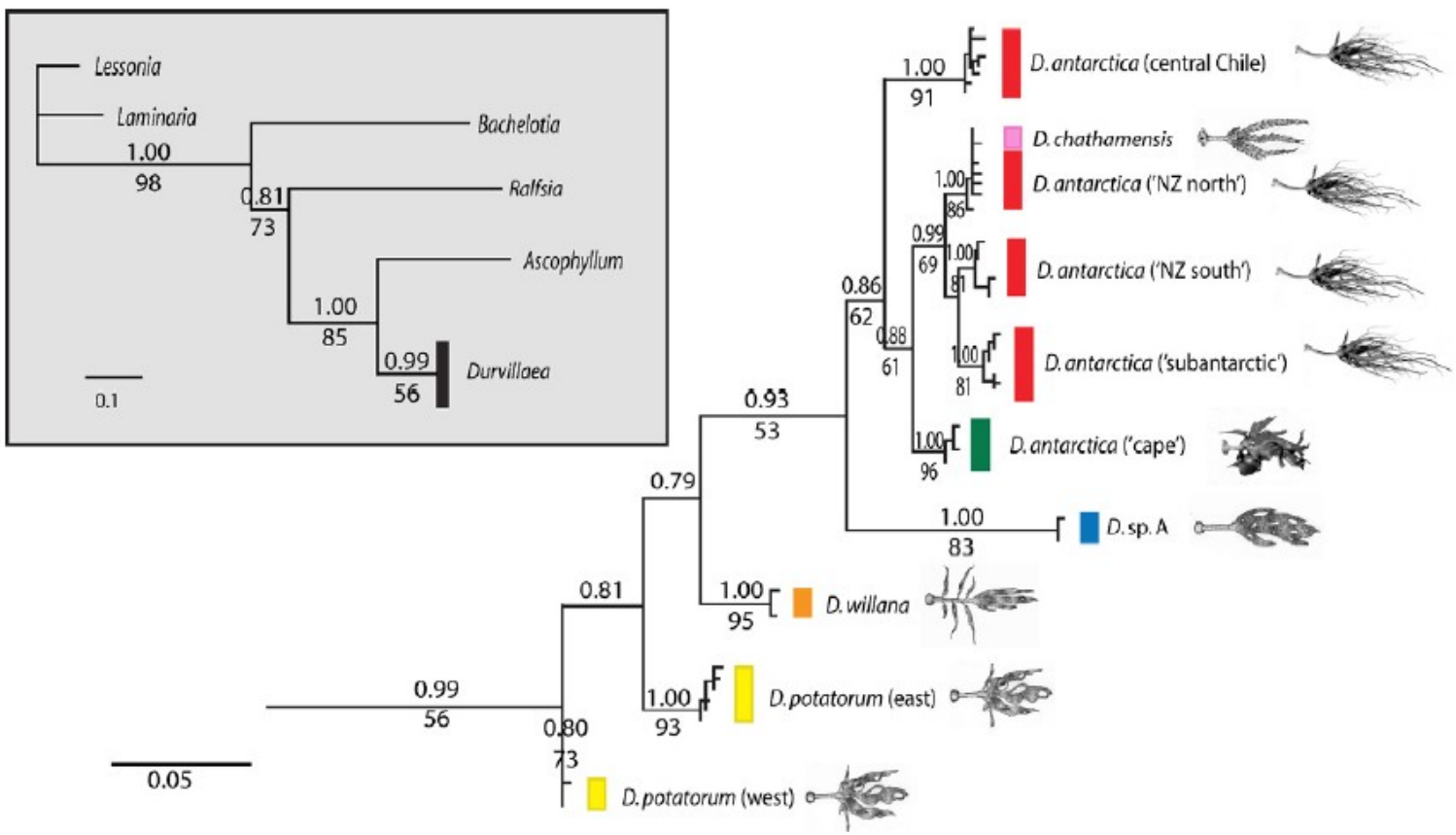

Fig. 3. Maximum-likelihood phylogeny of *Durvillaea* based on mitochondrial (COI) data. *Durvillaea* 'lineages' are identified by colored strips, with colors corresponding to those used in Fig. 1. Branches show Bayesian PP values (above the line) and ML bootstraps (>50%, below the line). The relationship of *Durvillaea* to the outgroup genera is shown (inset, upper left). Leaf-node images illustrate some of the important morphological differences among *Durvillaea* taxa (stylized drawings or photographs).

Fraser et al., 2010, Mol. Phyl. Evol. 57: 1301-1311.

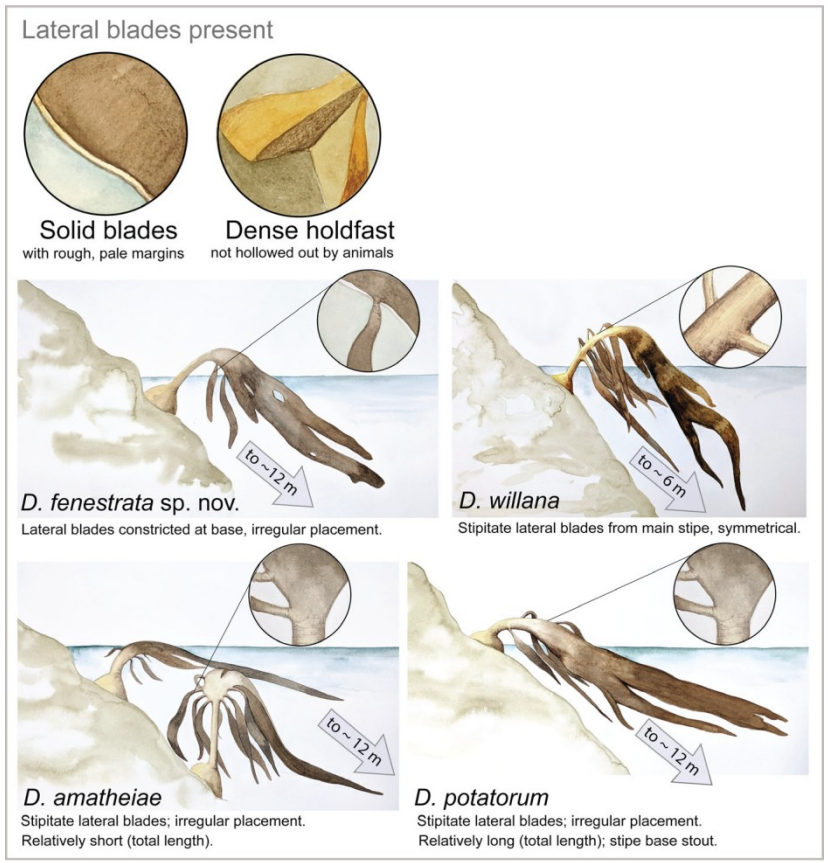

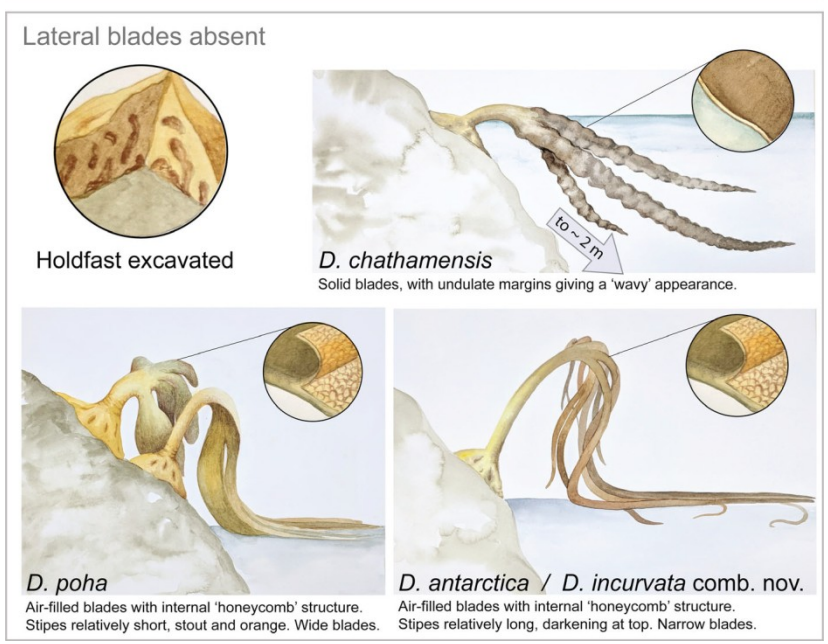

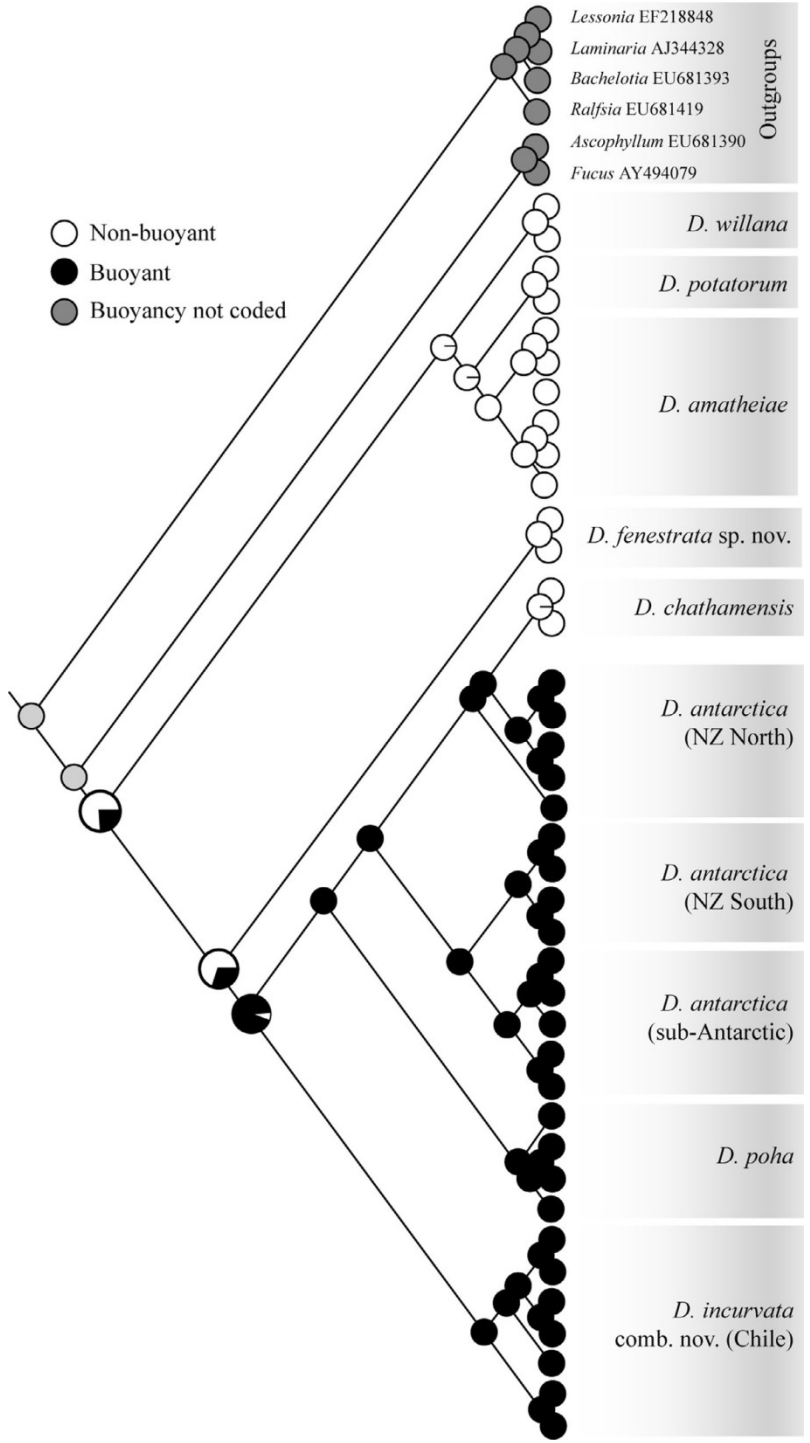

Fraser et al., 2019, J Phycol

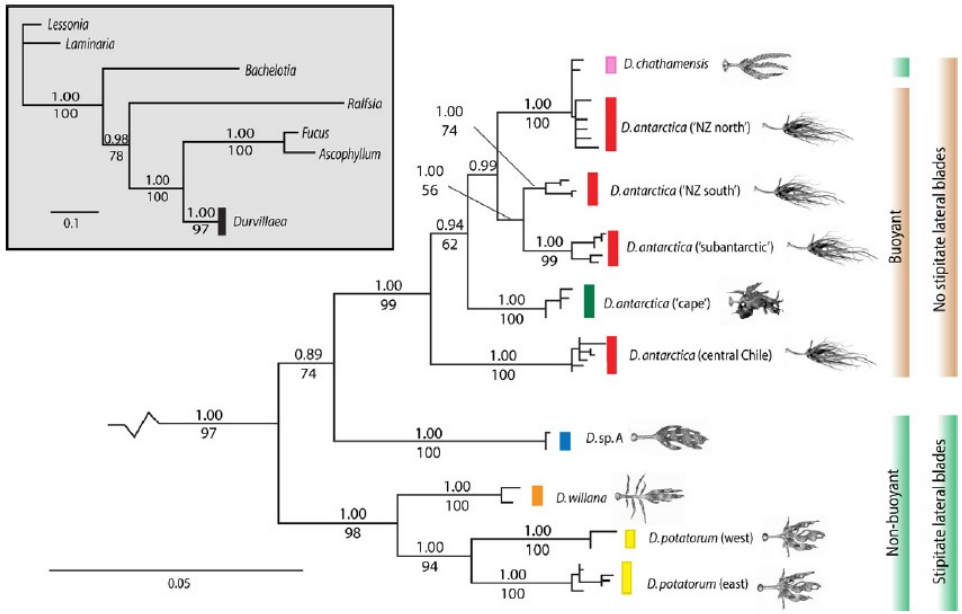

Fig. 6. Maximum likelihood phylogeny of *Durvillaea* based on concatenated (combined COI, *rbc*L, 18S and 28S) data. *Durvillaea* 'species' are identified by colored strips, with colors corresponding to those in Fig. 1. Branches show Bayesian PP values (above the line) and ML bootstraps (>50%, below the line, with those calculated by PhyML in parentheses). The relationship of *Durvillaea* to the outgroup genera is shown (inset, upper left). Leaf-node images illustrate some of the important morphological differences among *Durvillaea* taxa (stylized drawings or photographs). The presence/absence of stipitate lateral blades (a key diagnostic feature) is indicated on the far right.

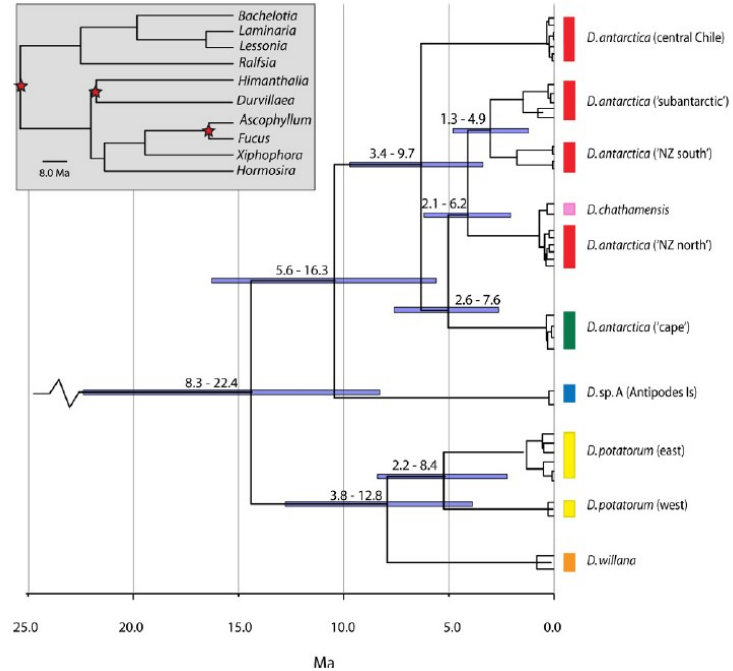

Fig. 7. Bayesian maximum clade consensus phylogeny of *Durvillaea* species and outgoup genera. This analysis is based on sequence data from three markers: COI, *rbc*L, and 28S. Outgroups have been removed from the tree for clarity, but are indicated schematically in the inset (upper left) with red stars showing the positions of calibrated nodes. Horizontal bars and associated number ranges show the 95% posterior probability of the age of each node. The scale bar indicates time in millions of years (Ma) from present.

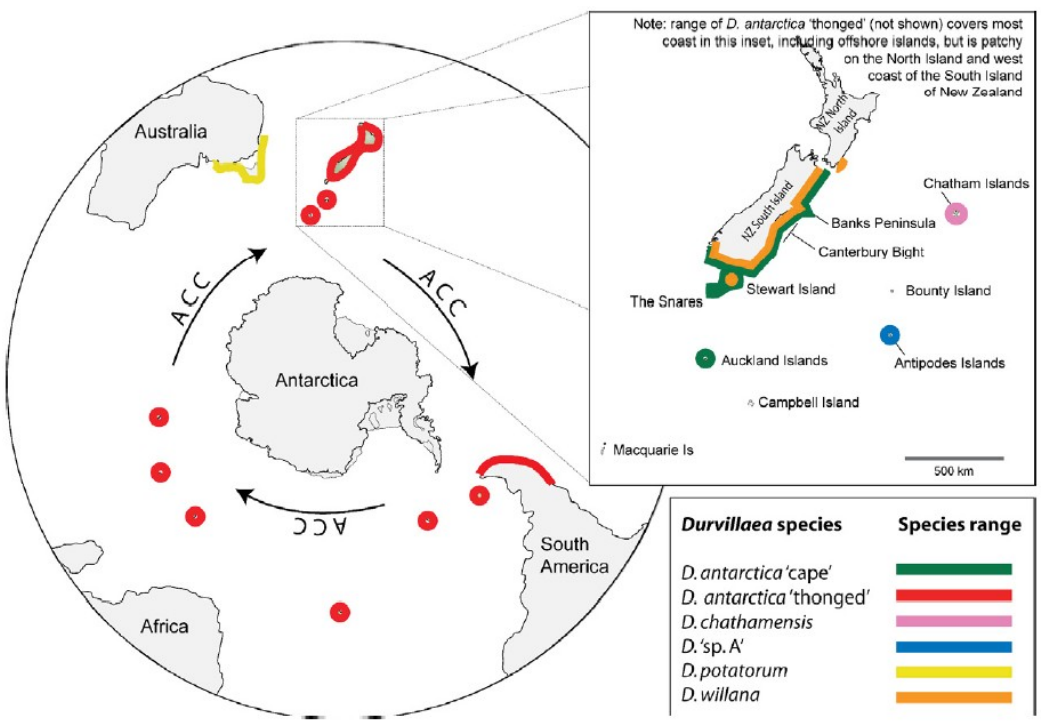

Fig. 1. Geographic range of each *Durvillaea* species recognized by Hay (1994), as well as the 'cape' form of *D. antarctica* (South and Hay, 1979; Fraser et al., 2009a). The general path of the Antarctic Circumpolar Current (ACC) is indicated on the global projection. Inset: New Zealand and NZ subantarctic region, where most diversity within the genus is found.

Fraser et al., 2010, Mol. Phyl. Evol. 57: 1301-1311.

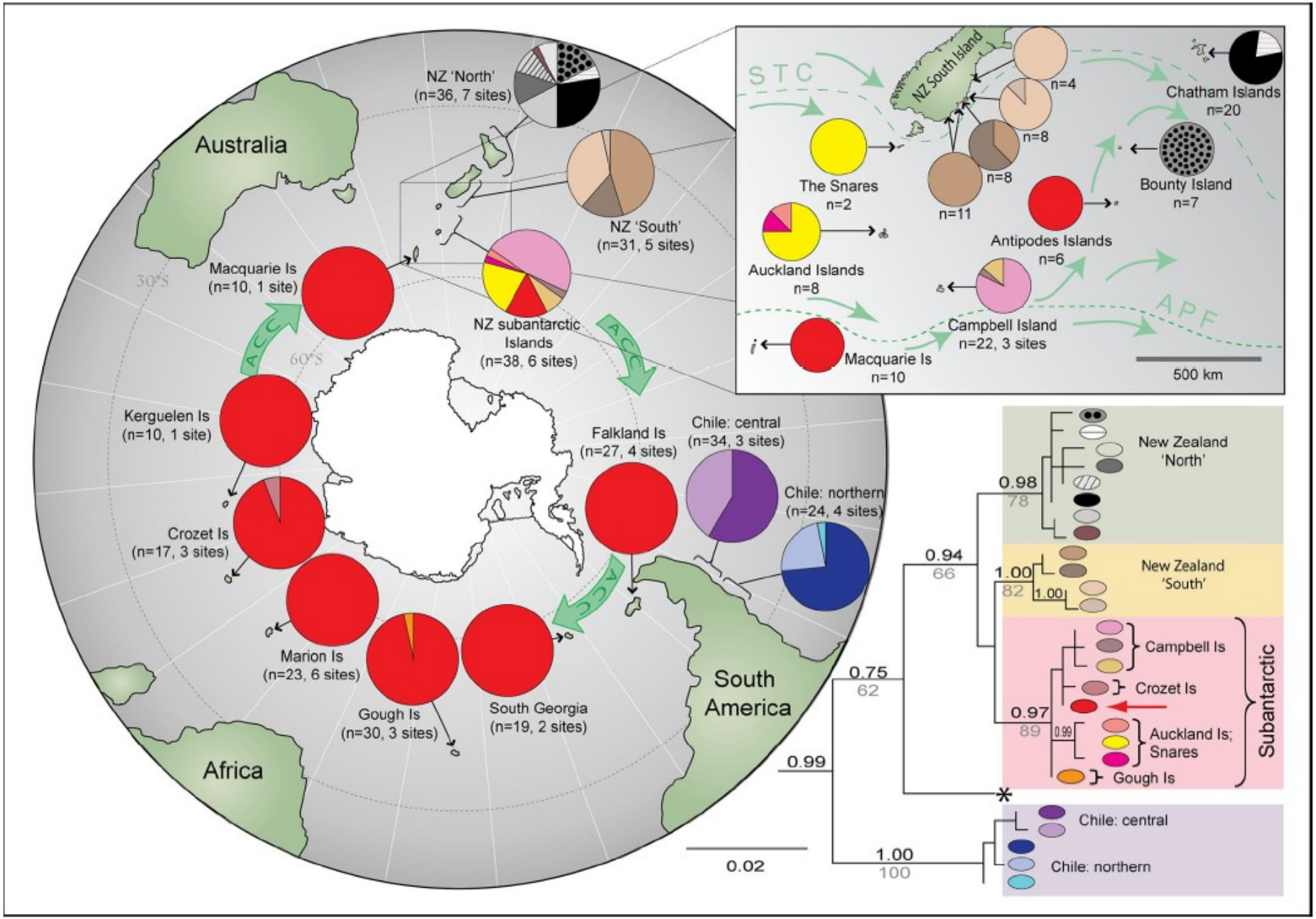

Fig. 1. Phylogeographic relationships within *D. antarctica* based on COI data. The phylogenetic tree (lower right corner) indicates haplotype relationships, with Bayesian PP values above branches and ML bootstraps below. Outgroup taxa have been removed for clarity. "NZ subantarctic" refers to the Snares, Auckland, Campbell, and Antipodes Islands. The morphologically and genetically distinct "cape" form of *D. antarctica*, recently identified by Fraser *et al.* (25) from southeastern NZ, is indicated by an asterisk. The global projection shows haplotype distributions and proportions at each locality. Diversity in the southern New Zealand region is illustrated at higher magnification (*Inset*, upper right). Green arrows show major surface currents.

Fraser et al., 2009, PNAS

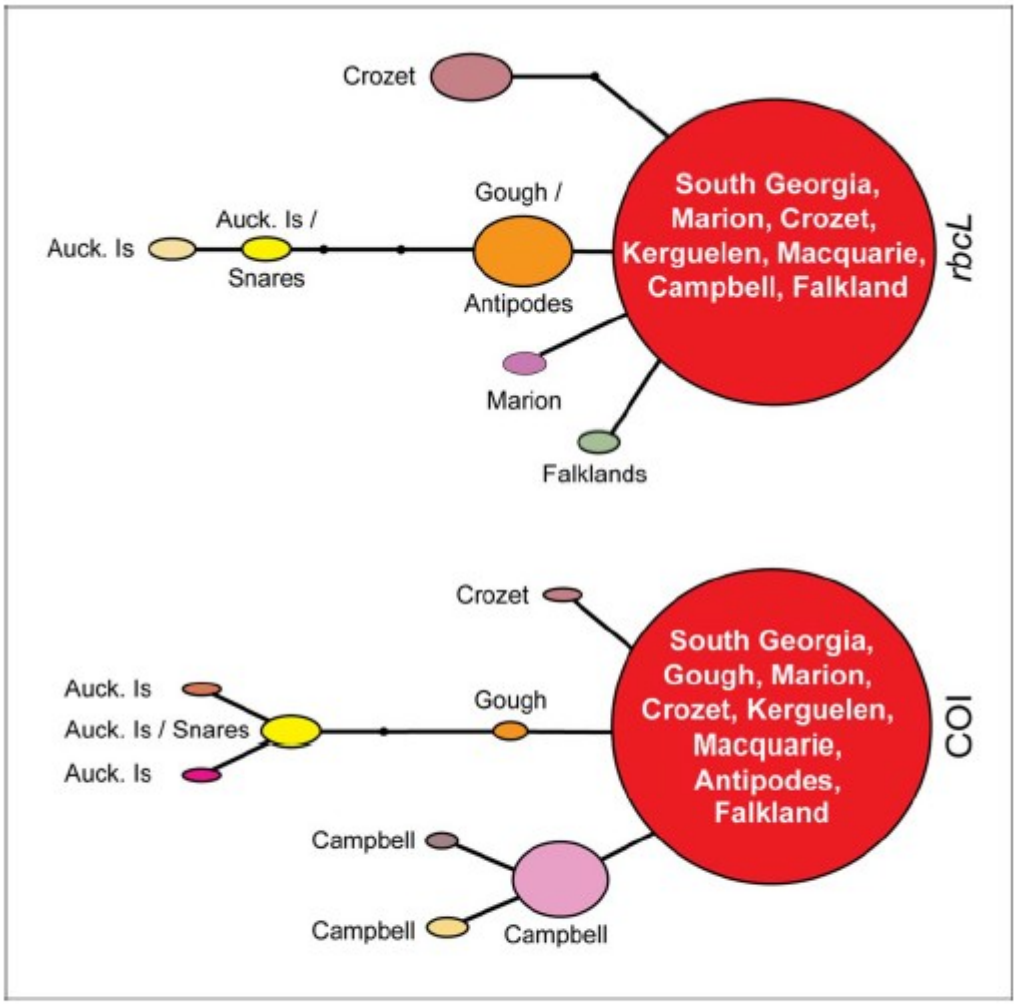

Fig. 2. Haplotype network diagrams for the "subantarctic" clade of *D. antarctica* for both mtDNA (COI) and chloroplast (*rbc*L) datasets. Circle size is scaled according to haplotype frequency. Black dots represent hypothetical haplotypes not detected in the current study.

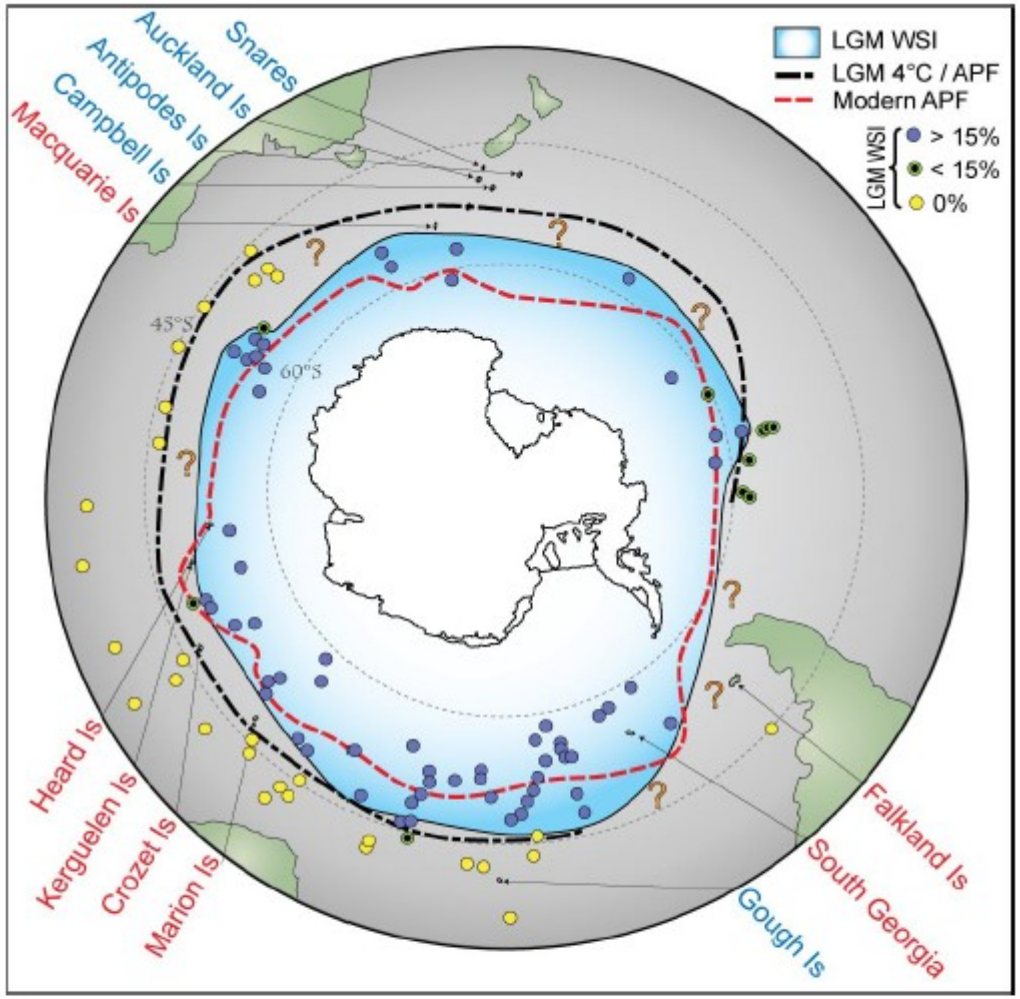

Fig. 3. Positions of the subantarctic islands in relation to present-day conditions and reconstructed LGM oceanographic features, including LGM WSI extent, modified from Gersonde *et al*. (13). Dot points indicate sediment core sites used to reconstruct LGM sea ice cover (after ref. 13): yellow dots contained no evidence of sea ice-associated diatoms, green dots indicate (minimal) evidence, and blue dots indicate high proportions of ice-indicator diatoms. Regions demarcated by question marks lack core data (13). Based on *D. antarctica* genetic data, red labels indicate "recolonized" islands putatively affected by LGM ice scour, whereas blue labels indicate putative "refugial" islands. The LGM 4 °C isotherm has been identified as a feature roughly equivalent, in terms of water properties and gradients, to the modern APF (13).

Fraser et al., 2009, PNAS

Fucus

Evolutionary geographic origins of *Fucus* and their phylogeny

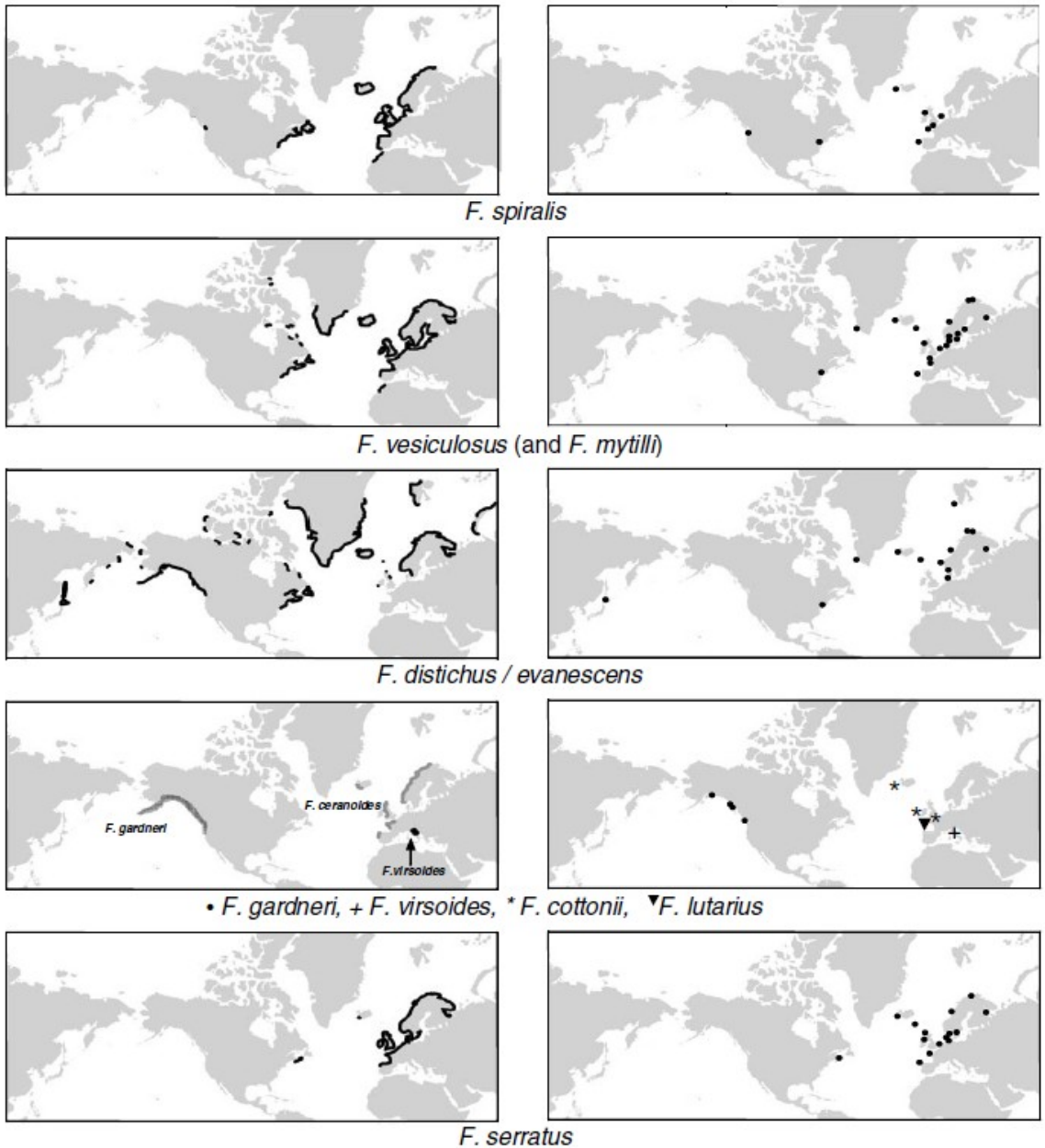

Fig. 1. Species distributions and sampling locations. Panels on the left show the ranges of each species of *Fucus* examined (adapted from Lüning, 1990). Panels on the right indicate approximate location of samples collected for this study. Distinction among *F. distichus, F. evanescens*, and *F. gardneri* in the northeastern Pacific remains unclear.

Coyer et al., 2006, Mol. Phyl. Evol.

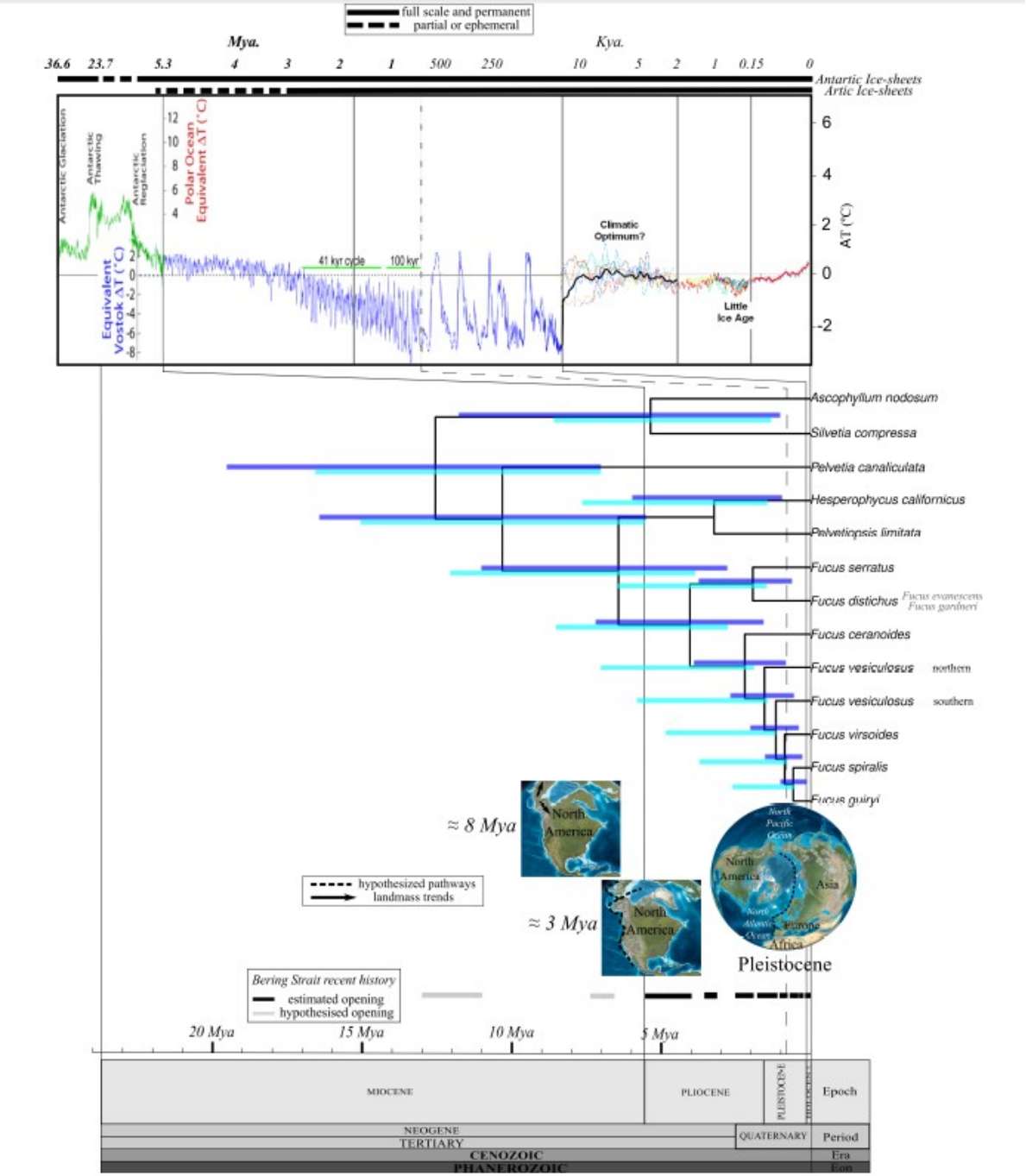

Figure 2 Bayesian dating of Fucaceae diversification. Simplified Bayesian dated phylogenetic reconstruction using the 13 coding loci. Node ages in million years (Myr) with their 95% HPD interval for both expansion growth (violet bars) and Yule speciation (cyan bars) models correspond to the time scale at the bottom of the Figure. Polytomies within species were collapsed for clarity, extracting the most divergent individuals (= leaf) from the Bayesian dating of Fucaceae diversification (for full tree see Additional file 4) Each paleogeographic reconstruction is placed at the estimated age (reproduced with permission of Dr. R. Blakey). Temperature graph shows paleoclimate reconstructions according to Zachos et al. ([40]; Paleocene to Miocene), Lisiecki et al. ([41]; Pliocene to Pleistocene) and Petit et al. ([39], Holocene) (reproduced with permission of Dr. R.A. Rohde). The ages and their correlation to the names on the geological timescale are based on Gradstein et al. [91]. Recent history of the Bering Strait is shown with the estimated and hypothesized openings [18,20].

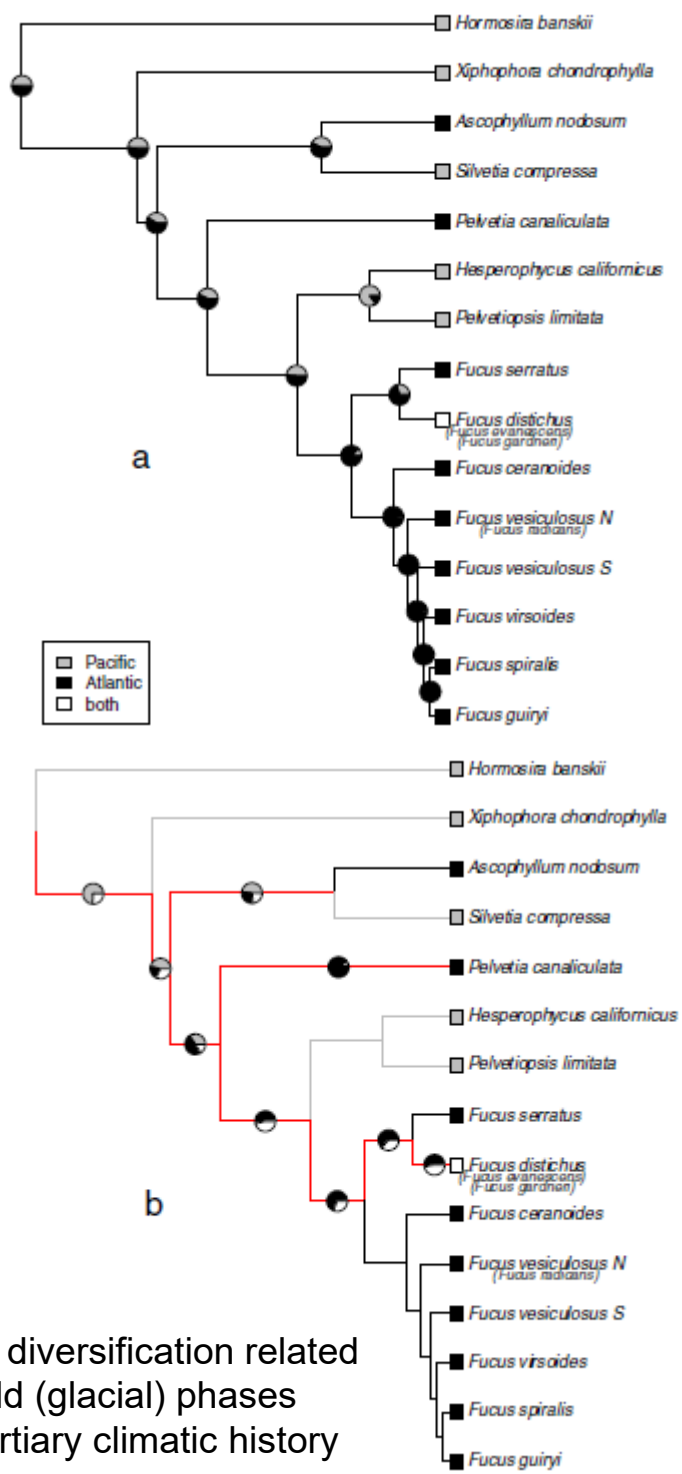

rapid diversification related to cold (glacial) phases of Tertiary climatic history

Cánovas et al., 2011, BMC Evol. Biol. 11:371.

Fucus vesiculosus – in tidal oceanic zones (eulittoral), cold seas, Baltic - sublitoral

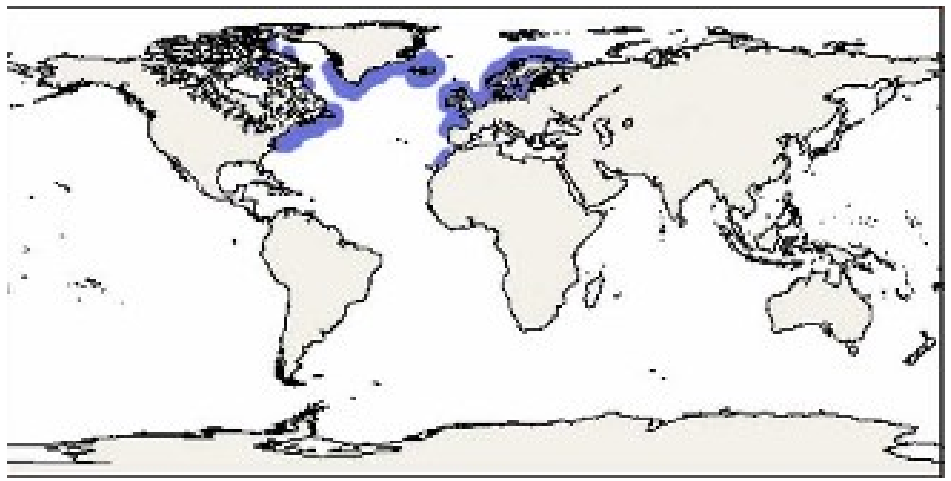

Fucus serratus – serrated margins of fyloides

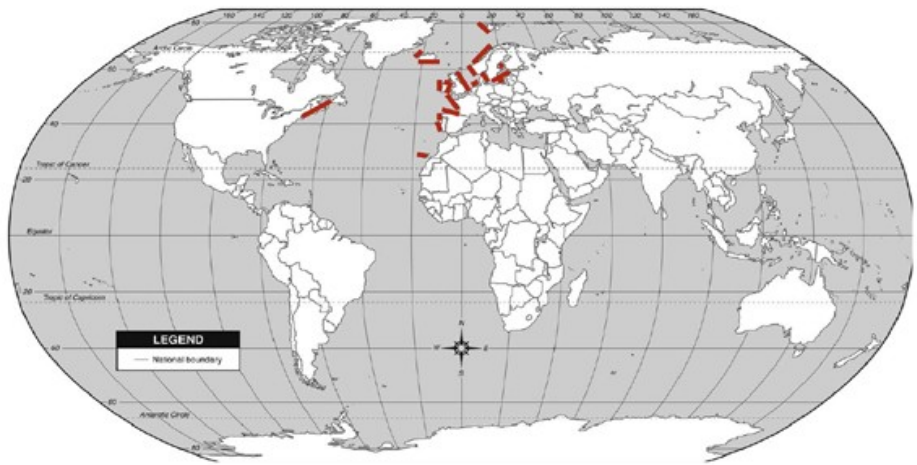

Adaptation of *Fucus serratus* to decreasing salinity in brackish waters

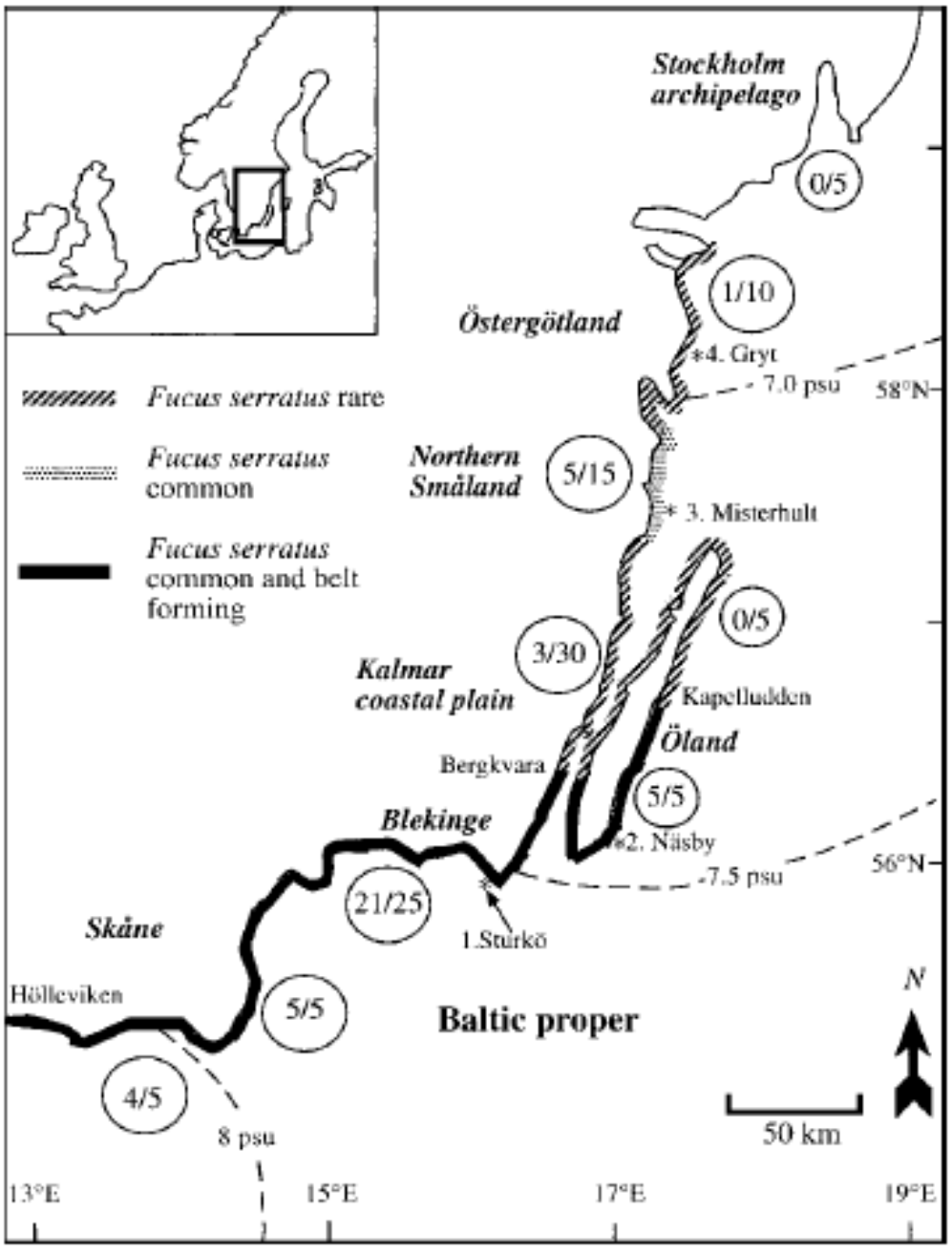

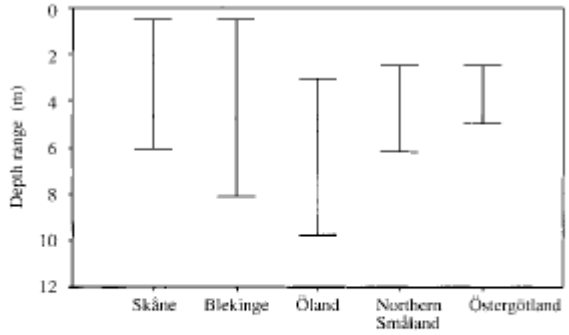

Fig. 2. Depth range of *Fucus serratus* in five regions of the Baltic proper based on 105 SCUBA diving transects.

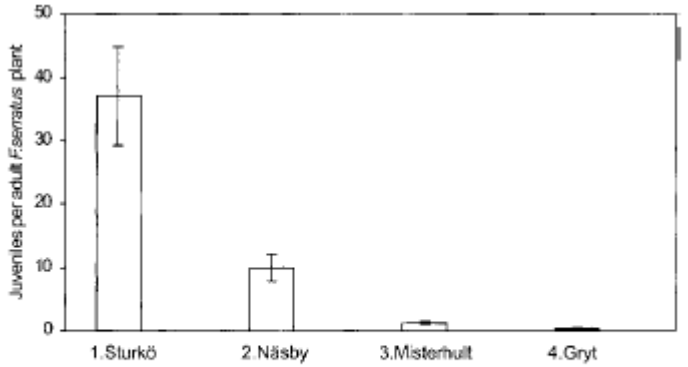

Fig. 3. Number of non-reproductive *Fucus serratus* plants (juveniles) (mean ± S. E.) per reproductive plant (adult) in Sites 1 to 4.

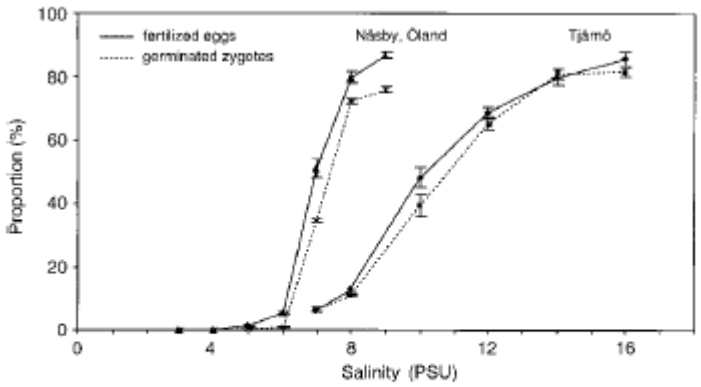

Fig. 4. Proportion of fertilised *Fucus serratus* eggs after 15 h and germination of zygotes (%) cultured at different salinities in natural seawater. The material from Näsby (Site

two sites – Kattegat and Baltic, locally adapted populations

critical stages of the life cycle at different salinities

Malm et al., 2001, Bot Mar 44: 101-108


F. spiralis

Microspeciation of *Fucus* in the Baltic

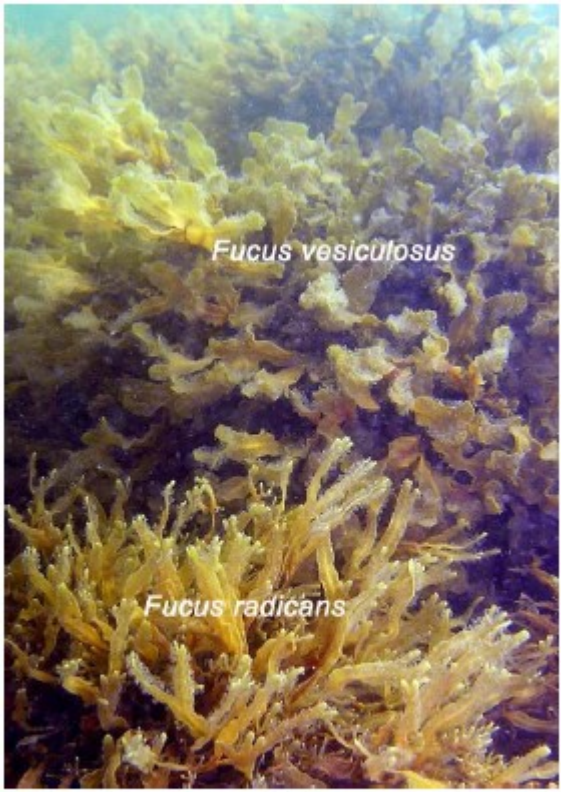

Figure 1
***Fucus radicans* and *F. vesiculosus*.** Picture showing both *Fucus* species living in sympatry without any environmental discontinuity in the SW Gulf of Bothnia (northern Baltic Se

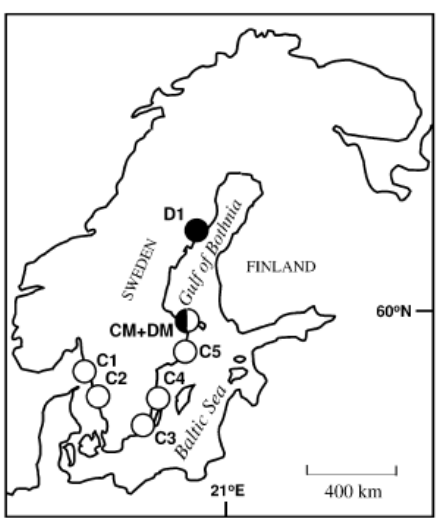

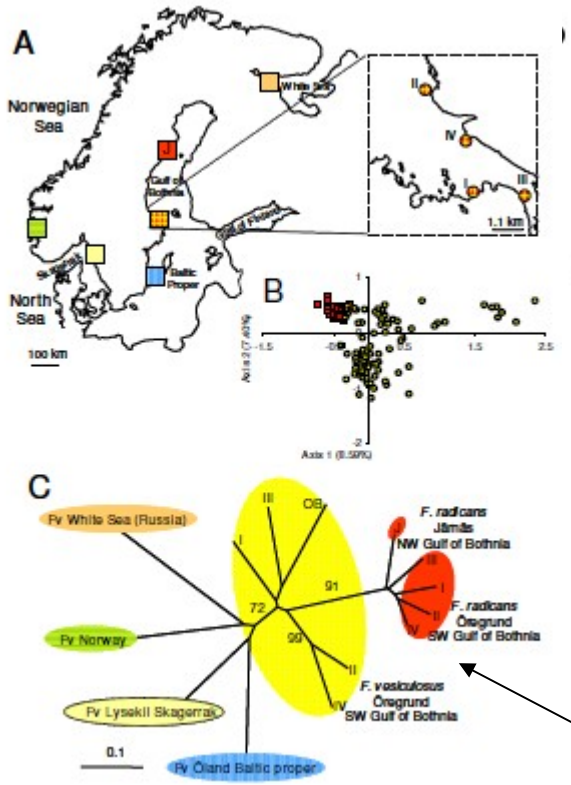

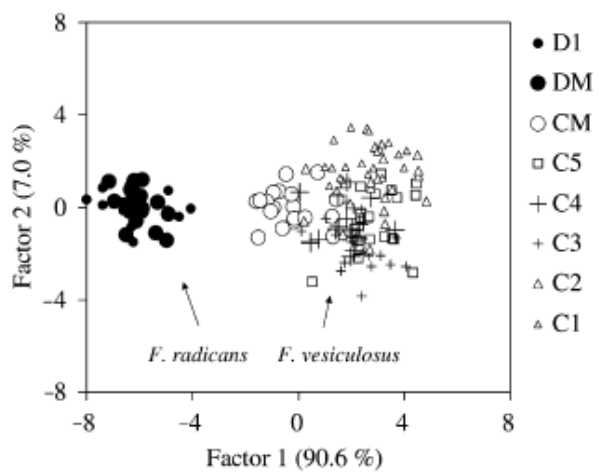

FIG. 6. Result of discriminant analysis of all populations based on five morphometric variables. Plot of discriminant function scores for each individual on the first two axes. Pillai's trace = 1.780, approx. F = 11.9, df = 35, 755, $P < 0.001$.

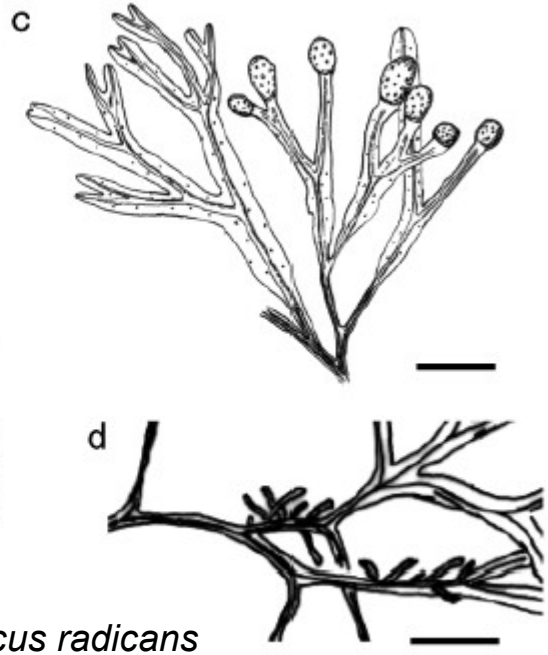

Fucus radicans

Baltic origin of the species

Bergstrom et al., 2005, J Phycol 41: 1025-1038
Pereyra et al. 2009, BMC Evol Biol 9: 70


F. radicans
F. vesiculosus

BUT - probable parallel speciation of *F. radicans* from *F. vesiculosus* in the Baltic Sea

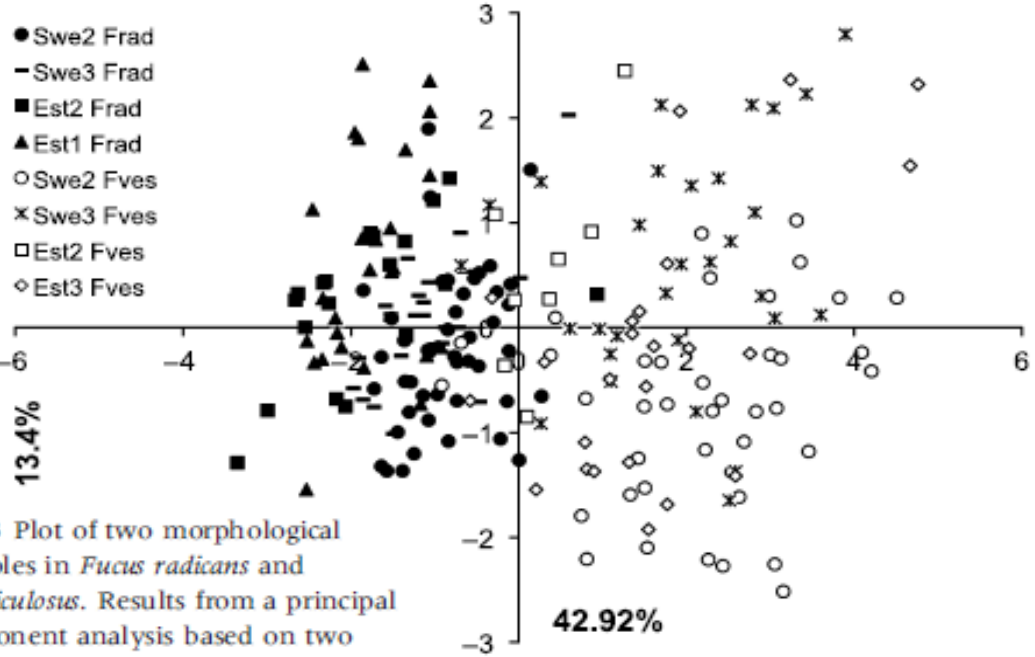

Fig. 3 Plot of two morphological variables in *Fucus radicans* and *F. vesiculosus*. Results from a principal component analysis based on two morphological variables with five measurements. Abbreviations from

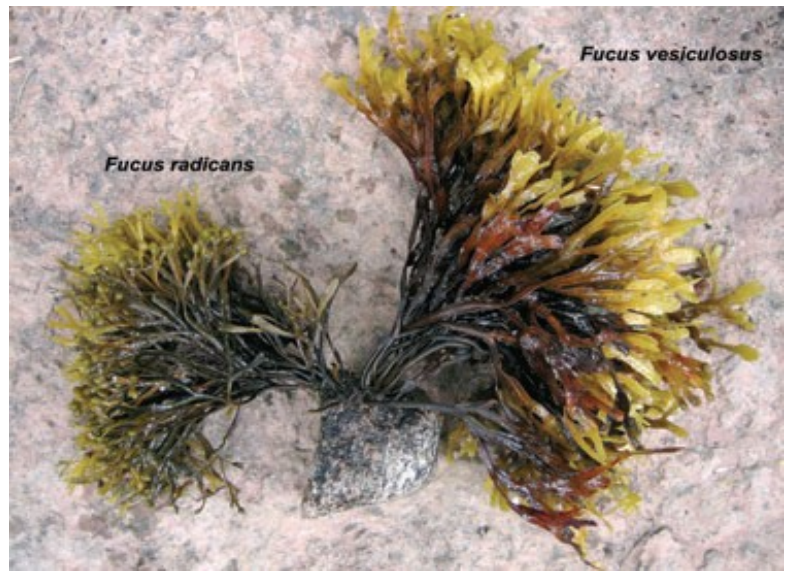

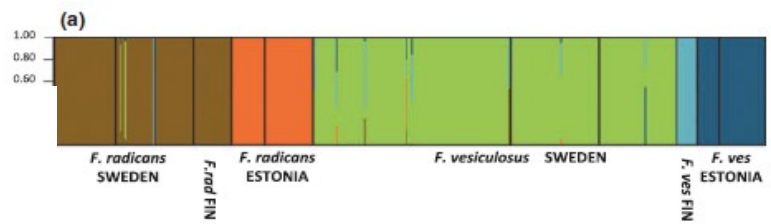

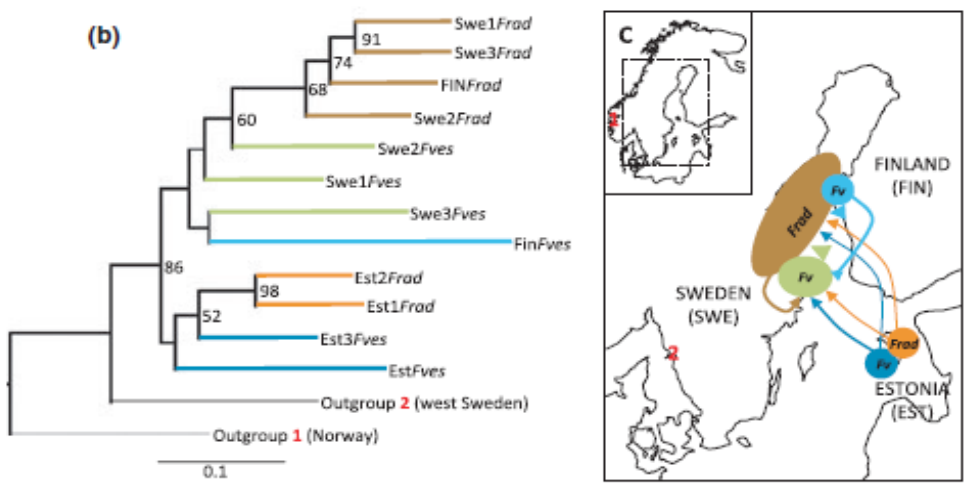

Fig. 4 Overall genetic differentiation between *Fucus* species in the Baltic Sea. (a) Combined histogram of Bayesian individual assignment test to illustrate the overall genotypic clustering of both species from all the sampling localities. Bars represent individual assignment probability into different genetic clusters depicted with colours, as in Fig. 2. (b) Neighbour-joining microsatellite-based population tree calculated with Cavalli-Sforza genetic distances. Out-group locations are indicated in Fig. 4c. (c) Map of the Baltic Sea with a superimposed gene flow network identifying the genetic sources among species and populations. Arrow thickness is proportional to the amount of gene flow to the indicated direction. Numbers 1 and 2 correspond to out groups *Fucus vesiculosus* from Eggholmen, Norway and Fiskebäckskil, west Sweden, respectively.

Pereyra et al., 2013, J. Evol. Biol.

Clonality (= genetic homogeneity) of *Fucus* population in relation to decreased salinity in the Baltic

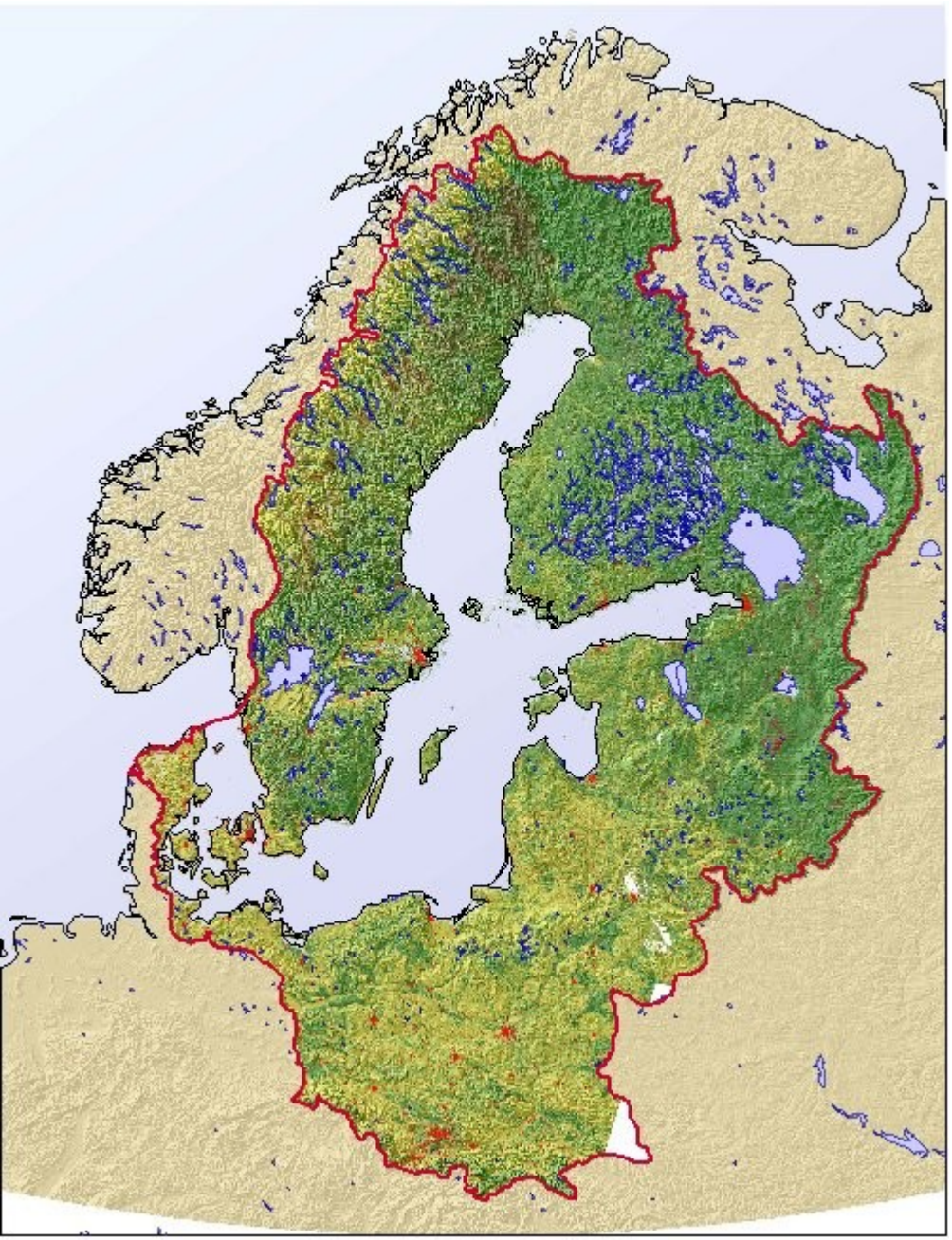

TABLE 1. Sampled locations, salinities, and number of thalli genotyped for two Baltic fucoid species, *Fucus radicans* and *F. vesiculosus*.

Sample	Region	Locality	Coordinates	Year	June salinity (PSU)	No. of thalli genotyped	
						Fucus radicans	*Fucus vesiculosus*
A	W Sweden	Kristineberg	58°15′ N, 11°27′ E	2003	>20.0	Absent	42
B	E Sweden	Öland	57°21′ N, 17°03′ E	2003	6.7	Absent	43
C	E Sweden	Öregrund	60°20′ N, 18°26′ E	2003	5.0	48	48
D	E Sweden	Djursten	60°23′ N, 18°24′ E	2007	5.0	49	51
E	NE Sweden	Bönhamn	62°53′ N, 18°18′ E	2007	3.8	30	34
F	NE Sweden	Järnäs	63°25′ N, 19°40′ E	2003	3.5	48	Absent
G	W Finland	Hällkalla	63°25′ N, 20°57′ E	2007	4.0	50	Absent
H	W Finland	Södra Vallgrund	63°09′ N, 21°13′ E	2007	4.3	50	16
I	W Finland	Märigrund	62°31′ N, 21°03′ E	2007	5.2	50	Not sampled
J	W Finland	Sälskär	62°19′ N, 21°10′ E	2007	5.5	44	Not sampled
K	Estonia	Pulli Panki	58°36′ N, 22°58′ E	2006	5.6	15	9
L	Estonia	Triigi	58°35′ N, 22°43′ E	2006	5.8	25	Absent
M	Estonia	Kõiguste	58°22′ N, 22°58′ E	2006	5.2	Absent	23

June salinities are averaged over 10 years (see text for details).
PSU, practical salinity units.

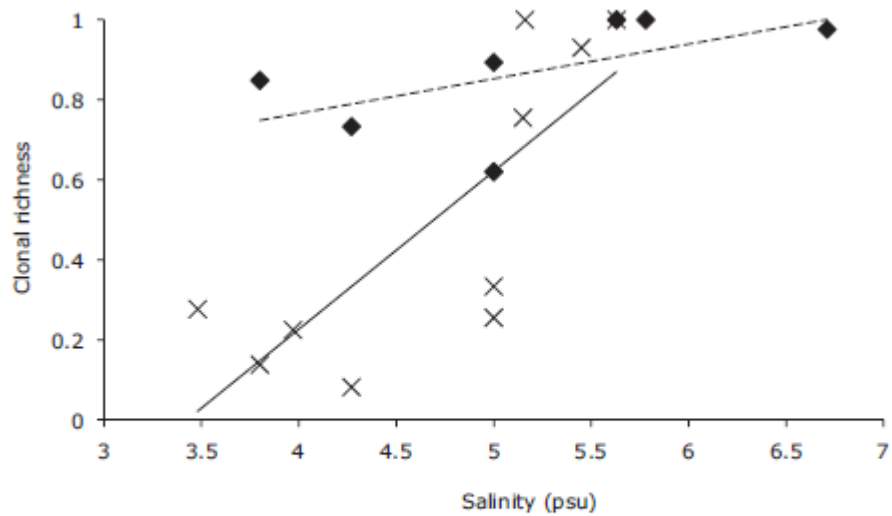

FIG. 2. Relationship between salinity and clonal richness of populations of *Fucus radicans* (crosses, dotted trend line, $R^2 = 0.62$, $P = 0.007$) and *F. vesiculosus* (diamonds, broken trend line, $R^2 = 0.34$, $P = 0.17$).

Johannesson et al., 2011, J. Phycol.

Ascophyllum (nodosum)

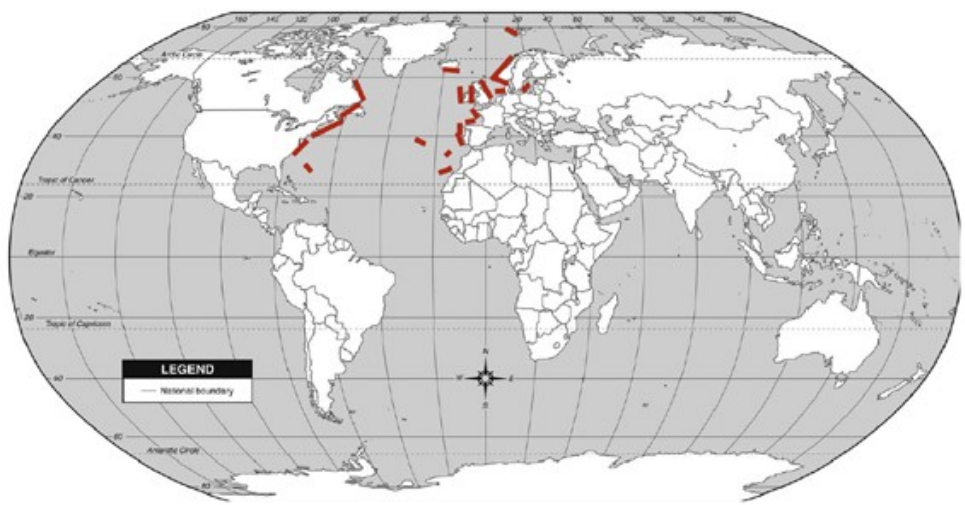

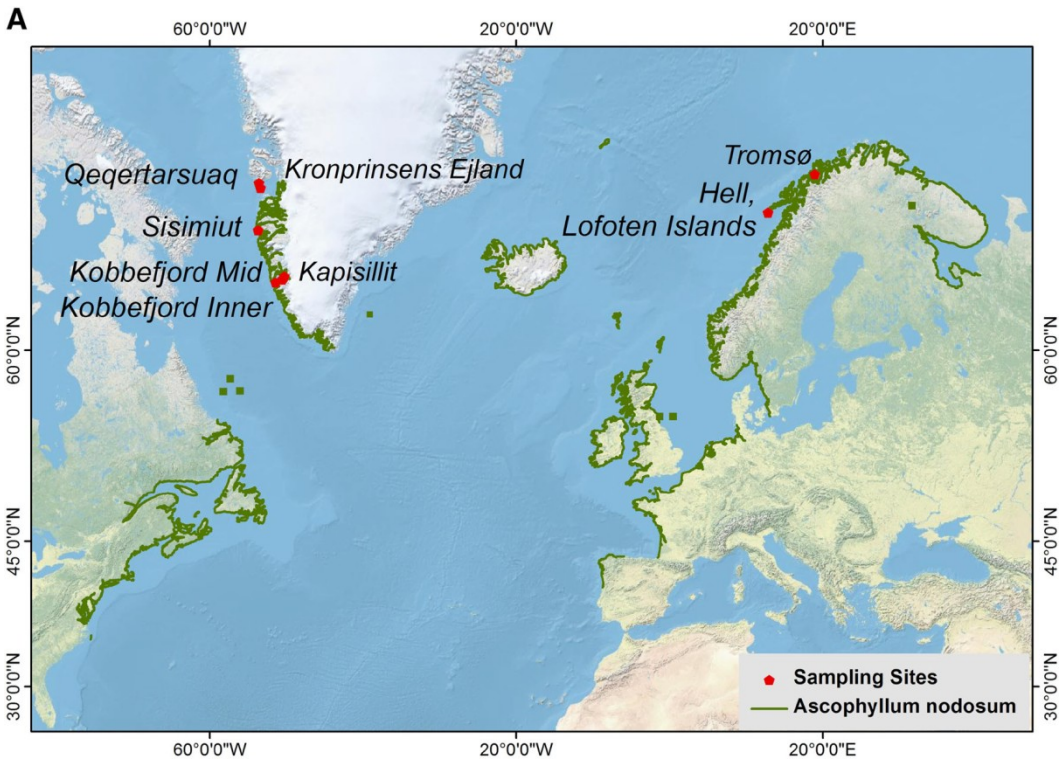

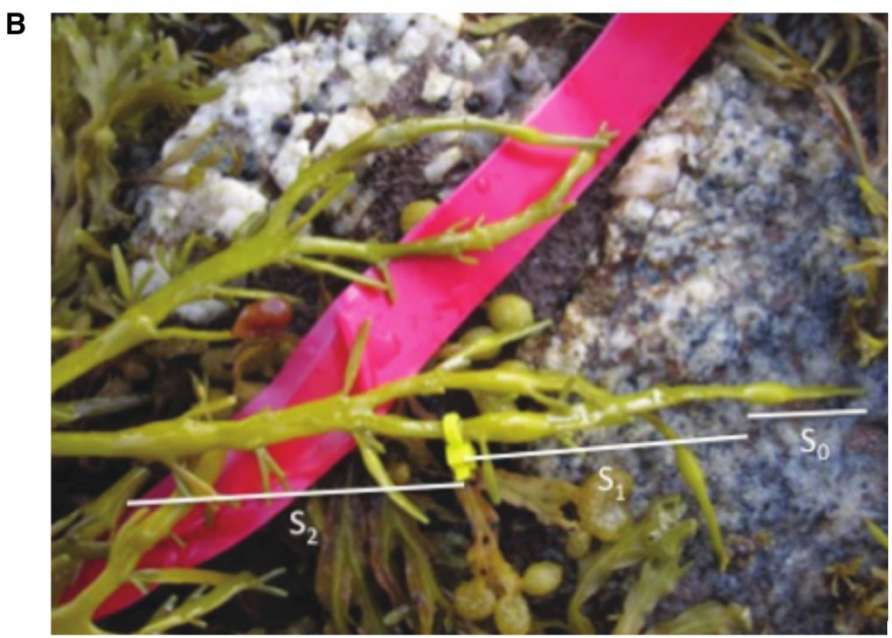

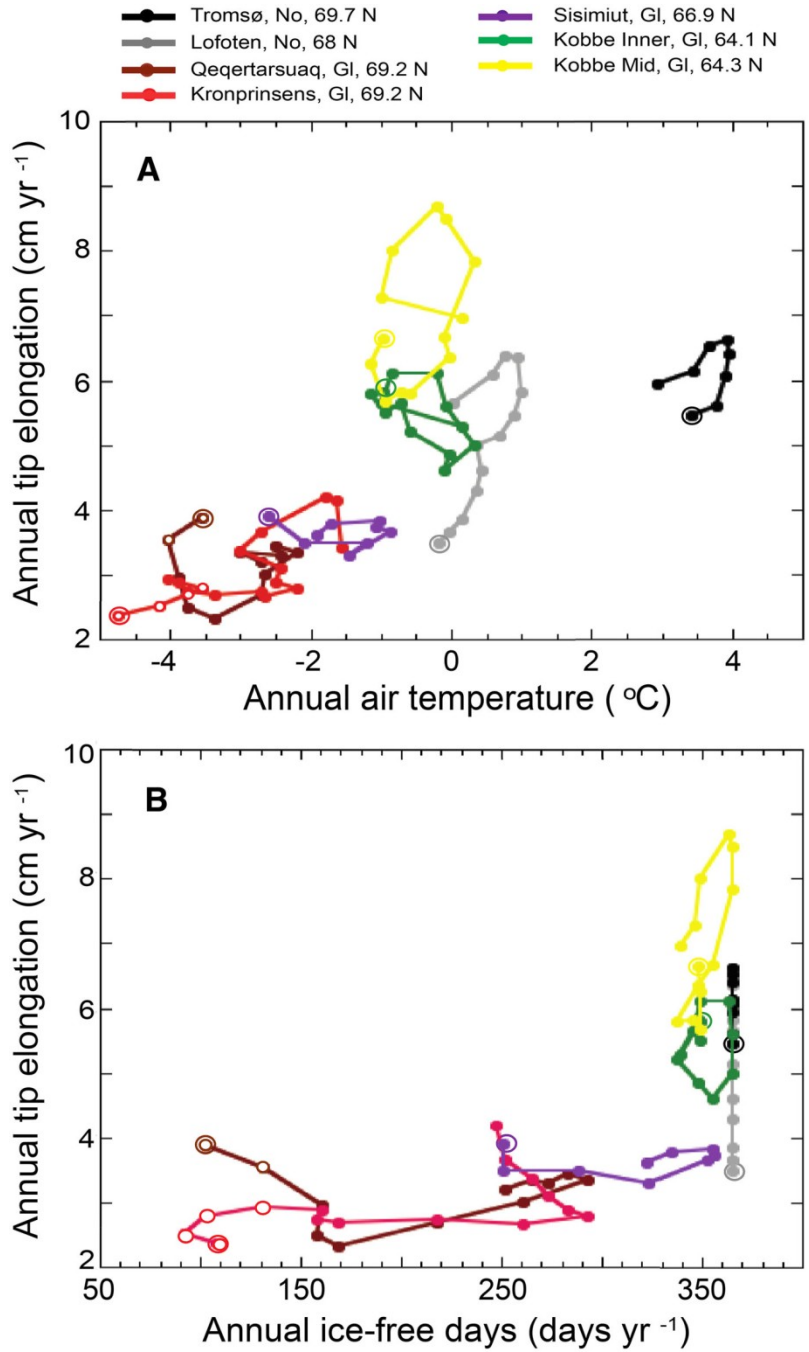

effect of warming in northern parts of the distribution area

Marba et al., 2017, Ambio

Sargassum – warm temperate to tropical waters

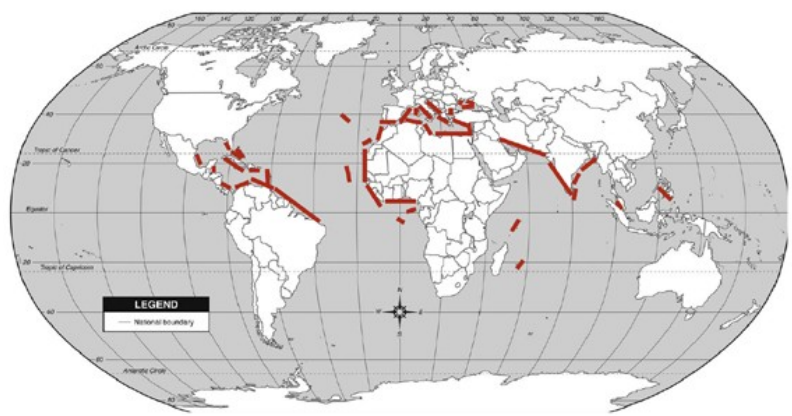

S. vulgare

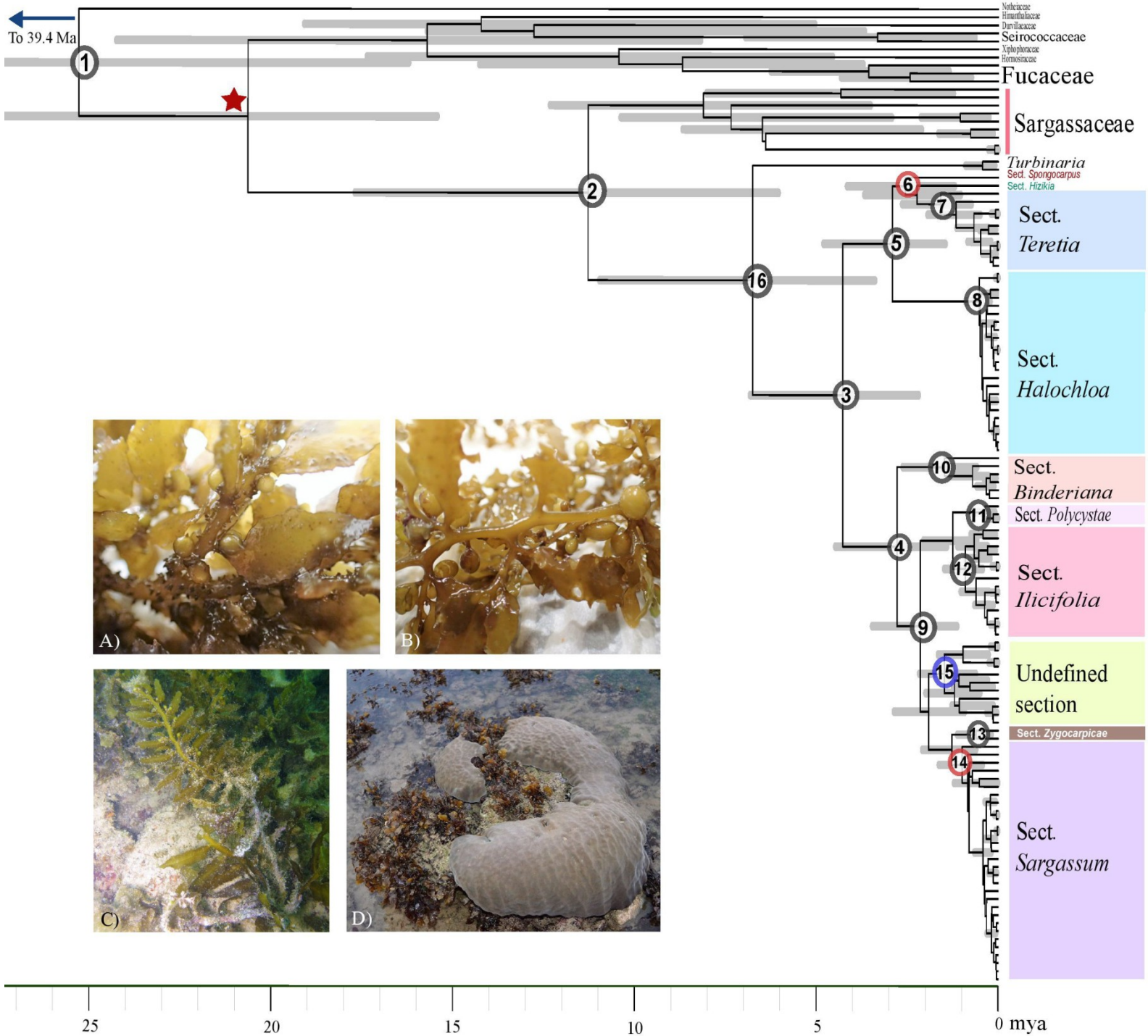

Yip et al., 2019

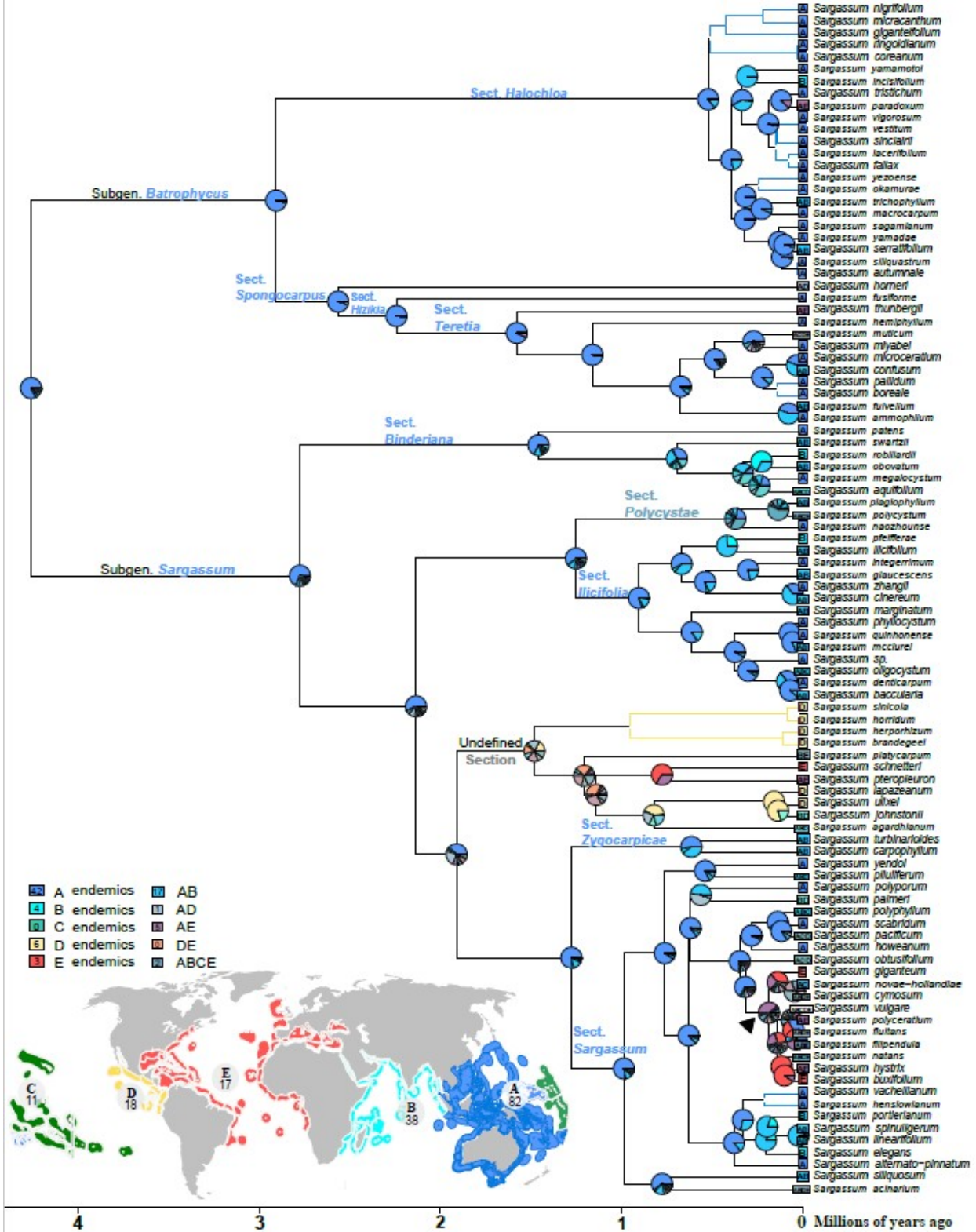

Yip et al., 2019

Sargassum – benthic and pelagic species (Sargasso sea)

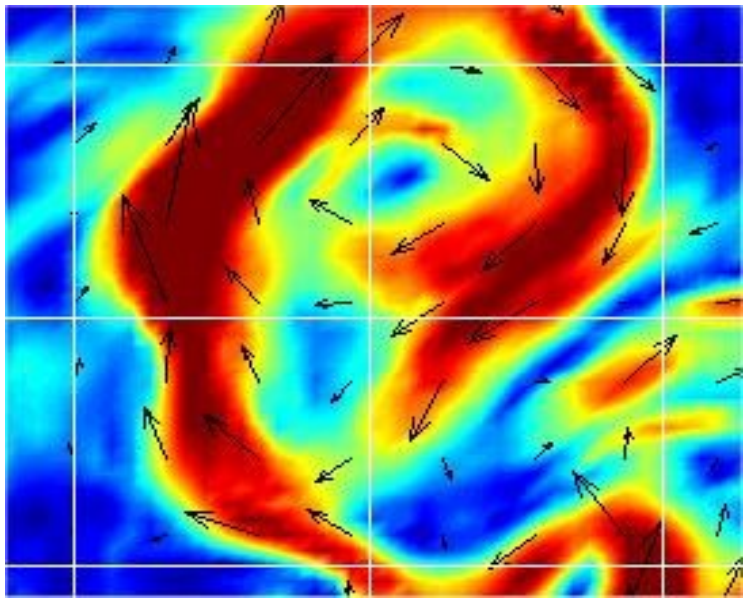

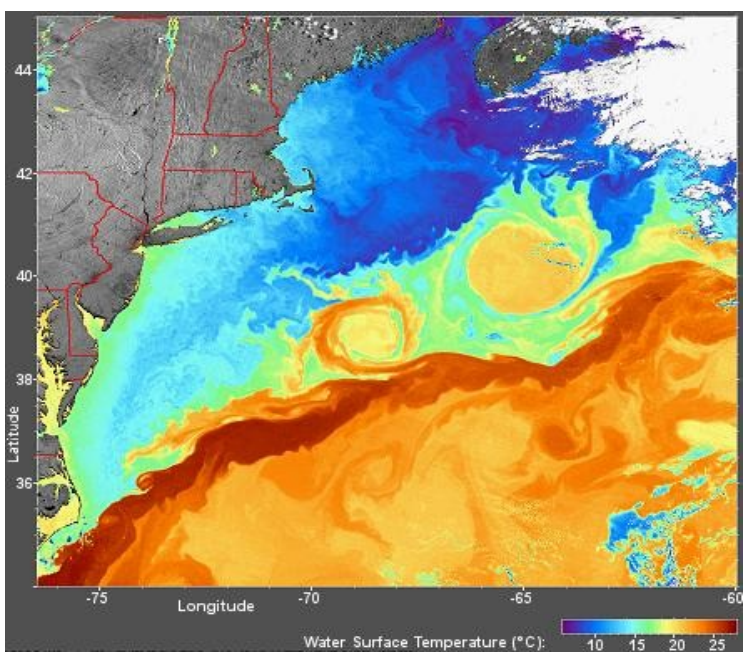

floating Sargassum in Brazil (Frenando Noronha) and Carribean

Sissini et al., 2017, Phycologia

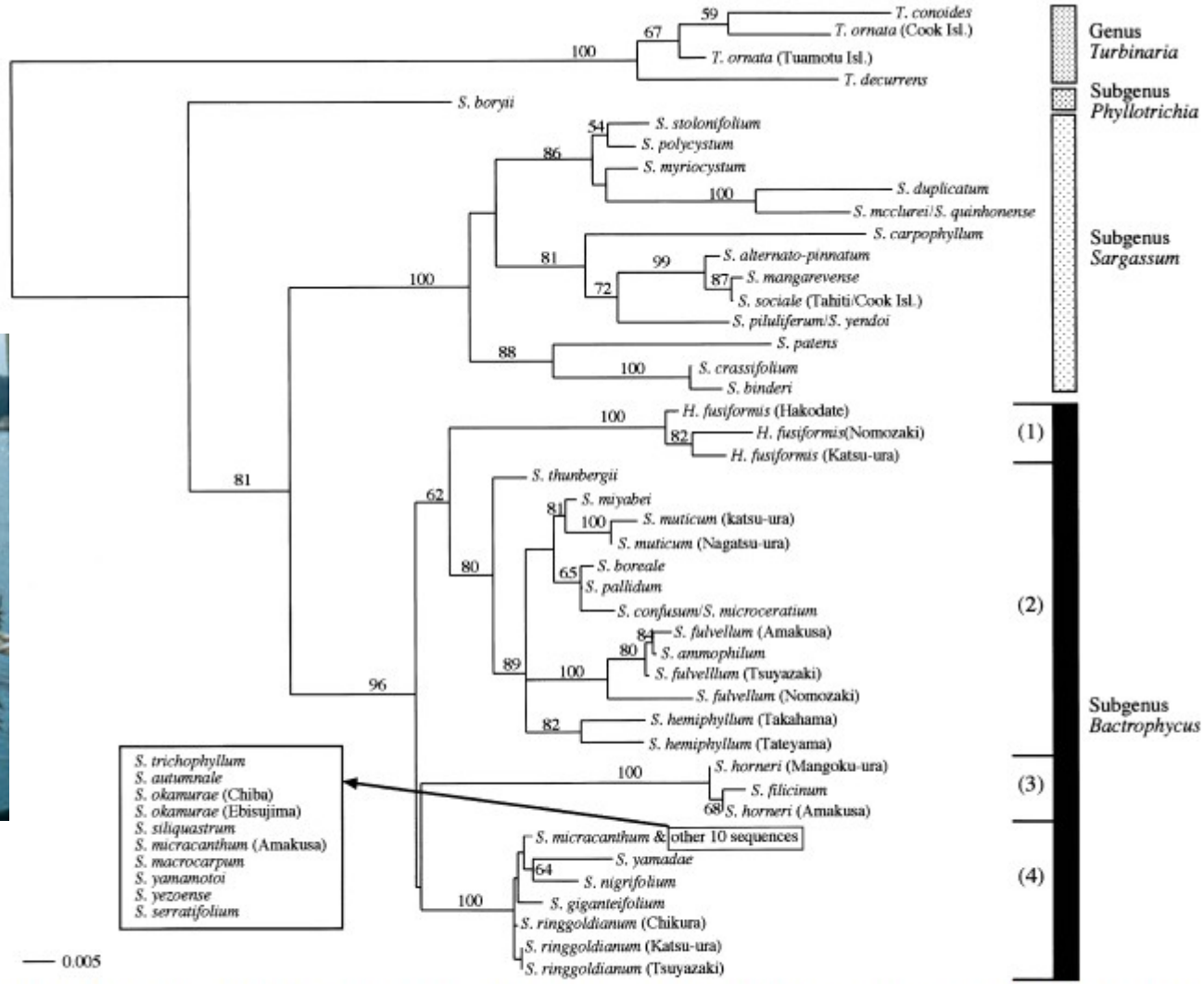

Fig. 1. Phylogenetic affinities within the genus *Sargassum*, implemented by the neighbor-joining method based on ITS-2 alignment. The numbers in parentheses (1) – (4) indicate the clade within the subgenus *Bactrophycus*, each corresponding to the sections as follows; (1) section *Hizikia*; (2) section *Teretia*; (3) section *Spongocarpus*; and (4) sections *Halochloa*/*Repentia*. The list of species enclosed by the square indicates the taxa which possessed exactly the same sequence as the one of *S. micracanthum*. The numbers at each node represent bootstrap value (1000 replicates). Scale bar = substitutions/site.

Hizikia belongs to *Sargassum* (subgenus *Bactrophycus*)

Stiger et al., 2003, Phycol. Res.

Turbinaria – a tropical genus

often grows in coral ecosystems

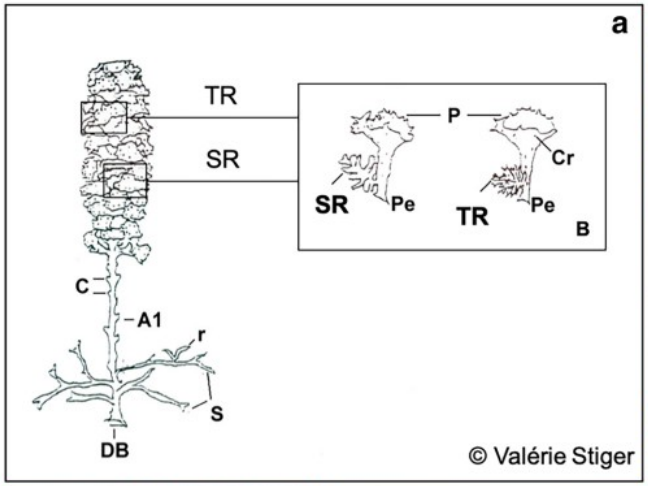

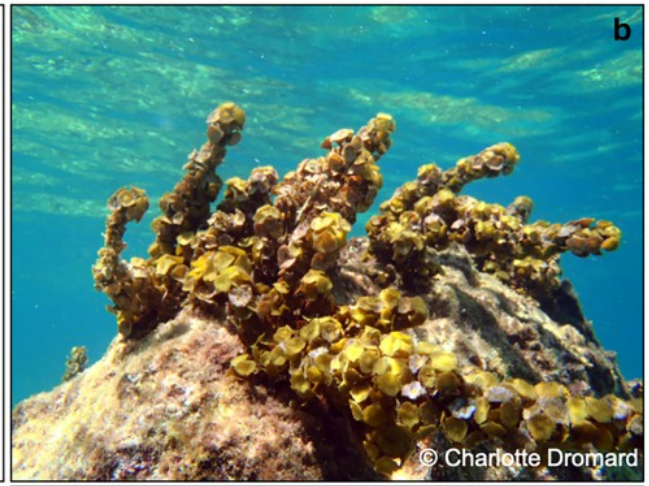

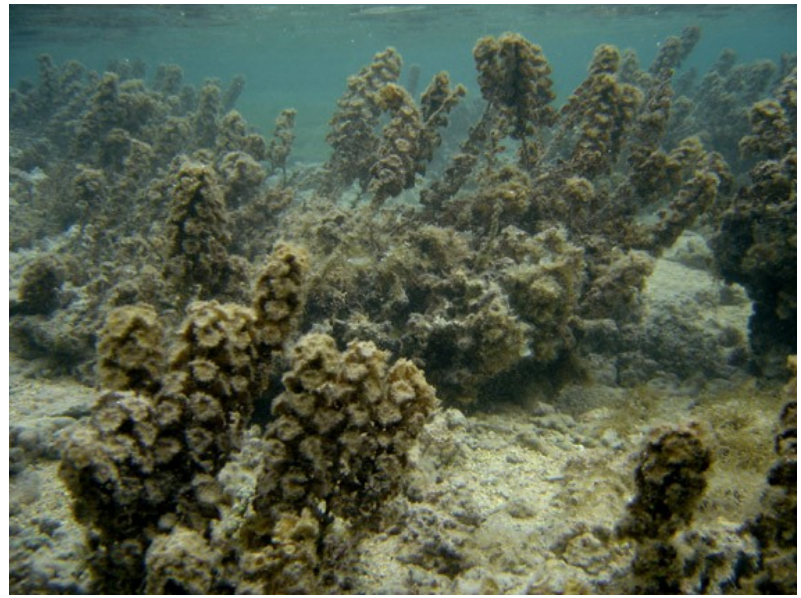

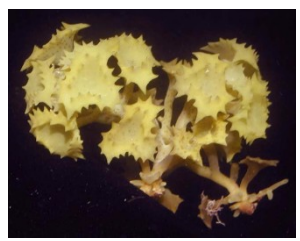

T. ornata

Fig. 1 General morphology of a thallus of *Turbinaria*, showing **a** the general aspect of the thallus and **b** detail of blades and receptacles, **c** individuals of *T. turbinata* from Guadeloupe (French West Indies, Atlantic Ocean), **d** *T. ornata* from French Polynesia (South Pacific Ocean), and **e** *T. decurrens* from Mayotte (Indian Ocean). A1: main axis; C: scars; Cr: cryptostomata; DB: basal disc; P: blades (pleuridies); SR: squat receptacle (female); TR: tapered receptacle (male or monoecious); r: clonal regrowth; S: runners

T. turbinata

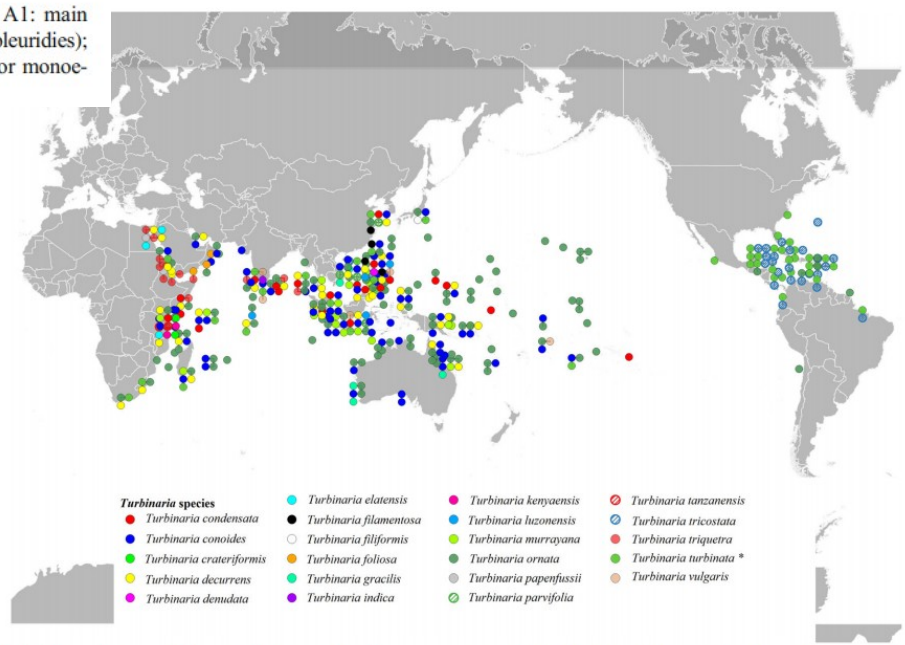

Fig. 2 Map illustrating the currently known distribution of *Turbinaria* species according to distribution data stored in Algaebase (Guiry and Guiry 2020) and unpublished data collected by C. Payri. Map created by Sylvie Fiat. * indicates type species

Zubia et al., 2020, J. Appl. Phycol.

Cystoseira s.l. – a Mediterranean fucalean lineage of Sargassaceae

Ericaria amentacea

Gongolaria barbata

Cystoseira compressa

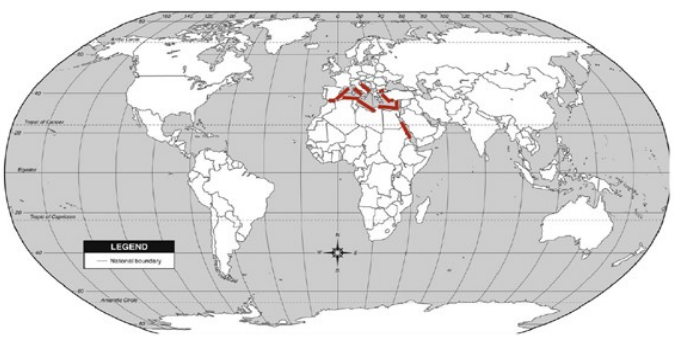

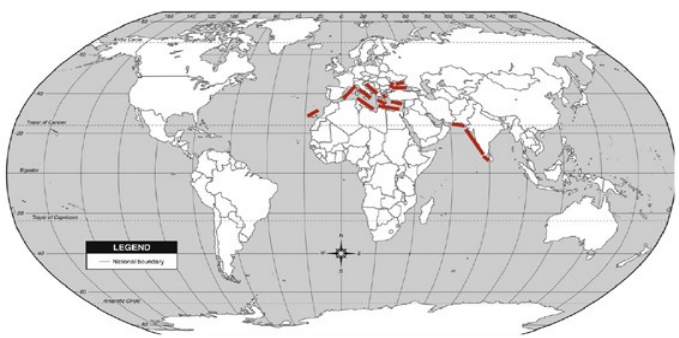

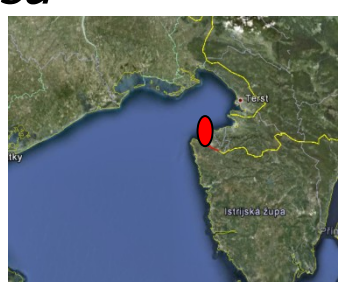

upper sublittoral; ecologically stable habitats


C. barbata, S. vulgare, C. compressa

phenological cycles of perennial thalli
phenotypic plasticity

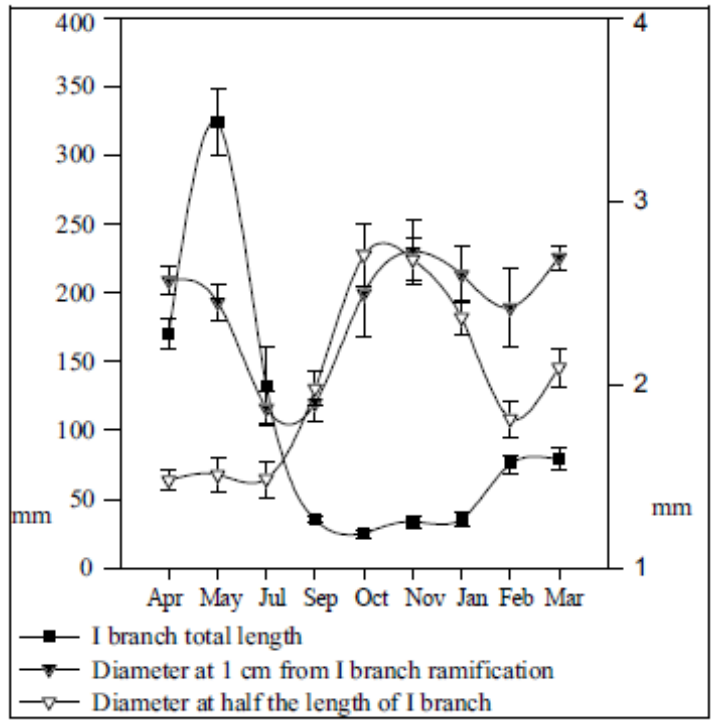

Fig. 3: Diagram of the I branches total length and diameter, measured at 1cm from the ramification and at half the length.

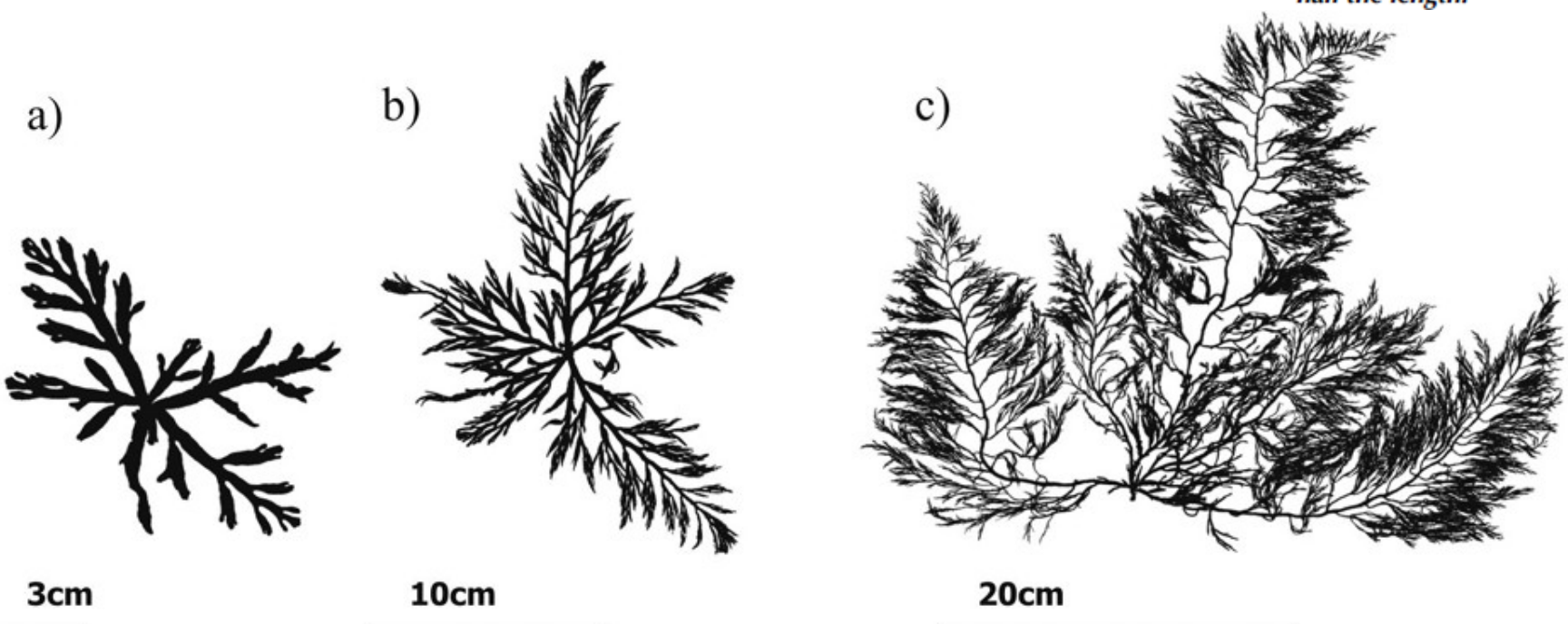

Fallace et al., 2005


profound seasonal phenological cycles

C. humilis

Neiva et al., 2023,
Eur. J. Phycol 58

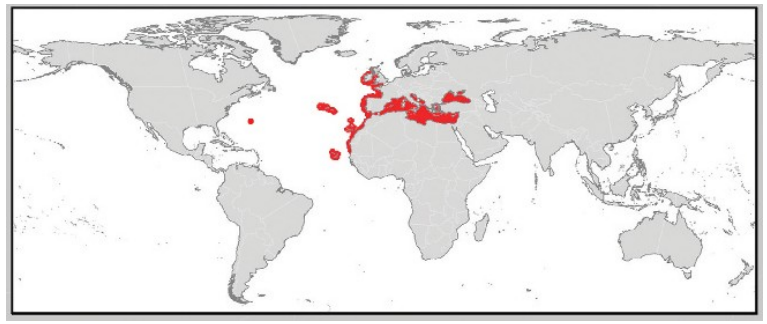

global distribution of *Cystoseira* s.l.

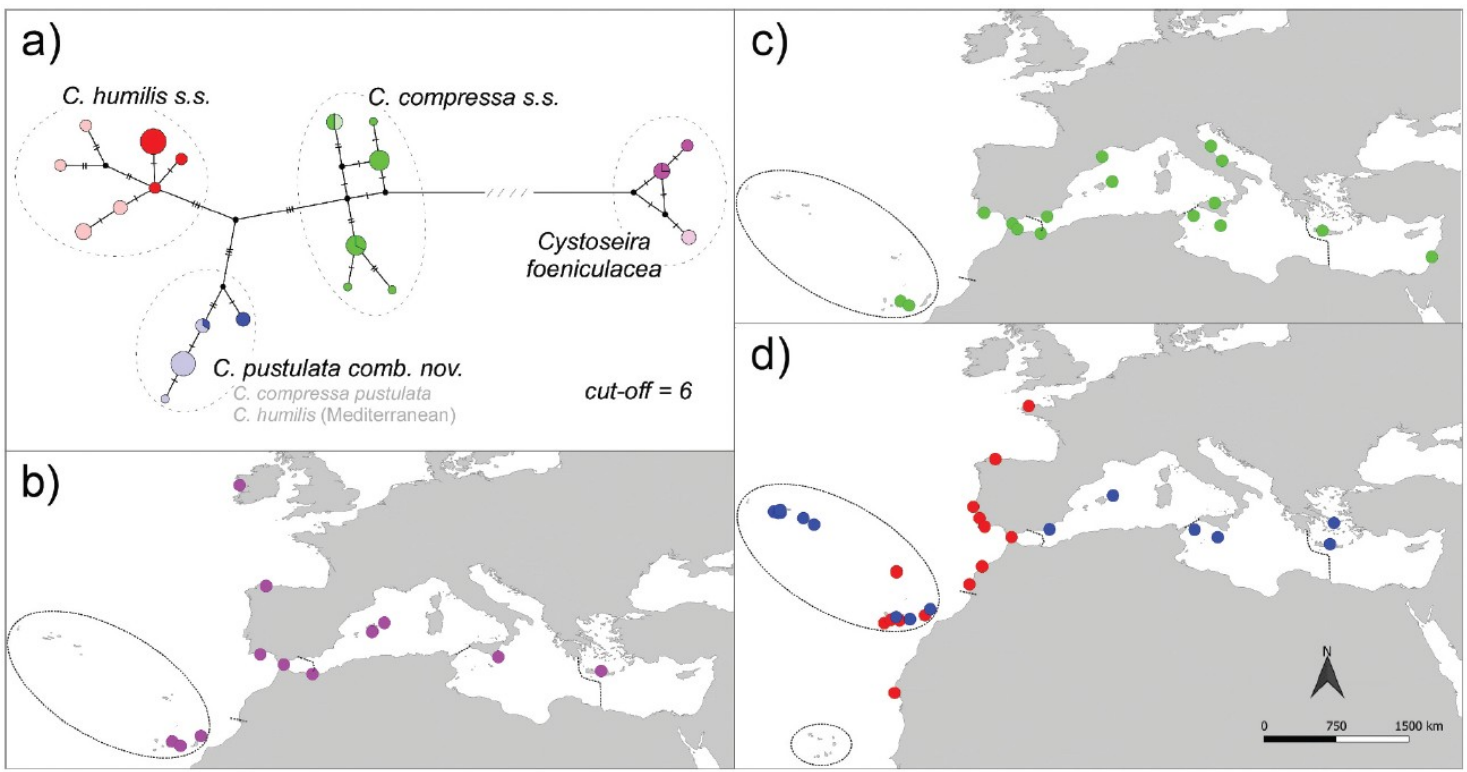

Fig. 2. Genetic entities and distribution of *Cystoseira* s.s. (**a**) *Cox*1 TCS haplotype network, with dashed circles delimiting inferred MOTUs (see discussion for taxonomic names). Haplotypes are represented by circles sized to their frequency. Pale colours indicate variation endemic to temperate Macaronesia (Azores, Madeira, Canary Islands), strong colours indicate haplotypes sampled elsewhere. Small dashes along the lines connecting haplotypes represent one bp mutation, larger dashes delimit major lineages, and black dots represent internal nodes. (**b–d**) Geographic sampling of each MOTU, using the same general colour code as in (**a**). Dashed lines separate major oceanographic regions as depicted in Fig. 1.

C. compressa

C. foeniculacea

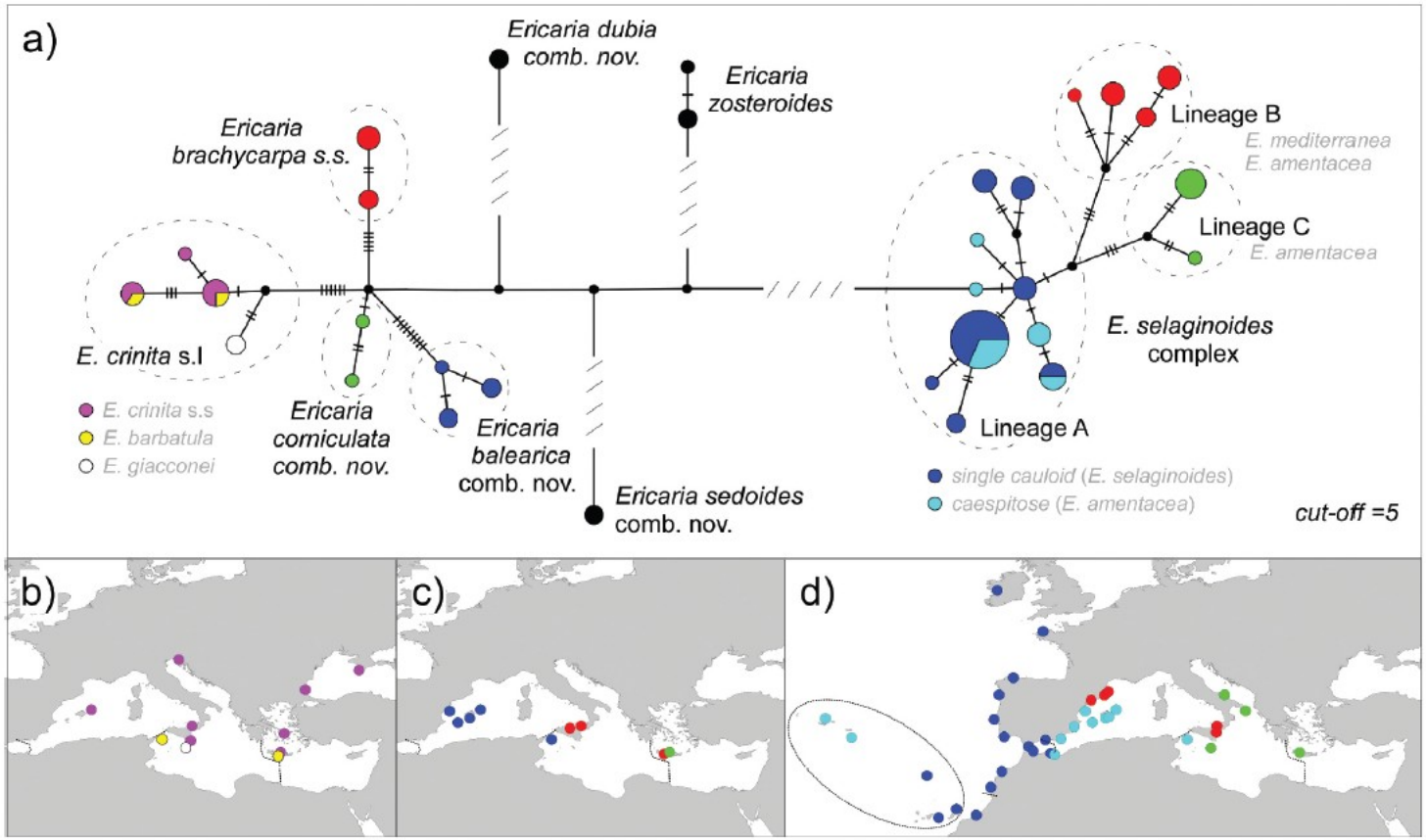

Fig. 3. Genetic entities and distribution of *Ericaria*. (**a**) *Cox*1 TCS haplotype network, with dashed circles delimiting inferred MOTUs (see discussion for taxonomic names). Haplotypes are represented by circles sized to their frequency. Small dashes along the lines connecting haplotypes represent one bp mutation, larger dashes delimit major lineages, and black dots represent internal nodes. (**b–d**) Geographic sampling of each MOTU, using the same colour code as in (a) with (**b**) depicting *E. crinita* s.l., (**c**) *E. corniculata, E. balearica* and *E. brachycarpa* s.s., and (**d**) *E. selaginoides* complex. Dashed lines separate major oceanographic regions as depicted in Fig. 1. *E. dubia, E. zosteroides* and *E. sedoides* were not mapped.

E.crinita

E. amentacea

Neiva et al., 2023, Eur. J. Phycol 58

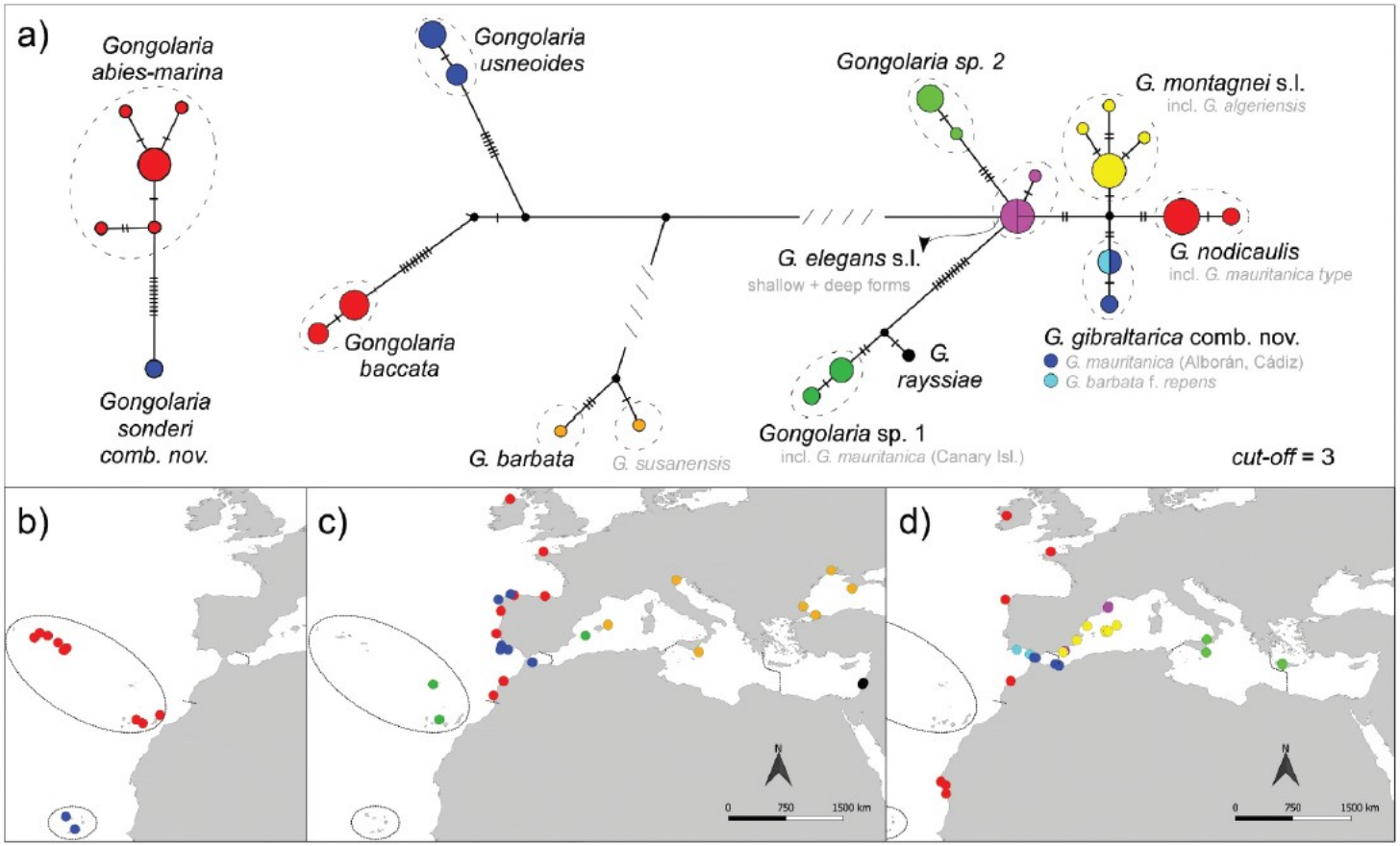

Fig. 4. Genetic entities and distribution of *Gongolaria*. (**a**) *Cox*1 TCS haplotype networks of clade A (left) and clade B (right), with dashed circles delimiting inferred MOTUs (see discussion for taxonomic names). Haplotypes are represented by circles sized to their frequency. Small dashes along the lines connecting haplotypes represent one bp mutation, larger dashes delimit major lineages, and black dots represent internal nodes. (**b–d**) Geographical sampling of each MOTU, using the same colour code as in (a) with (**b**) depicting *G. abies-marina* and *G. sonderi*, (**c**) *G. baccata, G. usneoides, G. barbata* (incl. Marzameni's '*G. susanensis*'), *G. rayssiae* and *Gongolaria* sp. 1, and (**d**) *G. nodicaulis, G. montagnei* s.l., *G. elegans* s.l. (incl. Columbrete's *G. sauvageauana*), *G. gibraltarica* and *Gongolaria* sp. 2. Dashed lines separate major oceanographic regions as depicted in Fig. 1.

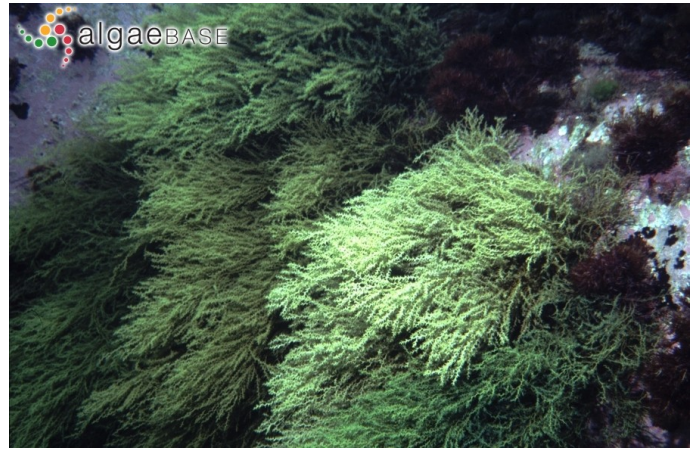

G. abies-marina

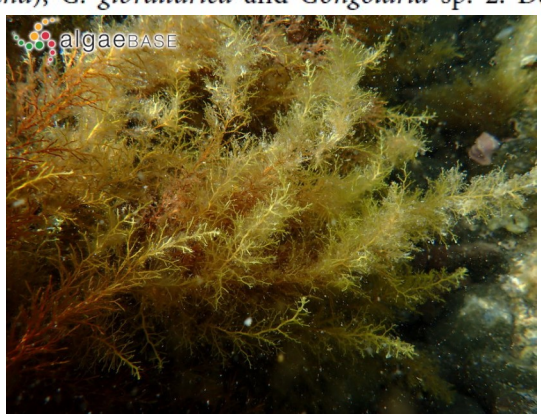

G. barbata

Neiva et al., 2023, Eur. J. Phycol 58

Recent decline of subtropical Fucales in the Mediterranean

Table 2
Status of the Fucales species on the Albères coast

Species	Abundance				Trend
	Sauvageau (1912)	Feldmann (1937a,b)	Gros (1978)	This study	
C. barbata	F	F	R	–	Extinct
C. caespitosa	F	F	R	R	Decrease
C. compressa f. *compressa*	VA	VA	VA	VA	=
C. crinita	F	F	R	–	Extinct
C. elegans	F	F	R	VR	Nearly extinct
C. foeniculacea f. *latiramosa*	R	–	–	–	Extinct
C. foeniculacea f. *tenuiramosa*	F	F	R	–	Extinct
C. funkii	R	R	–	–	Extinct
C. mediterranea	VA	VA	A	A	Decrease
C. sauvageauana	R	VR	–	–	Extinct
C. spinosa var. *compressa*	A	A	VR	–	Extinct
C. spinosa var. *spinosa*	R	?	VR	–	Extinct
C. zosteroides	F	F	F	R	Decrease
S. acinarium	?	R	–	–	Extinct
S. hornschuchii	?	F	–	–	Extinct
S. vulgare	R	F	–	–	Extinct

A: abundant, F: frequent, R: rare, VA: very abundant, VR: very rare, ?: unknown; –: not reported.

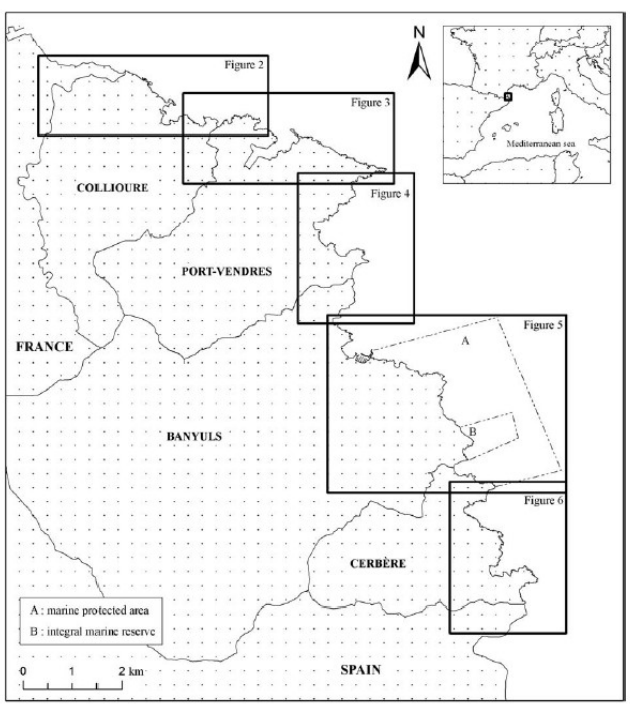

Fig. 1. The Albères coast.


Cystoseira compressa


Sargassum vulgare


Cystoseira barbata

Thibaut et al., 2005, Mar Pollut Bull 50: 1472-1489

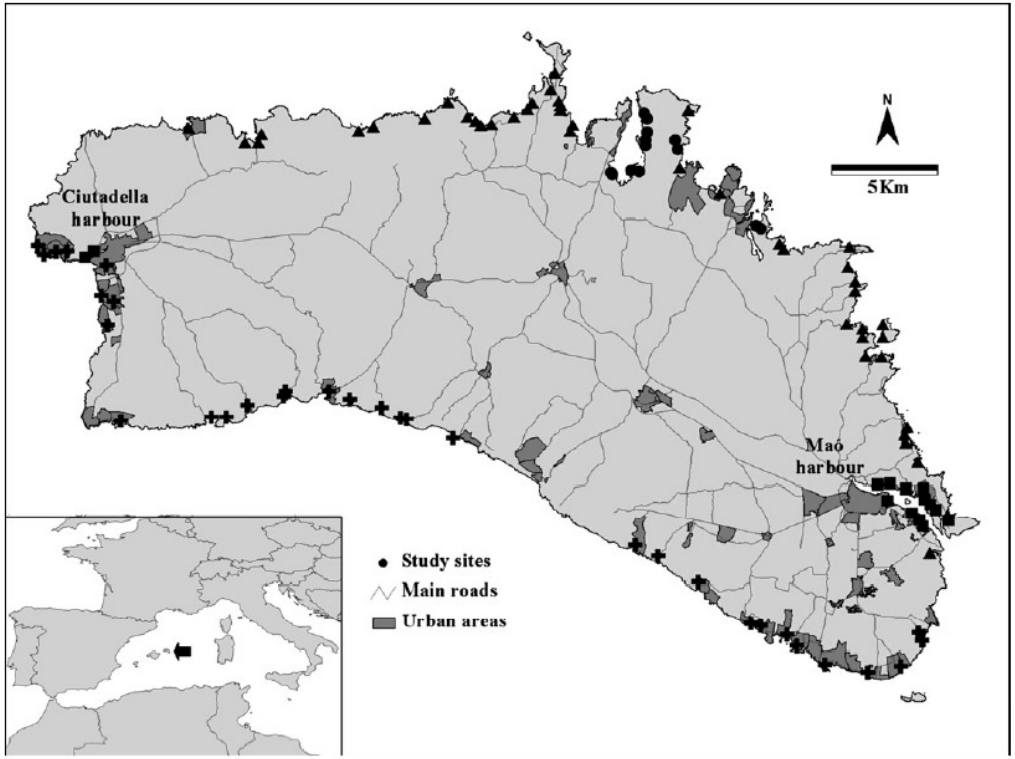

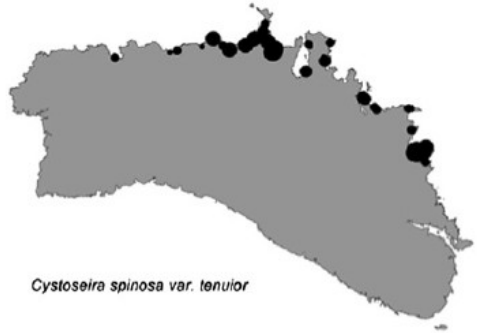

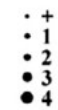

Fig. 1. Map of Menorca (Balearic Islands) showing location and type of the study sites (triangle: north, round: very sheltered, cross: south, square: harbour). Urban areas and main roads are represented and the most important harbours are indicated.

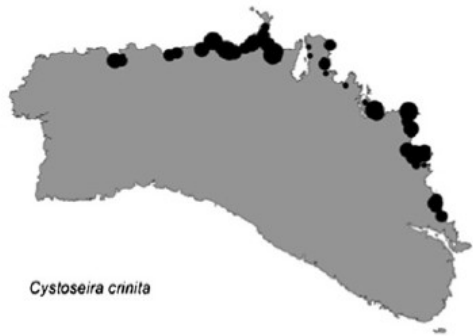

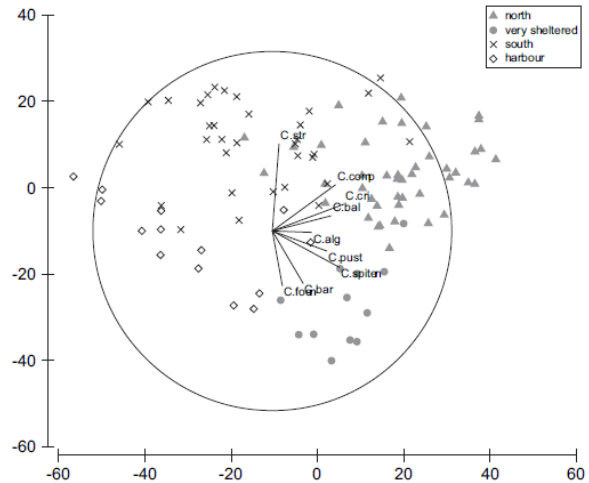

Fig. 4. Distance-based redundancy analysis showing direction of increasing abundances of different species along the study sites. C.str: *Cystoseira amentacea var. stricta*, C.comp: *C. compressa v. compressa*, C.cri: *C. crinita*, C.bal: *C. brachycarpa var. balearica*, C.alg: *C. algeriensis*, C.pust: *C. compressa v. pustulata*, C.spiten: *C. spinosa v. tenuior*, C.bar: *C. barbata*, C.foen: *C. foeniculacea v. tenuiramosa*. Axis I explains 63.9% variation out of the fitted model and 38.4% of the total variation, while axis II explains respectively 26.9% and 16.2% of the variation.

Sales & Ballesteros, 2009, Estuar. Coast. Shelf Sci. 84: 476-482.

Laminariales

- reduced microthallus (G) + foliose macrothallus (S)
- diplohaplontic cell cycle, heteromorphic, oogamy, no plurilocular zoidangia

Laminariales

taxonomic overview

Chordaceae (or Chordales) – 1 g, 6 sp (Chorda)

Pseudochordaceae (alternatively within Chordales) – 1 g, 2 sp

Akkesiphycaceae (alternatively within Chordales) – 1 g, 1 sp

Aureophycaceae – 1 g, 1 sp (Aureophycus)

Lessoniaceae – 4 g, 31 sp (incl. Ecklonia, Egregia, Lessonia)

Agaraceae – 5 g, 11 sp (incl. Agarum, Costaria)

Alariaceae – 8 g, 27 sp (incl. Alaria, Undaria)

Laminariaceae – 14 g, 63 sp (incl. Nereocystis, Macrocystis, Laminaria, Saccharina, Postelsia)

more details: algaebase.org

sporophyte
(fyloid, cauloid, haptera with rhizoides)

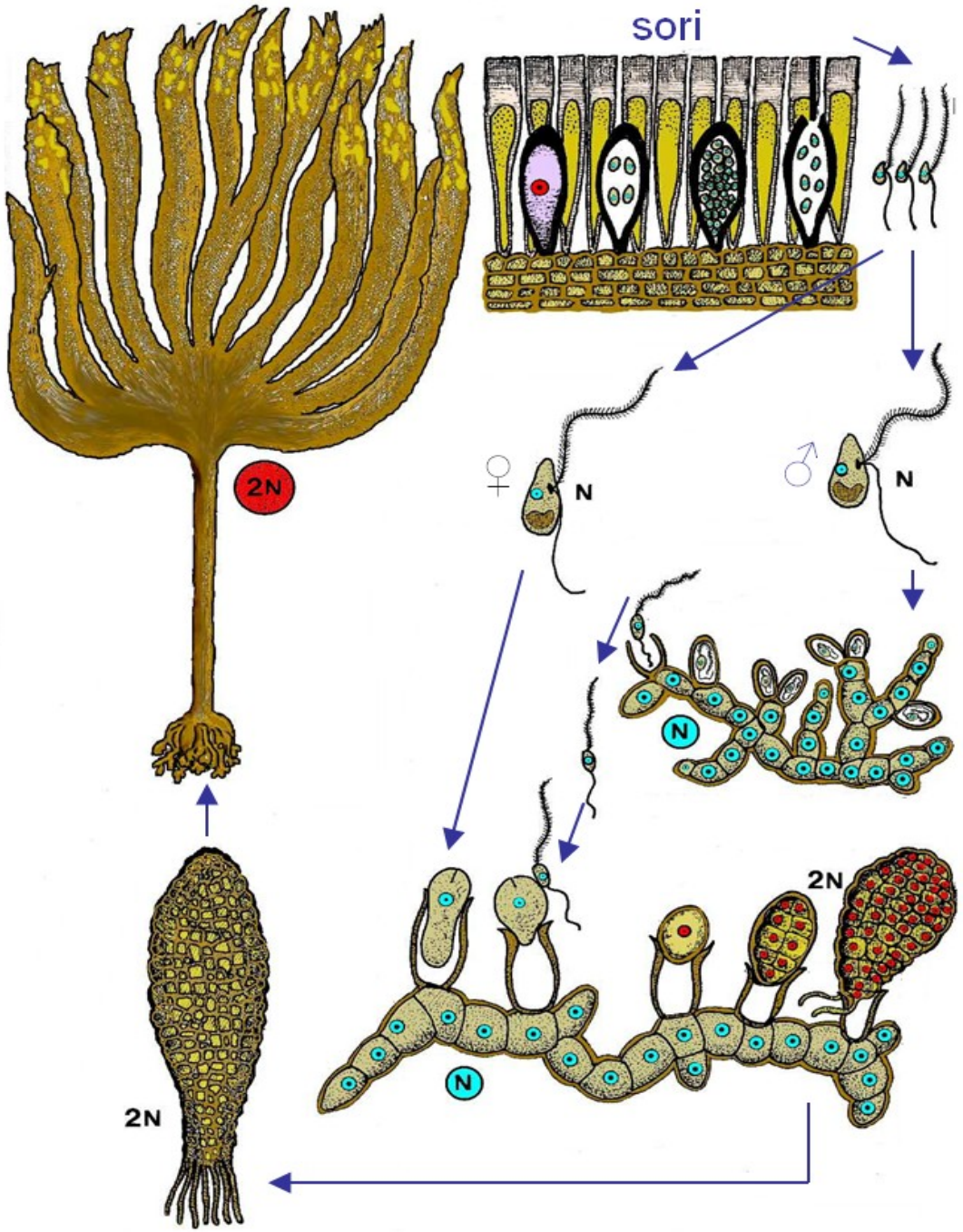

unilocular sporangia (+ paraphyses)

♂ gametophyte antheridia
(unilocular gametangia)

♀ gametophyte oogonia
(unilocular gametangia)

sporophyte structure and position of reproductive cells

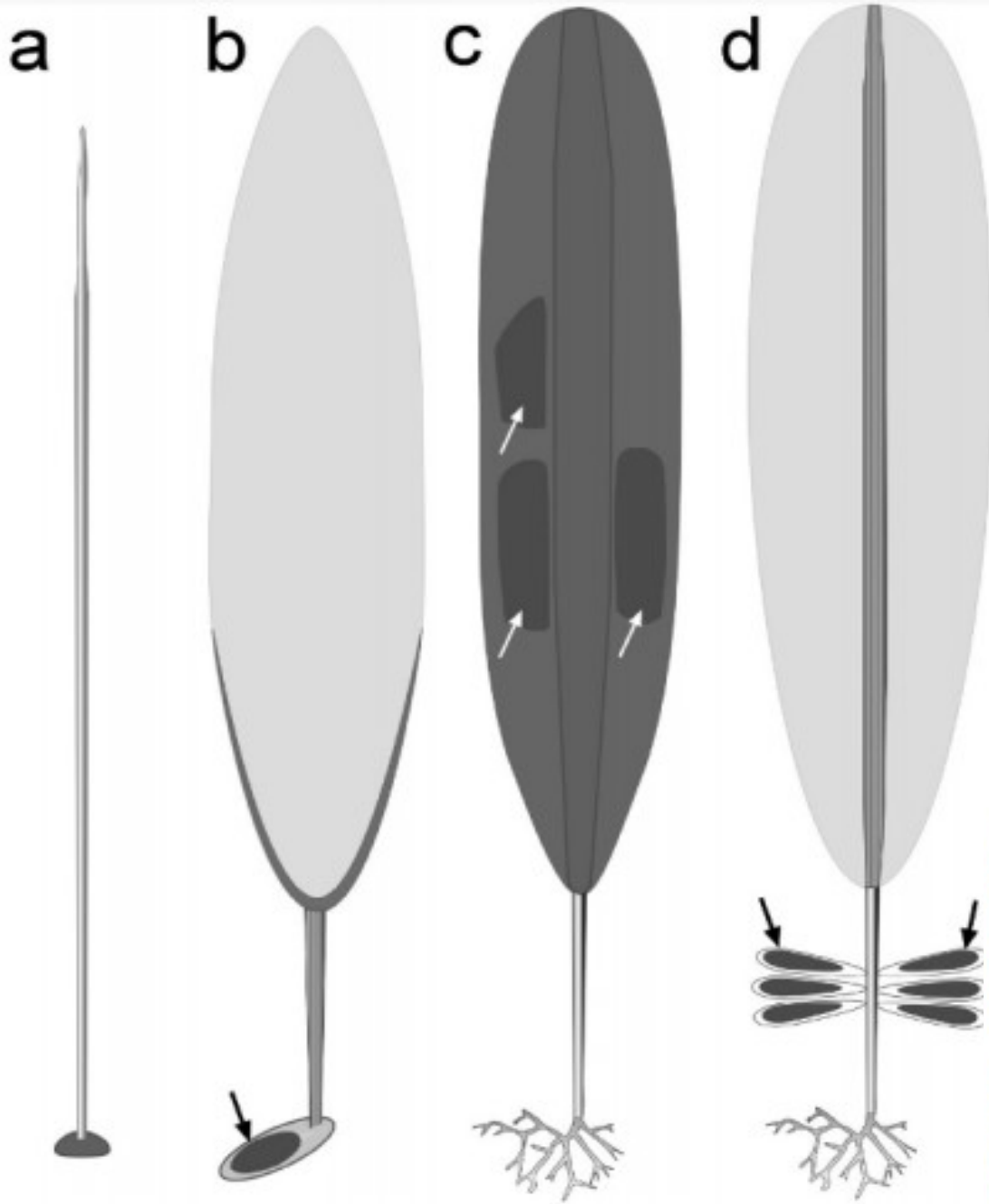

Figure 5 | Schematic presentation of basic morphology of different kelp species focusing the basic thallus structure and formation of reproductive cells. (a), Pseudochordaceae and Chordaceae having terete erect thallus and small discoidal holdfast. Unilocular zoidangia are formed on the entire surface of the erect thallus. (b), *Aureophycus aleuticus*. Erect thallus has characteristic flat stipe and thickened portion at the transitional zone to the blade. Sorus of unilocular zoidangia (arrow) is formed on the well-developed holdfast (basal system) of unilateral growth at an early stage of development. (c), Laminariaceae, erect thallus has thick blade and forms sorus on the blades (arrows). Most members, especially those with large erect thallus, have an epidermal rhizoidal holdfast. (d), Alariaceae, erect thallus with thin blade supported by thick midrib. Sori (arrows) are formed on the blade or on specialized blades near the base (sporophylls). [Illustration by H. Kawai].

Kawai et al., 2013, Sci Rep.

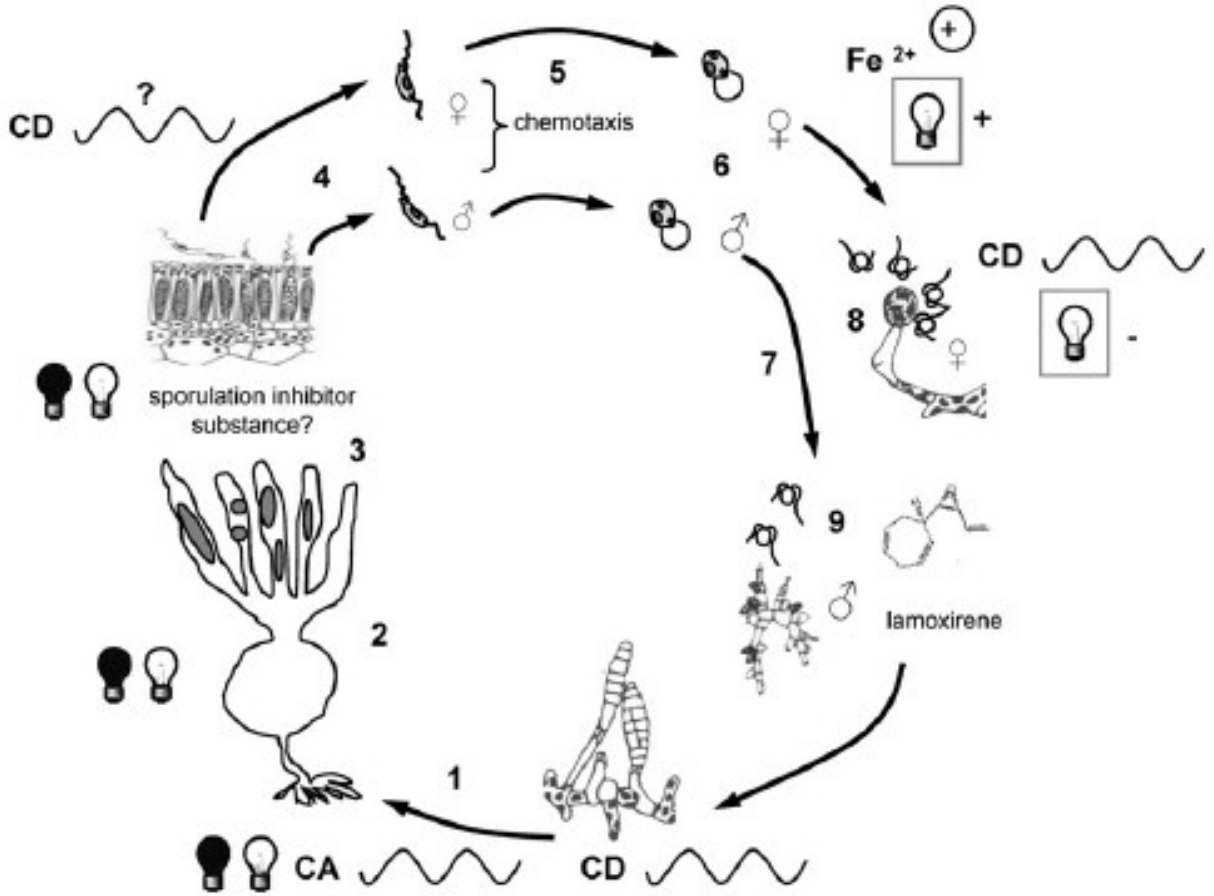

photoperiodic control

blue light control

CA circannual control

CD circadian control

1: growth: circadian [a], circannual [a] and photoperiodic control [b]

2: new blade: photoperiodic SD induction [c]

3: sporogenesis: photoperiodic SD induction [d], endogenous sporulation inhibitor? [e]

4: meiospore release: during night phase = circadian control? [f]

5: meiospore settlement: chemotactically controlled [g]

6: meiospore germination: autonomous (light independent) [h]

7: gametogenesis: induced by blue light and iron ions [i]

8: oogonium release: inhibited by blue light; under circadian control [j]

9: spermatozoid release and attraction to oogonium: induced by pheromone which is produced by oogonium [k]

Growth of sporophytes

light saturation: 20 -100 µmol m^{-2} s^{-1} [l]

minimal annual light requirement: 40-96 mol photons m^{-2} y^{-1} [m]

optimum temperatures: 5 – 15 °C [n]

nutrients modulate growth, but are not triggers [o]

Fertility:

gametophytes (optimum): 5-18 °C, 4-90 µmol photons m^{-2} s^{-1} [p]

sporophytes: 1 to 18 °C, 5-200 µmol photons m^{-2} s^{-1} [q]

Table 6. Reproductive period of selected *Laminaria* species worldwide

Species	Location	Month												Remarks	Reference
		J	F	M	A	M	J	J	A	S	O	N	D		
L. angustata	Hokkaido, Japan	S	–	–	–	–	S	S	S	S	S	S	S		Hasegawa (1972)[a]
		S	S	S	S	–	–	–	S	S	S	S	S	1-year plants	Kawashima (1983)
		–	–	–	–	–	S	S	S	S	S	S	S	2nd blade	
L. digitata	Calvados, France	S	S	S	S	S	S	S	S	S	S	S	S		Cosson (1976)
	Wales, UK	–	–	–	–	–	–	–	–	s	S	S	S		Harries (1932)
	Helgoland, Germany	–	–	–	s	s	S	S	S	S	S	S	s		Lüning (1982), Lüning (1988), Gehling & Bartsch (unpublished data)
	Cape Cod, USA	S	S	S	–	–	–	–	–	–	–	S	S		Sears & Wilce (1975)
L. ephemera	Vancouver Is., Canada	–	–	–	S	S	S	S	–	–	–	–	–		Druehl (1968), Klinger (1984)
L. farlowii	S California, USA	S	s	s	s	s	s	s	s	S	S	S	S		McPeak (1981)
	San Diego, USA	S	S	S	S	S	S	S	S	S	S	S	S		Dayton *et al.* (1999)
L. fragilis	Muroran and Hakodate, Japan	–	–	–	–	–	–	–	s	S	S	–	–		Miyabe (1957)
L. groenlandica	SE Alaska	s?	–	–	–	S	S	S	S	S	s	s	s		Calvin & Ellis (1981)
L. hyperborea	Isle of Man, UK	S	S	S	–	–	–	–	–	S	S	S	S		Kain (1975)
	Helgoland, Germany	S	S	S	s	–	–	–	–	–	–	S	S		Lüning (1982)
	Wales, UK	S	S	–	–	–	–	–	–	–	–	–	s		Harries (1932)
L. japonica	Hokkaido, Japan	S	S	S	S	S	S	S	S	–	–	–	–	Young sporophytes	Mizuta *et al.* (1999a,b)
	Japan	–	–	–	–	–	–	–	S	S	?	?	?	Sori from August onwards	Miyabe (1957)
L. longicruris	Long Island Sound, USA	S	S	S	S	S	s	s	s	s	S	S	S		Egan & Yarish (1990), van Patten & Yarish (1993)
	Nova Scotia, Canada	S	S	S	–	–	–	–	–	–	–	S	S	1-year plants	Chapman (1986)
		S	S	S	S	S	S	S	–	S	S	S	S	2-year plants	
		S	–	–	–	–	–	–	–	S	S	S	S	3-year plants	
L. ochotensis		–	–	–	–	–	–	–	s	S	?	?	?	Sori begin to appear in August	Miyabe (1957)
L. ochroleuca	Brittany, France	–	–	–	–	–	–	s	S	S	s	S	s	Summer to autumn fertility	Sauvageau (1918)
L. pallida	Cape of Good Hope, South Africa	S	S	S	S	S	S	–	–	–	–	–	S	Summer to autumn fertility	Dieckmann (1980)
L. religiosa	Hokkaido, Japan	–	–	–	–	–	–	–	–	S	S	S	S		Abe *et al.* (1982)
L. rodriguezii	Mediterranean Sea	–	–	–	S	S	S	S	S	S	S	–	–		Huvé (1955)
L. saccharina	Argyll, UK	S	S	S	S	S	S	S	S	S	S	S	S		Parke (1948)[a]
	Wales, UK	S	S	S	s	–	–	–	–	s	s	S	S		Rees (1928)[a], Harries (1932)
	Helgoland, Germany	S	–	–	–	–	–	–	–	s	S	S	S		Lüning (1982)
	Long Island Sound, USA	S	S	S	S	S	S	S	S	–	S	S	S	Annual population	Lee & Brinkhuis (1986)
	Cape Cod, USA	S	S	S	–	–	–	–	–	–	–	S	S	Most plants vegetative during reproductive period	Sears & Wilce (1975)
	British Columbia, Canada	S	–	–	S	S	S	–	–	S	S	S	S	Annual population	Druehl & Hsiao (1977)
L. setchellii	British Columbia, Canada	S	S	s	s	S	S	S	S	S	S	S	S	Sori in the field restricted to dissected blade portion	Druehl (1968), Klinger (1984)
L. sinclairii	Oregon, USA	–	S	S	S	–	–	–	–	–	S	S	–	In spring sori at tips of 2–3 cm blades; in autumn on old blades	Druehl (1968), Markham (1973)
L. solidungula	New Foundland, Canada	S	S	S	S	S?	–	–	–	–	–	S	S	Spore release next spring to summer	Hooper (1984)

Abbreviations: S: sori present; S: main fruiting period; s: sori present, but in relatively low quantity; –: no sori present or no information available.
[a]Cited by Lüning (1982).

Table 4. Examples of deepest *Laminaria* populations

Species	Location	Depth limits	Reference
L. abyssalis/brasiliensis	Off Brazilian coast	70–95 m	Joly & de Oliveira Filho (1967)
L. hyperborea	Aran Islands, Ireland	32 m	Lüning (1990)
L. ochroleuca	Strait of Messina, Italy	(60–) 95 m	Drew (1972), Giaccone (1972)
L. philippinensis	Off the Philippines	85 m	Petrov *et al.* (1973)
L. rodriguezii	Corsica, France	95 m	Fredj (1972)
L. saccharina	Spitsbergen	25 m	Hanelt (1998)
L. solidungula	Newfoundland, Canada	30 m	Whittick *et al.* (1982)

multigene phylogeny of Laminariales

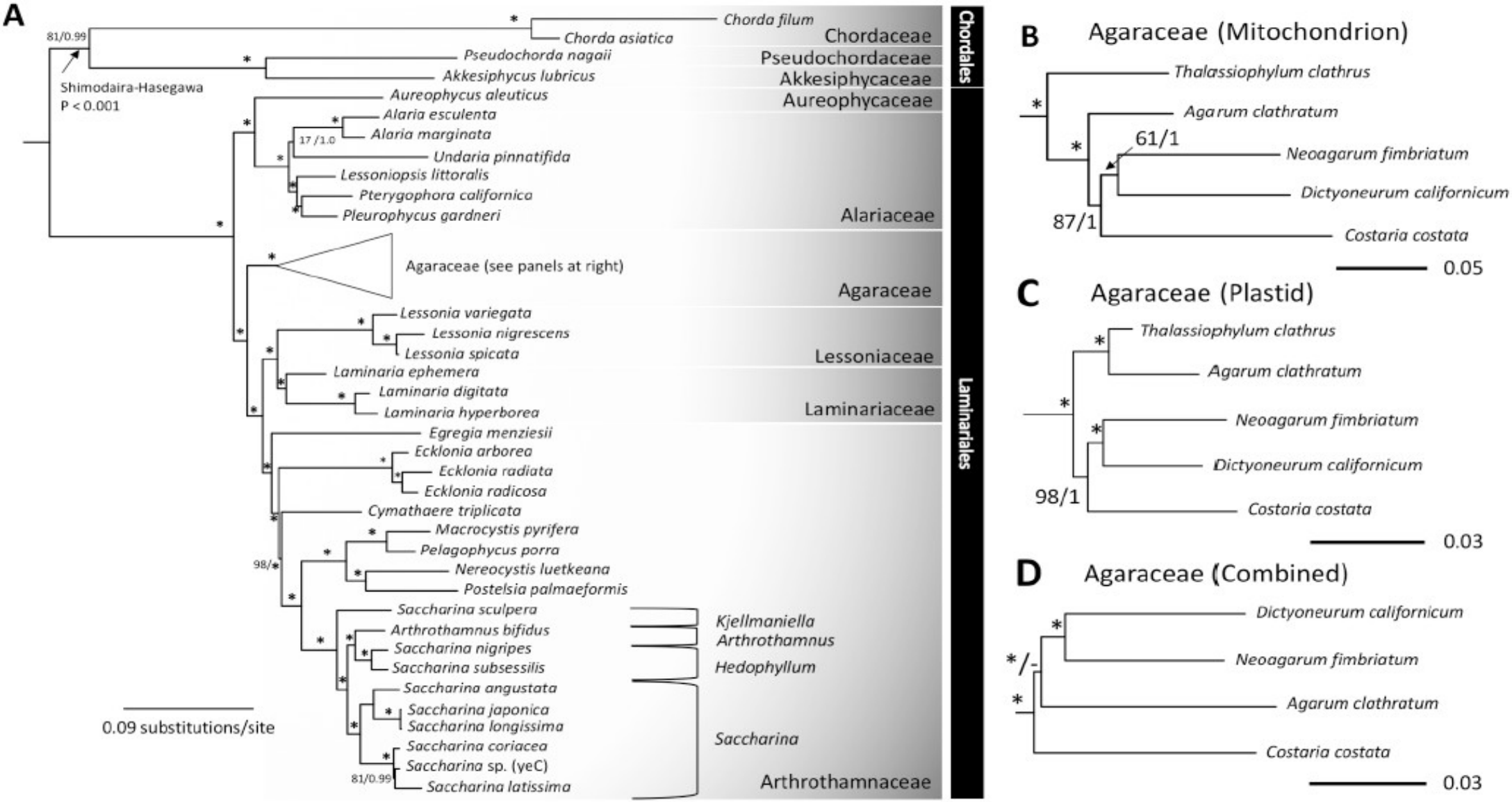

Starko et al., 2019, Mol Phyl Evol

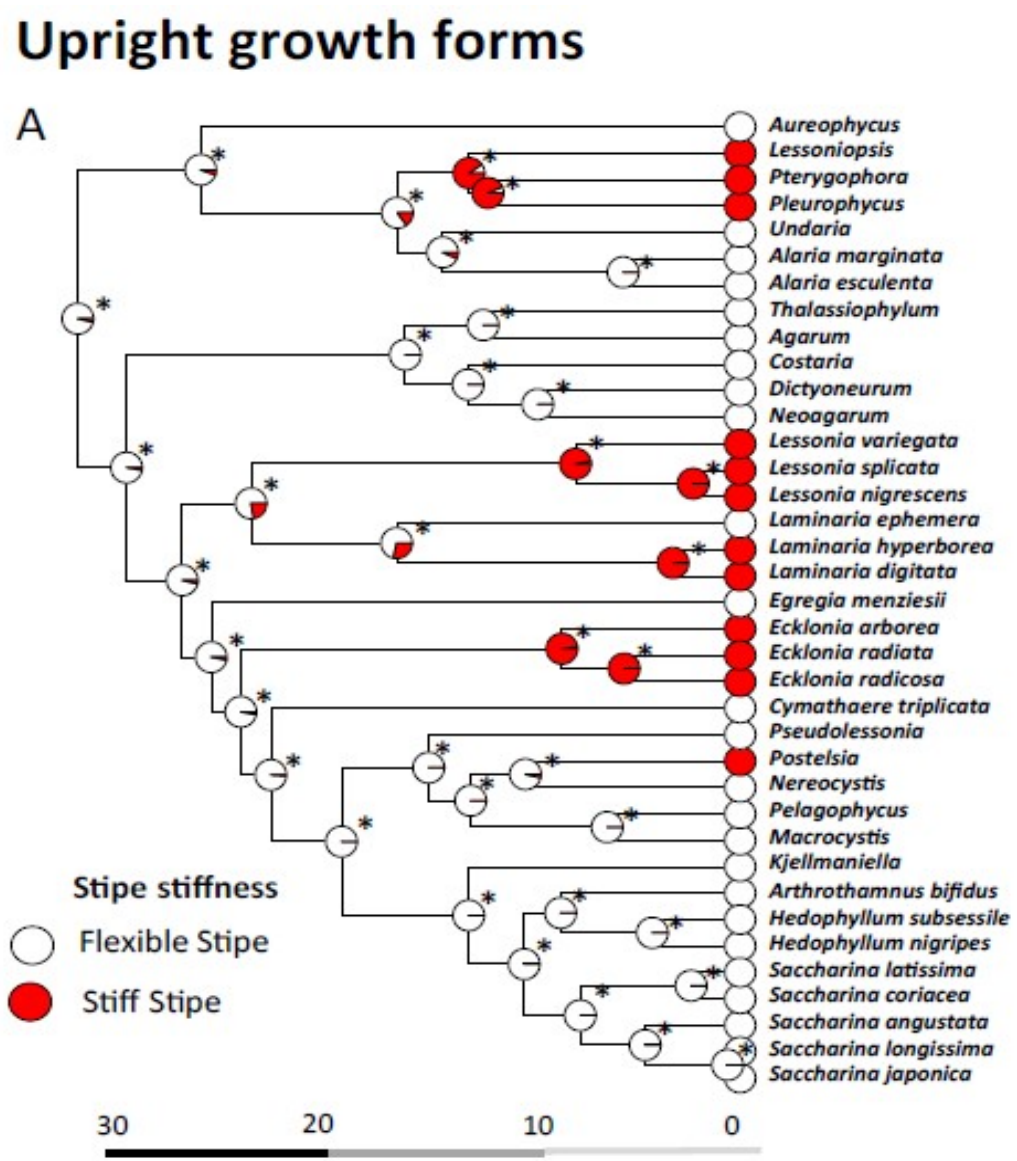

prostrate vs. erect

Starko et al., 2019, Mol Phyl Evol

Branching

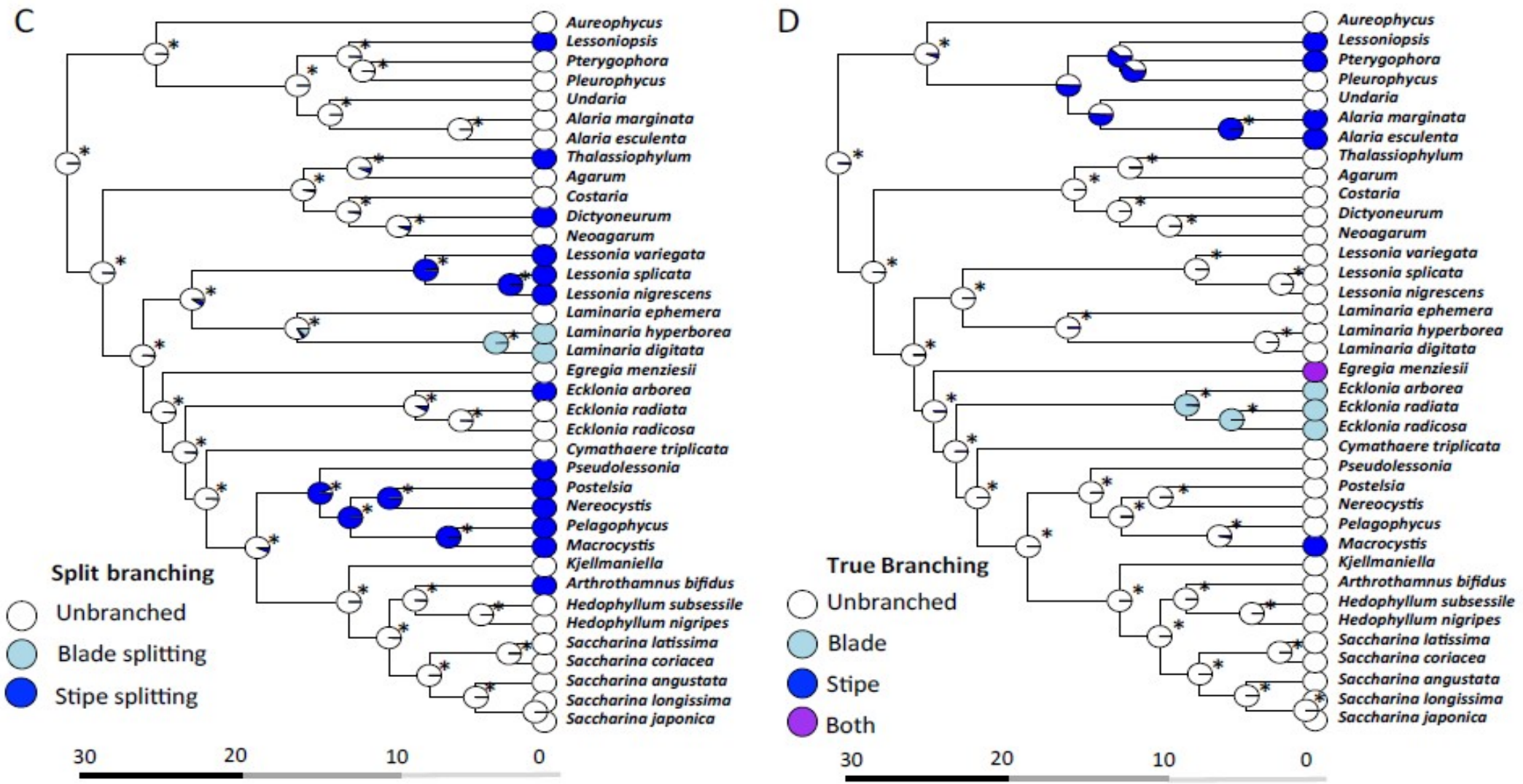

Starko et al., 2019, Mol Phyl Evol

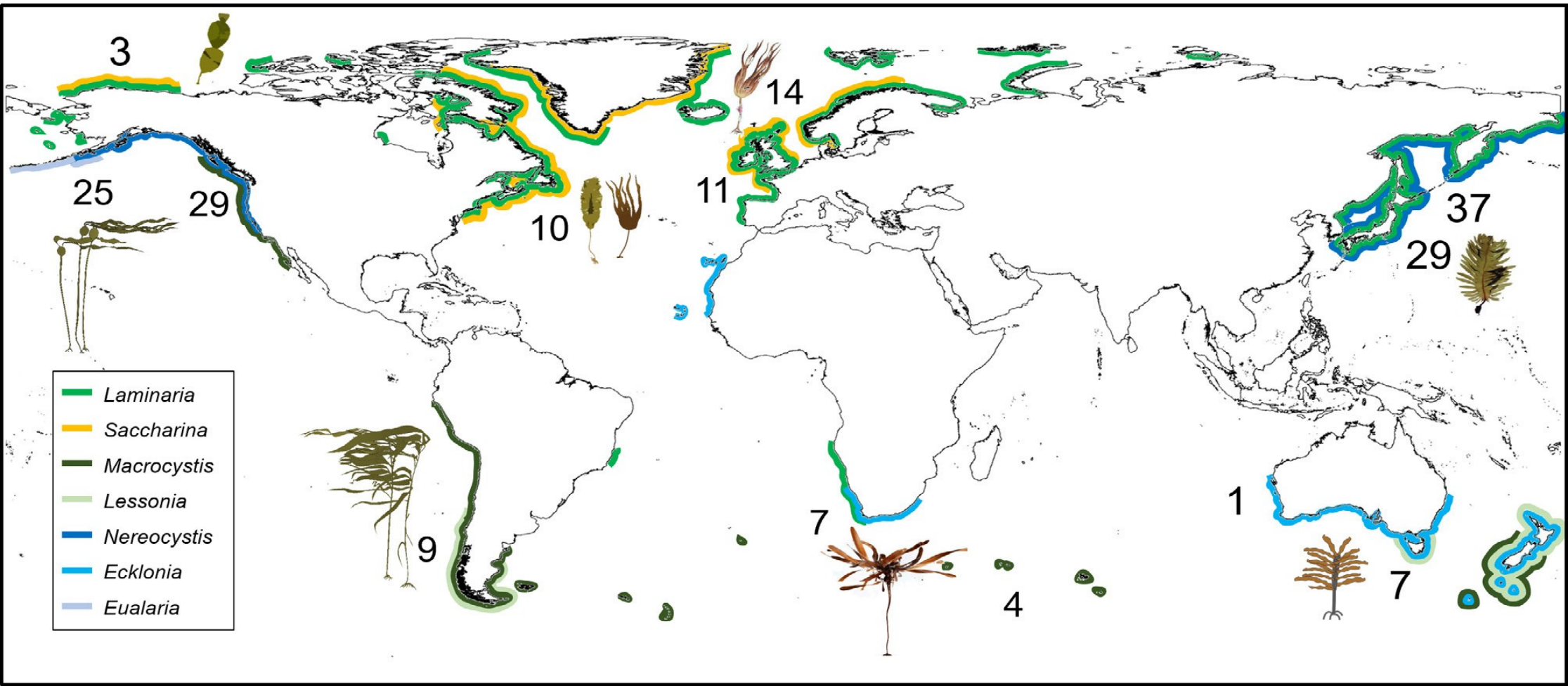

Wernberg et al., 2019, World Seas

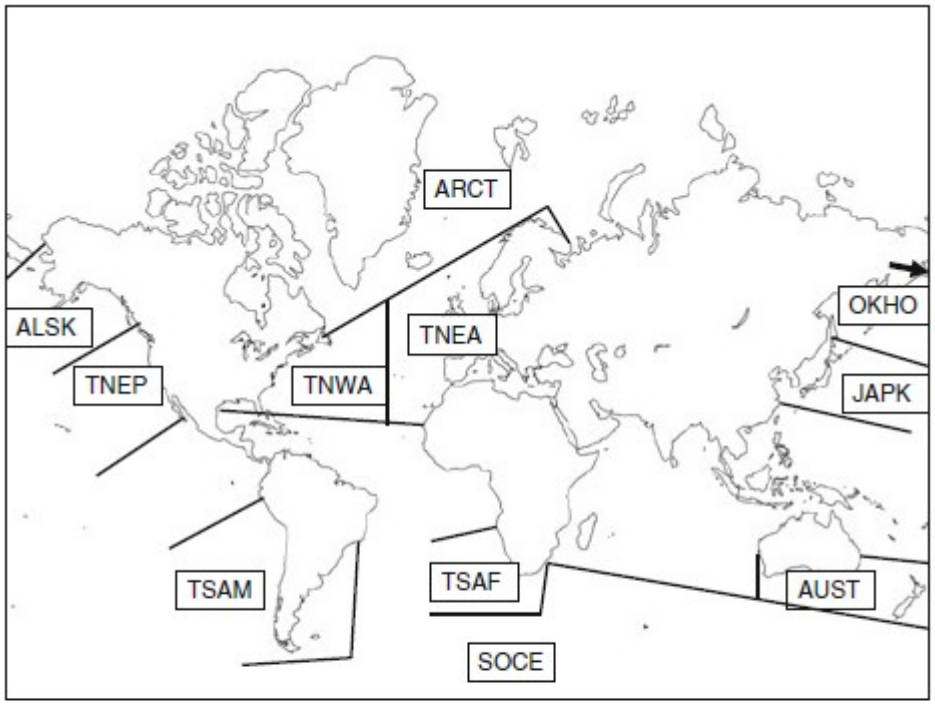

Fig. 1 The 11 world regions used for the biogeographical analysis (adapted from the system of Spalding et al. 2007, see text) (*TNEP* temperate Northeast Pacific, *ALSK* Alaska, *ARCT* Arctic, *TNWA* temperate Northwest Atlantic, *TNEA* temperate Northeast Atlantic, *OKHO* Okhotsk Sea, *JAPK* Japan, Korea, *TSAM* temperate South America, *SOCE* Southern Oceans, *TSAF* temperate South Africa, *AUST* Australasia)

Table 3 Numbers of species in each kelp family in each of 11 world marine regions (for explanation of region codes, see Table 2)

Family	OKHO	JAPK	ALSK	TNEP	ARCT	TNWA	TNEA	TSAM	SOCE	TSAF	AUST
Akkesiphycaceae	0	1	0	0	0	0	0	0	0	0	0
Chordaceae	1	4	1	1	1	1	1	0	0	0	0
Pseudochordaceae	0	2	0	0	0	0	0	0	0	0	0
Alariaceae	6	8	7	4	5	1	1	0	0	0	0
Costariaceae	3	3	4	5	1	1	0	0	0	0	0
Laminariaceae	19	14	13	16	7	7	8	2	2	2	1
Lessoniaceae	0	5	0	3	0	0	1	7	5	2	6
Total species	29	37	25	29	14	10	11	9	7	4	7
% Age of world species	**25.9**	**33.0**	**22.3**	**25.9**	12.5	8.9	9.8	8.0	6.3	3.6	6.3

Values with more than 20% of the world's species are highlighted

Table 4 Numbers of species in the most species-rich kelp genera in each of 11 world marine regions (for explanation of region codes, see Table 2)

	OKHO	JAPK	ALSK	TNEP	ARCT	TNWA	TNEA	TSAM	SOCE	TSAF	AUST
Alaria (15)	6	5	3	1	5	1	1	0	0	0	0
Laminaria (22)	6	2	4	6	4	4	6	1	1	1	0
Saccharina (20)	6	10	5	5	3	3	2	0	0	0	0
Ecklonia (7)	0	3	0	0	0	0	1	0	0	2	3
Eisenia (6)	0	1	0	2	0	0	0	3	0	0	0
Lessonia (9)	0	0	0	0	0	0	0	4	5	0	3

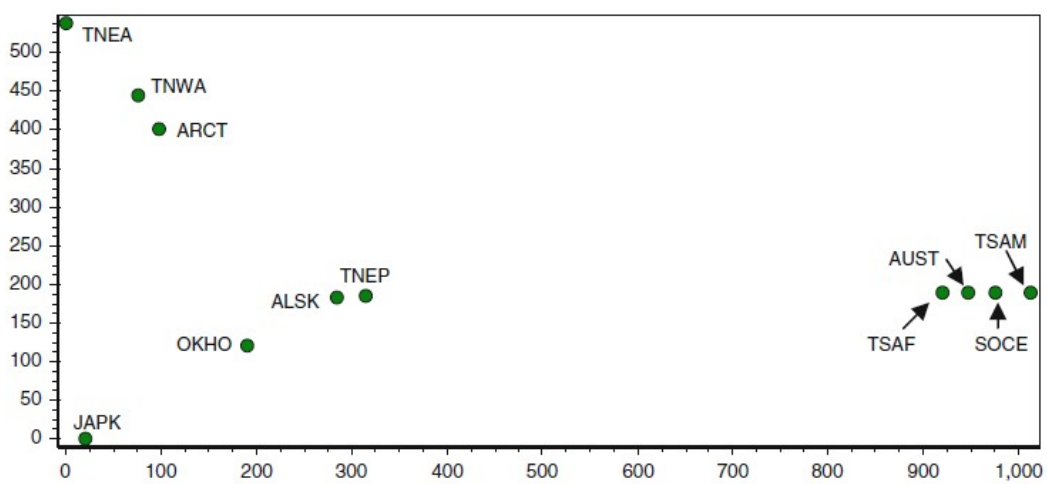

Fig. 4 DECORANA analysis of 11 world temperate marine regions, based on the kelp species that occur in them (Eigenvalues: Axis 1, 0.9414; Axis 2, 0.6482). Region codes as in Fig. 1

Bolton, 2010, Helgol. Mar. Res. 64: 263-279.

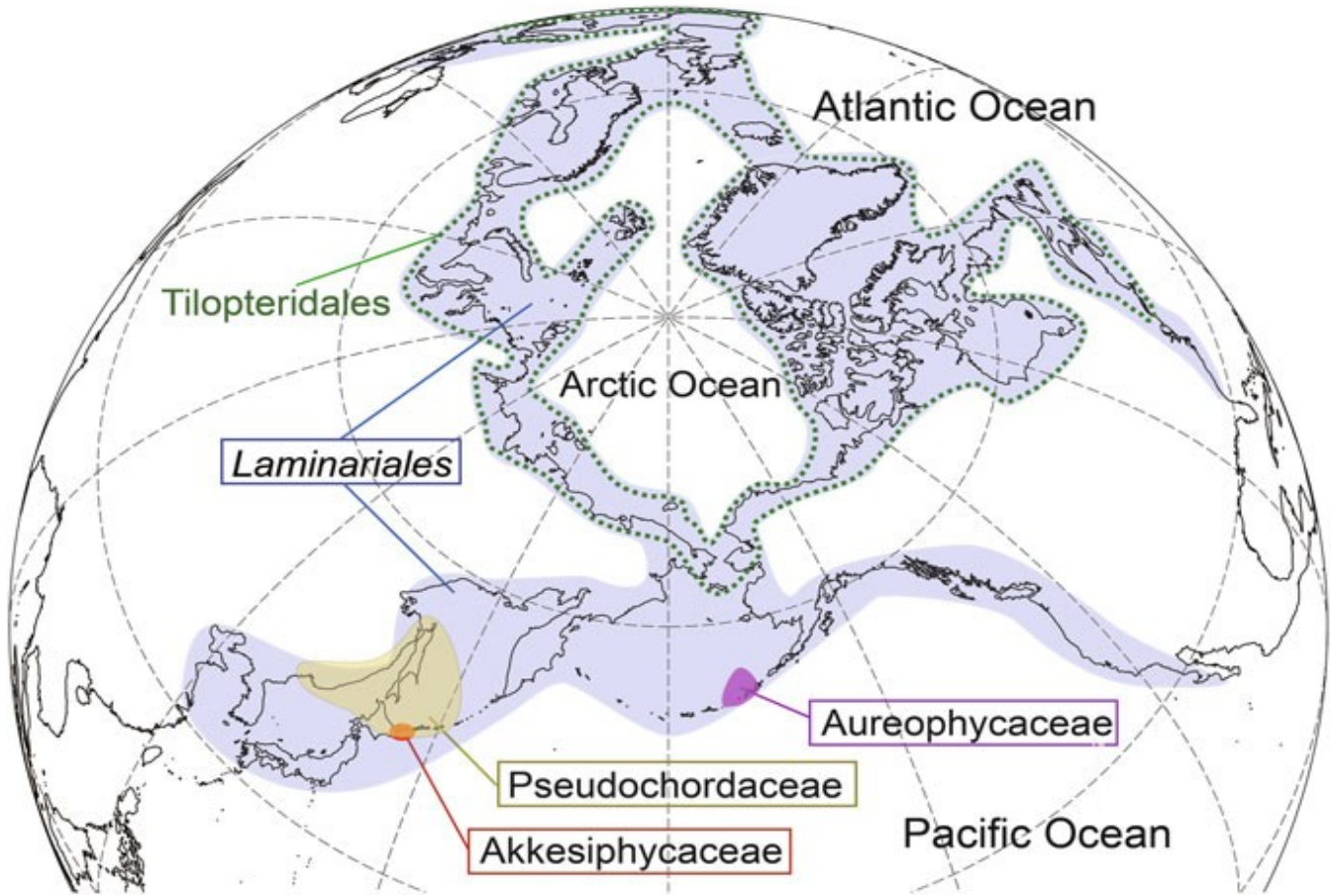

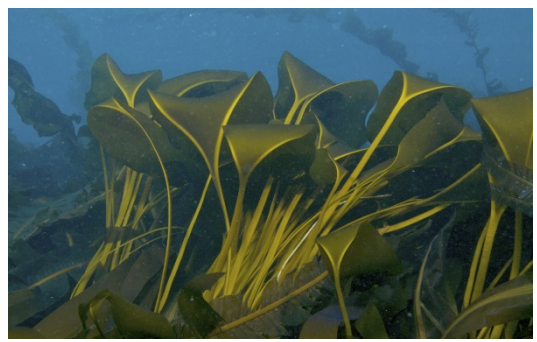

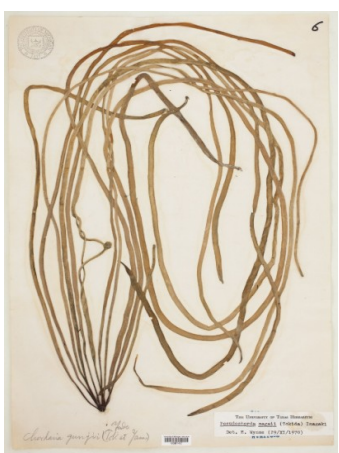

Kawai et al., 2016, In: Seaweed Phylogeography

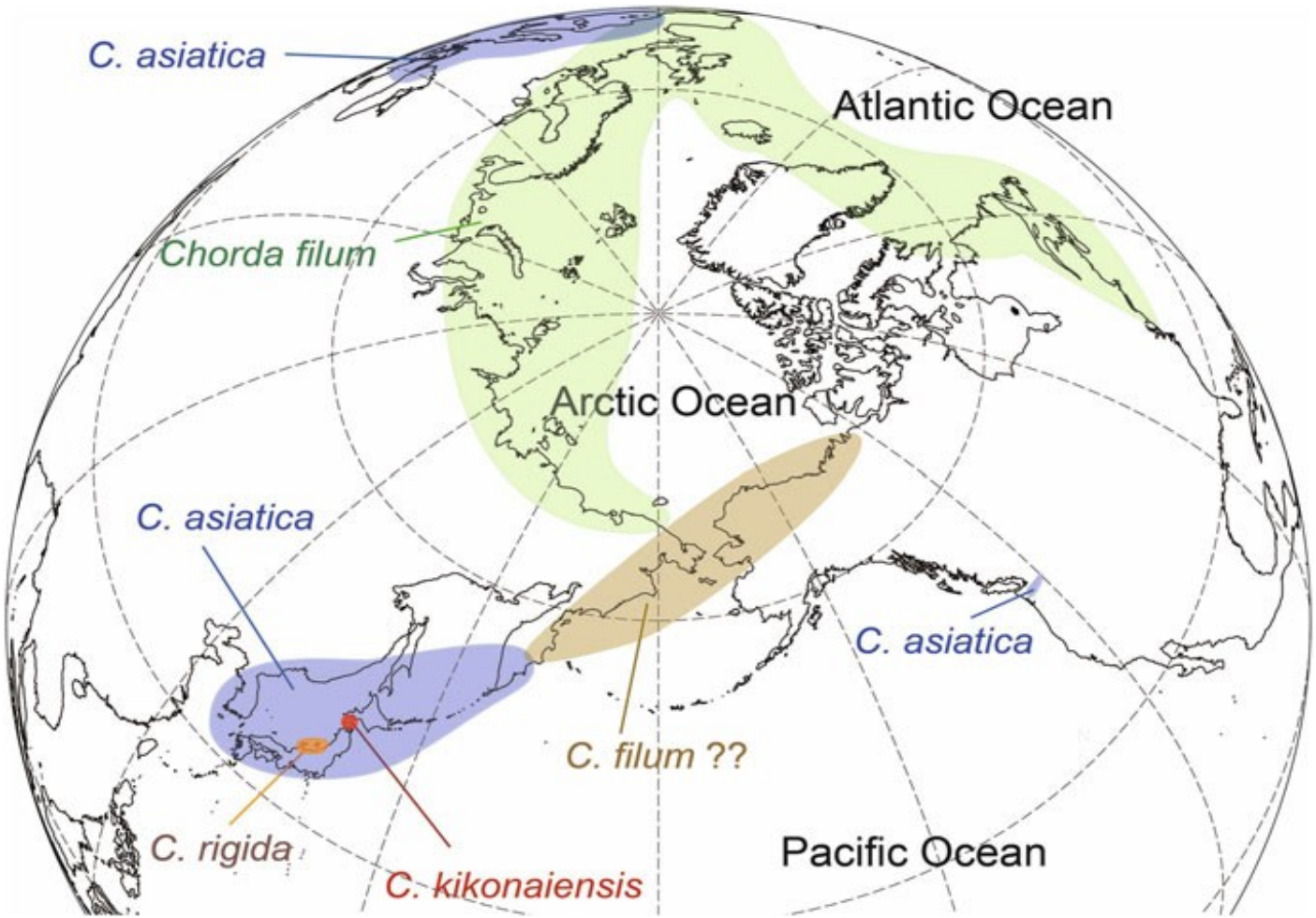

(incl. anthropogenic invasions)

Kawai et al., 2016, In: Seaweed Phylogeography

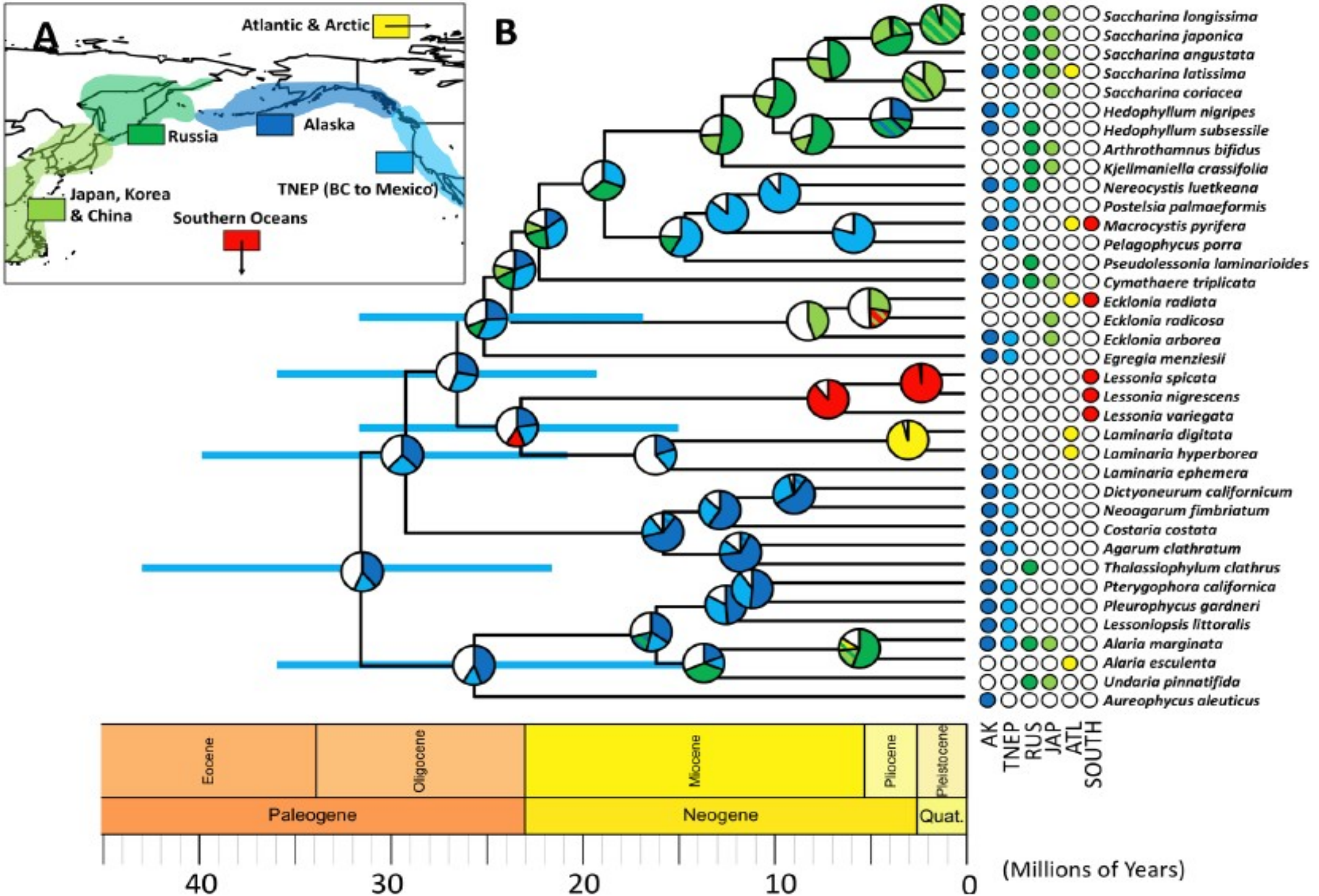

Starko et al., 2019, Mol Phyl Evol

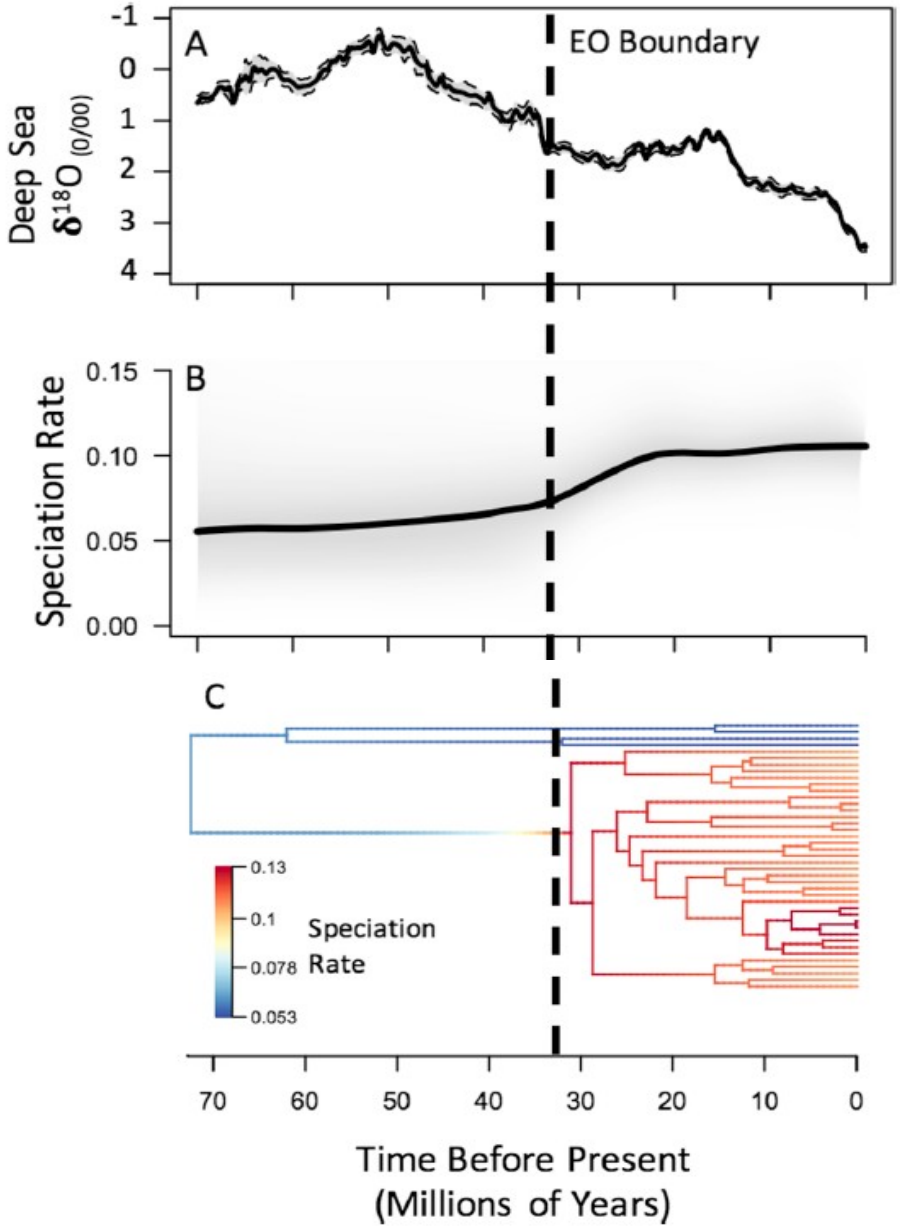

Fig. 3. Patterns of ocean climate and kelp diversification through deep time. (A) Pacific deep sea $\partial^{18}O$ (a proxy for ocean temperature) over the past 70 million years (data from Cramer et al 2009) (Cramer et al., 2009). Speciation rate plotted through time (B), and across the kelp phylogeny (C) as estimated using BAMM.

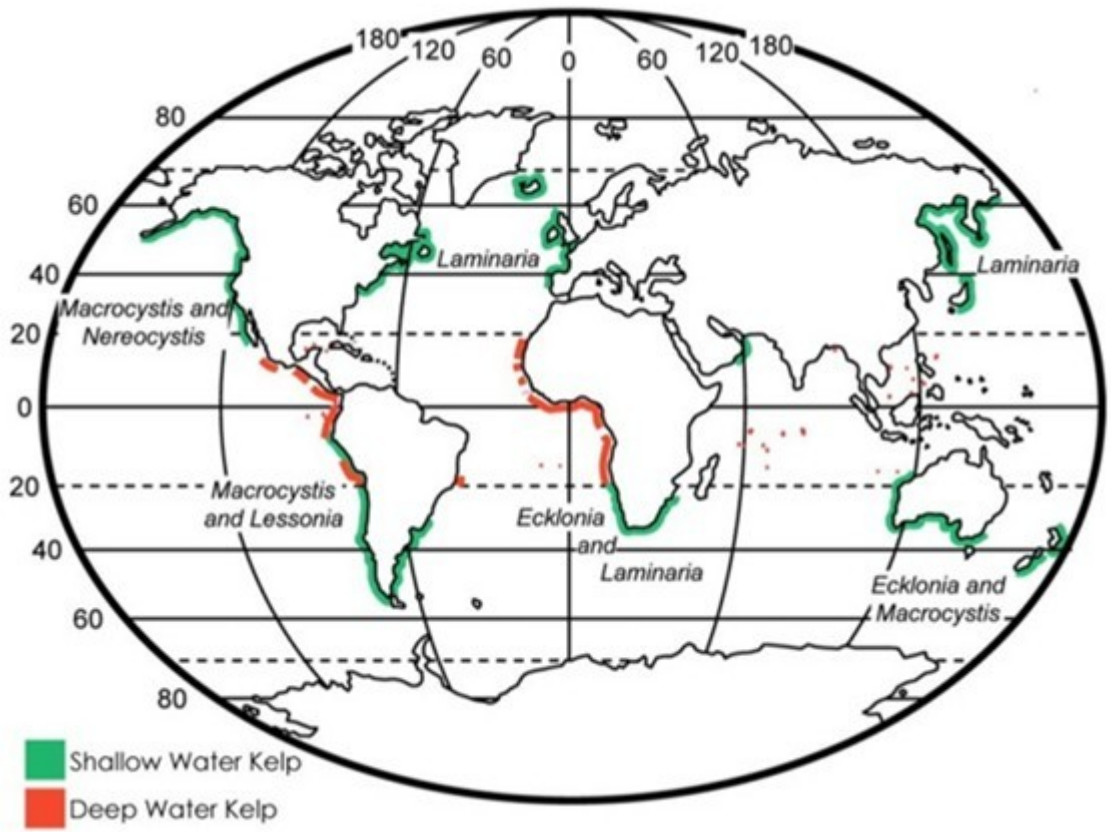
180
120
60
0
60
120
180
80
60
40
20
0
20
40
60
80
Laminaria
Laminaria
Macrocystis and
Nereocystis
Macrocystis
and Lessonia
Ecklonia
and
Laminaria
Ecklonia and
Macrocystis
Shallow Water Kelp
Deep Water Kelp

Aureophycus aleuticus

algaebase.org
Jewett & Clark, 2011

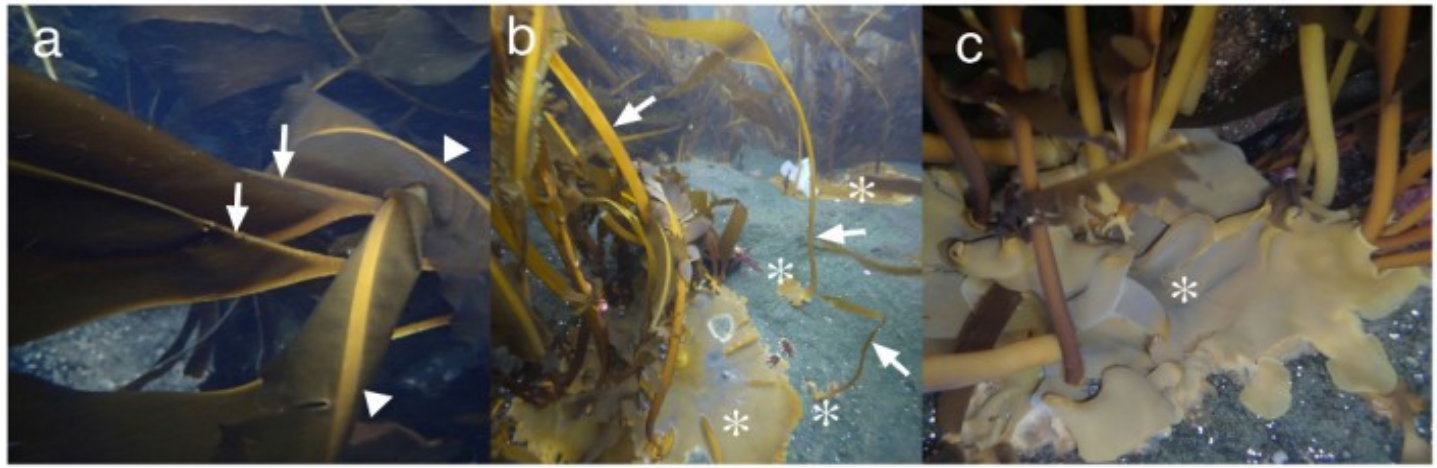

Figure 2 | Habit and morphology of *Aureophycus aleuticus* (St. George Is., 24 October 2012). (a), erect part of sporophyte with characteristic marginal thickening at the transitional zone between blade and stipe (arrows). Arrowheads show midribs of *Alaria* sp., growing mixed with *Aureophycus*. (b), Sporophytes of different developmental stages. Arrows show flattened stipes and asterisks show basal systems (discoidal holdfast forming sorus). Note that the basal systems show unilateral development in the early stages, and the iridescent color of the basal systems including those of rather young thalli showing signs of sorus formation. (c), developed basal systems overlapping each other, with iridescent color on the surface (asterisk) showing sorus formation. [Photographs by H. Kawai].

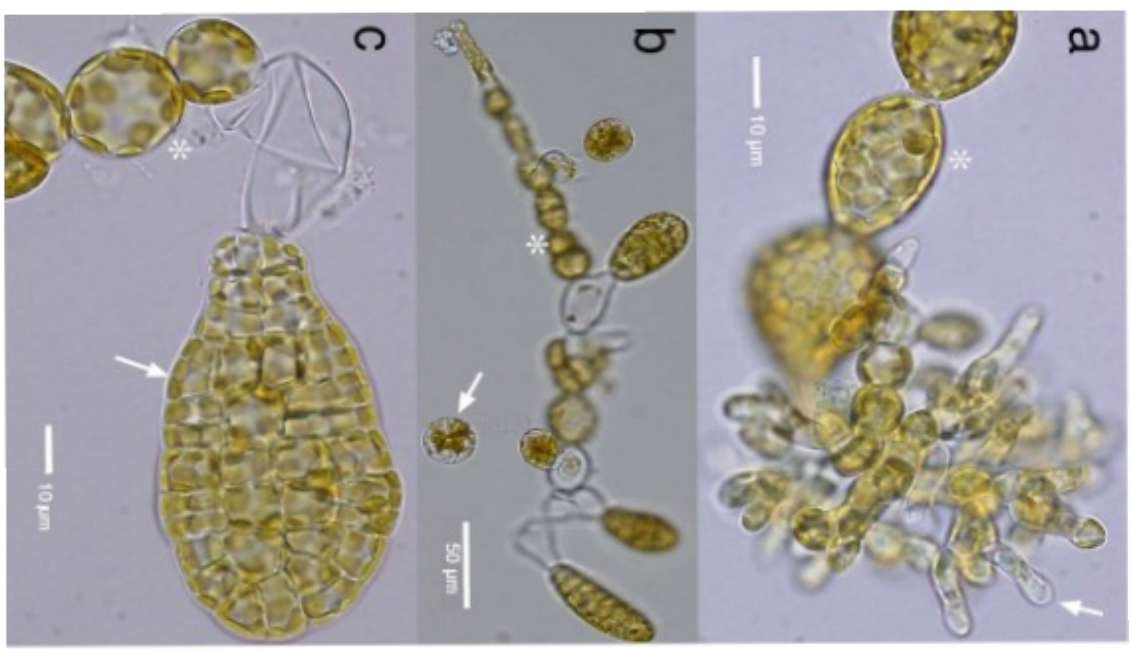

Figure 4 | Gametophytes and young sporophytes of *Aureophycus aleuticus*. (a), vegetative female gametophyte (left, asterisk) and fertile male gametophyte (right). Arrow shows antheridium. (b), Fertile female gametophyte (asterisk) and young sporophyte (embryos). Arrow shows zygote. (c), Fertile gametophyte (asterisk) with young sporophyte (arrow). [Photographs by H. Kawai].

Kawai et al., 2013, Sci. Rep.

Ecklonia

E. radiata

E. maxima - kelpak

Egregia

feather boa kelp

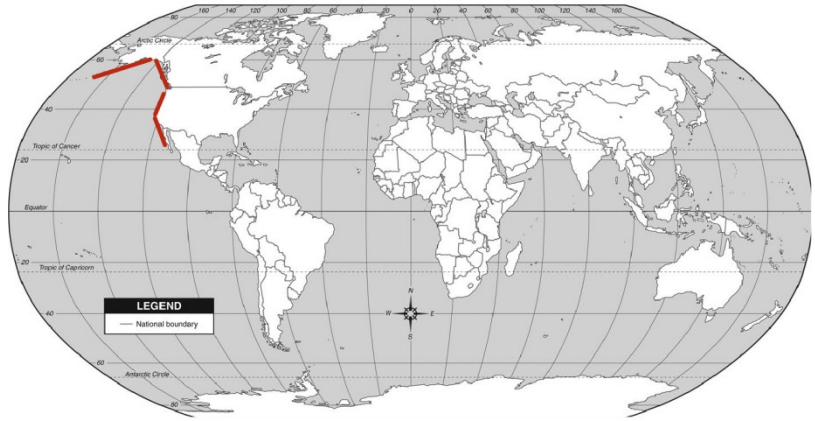

http://natural-history.main.jp

Lessonia

L. variegata

Neil & Nelson, 2016, NZ Seaweeds

Agarum

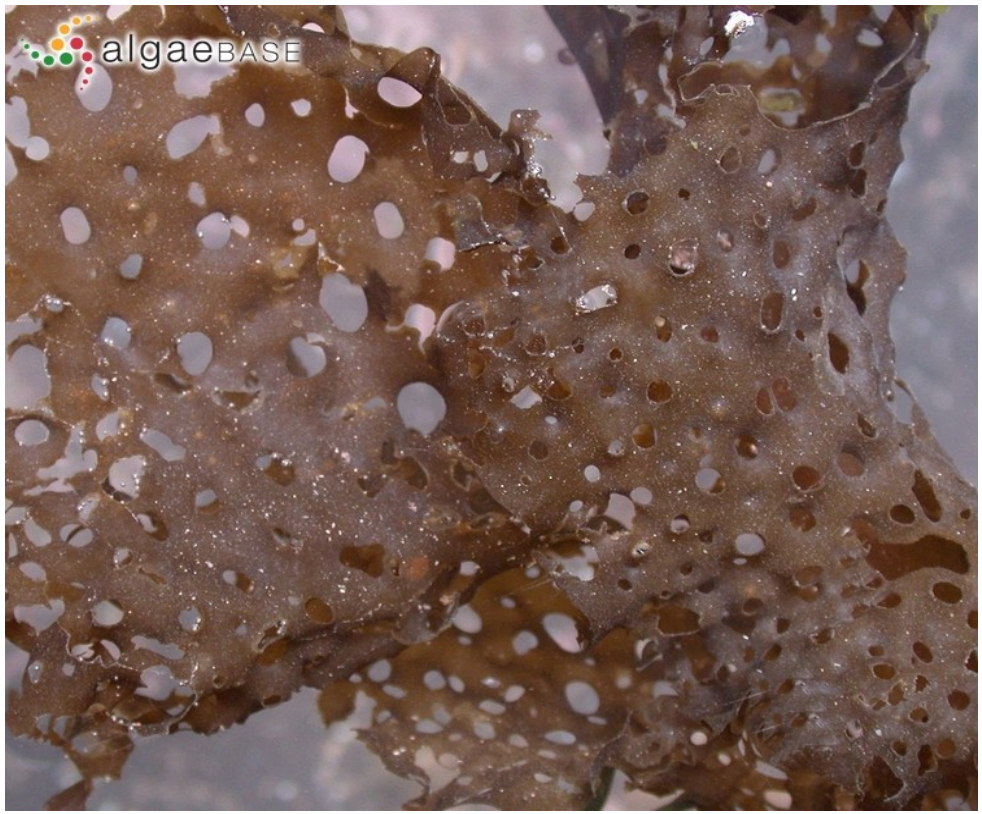

Costaria

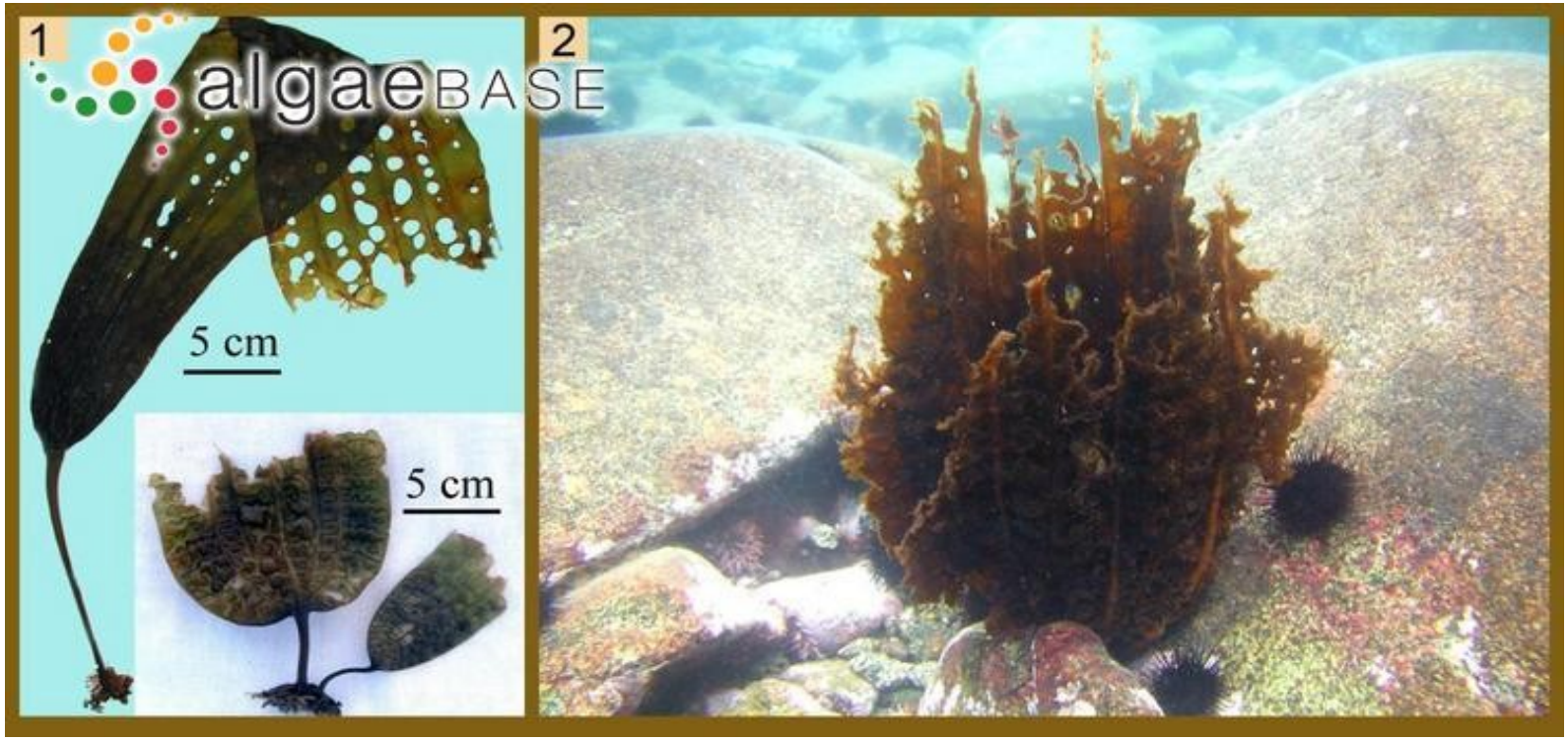

Alaria

Undaria (pinnatifida)

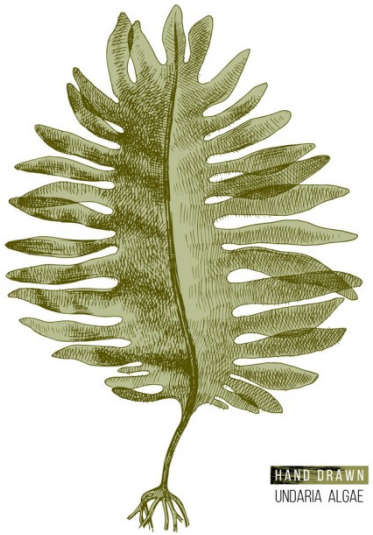

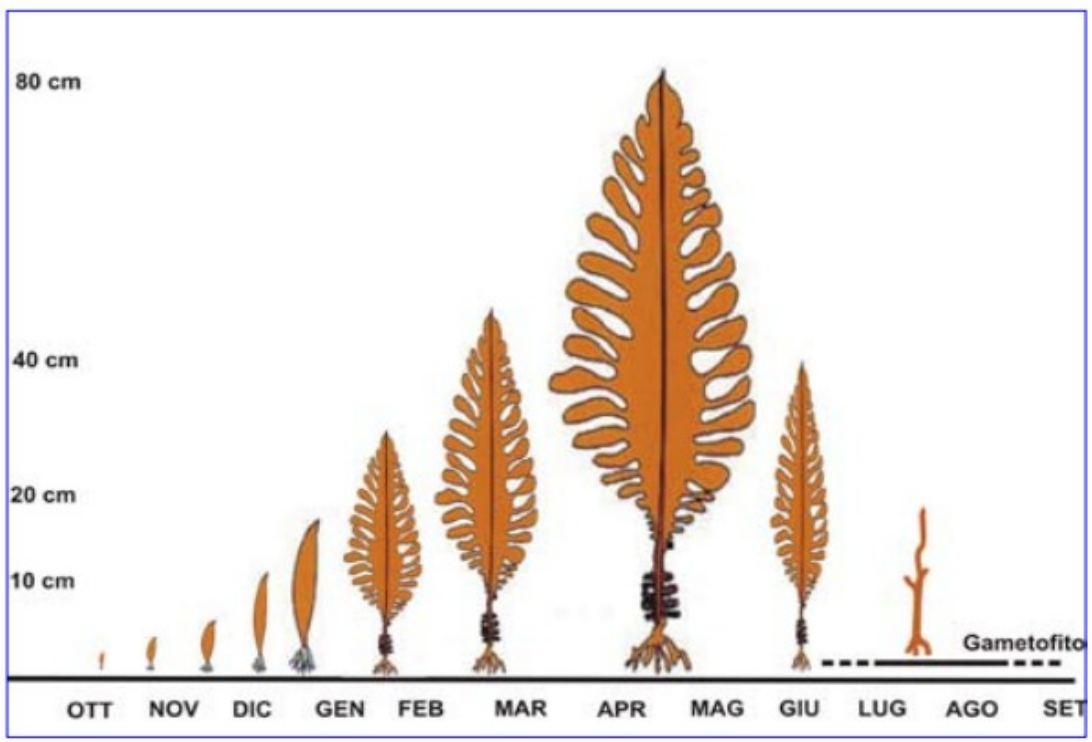

U. pinnatifida dynamics in Venice lagoon

Curiel & Marzocchi, 2010

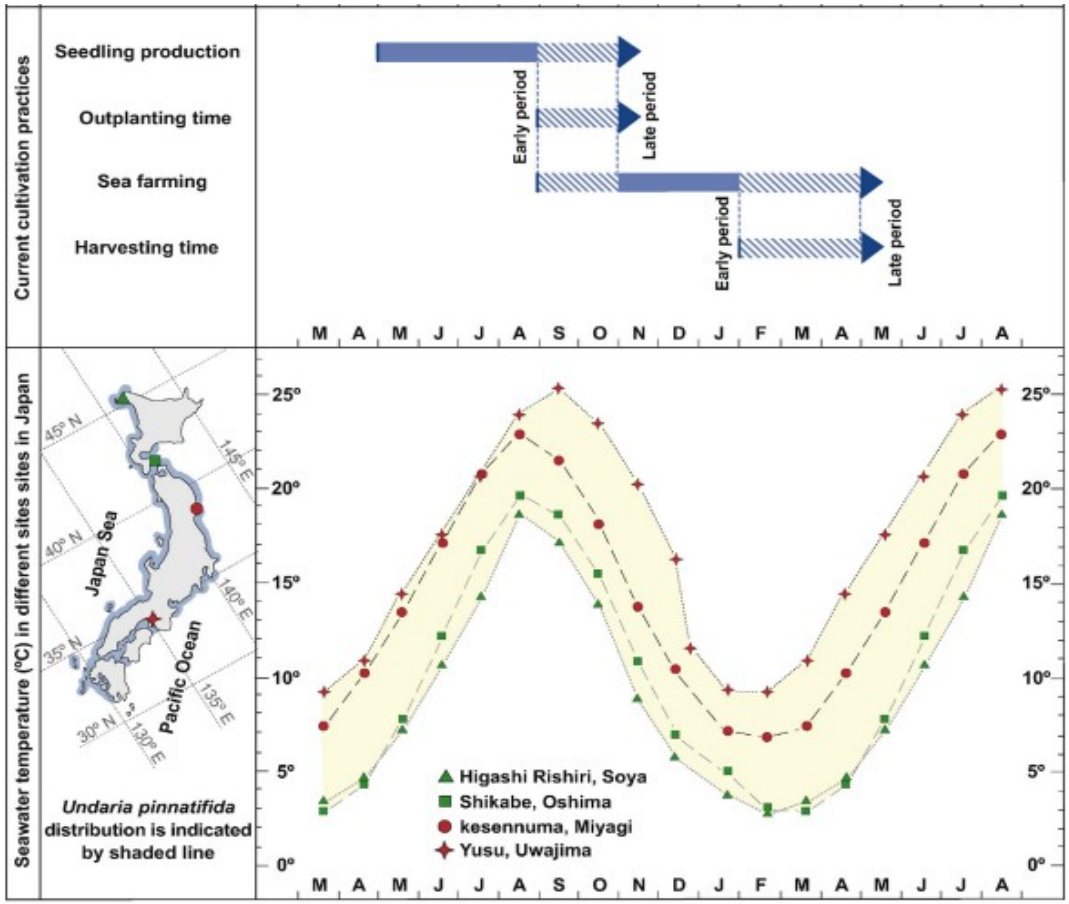

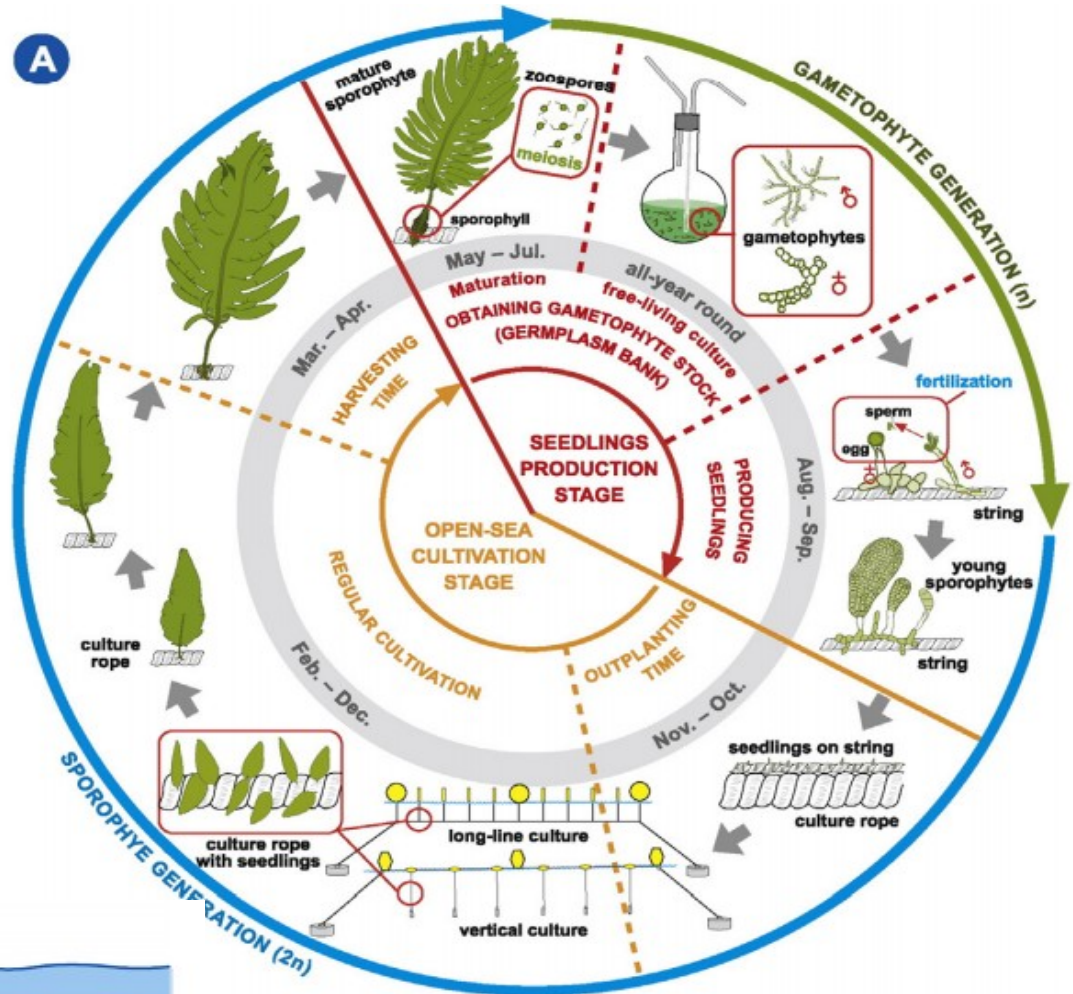

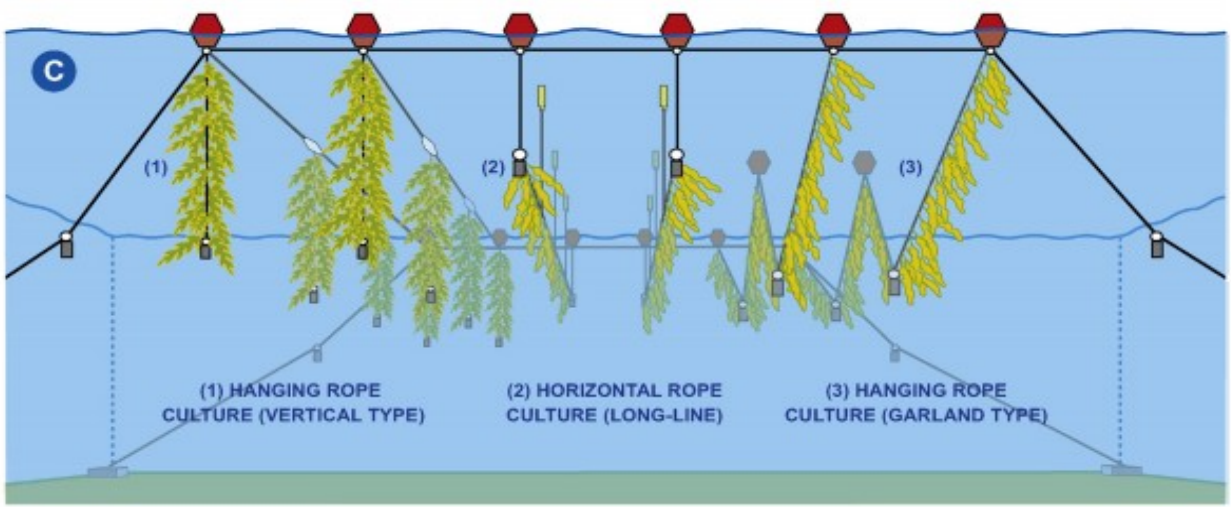

annual production of *U. pinnatifida* in aquacultures – cca 1.8 million tonnes; constituting possibly about 20% of total kelp production in agriculture

commercial culturing on U. pinnatifida in Japan and N Spain

Peteiro et al., 2016, Algal Res.

U. pinnatifida – wakame cultivation

En - Wakame, Fr - Wakamé, Es - Abeto marino

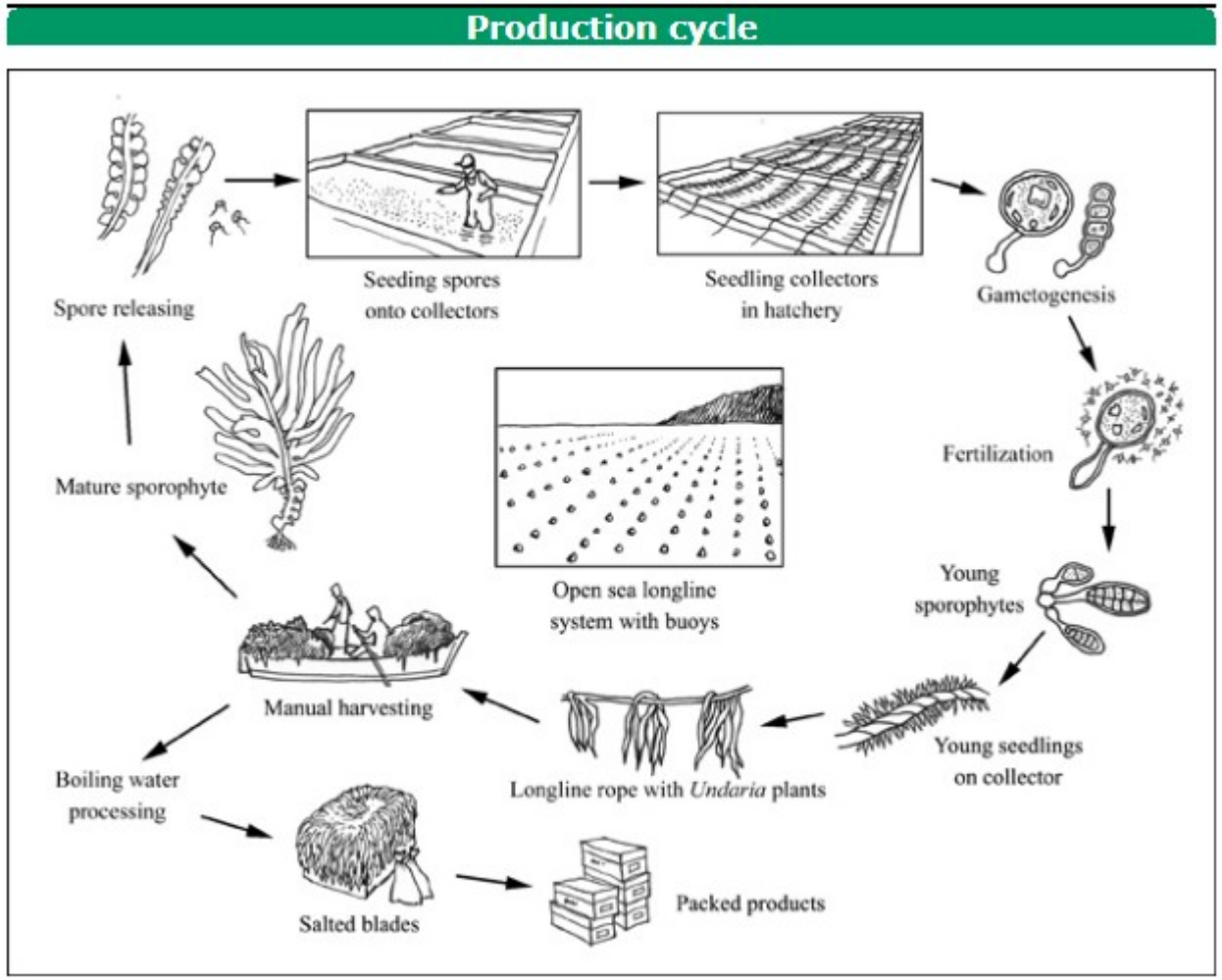

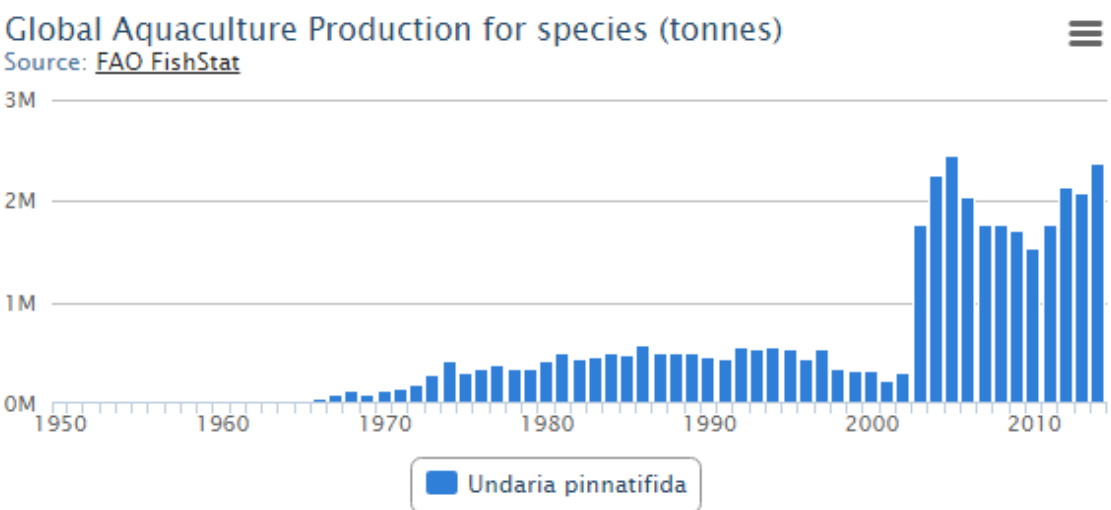

FAO, Fish. Aquacult. Dep., 2016

global invasion of
U. pinnatifida

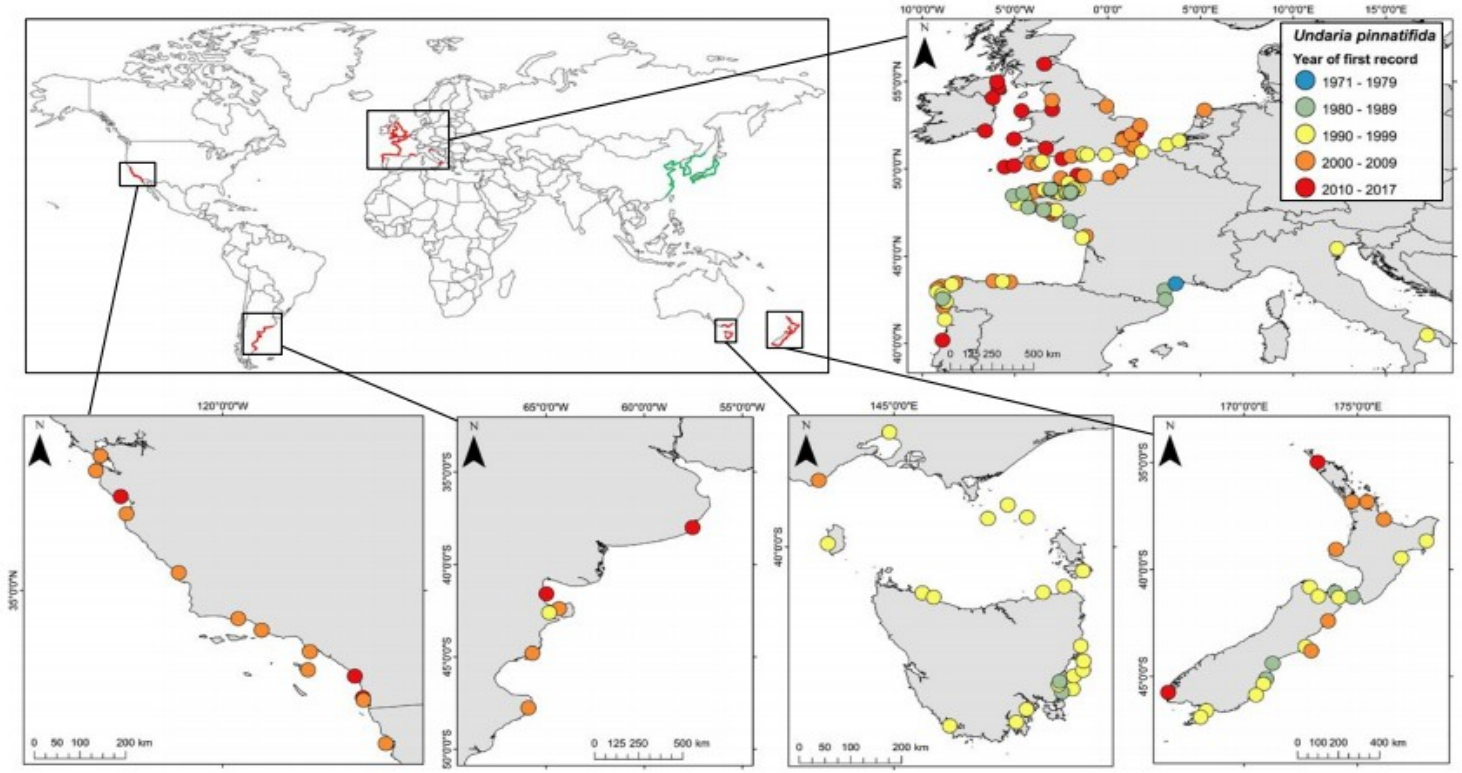

FIGURE 2 Approximate distribution of *Undaria pinnatifida*. Global map: Green = native range, red = non-native range. Regional maps: Each point represents a distinct location but does not indicate precise position or entire extent. See Table S1 for more information and references

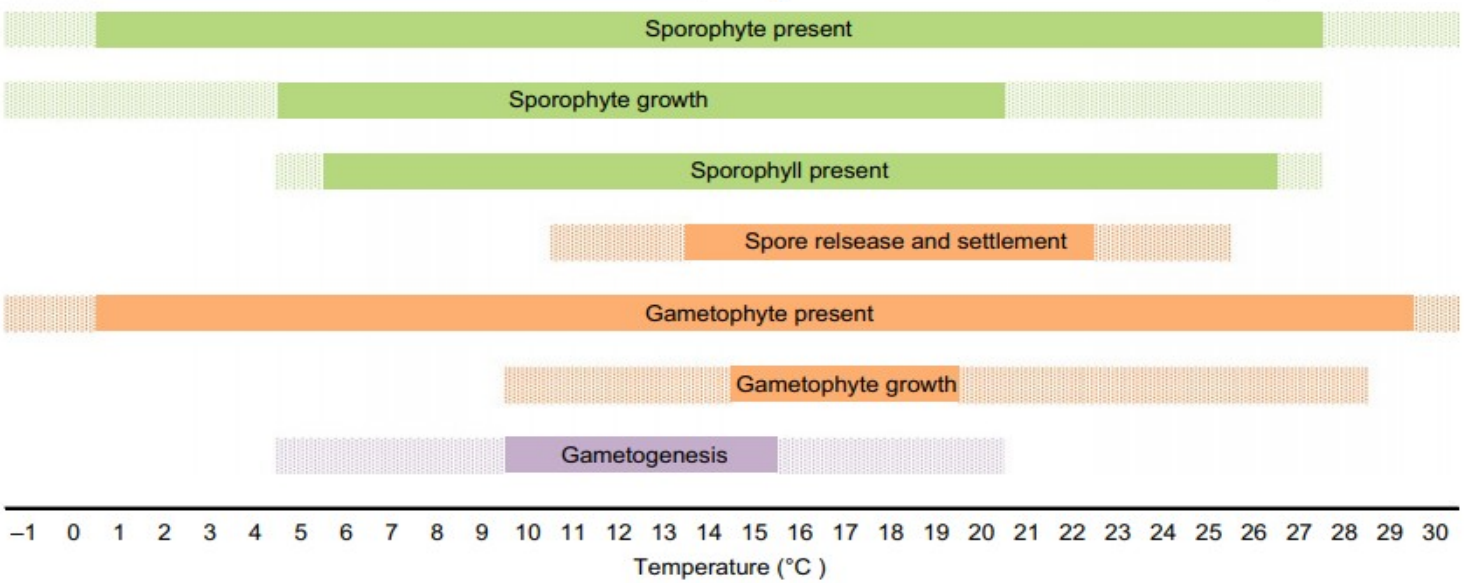

FIGURE 3 Thermal tolerances of the different life stages of *Undaria pinnatifida*. Lighter colors = life stage possible but may be limited. See in text for references

Epstein & Smale, 2017

Laminaria

- several very common species, kelp forests of N Hemisphere
- alginate industry
- biodiversity centre – NW Pacific coast (Alaska – California)

Most frequent European members of traditional *Laminaria*

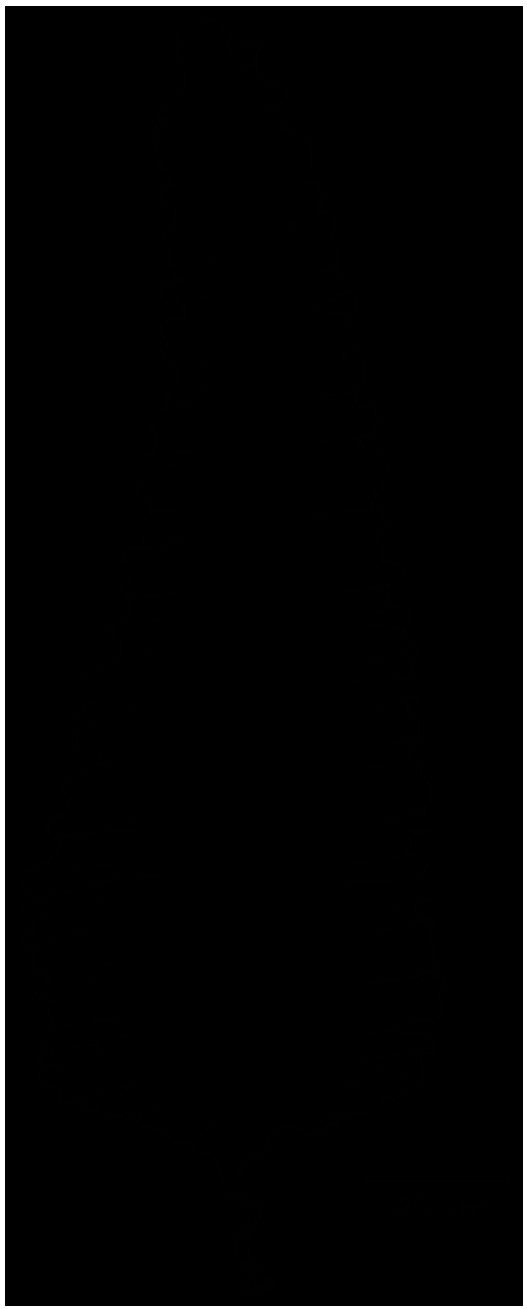

S. latissima

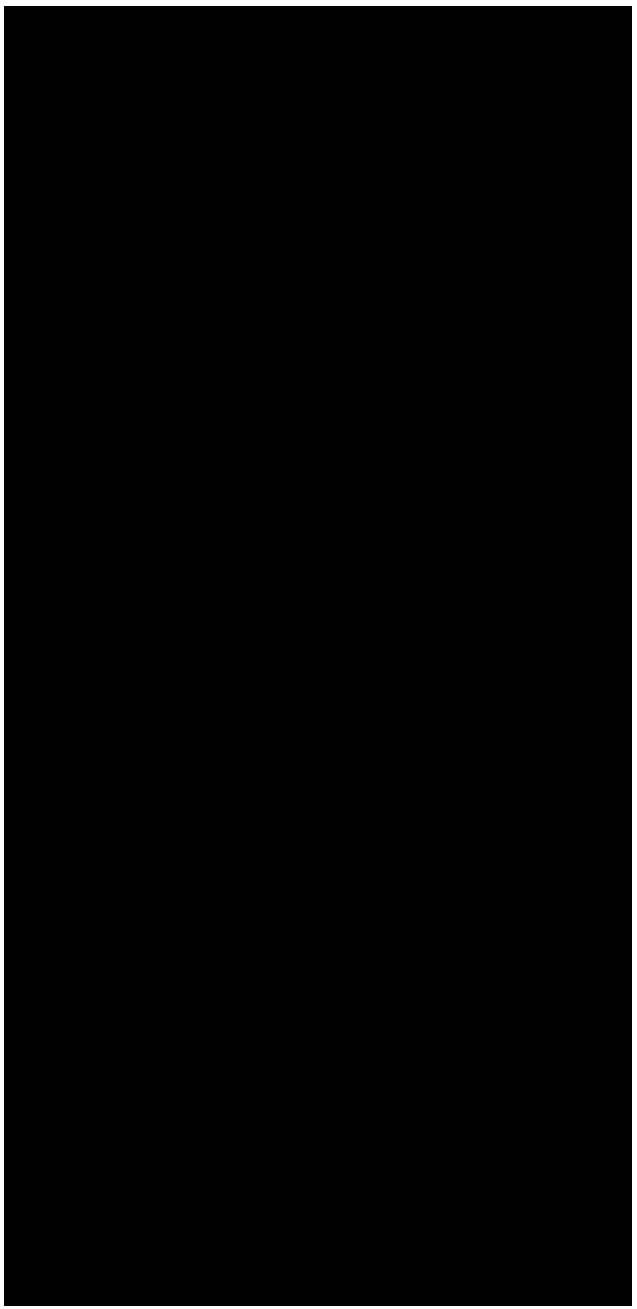

L. hyperborea

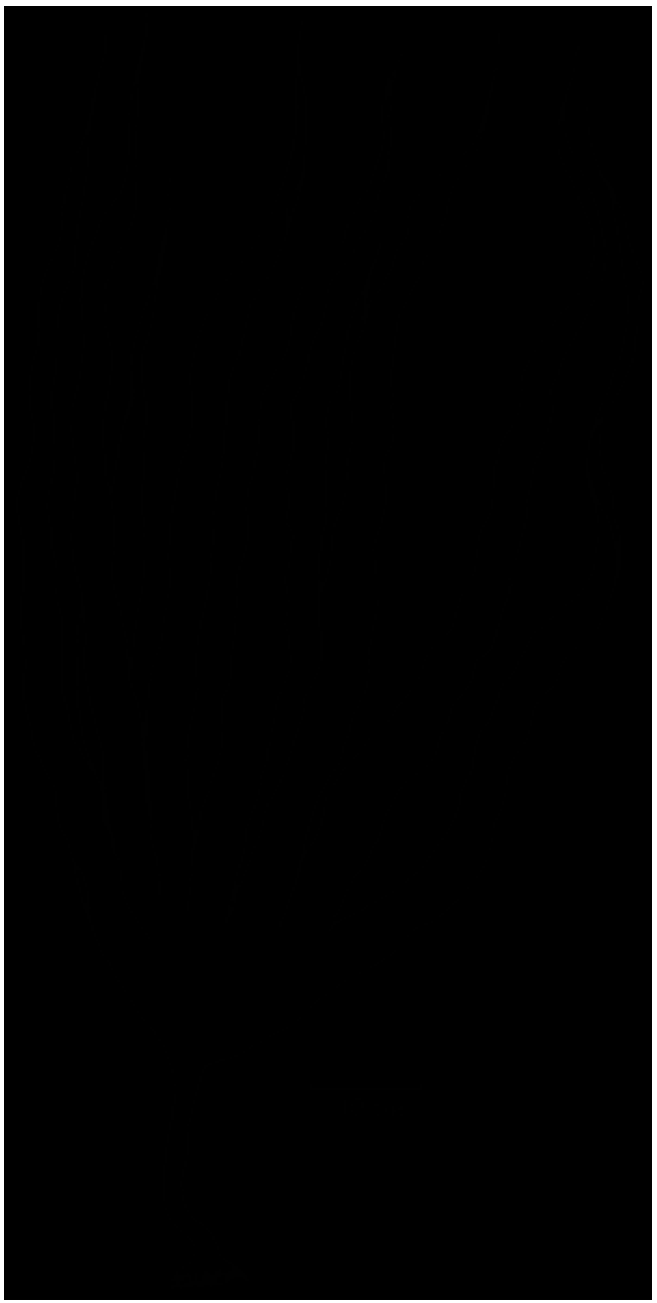

L. digitata

Laminaria hyperborea – canopy species of European kelp forests

Table 1. Current concept of species within the genera *Laminaria* Lamouroux and *Saccharina* Stackhouse

Species name	Most recent synonym(s)	Region of occurrence
***L. abyssalis* Joly et Oliveira 1967**		S Atlantic: deep-water off Brazil
L. appresirhiza Petrov et Vozzhinskaya 1970[a,b]		NW Pacific: Sea of Okhotsk
L. brasiliensis Joly et Oliveira 1967[c]		S Atlantic: deep-water off Brazil
L. complanata (Setchell et Gardner) Muenscher 1917[d]		NE Pacific: restricted occurrence in Washington and British Columbia
***L. digitata* (Hudson) Lamouroux 1813**		N Atlantic
***L. ephemera* Setchell 1901**		NE Pacific
***L. farlowii* Setchell 1893**		NE Pacific
L. gurjanovae Zinova 1964[a]		NW Pacific: Kamchatka, Sakhalin
***L. hyperborea* (Gunnerus) Foslie 1884**		NE Atlantic
L. inclinatorhiza Petrov et Vozzhinskaya 1970[a]		NW Pacific: Sea of Ochotsk
***L. longipes* Bory de Saint-Vincent 1826[f]**		NE Pacific
L. multiplicata Petrov et Suchovejeva 1976[a]		NW Pacific: Sea of Ochotsk
L. nigripes Agardh 1868[a,g]		N Atlantic: Arctic
***L. ochroleuca* Bachelot de la Pylaie 1824**		NE Atlantic, Mediterranean Sea
***L. pallida* Greville 1848[h]**	*L. schinzii* Foslie 1893	S Atlantic
L. philippinensis Petrov et Suchovejeva 1973[a,i]		NW Pacific: deep water off Philippines
***L. rodriguezii* Bornet 1888**		Mediterranean Sea
L. sachalinensis (Miyabe) Miyabe 1933		NW Pacific: Japan
***L. setchellii* Silva 1957**		NE Pacific
***L. sinclairii* (Harvey ex Hooker et Harvey) Farlow, Anderson et Eaton 1878**		NE Pacific
***L. solidungula* Agardh 1868**		N Atlantic: Arctic
***L. yezoensis* Miyabe 1902**		N Pacific
***S. angustata* (Kjellman) Lane, Mayes, Druehl et Saunders 2006**	*L. angustata* Kjellman 1885	NW Pacific: Japan
S. cichorioides (Miyabe) Lane, Mayes, Druehl et Saunders 2006[j]	*L. cichorioides* Miyabe 1902	NW Pacific: Japan
S. coriacea (Miyabe) Lane, Mayes, Druehl et Saunders 2006[k]	*L. coriacea* Miyabe 1902	NW Pacific: Japan
***S. sculpera* (Miyabe) Lane, Mayes, Druehl et Saunders 2006**	*Kjellmaniella crassifolia* Miyabe 1902	NW Pacific: Japan
***S. dentigera* (Kjellman) Lane, Mayes, Druehl et Saunders 2006**	*L. dentigera* Kjellman 1889	NE Pacific: Alaska
S. diabolica (Miyabe) Lane, Mayes, Druehl et Saunders 2006[k,l]	*L. diabolica* Miyabe 1902	NW Pacific: Japan

(*continued*)

Bartsh et al., 2008, Eur. J. Phycol. 43: 1-86.

Table 1. Continued

Species name	Most recent synonym(s)	Region of occurrence
***S. groenlandica* (Rosenvinge) Lane, Mayes, Druehl et Saunders 2006**[e,m]	*L. groenlandica* Rosenvinge 1893 (sensu Druehl, 1968)	NE Pacific: California to British Columbia
	L. bongardiana Postels et Ruprecht 1840[a]	N Pacific: Alaska, Commander Islands
***S. gyrata* (Kjellman) Lane, Mayes, Druehl et Saunders 2006**	*Kjellmaniella gyrata* (Kjellman) Miyabe 1902	NW Pacific: Japan
***S. japonica* (Areschoug) Lane, Mayes, Druehl et Saunders 2006**[l]	*L. japonica* Areschoug 1851	NW Pacific: Japan
	L. fragilis Miyabe 1902	
***S. kurilensis* (Miyabe et Nagai) Lane, Mayes, Druehl et Saunders 2006**	*Cymathaere japonica* Miyabe et Nagai 1940	NW Pacific: Kurile Islands
***S. latissima* (Linnaeus) Lane, Mayes, Druehl et Saunders 2006**	*L. saccharina* (Linnaeus) Lamouroux 1813	N Atlantic and N Pacific
	L. faroensis (Børgesen) Børgesen 1902[n]	NE Atlantic
	L. agardhii Kjellman 1877[o]	NW Atlantic: Canada
	L. groenlandica Rosenvinge 1893 (NW Atlantic form)[m]	NW Atlantic: Canada
S. longicruris (Bachelot de la Pylaie) Lane, Mayes, Druehl et Saunders 2006[p]	*L. longicruris* Bachelot de la Pylaie 1824	NW Atlantic: Canada
S. longipedalis (Okamura) Lane, Mayes, Druehl et Saunders 2006[k]	*L. longipedalis* Okamura 1896	N Pacific: Japan to Washington
S. longissima (Miyabe) Lane, Mayes, Druehl et Saunders 2006[k]	*L. longissima* Miyabe 1902	NW Pacific: Japan
S. ochotensis (Miyabe) Lane, Mayes, Druehl et Saunders 2006[l,q]	*L. ochotensis* Miyabe 1902	NW Pacific: Japan
S. religiosa (Miyabe) Lane, Mayes, Druehl et Saunders 2006[l,q,r]	*L. religiosa* Miyabe 1902	NW Pacific: Japan
***S. sessilis* (Agardh) Kuntze 1891**	*Hedophyllum sessile* (Agardh) Setchell 1901	NE Pacific and Kamchatka
S. subsimplex (Setchell et Gardner) Widdowson, Lindstrom et Gabrielson 2006[a,e]	*L. subsimplex* (Setchell et Gardner) Miyabe et Nagai 1933	NE Pacific: Bering Sea
S. yendoana (Miyabe) Lane, Mayes, Druehl et Saunders 2006[s]	*L. yendoana* Miyabe 1936	NW Pacific: Japan

All names listed have been in use since Kain (1979); doubtful earlier taxa are excluded. For an overview of synonymized and doubtful taxa and more taxonomic references see www.algaebase.org. Distribution extracted from Kain (1979), Lüning (1990) and Guiry & Guiry (2007). Species considered to be currently valid are in bold type.

[a] Taxonomic position unclear. [b]Similar to *L. digitata*; sporangia on one side only, mucilage ducts medially placed and widely spaced (Olga Selivanova, pers. comm. Algaebase version 4.2, 13 Nov 2006). [c]Relationship between *L. abyssalis* and *L. brasiliensis* unclear; it seems probable that just one species is involved due to the restricted occurrence of both. [d]For distribution see also Druehl (1969); he assumes affinity to Arctic *L. digitata* f. *complanata*, but basionym is *L. saccharina* f. *complanata* Setchell et Gardner (Algaebase, vers. 4.2). [e]Petrov (1972) included *L. groenlandica* in his concept of *L. bongardiana*; Lüning & tom Dieck (1990) supported this idea, suggesting similarities to N Atlantic *L. digitata* which were not corroborated by hybridization studies (tom Dieck, 1992); Gabrielson *et al*. (2006) synonymized *L. bongardiana* and *L. groenlandica* with *Saccharina subsimplex*; Lane *et al*. (2006) transferred NE Atlantic *L. groenlandica* to *S. groenlandica*. [f]Molecular data from a population outside the currently recognized range for the species (San Juan Island) indicate a closer relationship to *Laminaria* than to *Saccharina* (Lane, pers. comm.); although this needs confirmation, the transfer to the genus *Saccharina* proposed by Lane *et al*. (2006) is not followed here. [g]Close relation to *L. digitata* (Kain, 1979), but taxonomic position still unclear. [h]Conspecificity with *L. schinzii* was suggested by Stegenga *et al*. (1997) as *L. pallida* and *L. schinzii* were interfertile (F1 generation) (tom Dieck & de Oliveira, 1993). [i]First published in Petrov *et al*. (1973); deep-water population. [j]Lane *et al*. (2006) assume conspecificity with *S. latissima* due to identical ITS sequences. [k]Lane *et al*. (2006) assume conspecificity with *S. japonica* due to identical ITS sequences. [l]According to Yotsukura *et al*. (2006), *S. japonica*, *S. religiosa*, *S. ochotensis* and *S. diabolica* are considered to be one biological species. [m]'Taxonomic relationship between N Atlantic and N Pacific plants unclear' (Druehl, 1969); N Atlantic *L. groenlandica* has been synonymized with *L. cuneifolia* and then with *L. saccharina* (Wilce, 1960; Kain, 1979), a concept which is followed here; N-Pacific plants differ by frequent fingering of the blade (Druehl, 1968). [n]According to partial LSU rDNA, ITS rDNA and AFLP data *L. faroensis* has a sub-species status to *L. saccharina* (Erting *et al*., 2004); Kain (1979) also suggested it to be a 'genetic strain'. [o]According to Chapman (1975), who discounted duct anatomy as taxonomic character; Kain (1979) and later Bhattacharya *et al*. (1991) suggest conspecificity with *L. longicruris* and *L. saccharina*. [p]There is much evidence (Kain,1979: duct and stipe anatomy; Lüning *et al*., 1978: hybridization studies; Bhattacharya *et al*., 1991: 18S rDNA, rDNA (LSU); Cho *et al*., 2000: RuBisCo spacer; Lane *et al*., 2006: ITS) that *S. longicruris* is conspecific with *S. latissima*. [q]According to Lane *et al*. (2006), there is only one base pair difference in ITS sequence between *S. ochotensis*/*S. religiosa* and *S. japonica*. [r]Yoon *et al*. (2001) suggest conspecificity of *S. religiosa* with *S. japonica* due to identical RuBisCo spacer sequences. [s]Druehl & Masuda (1973) state close morphological relation of *S. yendoana* to *S. cichorioides* which, in turn, has identical ITS sequences to *S. latissima* (Lane *et al*., 2006).

Alaria esculenta

Laminaria digitata

Laminaria hyperborea

Laminaria ochroleuca

Laminaria rodriguezii

Laminaria saccharina

Phyllariopsis breviceps

Phyllariopsis purpurascens

Saccorhiza dermatodea

Saccorhiza polyschides

Undaria pinnatifida

Nereocystis – annual plant, length up to 40 m

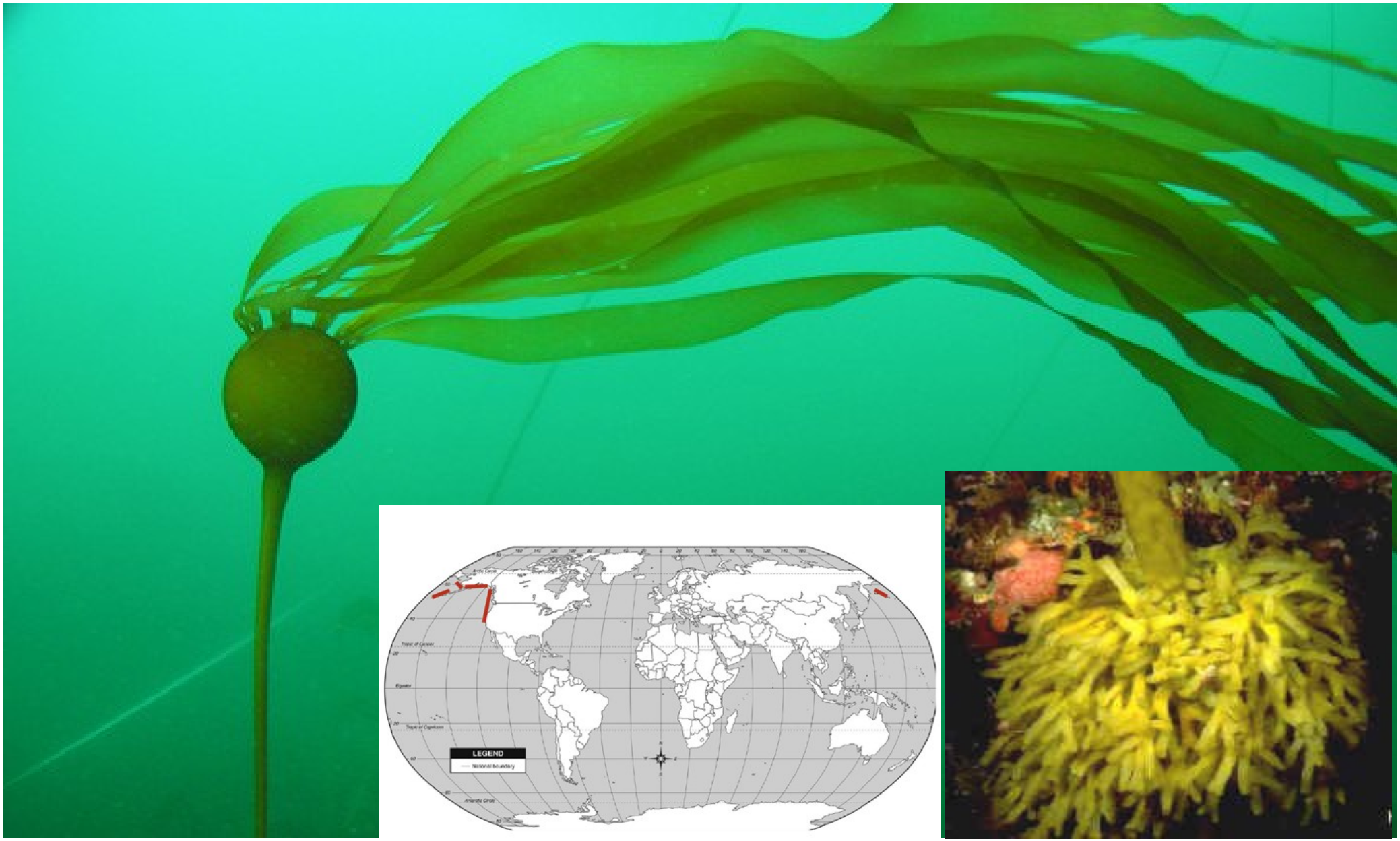

měchýřky – až 12% CO (!)

Macrocystis – sublitoral, length up to 60m, weight 300 kg

Macrocystis pyrifera

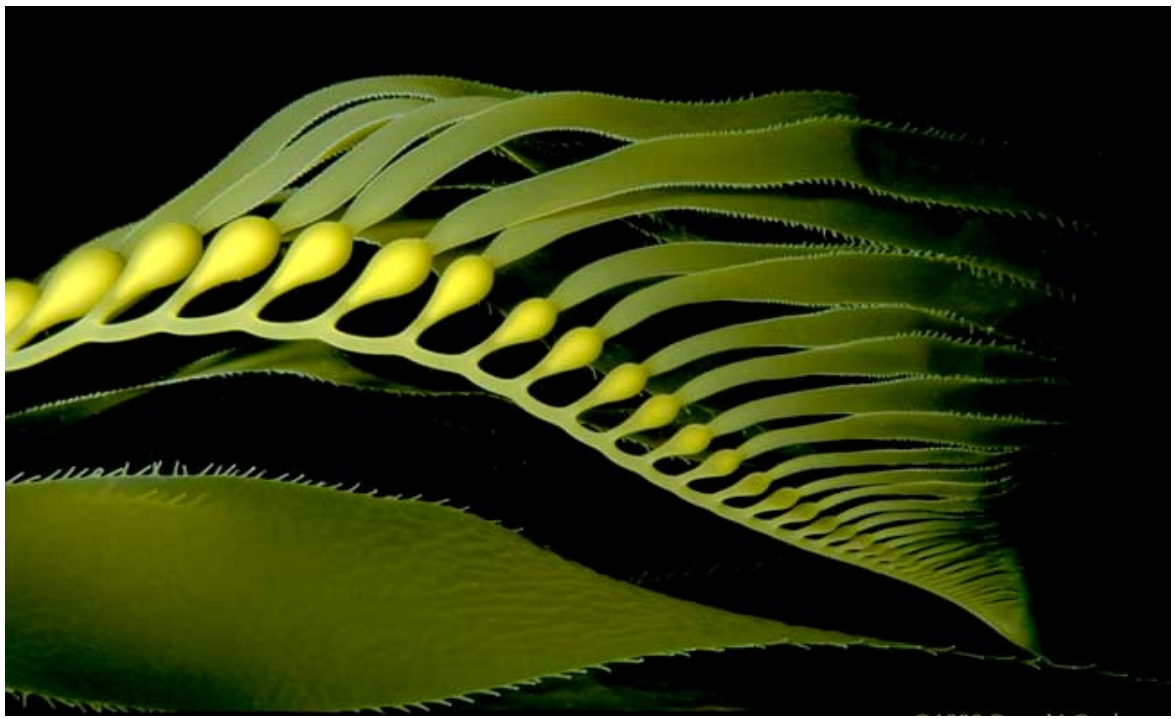

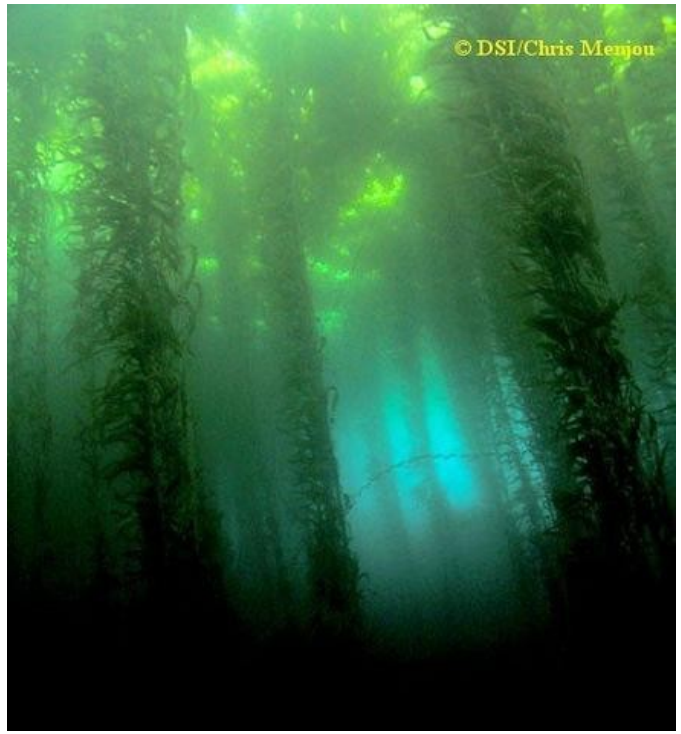

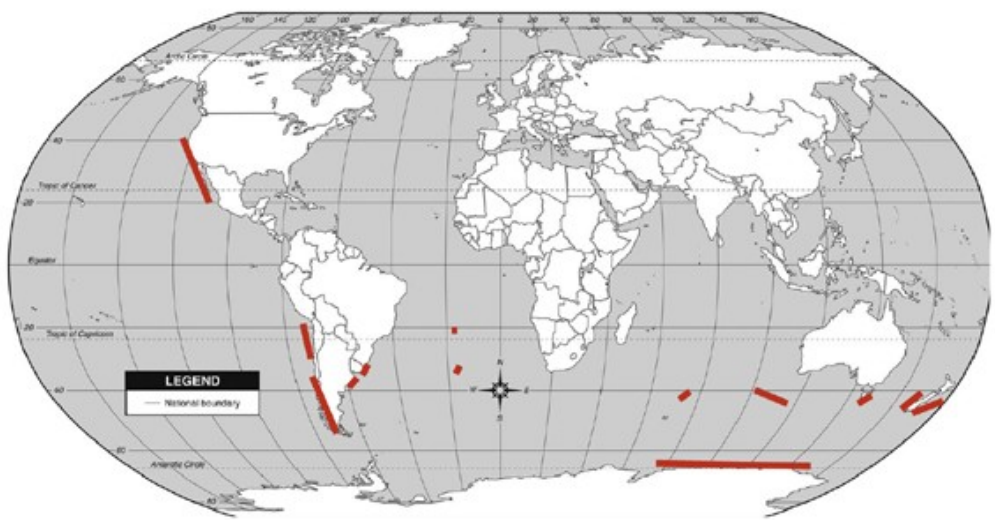

Evolutionary geographic origins of the genus *Macrocystis*

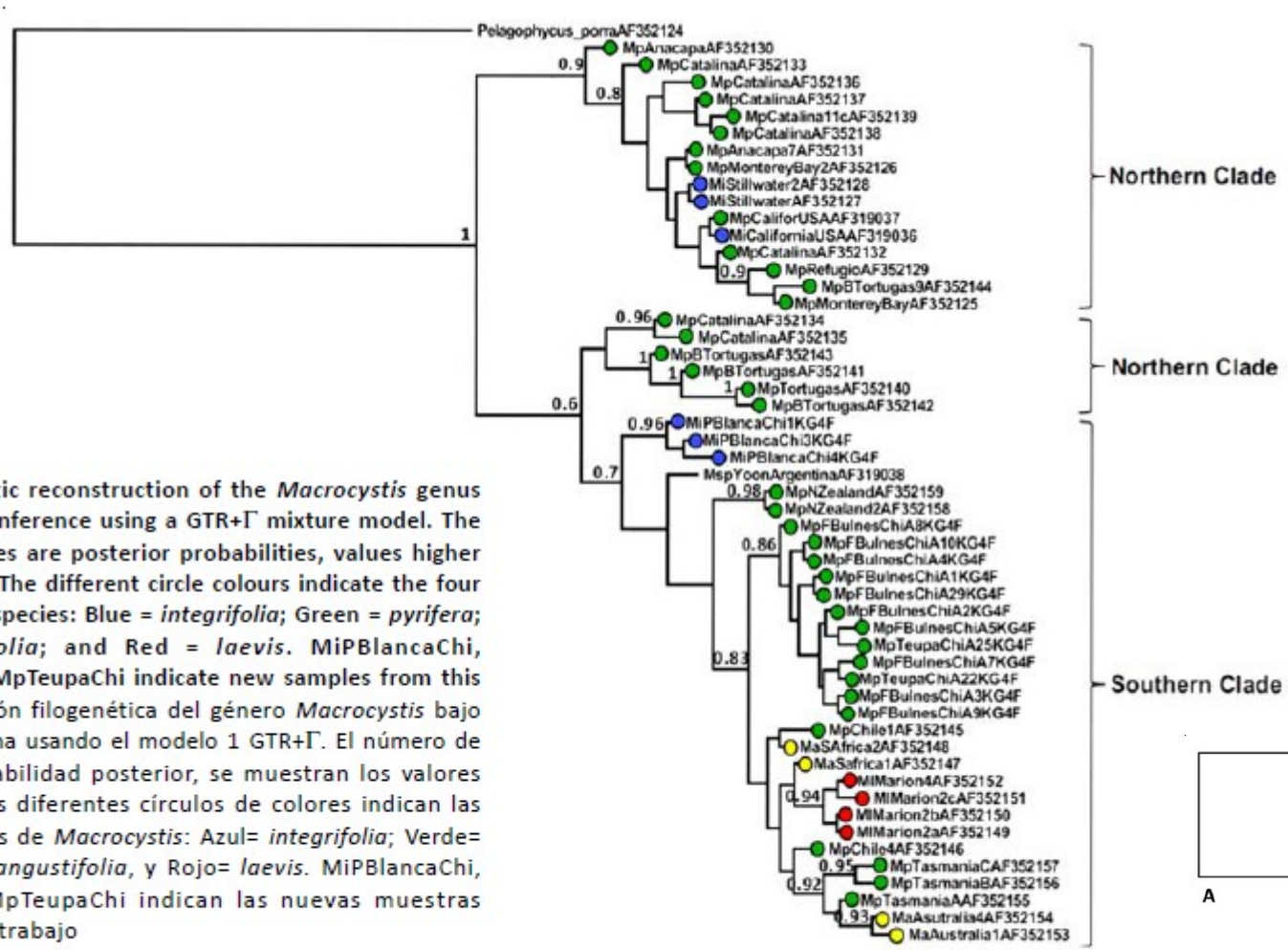

Figure 1. Phylogenetic reconstruction of the *Macrocystis* genus under the Bayesian inference using a GTR+Γ mixture model. The numbers at the nodes are posterior probabilities, values higher than 0.5 are shown. The different circle colours indicate the four *Macrocystis* morphospecies: Blue = *integrifolia*; Green = *pyrifera*; Yellow = *angustifolia*; and Red = *laevis*. MiPBlancaChi, MpFBulnesChi, and MpTeupaChi indicate new samples from this work / Reconstrucción filogenética del género *Macrocystis* bajo la inferencia Bayesiana usando el modelo 1 GTR+Γ. El número de los nodos son probabilidad posterior, se muestran los valores superiores a 0,5. Los diferentes círculos de colores indican las cuatro morfoespecies de *Macrocystis*: Azul= *integrifolia*; Verde= *pyrifera*; Amarillo= *angustifolia*, y Rojo= *laevis*. MiPBlancaChi, MpFBulnesChi, y MpTeupaChi indican las nuevas muestras aportadas por este trabajo

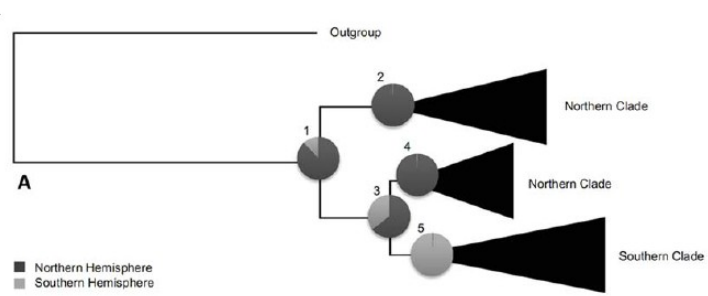

A) Hemisphere

Node	Ancestral State	
	Northern Hemisphere	Southern Hemisphere
1	0.88 ± 0.13	0.12 ± 0.13
2	0.99 ± 0.01	0.01 ± 0.01
3	0.64 ± 0.22	0.36 ± 0.22
4	0.99 ± 0.01	0.01 ± 0.01
5	0.01 ± 0.01	0.99 ± 0.01

Table 1. The probability values for each ancestral state of (A) Hemisphere, (B) Ocean, and (C) Morphology of *Macrocystis*. The probability values are reported with 10 times the standard error based on the BMCMC approach / Valores de probabilidad de cada estado ancestral para (A) Hemisferio, (B) Océano y (C) Morfología de *Macrocystis*. Los valores de probabilidad son reportados con 10 veces el error estándar basado en la aproximación BMCMC

probable Northern origin of the genus

Astorga et al., 2012, Rev. Biol. Mar. Oc.

Saccharina

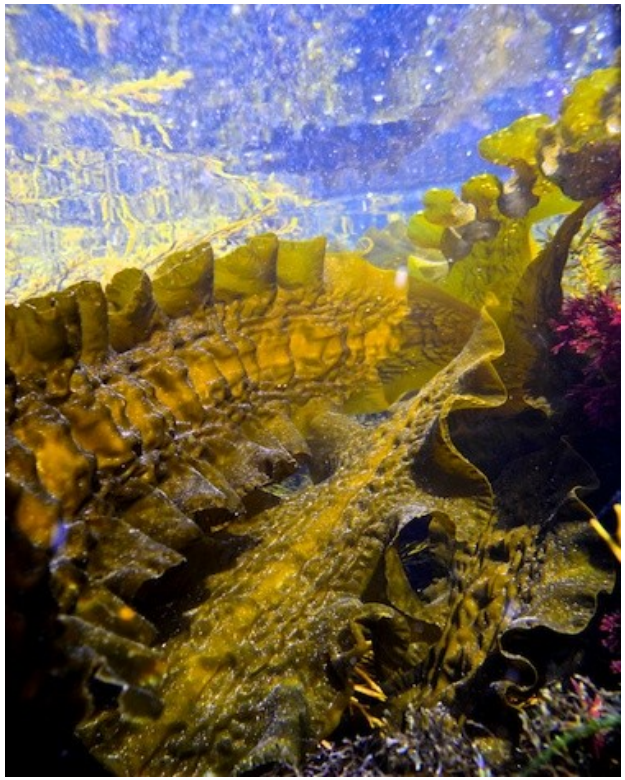

S. japonica

S. latissima

seaweed.ie

Saccharina

- separated from Laminaria
- circumboreal genus (*S. latissima*, *S. japonica*)

(kombu)

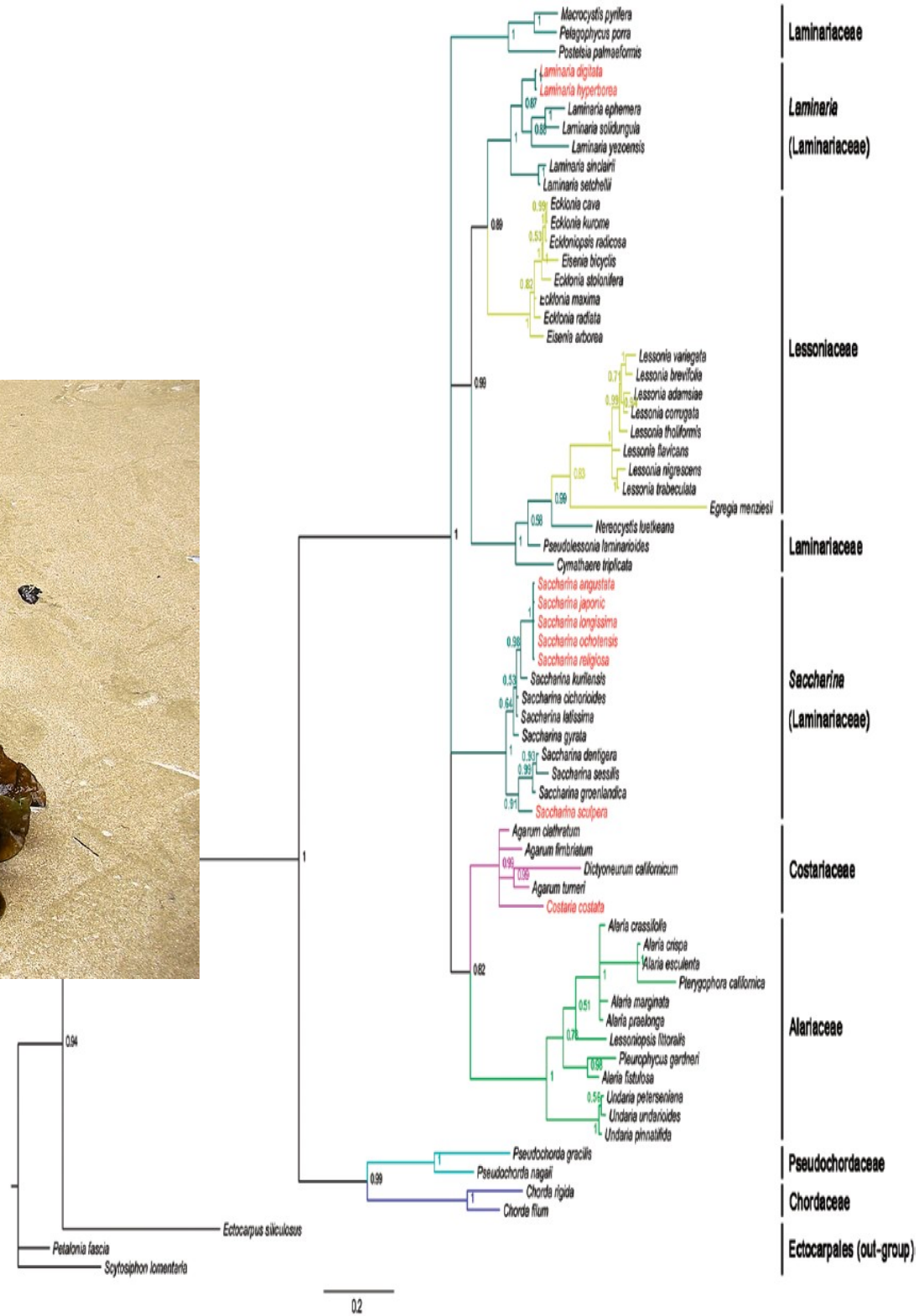

Chi et al., 2014, Acta Oceanol Sin

Postelsia (palmaeformis)

sea palm

Chorda filum – 0.3 to 5 m long strands, filled by air

paraphyses (and hairs)
cover the thallus

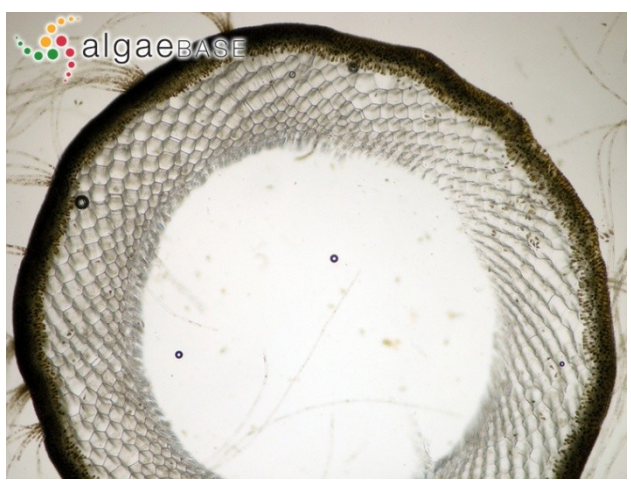

cold temperate/subarctic alga,
ephemeral thalli, penetrates deep into the brackish water habitats

Ectocarpales

- simple, uniseriate filaments
- diplohaplontic cell cycle, isomorphic or slightly heteromorphic

Ectocarpus siliculosus

- delicate, filamentous tufts
- very common, cosmopolitan species

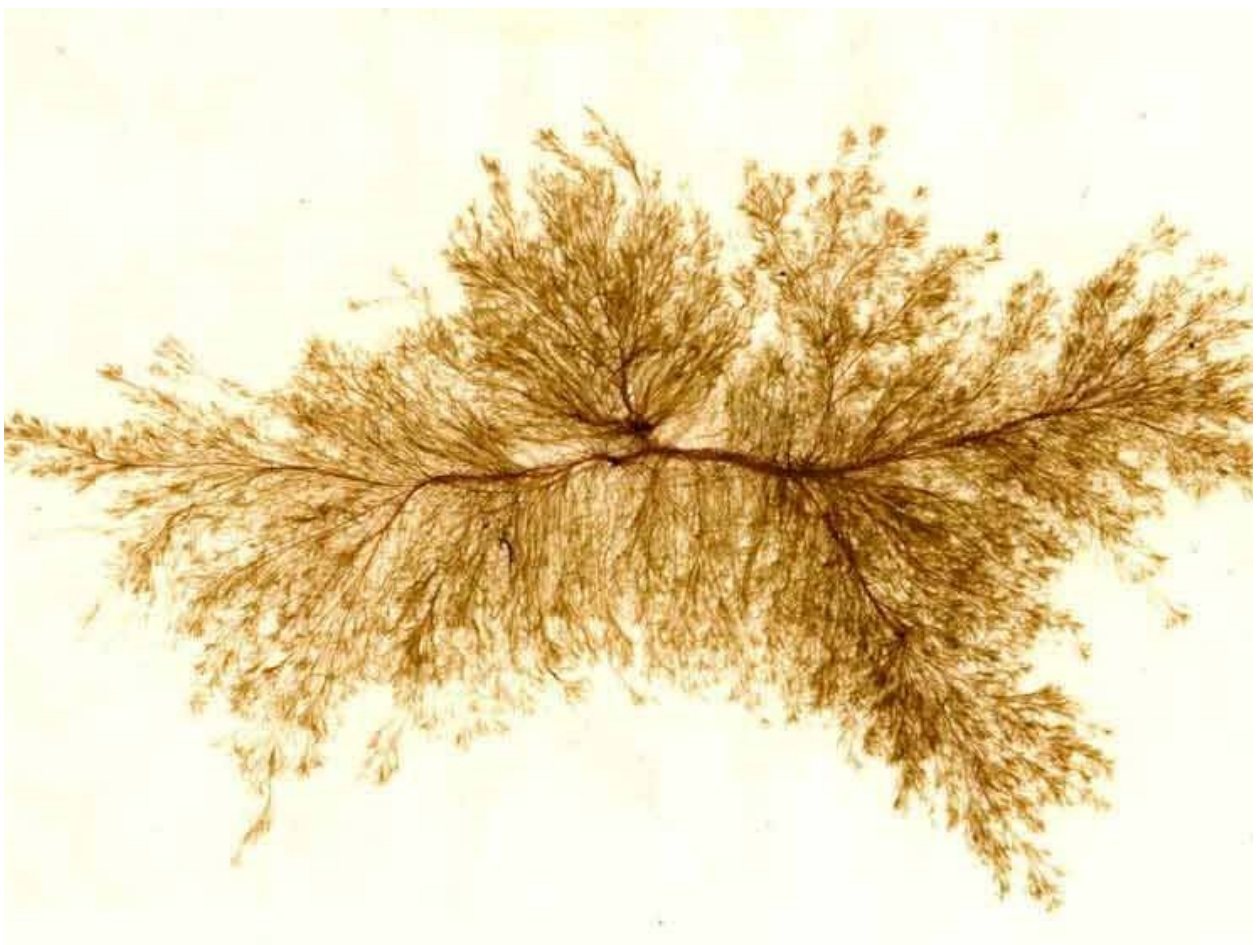

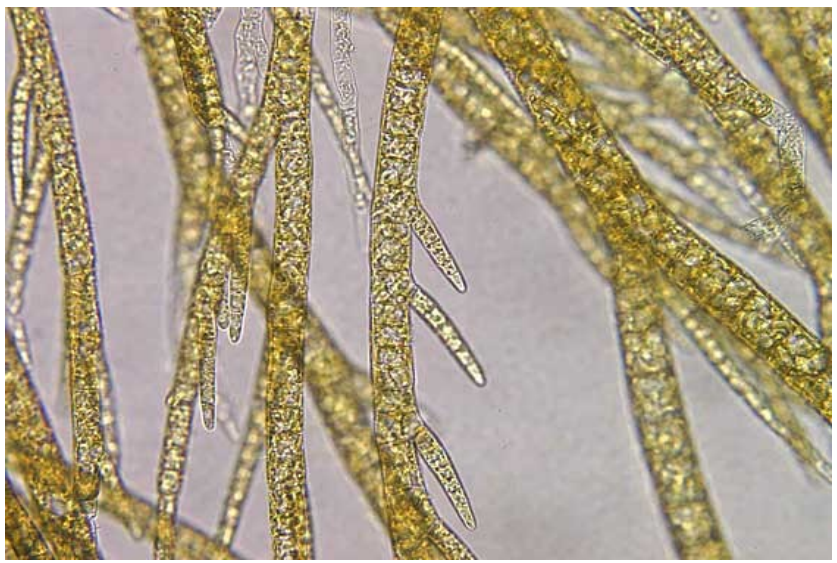

Pylaiella littoralis

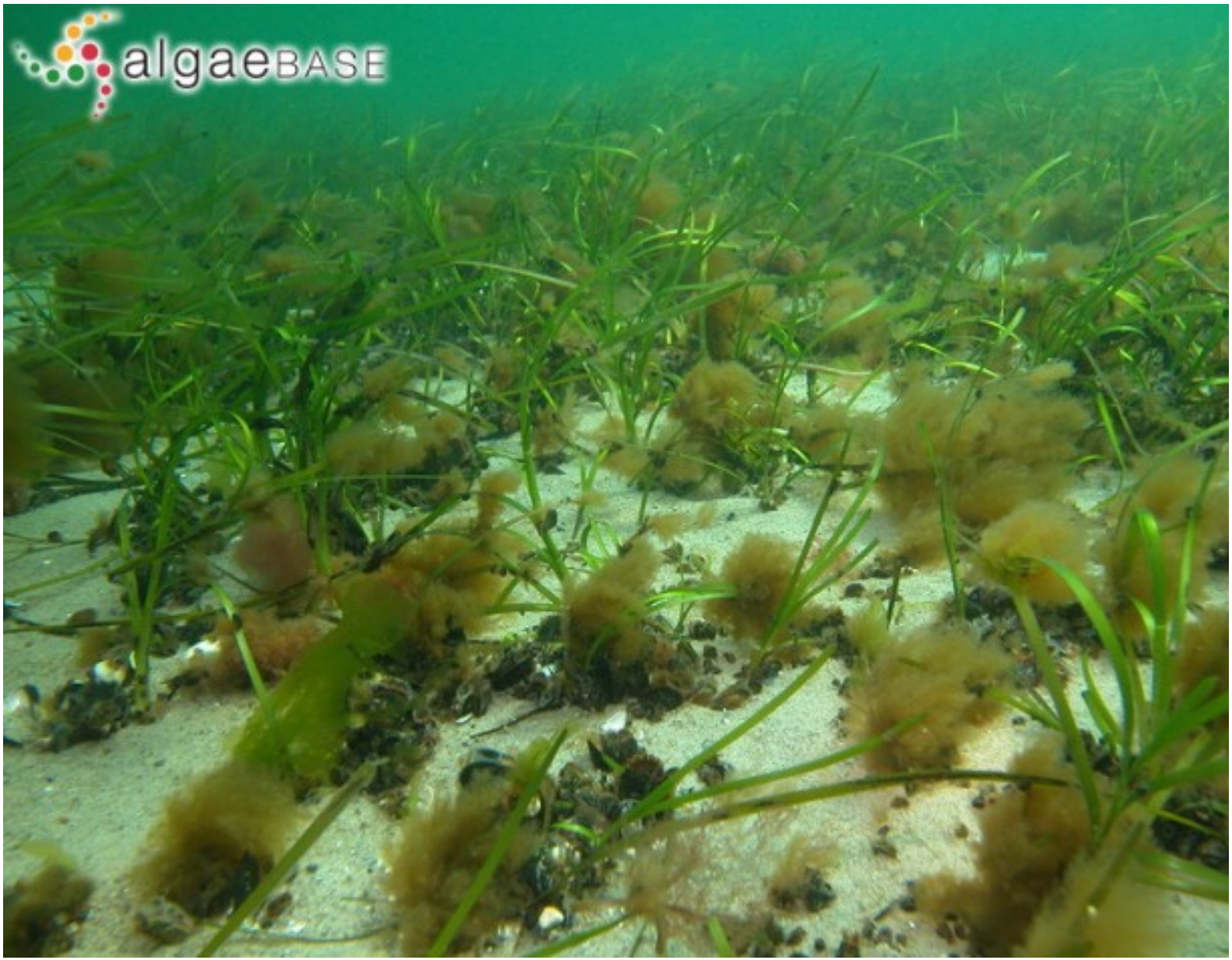

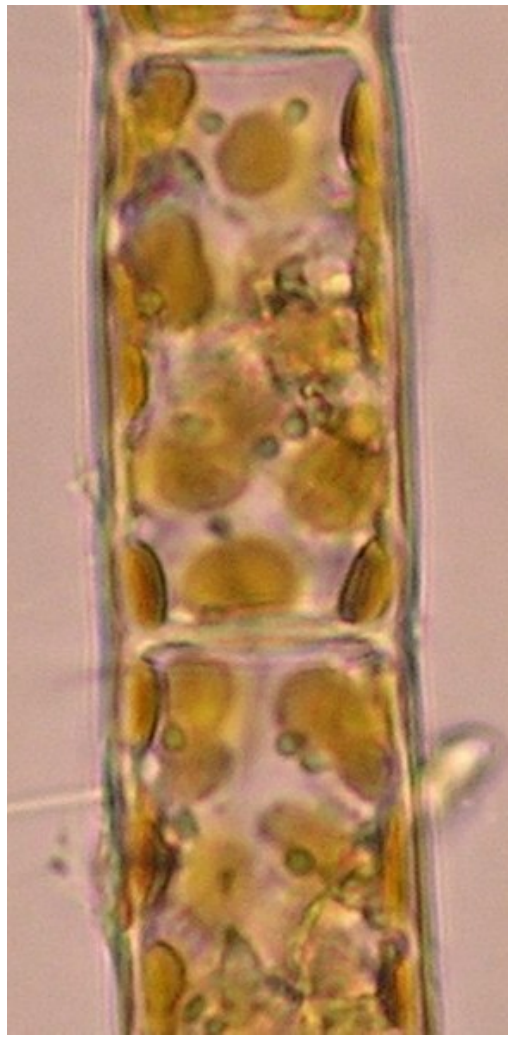

abundant cold water species, often in brackish waters,
dominant as annual epiphyte in the Baltic


Pylaiella littoralis

♂ gametophyte

♀ gametophyte

plurilocular sporangia

plurilocular gametangia

plurilocular sporangia

unilocular sporangia

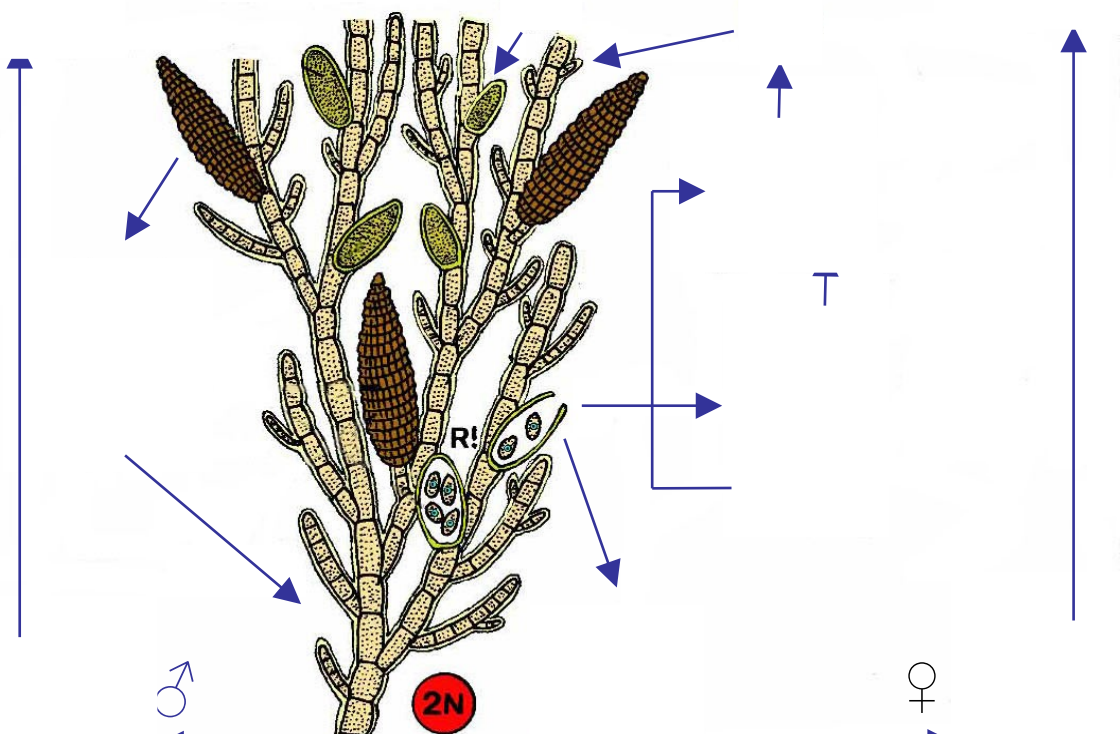

Colpomenia

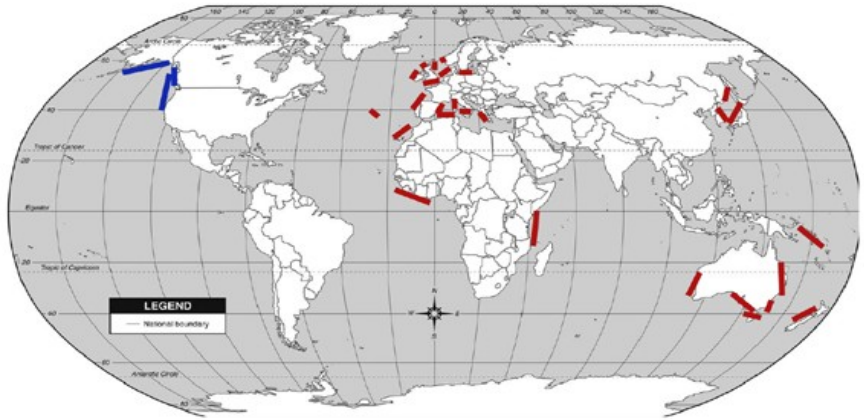

Colpomenia peregrina

ephemeral thalli, saccate gametophytes,

invasive species, origin in NW Pacific

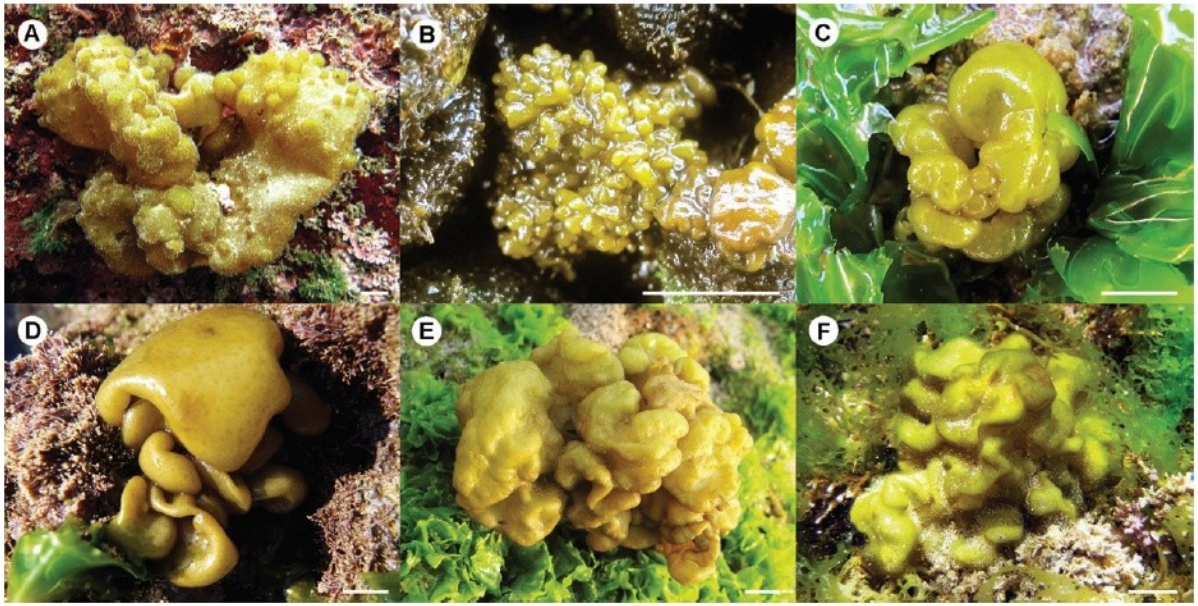

Figure 1 *Colpomenia sinuosa*: variable morphology and habit.
(A) Group Ia, Sasudong, Jeju, Korea (8 Jul. 2011); (B) group Ic, Punta Santa Ana, Magallanes, Chile (31 Oct. 2011); (C) group Ie, Praia Rasa, Búzios, Brazil (24 Oct. 2011); (D) group II, Heraklion, Crete Island, Greece (11 Jan. 2011); (E) group IIIa, Daedonghae, Hainan, China (9 Mar. 2009); (F) group IIIb, Bulusan, Philippines (3 Feb. 2010). Scale bars are 1 cm.

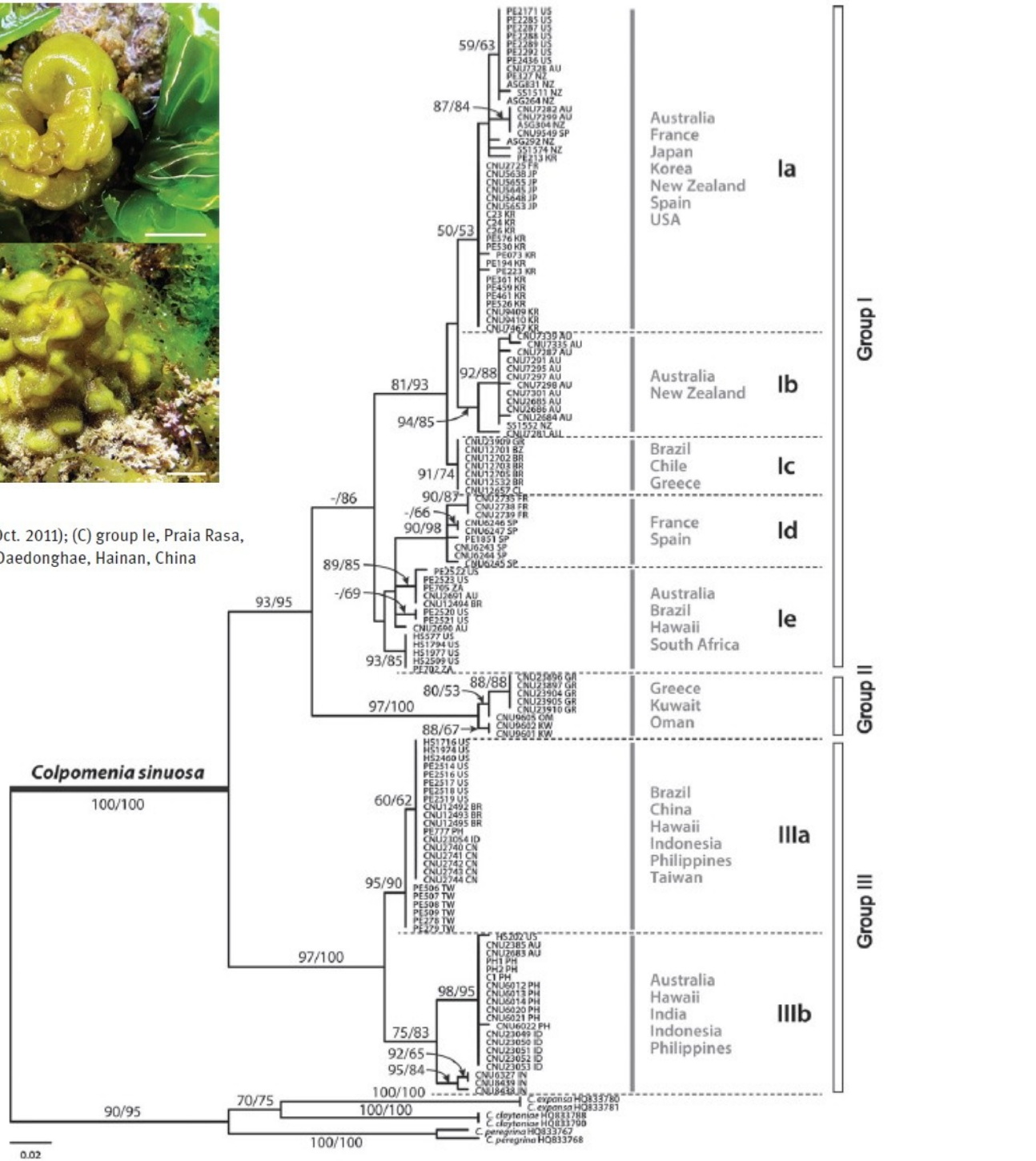

Figure 2 *Colpomenia sinuosa*: ML tree inferred from the phylogenetic analysis of *cox*3 sequences.
Values shown near branches are bootstrap values (1000 iterations) from the data (ML/MP). Only bootstrap values >50% are shown. Branch lengths are proportional to the number of substitutions per site.

Lee et al., 2013, Bot. Mar. 56: 15-25.

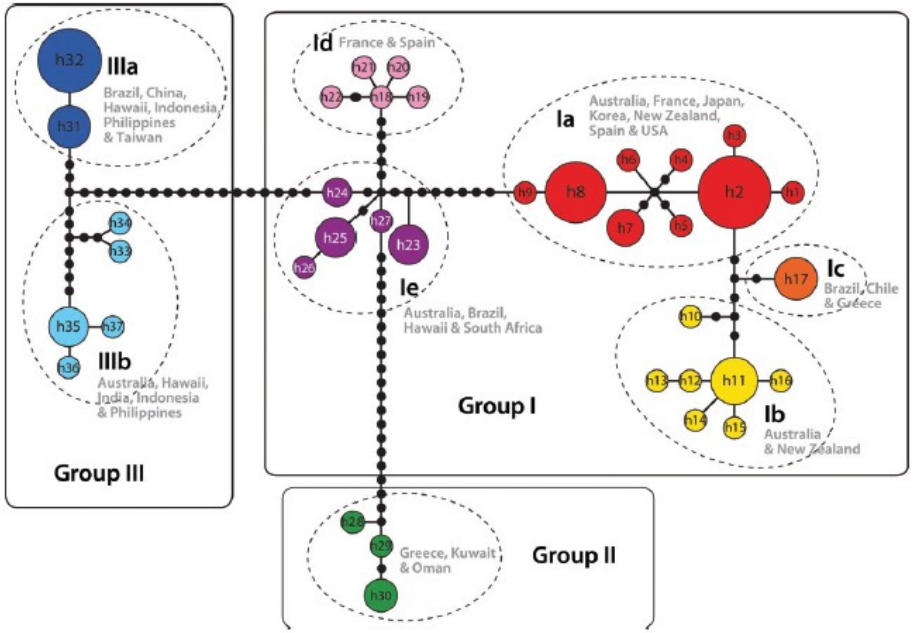

Figure 5 *Colpomenia sinuosa*: statistical parsimony network for 37 *cox*3 haplotypes.
Each circle represents a haplotype and circle size is proportional to strain frequency. Black solid lines delineate the three major groups (I, II, and III). Lines between haplotypes are single mutational steps; small black dots indicate missing haplotypes (either extinct or not sampled).

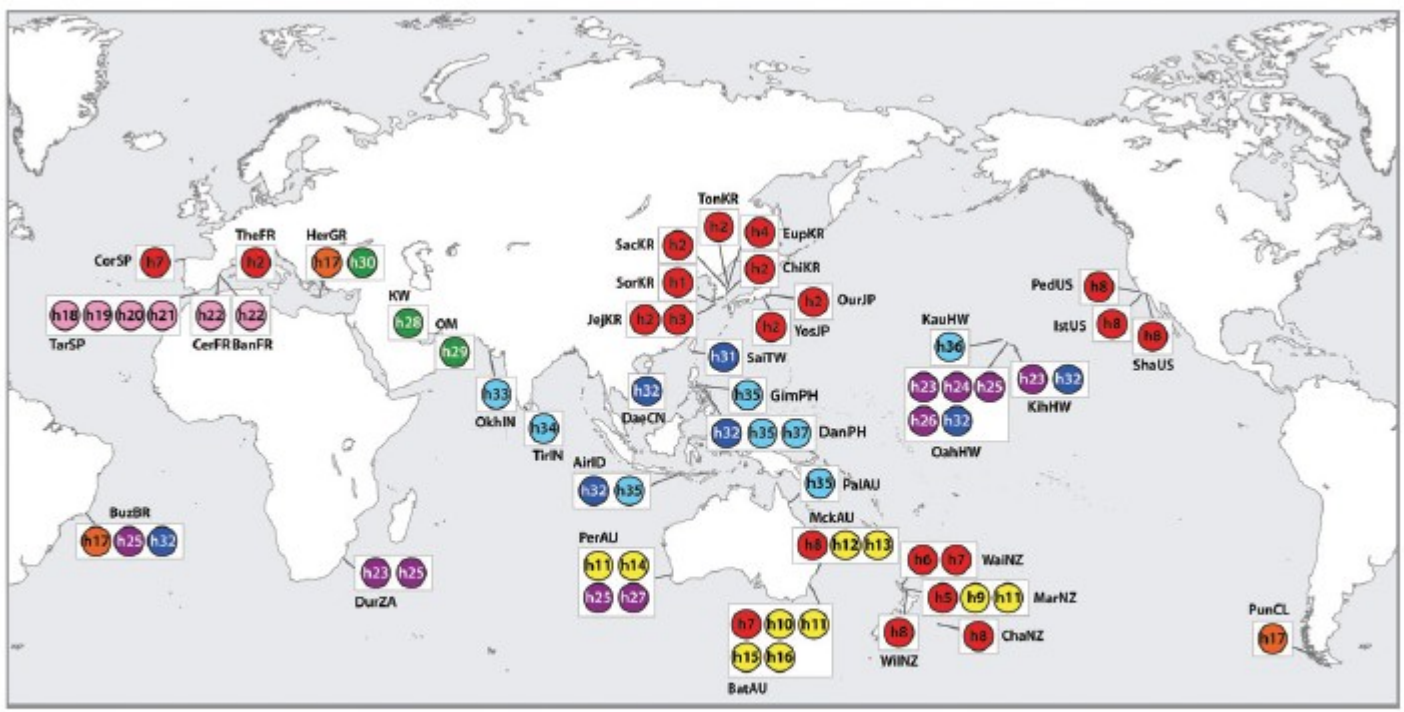

Figure 4 *Colpomenia sinuosa*: distribution map of the *cox*3 haplotypes.
Circles indicate haplotypes, and boxes indicate locations in which more than two haplotypes were found. Different colors are given for group II and subgroups of group I and III, as indicated in Figure 5. Abbreviations explained in Table 1.

former
Scytosiphonales

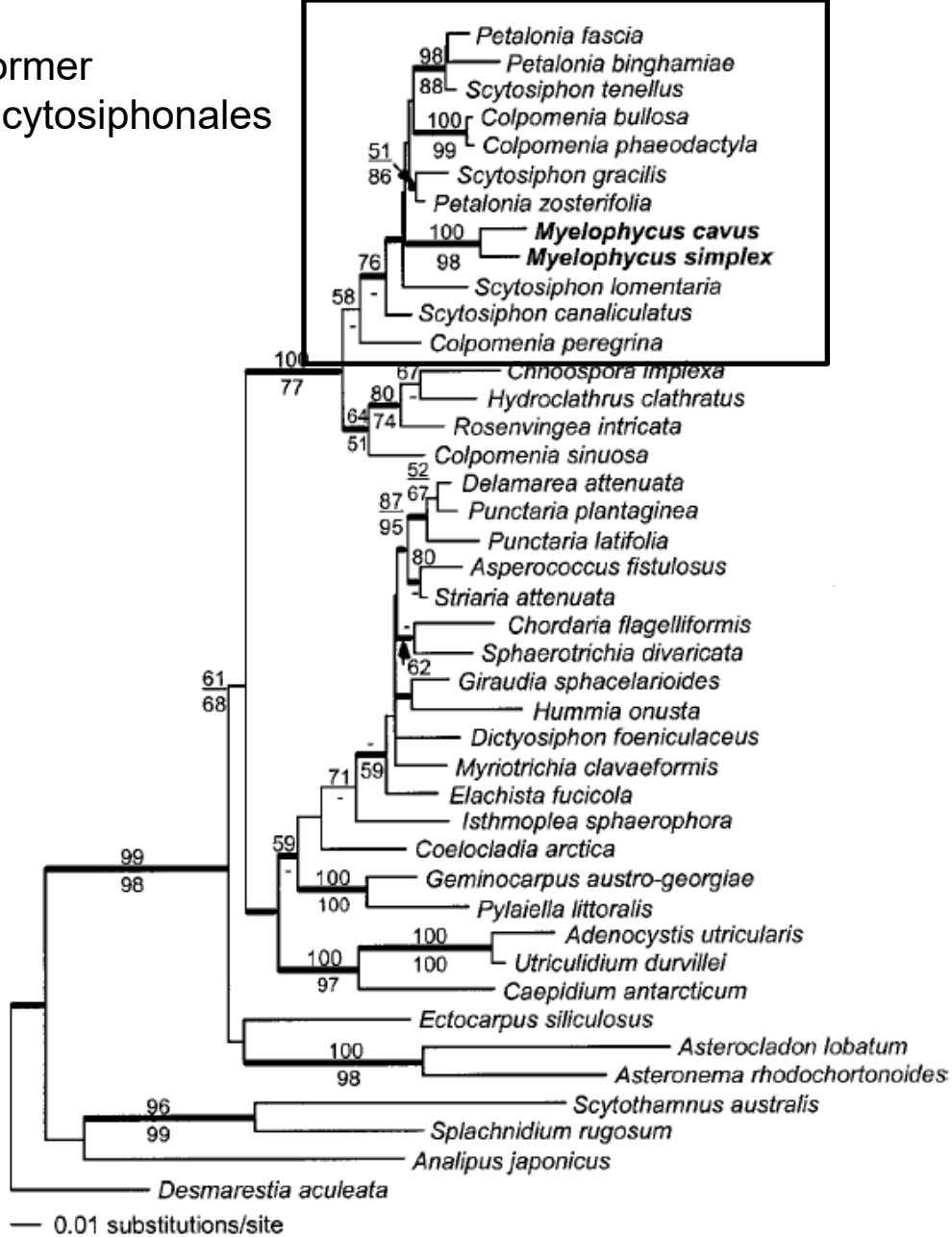

Fig. 10. Maximum likelihood tree for *Myelophycus* and relatives estimated from *rbc*L sequence data (GTR + I + Γ model, -Log likelihood = 9745.20; I = 0.5984; Γ = 0.9113; A ↔ C = 1.227, A ↔ G = 4.55; A ↔ T = 1.207; C ↔ G = 1.314; C ↔ T = 10.16; and G ↔ T = 1). Thicker branches represent the posterior probabilities (>95%) from Bayesian analysis. Bootstrap values (>50%) are given above (MP) and below (ME) branches. The alternative hypothetical topologies of the *rbc*L tree are shown with numbered arrows, indicating the constrained monophyly with *Myelophycus* for Shimodaira-Hasegawa test.

Petalonia fasciata


Scytosiphon lomentaria

Scytosiphon lomentaria

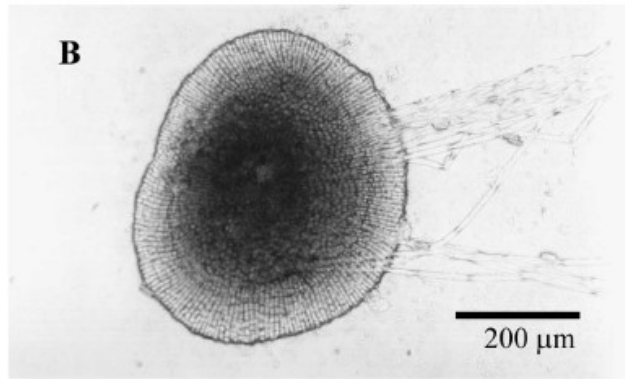

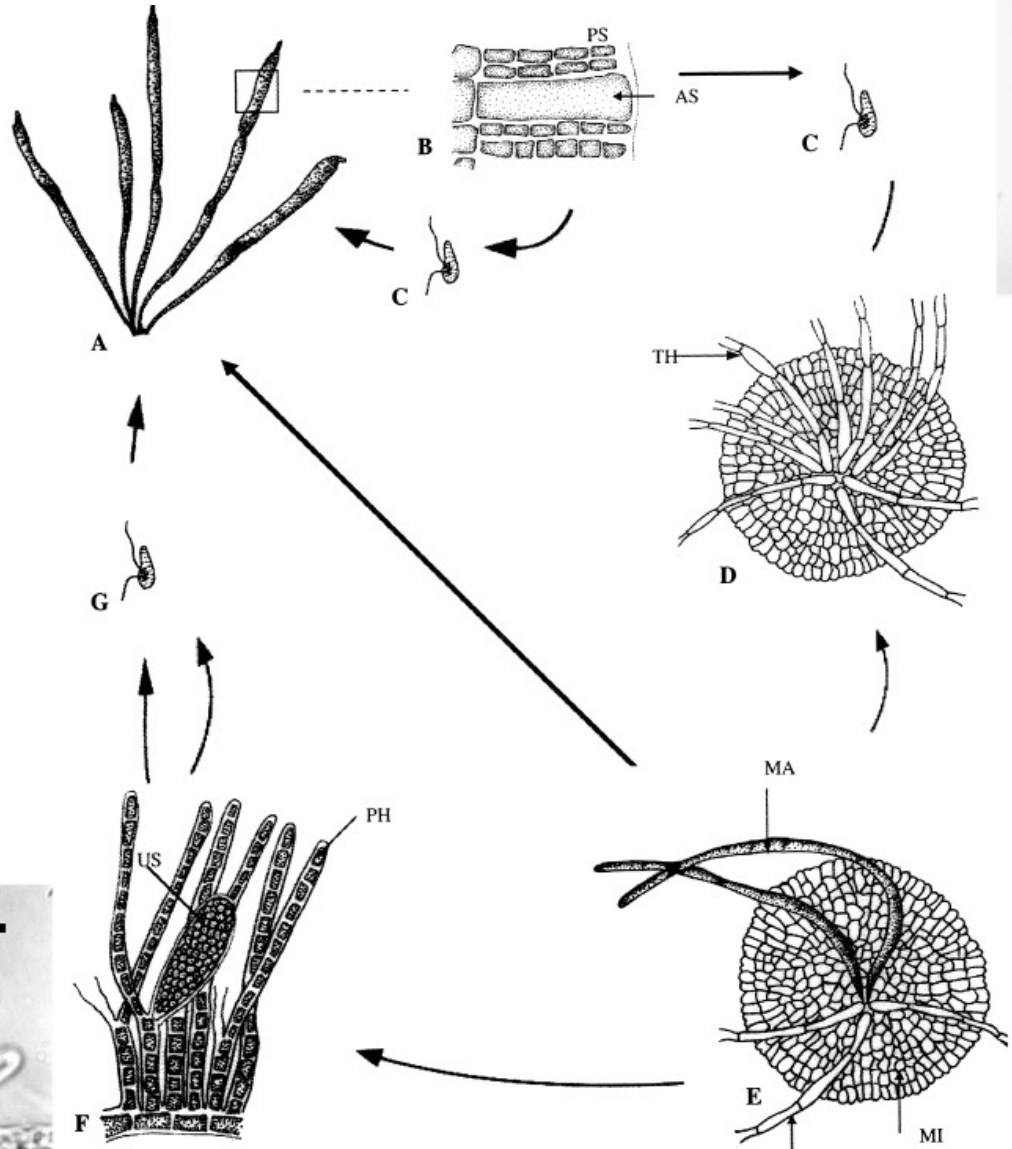

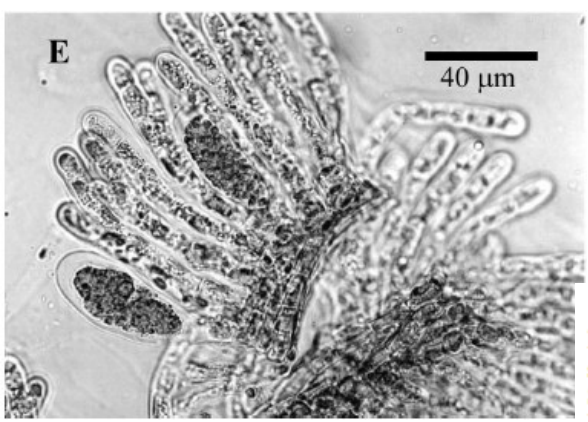

FIG. 4. Diagrammatic illustrations of the life history of Azorean *Scytosiphon lomentaria* in culture. (A) Macrothallus with plurilocular sporangia. (B) Transverse section of a small portion of macrothallus with plurilocular sporangia. (C) Spore from the plurilocular sporangia (plurispore). (D) Crustose microthallus. (E) Crustose microthallus with erect blades and true hairs emerging. (F) Squashed microthallus with unilocular sporangia and paraphyses. (G) Spore from the unilocular sporangia (unispore). AS, ascocyst; MA, macrothallus; MI, microthallus; PH, paraphyses; PS, plurilocular sporangia; TH, true hair; US, unilocular sporangia.

Parente et al., 2003, J. Phycol. 39: 353-359.

Dictyosiphon foeniculaceus

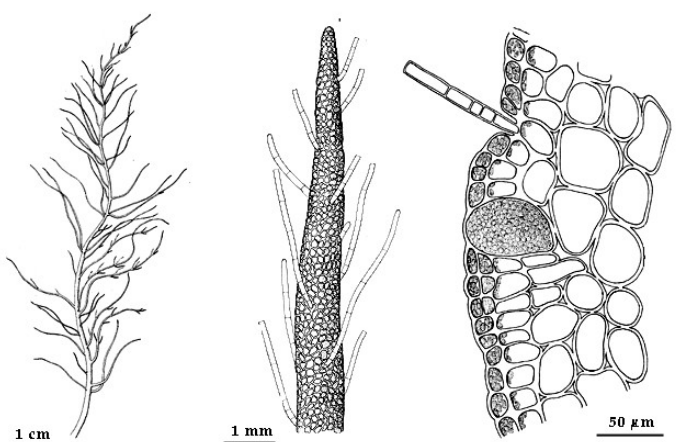

Adenocystis

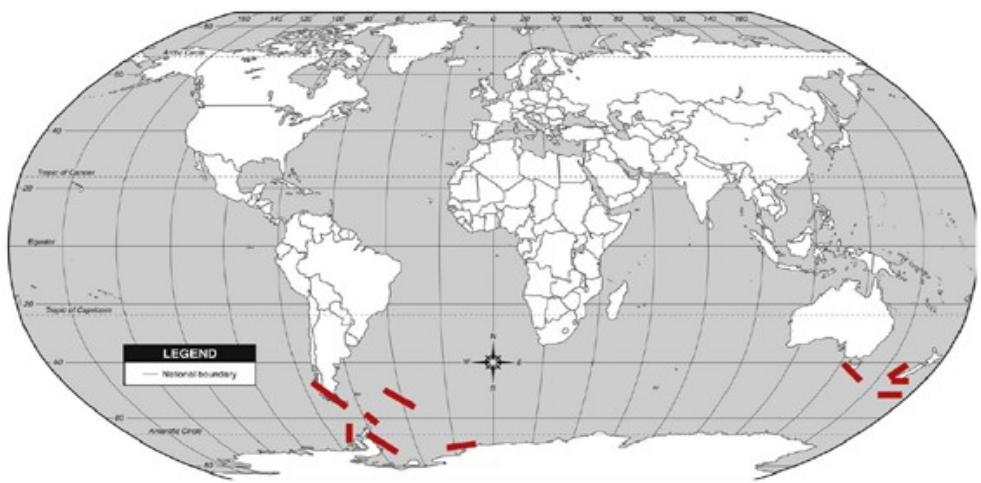

Adenocystis utricularis

Splachnidium

S. rugosum

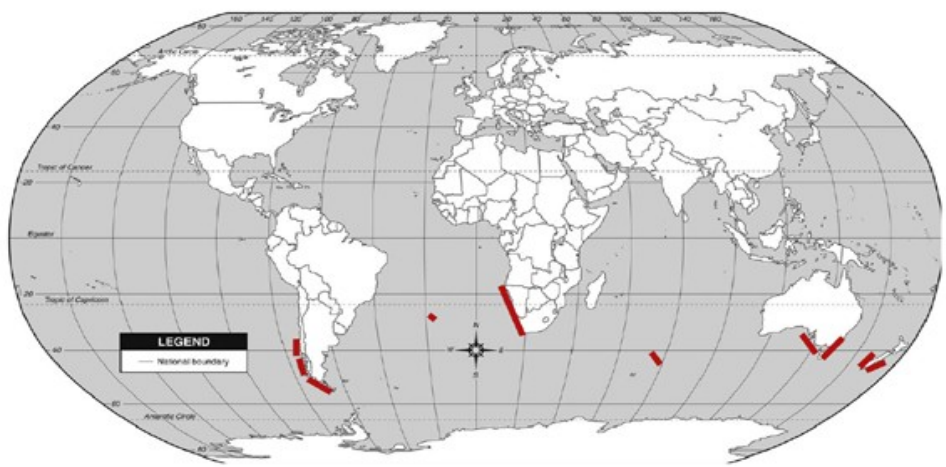

Utilization of brown algae

- Scandinavia, Faroe Islands – grazing by sheep
- fuel, composting, roofs
- production of soda, potash, iodine (1930s)

Læsø, Denmark

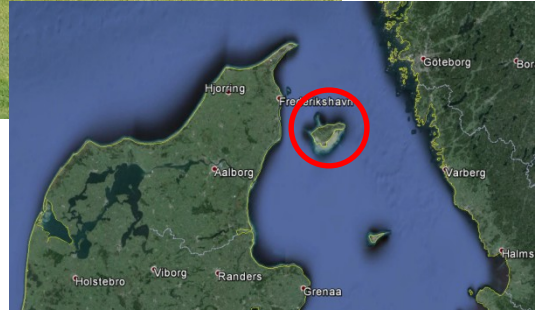

Utilization of brown algae - cultivation

Utilization of brown algae - food

kombu - *Laminaria*

Utilization of brown algae - food

wakame - *Undaria*

Utilization of brown algae - food

hiziki - *Hizikia*

Utilization of brown algae - alginates

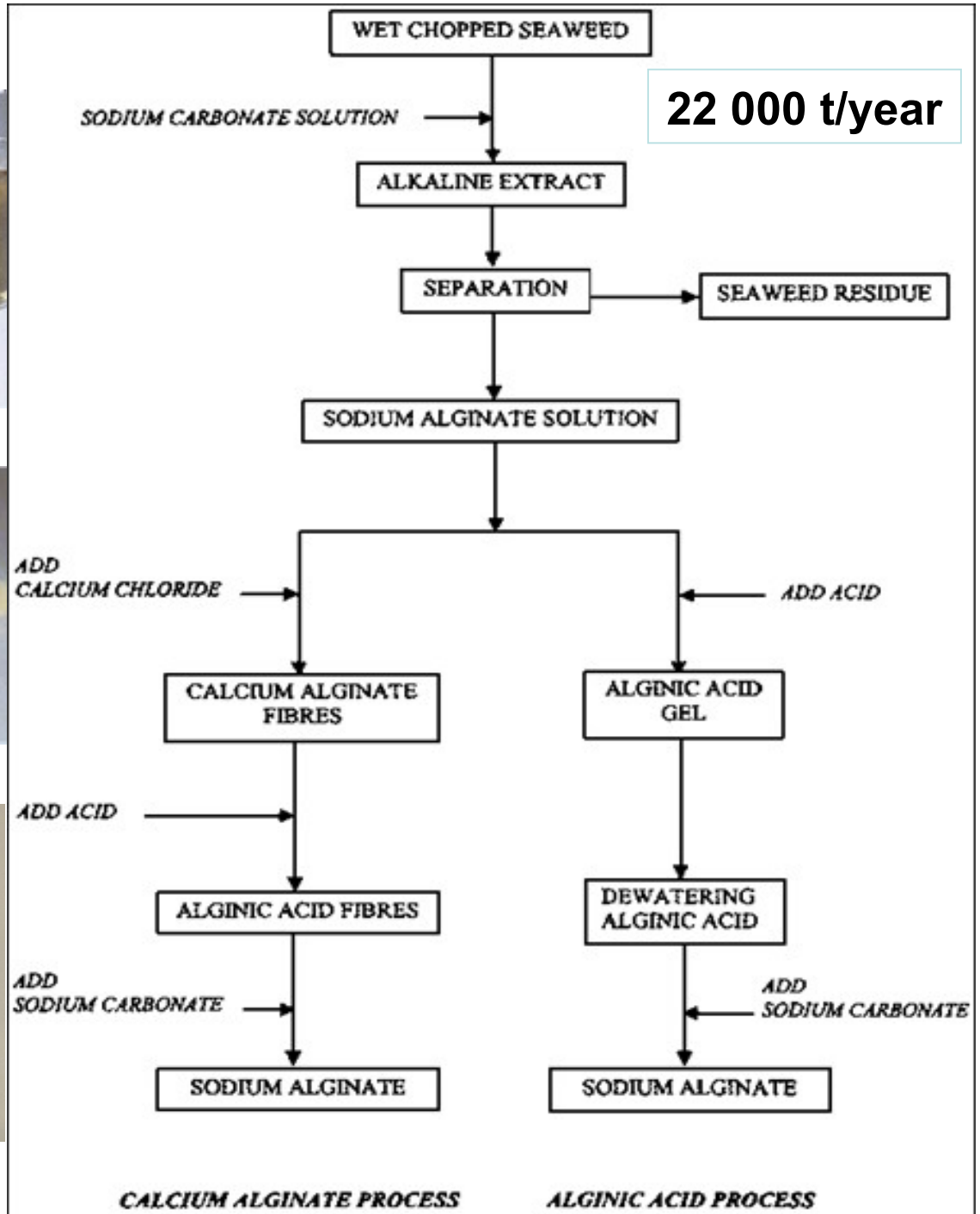

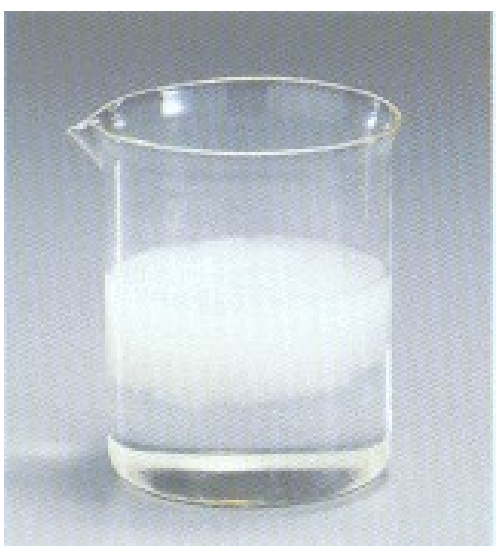

Utilization of brown algae - alginates

food industry

Utilization of brown algae - alginates

food industry

Product	E num-ber	Origin	Used as	Typical products
Alginates and various derivatives (e.g. Sodium alginate, Propylene glycol alginate)	E400-405	Large brown seaweeds such as *Laminaria hyperborea*, *Ascophyllum nodosum* and *Macrocystis* species	Emulsifier, suspending, stabiliser, gelling agent, thickner.	Ice-creams, milk shakes, instant desserts, custard tarts. Suspending agent in soft drinks. Spreads and many others.
Agar	E406	Mainly species of *Gelidium*, *Pterocladia*, and *Gracilaria*	Emulsifier, stabiliser, gelling agent, thickner.	Ice-creams, tinned goods, glazes for meats, etc.
Carrageenan	E407	Mainly *Eucheuma*, *Betaphycus*, *Kappaphycus*, amd *Chondrus crispus*	Emulsifier, stabiliser, gelling agent, thickner.	Ice-creams, milk shakes, instant desserts, custard tarts. Suspending agent in soft drinks. Spreads and many others.

Utilization of brown algae - alginates

farmaceutics, cosmetics

Utilization of brown algae - alginates

slim down diets – satiety

Utilization of brown algae - alginates

building materials

Utilization of brown algae - fucoidane

cell wall polysaccharides; used as dietary supplements

Utilization of brown algae seaweed baths

treatment of rheumatism and arthritis

Utilization of brown algae alginate batteries

Brown algae could help your smartphone keep its charge

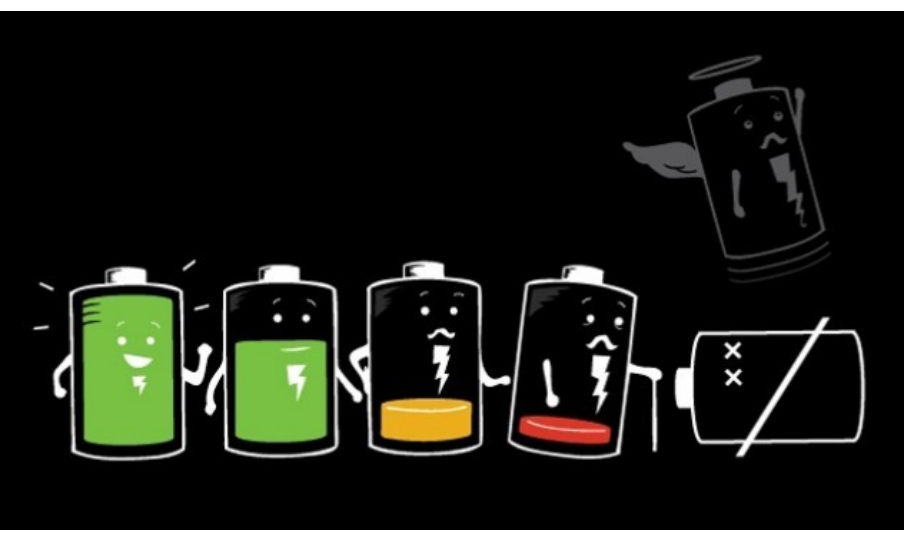

Current battery electrodes are made from graphite, but it's hoped by switching to silicon, larger capacity and longer life Li-ion batteries could be a reality. The only problem is that we need to find something that can can bind effectively onto silicon electrodes. Current batteries use Polyvinylidene Fluoride (PVDF) which in addition to being toxic isn't very good at binding to silicon.

Luckily, they've found something that works better, and is substantially more environmentally friendly. Alginate is a polymer harvested from fast growing brown seaweed, and it's more efficient than PVDF with both silicon and graphite. The way it works is that the alginate forms a protective film on top of the silicon electrode to stop the electrolyte solvent from washing onto the surface of silicon particles, preventing the battery from decomposing.

seaweed art

(belongs to the land-art styles)